

## **Electrospun fibres for supply air filtration in residential buildings**

*an experimental study*

Orlando, Roberta

DOI (link to publication from Publisher):  
[10.54337/aau468596978](https://doi.org/10.54337/aau468596978)

Publication date:  
2021

Document Version  
Publisher's PDF, also known as Version of record

[Link to publication from Aalborg University](#)

Citation for published version (APA):  
Orlando, R. (2021). *Electrospun fibres for supply air filtration in residential buildings: an experimental study*. Aalborg Universitetsforlag.

### **General rights**

Copyright and moral rights for the publications made accessible in the public portal are retained by the authors and/or other copyright owners and it is a condition of accessing publications that users recognise and abide by the legal requirements associated with these rights.

- Users may download and print one copy of any publication from the public portal for the purpose of private study or research.
- You may not further distribute the material or use it for any profit-making activity or commercial gain
- You may freely distribute the URL identifying the publication in the public portal -

### **Take down policy**

If you believe that this document breaches copyright please contact us at [vbn@aub.aau.dk](mailto:vbn@aub.aau.dk) providing details, and we will remove access to the work immediately and investigate your claim.



# **ELECTROSPUN FIBRES FOR SUPPLY AIR FILTRATION IN RESIDENTIAL BUILDINGS: AN EXPERIMENTAL STUDY**

**BY  
ROBERTA ORLANDO**

DISSERTATION SUBMITTED 2021



**AALBORG UNIVERSITY**  
DENMARK





---

---

# Electrospun fibres for supply air filtration in residential buildings: an experimental study

---

---

Ph.D. Dissertation  
Roberta Orlando

Aalborg University Copenhagen  
Department of the Built Environment  
AC Meyers Vænge 15 DK-2450 Copenhagen SV

Dissertation submitted: December 2021

PhD supervisor: Professor Alireza Afshari  
Aalborg University

Assistant PhD supervisor: Associate Professor Peter Fojan  
Aalborg University

PhD committee: Senior Researcher Helle Vibeke Andersen (Chair)  
Aalborg University, Denmark

Professor Ioannis S. Chronakis  
Technical University of Denmark, Denmark

Associate Professor Christophe Duwig  
KTH Royal Institute of Technology - Mechanics, Sweden

PhD Series: Faculty of Engineering and Science, Aalborg University

Department: Department of the Build Environment

ISSN (online): 2446-1636  
ISBN (online): 978-87-7573-967-7

Published by:  
Aalborg University Press  
Kroghstræde 3  
DK – 9220 Aalborg Ø  
Phone: +45 99407140  
aauf@forlag.aau.dk  
forlag.aau.dk

© Copyright: Roberta Orlando

Printed in Denmark by Rosendahls, 2022

# Abstract

Air pollution is considered one of the major risks to human health and the environment and consists of a mixture of particles and gaseous contaminants. Indoor air quality is strongly affected by air pollution, which either originates from indoor sources or enters buildings from the outdoor environment. As people nowadays spend most of their time indoors, exposure to indoor air pollutants represents a crucial public health risk.

Supply air filtration prevents outdoor pollutants (contaminants that would worsen the indoor air quality) from entering buildings. Among the various ventilation system designs, natural ventilation usually does not support the use of supply air filtering. Moreover, natural ventilation systems can only handle rather low pressure drops because they do not rely on mechanical supply fans to distribute the air. Therefore, traditionally, existing naturally ventilated buildings, mostly residential, cannot rely on supply air filtration solutions to reduce indoor pollution levels.

The objective of this study is to develop a novel air filter that can be installed in residential buildings with naturally supplied outdoor air. Such filters could improve indoor air quality with only a small effect on building energy use. Hence, such a filter would have to remove both particles and gaseous pollutants while introducing a negligible pressure drop into the ventilation system.

This thesis presents the development of filter materials, the investigation and analysis of the filter materials' performance and the advantages and disadvantages of the proposed solutions. Electrospun fibre filters are the subject of this experimental study. The fibres are fabricated with diverse polymer-based solutions divided in two generations of filters and doped with activated charcoal (AC) and titanium dioxide ( $\text{TiO}_2$ ), either separately or in combination. The experimental investigation measured the pressure drop, the particle filtration efficiency and the VOC removal capacity of the filters.

After the experimental investigation on the first generation of filters, the second generation showed overall improved performance, both in terms of pressure drop and

pollutants removal. These filters optimised the ratio between pressure drop and particle filtration efficiency while also removing toluene from the polluted air. Based on the findings of this experimental study, it can be concluded that the developed ultrathin electrospun filters are a potential solution to improve conditions in existing naturally ventilated buildings, achieving better indoor air quality with a limited effect on the building energy use.

# Resumé

Luftforurening betragtes som en af de største risici for menneskers sundhed og for miljøet generelt. Derfor har tilstedeværelsen af luftforurening indendørs en kraftig og negativ indvirkning på den indendørs luftkvalitet. Luftforurening, som består af en blanding af partikler og forurenende gasser, kan både have indendørs og udendørs kilder. Opstår luftforureningen udendørs, kan den transporteres ind i en bygning via ventilation eller infiltration. Fordi mennesker i dag bruger størstedelen af deres liv indendørs, udgør problemer med indendørs luftforurening og lav luftkvalitet en risiko for folkesundheden.

Filtrering af tilluft forhindrer forurening fra udendørs kilder i at trænge ind i bygninger. Naturlig ventilation, som er et blandt flere ventilationsprincipper, tillader normalt ikke filtrering af tilluft. Fordi der ved naturlig ventilation ikke gøres brug af mekaniske ventilatorer, så kan naturlige ventilationssystemer kun håndtere relativt lave tryktab over systemet. Derfor har der i eksisterende naturligt ventilerede bygninger (som primært er boliger) ikke været tradition for at filtrere tilluft for at reducere indendørs luftforurening.

Formålet med dette projekt er at udvikle et innovativt filter, der kan installeres i beboelsesejendomme, hvor tilluft tilføres 'naturligt' (f.eks. gennem udeluftventiler). Sådanne filtre ville kunne forbedre den indendørs luftkvalitet uden større påvirkning af en bygnings energibehov. Derfor vil et sådant filter skulle kunne fjerne både partikler og forurenende gasser, uden at det samtidigt medfører en betydelig stigning i tryktabet over et ventilationssystem.

Denne afhandling præsenterer udviklingen af filtermaterialer, undersøgelsen og analysen af filtermaterialernes ydeevne samt fordele og ulemper ved de udviklede løsninger. Fokuset for dette eksperimentelle studie er elektrospundne fiberfiltre. Fibrene er fremstillet ved forskellige polymerbaserede løsninger udviklet over to generationer. De elektrospundne fibre er blevet tilsat aktivt kul (AC) og titaniumdioxid ( $\text{TiO}_2$ ). Tilsætningsstofferne individuelle og kombinerede effekter er blevet undersøgt. Som led i det

eksperimentelle arbejde er der gennemført måling af tryktab over udviklede filterløsninger, effektivitet ved filtrering af partikler og kapacitet for at fjerne flygtige organiske forbindelser (VOC'er).

Første generation af udviklede filtermaterialer blev undersøgt eksperimentelt. Anden generation viste en generel forbedring i ydeevne. Der blev målt forbedringer med hensyn til tryktab, effektivitet ved filtrering af partikler og kapacitet for at fjerne VOC'er. Filtermaterialerne i anden generation optimerede på forholdet mellem tryktab og effektivitet ved filtrering af partikler, samtidigt med at de også fjernede toluen fra den forurenede luft. Baseret på resultaterne af dette eksperimentelle studie kan det konkluderes, at de udviklede ultratynde elektropsundne filtre er en potentiel løsning til at forbedre forholdene i eksisterende naturligt ventilerede bygninger og opnå bedre indendørs luftkvalitet uden større påvirkning af en bygnings energibehov.

# Preface

**Thesis Title:** Electrospun fibres for supply air filtration in residential buildings:  
an experimental study  
**Ph.D. Student:** Roberta Orlando  
**Supervisors:** Professor Alireza Afshari, Aalborg University  
Associate Professor Peter Fojan, Aalborg University

The study presented in this thesis was conducted partly at the Department of Materials and Production and partly at the Department of the Built Environment at Aalborg University from October 2018 to December 2021. The experimental work was performed at the Department of Materials and Production at Aalborg University, at the Department of Chemistry at the University of Copenhagen and at the Department of Building Science at Tsinghua University. Financial support was provided by the Danish Landowners' Investment Association (Grundejernes Investeringsfond, No. 9026310), the Department of the Built Environment and the Department of Materials and Production (AAU). The author is deeply grateful for the opportunity provided by the funding organisations. The main body of this thesis consists of the following papers:

- [1] R. Orlando, P. Fojan, J. Mo, N. C. Bergsøe and A. Afshari, "Single-Stage Air Filtration of Particles and Gaseous Contaminants in Buildings: A Literature Study", *IOP Conference Series: Earth and Environmental Science*, vol. 588, 032073, 2020. <https://doi.org/10.1088/1755-1315/588/3/032073>
- [2] R. Orlando, P. Fojan, M. S. Johnson, N. C. Bergsøe and A. Afshari, "Electrospun nanofiber air pollution filters: An experimental study", In Proceedings for *The 16th Conference of the International Society of Indoor Air Quality & Climate*, Indoor Air 2020.

- [3] R. Orlando, M. Polat, A. Afshari, M. S. Johnson and P. Fojan, "Electrospun Nanofibre Air Filters for Particles and Gaseous Pollutants", *Sustainability*, vol. 13, no. 12, 6553, 2021. <https://doi.org/10.3390/su13126553>
- [4] R. Orlando, Y. Gao, P. Fojan, J. Mo and A. Afshari, "Filtration performance of ultrathin electrospun cellulose acetate filters doped with  $\text{TiO}_2$  and activated charcoal", *Buildings*, vol. 11, no. 11, 557, 2021. <https://doi.org/10.3390/buildings11110557>
- [5] R. Orlando, A. Afshari and P. Fojan, "Cellulose Acetate-based composite fibre membranes for toluene removal", Submitted in Journal of Industrial Textiles (November 2021).

This thesis has been submitted for assessment in partial fulfilment of the Ph.D. degree. The thesis is based on the submitted or published scientific papers listed above. The dissertation is paper-based, and the papers are used directly in the main body of the thesis. As part of the assessment, co-author statements have been made available to the assessment committee and are also available at the Faculty. The thesis is not acceptable for open publication in its present form but only for limited and closed circulation, as copyright may not be ensured.



# Acknowledgements

First, I would like to express my sincere and deep gratitude to my supervisor, Professor Alireza Afshari, for his continuous guidance, supervision and shared expertise. He gave me the opportunity to pursue a doctoral degree and truly supported me as I researched and wrote the thesis, guiding me and keeping me on the right path.

My deepest appreciation to my co-supervisor, Associate Professor Peter Fojan, for the extensive knowledge he shared with me. I am deeply grateful for the incredible amount of time we spent working together in the laboratory as he guided my experimental research and for his support during the analysis and writing phase of my doctoral research. This work would not have been possible without his support.

Special thanks go also to Professor Matthew S. Johnson for his unsparing guidance and valuable discussions during my experimental work at the Department of Chemistry at the University of Copenhagen. Furthermore, I would like to thank the wonderful colleagues and students of Matthew's group for their support and assistance during my stay there.

I thankfully acknowledge Professor Jinhan Mo and Yilun Gao for their collaboration, kind support and insights during the second experimental phase of my Ph.D. project. They gave me the opportunity to finish my study through remote collaboration during the COVID pandemic, and I am grateful for their willingness to work with me in such unprecedented conditions.

I would also like to thank Niels C. Bergsøe, who was my co-supervisor in the initial part of the project and whose precise comments and assistance were invaluable. I extend my gratitude to all my colleagues at Aalborg University in both the Departments I worked for their support and the pleasant work environment during the past three years. Thank you for sharing your thoughts, insights and friendly talks during this time.

I would like to thank all the people who have encouraged me during my doctoral studies, including my friends and family both close and far. Their words of support made

this journey not so lonely after all. I would like to mention and thank my grandmother Rosetta for her reminder to pursue what brings me joy in life. With her wise advice and delicate presence, she shaped the person I am today. Furthermore, I would like to express my warmest thanks to my amazing parents, Silvia and Paolo, and my wonderful siblings, Francesca, Lorenza and Luca. Their support in difficult times and the joy we shared when reaching important goals have made this journey richer and even more valuable. Thank you for being my compass, my inspiration and my greatest value in life. I would not be who I am today without you.

The last important acknowledgement and gratitude from the bottom of my heart go to Daniel, my partner in this life. His endless support, kind and reassuring words and tireless encouragement despite difficult times made the greatest difference for me. His positive attitude and his strong belief in my potential helped me see the journey through. Thank you for the laughs, for listening to me and for being such a loving person. I would not have completed this study without you next to me.

Roberta Orlando  
Aalborg University, December 14, 2021

*To my beloved mother, Silvia,  
passionate about science, who inspired me and supported me throughout my journey*



# Contents

<b>Abstract</b>	<b>iii</b>
<b>Resumé</b>	<b>v</b>
<b>Preface</b>	<b>vii</b>
<b>Acknowledgements</b>	<b>ix</b>
<b>I Introduction</b>	<b>1</b>
<b>1 Introduction</b>	<b>3</b>
1.1 Background . . . . .	3
1.2 Objectives and scope . . . . .	7
1.2.1 Limitations . . . . .	7
1.3 Outline of the thesis . . . . .	8
<b>2 Air pollution</b>	<b>11</b>
2.1 Ambient air pollution . . . . .	11
2.1.1 Outdoor air particle pollution . . . . .	12
2.1.2 Outdoor gaseous pollutants . . . . .	13
2.1.3 Consequences of outdoor air pollution . . . . .	15
2.2 Indoor air quality . . . . .	16
2.2.1 The relationship between outdoor contaminants and indoor air quality . . . . .	19
2.2.2 Indoor air pollutants and their impacts . . . . .	21
2.2.3 Improving indoor air quality . . . . .	22

<b>3</b>	<b>Air filtration technologies</b>	<b>25</b>
3.1	An introduction to filtration . . . . .	25
3.1.1	Fundamentals of filtration mechanisms . . . . .	26
3.2	Air filtration in HVAC systems . . . . .	29
3.2.1	Ventilation strategies . . . . .	29
3.2.2	Air filter performance . . . . .	33
3.2.3	Classification of HVAC filters . . . . .	39
3.2.4	Air filtration and purification technologies . . . . .	40
3.2.5	Combined air filtration systems . . . . .	46
3.3	Electrospun fibre filters . . . . .	48
3.4	Electrospinning . . . . .	52
3.4.1	Electrospinning governing parameters . . . . .	57
3.4.2	Fundamentals of the theoretical background and phenomena governing the electrospinning process . . . . .	59
<b>II</b>	<b>Research Papers</b>	<b>65</b>
<b>4</b>	<b>Paper I</b>	<b>69</b>
	Single-Stage Air Filtration of Particles and Gaseous Contaminants in Buildings: A Literature Study . . . . .	71
<b>5</b>	<b>Paper II</b>	<b>75</b>
	Electrospun nanofiber air pollution filters: An experimental study . . . . .	77
<b>6</b>	<b>Paper III</b>	<b>83</b>
	Electrospun Nanofibre Air Filters for Particles and Gaseous Pollutants . . . .	85
<b>7</b>	<b>Paper IV</b>	<b>103</b>
	Filtration performance of ultrathin electrospun cellulose acetate filters doped with $\text{TiO}_2$ and activated charcoal . . . . .	105
<b>8</b>	<b>Paper V</b>	<b>121</b>
	Cellulose Acetate-based composite fibre membranes for toluene removal . . .	123

<b>III</b>	<b>Discussion and Conclusions</b>	<b>143</b>
<b>9</b>	<b>Discussion</b>	<b>145</b>
9.1	Air filter performance . . . . .	145
9.2	Overall discussion . . . . .	151
<b>10</b>	<b>Conclusions</b>	<b>153</b>
10.1	Conclusion . . . . .	153
10.2	Future research . . . . .	154
	<b>Bibliography</b>	<b>155</b>

# List of Figures

2.1	Classification of particles based on their aerodynamic diameter from different sources (adapted from [32]). . . . .	12
2.2	Pathways and sources of indoor air pollution. . . . .	20
3.1	Filtration mechanisms: (a.) surface straining, (b.) depth straining, (c.) depth filtration and (d.) cake filtration (adapted from [109]). . . . .	28
3.2	Natural ventilation techniques: (a.) single-sided ventilation, (b.) cross-flow ventilation, (c.) stack-ventilation (adapted from [117]). . . . .	30
3.3	Principles of mechanical ventilation systems: (a.) mechanical extract ventilation, (b.) mechanical supply ventilation, (c.) balanced mechanical ventilation (adapted from [112]). . . . .	31
3.4	Illustration of the different filtration mechanisms involved in mechanical filtration (adapted from [120]). . . . .	34
3.5	Schematic representation of the flow regime in relation to the Knudsen number (adopted from [136]). . . . .	38
3.6	Interaction mechanisms between adsorbent and adsorbate during physisorption and chemisorption (adapted from [156]). . . . .	42
3.7	Mechanism of the PCO of VOCs with UV light using $\text{TiO}_2$ as catalyst (adapted from [165]). . . . .	44
3.8	Scheme of a basic electrospinning setup. (a) Examples of types of feeding configuration (a1) single needle (a2) coaxial needle (a3) multineedle. (b) Examples of types of collector (b1) flat plate collector (b2) parallel electrodes (b3) rotating drum. . . . .	55
3.9	Coalescence of PU nanofibres. DMF is the solvent used for dissolving the polymer. . . . .	63



9.1 Pressure drop of the fabricated filters recorded at a face velocity of 0.053  
m s<sup>-1</sup>. . . . . 147

# List of Tables

2.1	Major chemical components and related sources of airborne particles grouped by size [32, 39–41]. . . . .	14
2.2	Current WHO air quality guidelines and EU air quality standards [6, 8].	17
2.3	Sources and impacts of indoor air pollutants [88, 98, 99, 104–106]. . . .	23
3.1	Various filter media types and their applications [107]. . . . .	27
3.2	Classification and requirements of air filters (ISO 16890) [140] . . . . .	40
3.3	Air filter performance of electrospun fibre filters. . . . .	51
3.4	Commonly electrospun polymers and their application. . . . .	53
3.5	Electrospinning governing parameters. . . . .	57
9.1	Quality factors of the produced filters. . . . .	149

# Nomenclature

The following list presents the abbreviations and symbols that are used most frequently in the body of the dissertation.

## Abbreviations

<i>AC</i>	Activated charcoal
<i>CA</i>	Cellulose acetate
<i>DMF</i>	N,N-dimethylformamide
<i>HEPA</i>	High-Efficiency Particulate Air
<i>HVAC</i>	Heating, Ventilation and Air Conditioning
<i>IAQ</i>	Indoor Air Quality
<i>PCO</i>	Photocatalytic Oxidation
<i>PM<sub>x</sub></i>	Particulate Matter with aerodynamic diameter below x $\mu\text{m}$
<i>PU</i>	Polyurethane
<i>PVA</i>	Polyvinyl alcohol
<i>TCD</i>	Tip-to-Collector Distance
<i>TiO<sub>2</sub></i>	Titanium dioxide
<i>TVOCs</i>	Total Volatile Organic Compounds
<i>VOCs</i>	Volatile Organic Compounds

*WHO* World Health Organisation

### Variables and Parameters

$\alpha$	Filter packing density
$\Delta p$	Pressure drop (Pa)
$\eta$	Filtration efficiency/removal capacity of a filter
$\lambda$	Mean free path of gas molecules (nm)
$A$	Filter cross-sectional area (m <sup>2</sup> )
$C_{down}$	Pollutant concentration downstream of a filter
$C_{up}$	Pollutant concentration upstream of a filter
$d_f$	Fibre diameter of a filter (nm, $\mu\text{m}$ )
$Kn$	Knudsen number
$Q$	Air flow rate (m <sup>3</sup> h <sup>-1</sup> )
$Q_f$	Quality factor (Pa <sup>-1</sup> )
$V_f$	Face velocity (m s <sup>-1</sup> )

# Part I

## Introduction



# Chapter 1

## Introduction

### 1.1 Background

#### *Indoor air quality and air pollution*

Air filtration plays a vital role in maximising indoor air quality while minimising energy usage. As part of the ventilation system, air filters prevent building users from exposure to air pollutants and protect the air handling system and equipment from becoming damaged and ineffective due to contamination. Air filters' ability to remove air pollutants from the air supply brings fresh and clean air into the building from the outdoor environment; outdoor air can be heavily polluted, especially in urban and industrialised areas. Nowadays, air pollution is one of the major concerns for human health and the environment. Air pollution is a mixture of several components. These include both solid pollutants, such as particles of various sizes ranging from a few nm to tens of micrometres, and gaseous compounds, such as ozone ( $O_3$ ), nitrogen dioxide ( $NO_2$ ), carbon monoxide (CO) and volatile organic compounds (VOCs).

Exposure to pollution has been linked to negative impacts on the immune [1], respiratory and cardiovascular systems [2–4]. It contributes to lung cancer [5] and premature mortality [3]. As a result, the European Union has developed a set of health-based standards for several pollutants present in the air. These include particles as well as  $O_3$ , CO and VOCs such as benzene and polycyclic aromatic hydrocarbons [6]. Denmark has adopted these standards as the basis of the Danish air quality requirements [7]. The World Health Organisation (WHO) has also defined air quality guidelines for average

outdoor particle concentrations of  $\text{PM}_{10}$ ,  $\text{PM}_{2.5}$  and for gaseous compounds like sulphur dioxide ( $\text{SO}_2$ ),  $\text{NO}_2$ ,  $\text{O}_3$  and CO [8]. In regards to the indoor environment, the WHO guidelines focus on gaseous pollutants like VOCs such as benzene and formaldehyde, CO and radon, which are typical indoor pollutants that harm human health [9]. Nevertheless, 91% of the world population lives in areas where the WHO guidelines are not met, and indoor air pollution is still not constantly monitored in most countries. Consequently, air pollution is the cause of 4.2 million deaths per year [10]. The loss of life expectancy due to air pollution is estimated to be 2.9 years, which exceeds that of all forms of violence, HIV/AIDS and smoking [11].

As people spend most of their time indoors, most exposure to air pollution happens inside buildings. The most frequent short-term symptoms of exposure to poor indoor air quality are headaches; irritation of the eyes, nose and throat; fatigue [12] and asthma [13]. These health effects also cause a loss of productivity and increased absenteeism in workplaces [14].

Indoor pollution concentration is influenced by both outdoor and indoor sources [15]. Outdoor pollutants are generated through industrial and agricultural processes, such as the combustion of fossil fuels (domestic heating, vehicles and power generation) and waste incineration. Typical indoor sources of pollution include cleaning products, office equipment, cooking and biological sources such as people, pets or mould [16]. Outdoor pollution significantly increases the indoor pollutant concentration, as it is the dominant source of indoor particles [17]. In this context, outdoor-to-indoor pollution transport can be reduced by implementing supply air filters within the ventilation system, thereby improving indoor air quality.

### *Air filtration technology and its challenges*

Air filtration technologies deal with different pollutants, which require different mechanisms to be removed or degraded. Air filters can be rather selective in which pollutant type they can remove; each filter has its own advantages and limitations. The result is rather cumbersome and complicated multi-stage air filtration systems to handle air pollution. The simultaneous removal of particles and gaseous pollutants is a key challenge that must be solved, and a better understanding of the mechanisms for the simultaneous removal of multi-pollutants is needed. Combining multi-stage devices into a single-stage air filter is an attractive yet underexplored potential solution.

The balance between healthy air quality, building energy use and heating, ventilation and air conditioning (HVAC) system efficiency is linked to HVAC components including



air filters and their performance. Several criteria should be considered when designing new air filters. To improve total building efficiency, a filter with a low pressure drop should be fabricated to reduce energy use without compromising the filter's pollutant removal capacity. The challenge should be solved by implementing air filters that would not add complexity to the ventilation systems. Finally, solutions that require easy production, cost-effective operation and maintenance should be favoured to ensure their widespread implementation in buildings.

*Building energy use: The role of HVAC and air filtration*

The purpose of an HVAC system is to compensate for shortcomings in the interactions between building structure, building use and the outdoor climate to achieve the thermal climate, air quality and air purity that the occupants require for the use of the building. Three major mechanical ventilation systems are available: exhaust ventilation systems, supply ventilation systems and balanced ventilation systems. Exhaust ventilation and balanced ventilation systems rely on outdoor air supply through vents in windows and walls. Natural and hybrid ventilation systems are also used. Natural ventilation systems do not integrate a supply air filtration in their traditional design. Nevertheless, to ensure and maintain a healthy indoor air quality without affecting energy use, a low pressure drop air filter should be installed on the air supply intake.

According to the International Energy Agency, the building sector accounts for 28% of energy-related CO<sub>2</sub> emissions, two-thirds of which are from rapidly growing electricity use. In fact, buildings consume more than 55% of global electricity [18]. HVAC systems account for approximately 35% of the total energy used by commercial and residential buildings [19]. Therefore, HVAC systems play an important role in the total energy use of the building sector.

The recent outbreak of the COVID-19 pandemic could affect the use of HVAC in buildings in the future. To prevent the spread of contagious diseases, experts from REHVA [20] and ASHRAE [21] recommend increasing the use of outdoor air and the rate of air change, inspecting and maintaining HVAC systems and implementing the use of MERV-13 filters for improved filtration. Consequently, it is even more important today for HVAC systems to operate as efficiently as possible [22]. HVAC components' energy use varies considerably depending on several factors, including building parameters such as building type, glazing percentage and properties, occupancy pattern, the level of internal gains and building location and climate. Furthermore, the ventilation design (natural or mechanical ventilation) and operation time and schedule – which can vary

depending on the building type (residential or commercial) and occupancy – play an important role in the system’s energy use. Fans, which are responsible for air distribution, account for  $\sim 34\%$  of the total energy use of the HVAC system on average [23]. The power required to run an HVAC fan depends on system design parameters such as air flow and flow resistance as well as on the fan system’s efficiency. The air flow rate and fan system efficiency are determined, in turn, by the system’s needs, the equipment selection and the building requirements, while the flow resistance depends on the component selection and the ventilation system design submitted to the airstream. Air filters are a component that introduces air resistance into the system. Their contribution to the total system pressure drop is in the range of 20–50%, depending on the loading conditions, filter efficiency and system configuration [24].

### *Climate and buildings policies*

The European Union has formulated the European Green Deal with the aim of becoming the first climate-neutral continent by achieving net-zero carbon dioxide ( $\text{CO}_2$ ) emissions by 2050 [25]. In the last report on the Energy Efficiency Directive, published in 2020, the European Commission has stated that a significantly higher energy efficiency effort from the EU Members States is necessary to meet the 2030 target (a reduction of 39–41% in primary energy consumption and 36–37% in final energy consumption). The energy-saving campaign that EU countries promoted in 2018 was not enough to reach the 2020 target when excluding the impact of COVID-19 on energy demand [26].

The European buildings policy has its foundation in the Energy Performance of Buildings Directive (EPBD, 2010/31/EU), which promotes the improvement of buildings’ energy performance. Furthermore, it is stated that Member States shall take the necessary measures to guarantee the requirements of minimum energy performance, which ‘[...]/ shall take account of the general indoor climate condition, in order to avoid possible negative effect such as inadequate ventilation’ [27]. From a Danish perspective, in the Danish Building Code (BR18), it is declared that ‘buildings must be ventilated to provide satisfactory air quality’ [28]. Therefore, the focus lies on reducing buildings’ energy use while promoting healthy indoor air conditions at both the European level and the Danish national level.

## 1.2 Objectives and scope

The main objective of this Ph.D. project is to develop knowledge about solutions for satisfactory indoor air quality at the lowest possible energy use for a given activity in a building. The aim was to develop a single-stage filter that can be implemented as a supply air filtration system for residential buildings, especially those relying on natural ventilation.

The main hypothesis of this study is that the novel filter would be able to simultaneously remove solid and gaseous pollutants and that it would have a lower impact on building energy use compared to conventional filters. The ratio between indoor air quality and energy use will then be optimised.

The Ph.D. project consisted of performing several tasks in order to evaluate the hypothesis and achieve the research objective.

- The air filtration technologies present on the market and investigated in previous studies in the literature were reviewed to assess solutions that would meet the objective of the Ph.D. study. Electrospun fibre filters were identified as a potential solution. These filters showed promising results by combining active chemistry on the filter surface to remove both particles and gaseous pollutants while maintaining a low pressure drop.
- Several electrospun nano- and microfibre materials were developed in the laboratory using various polymers and additive materials, various electrospinning configurations and methods to activate the polymer-based fibres towards gaseous pollutants. Two generations of filters were fabricated.
- The performance of the developed materials was assessed under control conditions in the laboratory. Pressure drop, filtration efficiency and removal or degradation of gaseous pollutants were investigated. A detailed and critical analysis of the performance was conducted to identify the advantages and limitations of the produced filters.

### 1.2.1 Limitations

The aim of this work was to fabricate filter materials that could be produced by a fast and reliable production method. A parameter analysis of the filter production with electrospinning in terms of process, solution and ambient parameters was completed with the aim of optimising air filter performance.

The project's focus was on the fabrication of novel filter materials and the experimental investigation of their filtration performance in a laboratory environment from a short-term perspective. The work does not include a modelling study such as a multi-physics simulation environment or a computational fluid dynamic simulation of a filtration system.

Therefore, the study has focused on performance under controlled conditions. The results are related to the initial performance of the material, as long-term investigations involving installation in a building were not possible given the project's timeframe. Nevertheless, the investigated materials were selected with the aim of long-term use in a filtration system.

### 1.3 Outline of the thesis

The thesis is divided into three parts for a total of ten chapters.

**Part I** includes **Chapters 1–3** and presents the background, theories and results in the literature on the core topics of the research project:

- **Chapter 1** presents the background, objectives and scope of the Ph.D. project, which delimit the work conducted for this thesis. The project's limitations are also described.
- **Chapters 2–3** focus on the literature on air pollution and filtration technologies, with special regards to electrospun nanofibre filters. Theories that are pertinent to the conducted research are discussed in these chapters.

**Part II** comprises in **Chapters 4–8** and includes the research papers written and published throughout the Ph.D.:

- **Chapter 4** describes the literature review performed at the beginning of the work, which drove the decisions related to the research objectives of the Ph.D. project.
- **Chapter 5** describes the investigation of the first generation of developed filters, presenting the preliminary results of the materials' filtration performance.
- **Chapter 6** extends the work related to **Chapter 5**, investigating the first generation of filter materials by characterising the nanofibres and presenting extensive filtration performance results.

- **Chapter 7** presents the results of the second generation of filters, which was designed to improve the filtration performance from **Chapter 5** and **6**. A new fabrication method is described and novel composite materials are introduced. The study focused on particle filtration.
- **Chapter 8** finalises the study on the second generation of filter, investigating the removal of gaseous compounds by the novel materials.

**Part III** concludes the thesis and synthesises the scientific output of the Ph.D. project. In **Chapter 9**, the results from the papers are brought together to discuss the global outcome of the research project. **Chapter 10** frames the final conclusions and suggests future research.



# Chapter 2

## Air pollution

### 2.1 Ambient air pollution

Air pollution is a complex mixture of several substances that can harm human health, living resources and ecological systems. There are many types of air pollutants. They can be classified by their physical state as solids, such as particles or particulate matter; gases, such as ozone, carbon monoxide, toluene and formaldehyde; and biological molecules, such as viruses or bacteria. They can also be classified based on their sources, whether natural or anthropogenic. *Primary pollutants* are those emitted directly into the atmosphere. *Secondary* pollutants are those produced within the atmosphere from chemical reactions with other pollutants (e.g. ozone and gas-to-particle conversion processes) or atmospheric gases [29, 30].

Air pollution concentration also varies based on weather and location. Air quality in urban areas is affected by industrial and traffic-related emissions, which result in heavier air pollution compared to rural areas. Outdoor air in arid and semi-arid areas presents large-particle pollution due to the presence of mineral dust typical of deserts, which is one of the largest contributors of naturally produced particles [29]. There are also clear differences between Western industrialised countries and middle- and low-income nations. In the former, the policies and technological development of relevant industrial sectors help to contain the emission of pollutants. On the other hand, in middle- and low-income countries, widespread industrialisation and urbanisation result in large urban centres with air quality amongst the poorest in the world. Furthermore, these countries' protective and preventive measures are still in an early stage [31].

### 2.1.1 Outdoor air particle pollution

Particle pollution, also called atmospheric aerosol or particulate matter (PM), indicates a mixture of liquid droplets and solid particles suspended in the air [32]. The particles can vary widely in terms of particle size, concentration and chemical composition. The aerodynamic diameter is commonly used to categorise particles; this measure represents the diameter of a spherical particle that has the same settling velocity as the particle that is to be characterised and a density of  $1 \text{ g cm}^{-3}$  [33]. The period of time that particles with an aerodynamic diameter larger than  $30 \text{ }\mu\text{m}$  are suspended in air before deposition is relatively short compared to smaller particles and such large particles are therefore rarely the subject of studies [34]. Conversely, particles with an aerodynamic diameter  $<10 \text{ }\mu\text{m}$  ( $\text{PM}_{10}$ ) pose the greatest problems for human health and the environment [35]. These particles are grouped into coarse, fine and ultrafine particles, characterized by aerodynamic diameters of  $<10 \text{ }\mu\text{m}$  ( $\text{PM}_{10}$ ),  $<2.5 \text{ }\mu\text{m}$  ( $\text{PM}_{2.5}$ ) and  $<0.1 \text{ }\mu\text{m}$  ( $\text{PM}_{0.1}$ ), respectively. The size classification linked to the particle types is presented schematically in Figure 2.1. The size distinction between particles is essential because different particle sizes present differences in formation, modification, atmospheric residential time, removal, physical and chemical properties and consequences to human health and the environment [29].

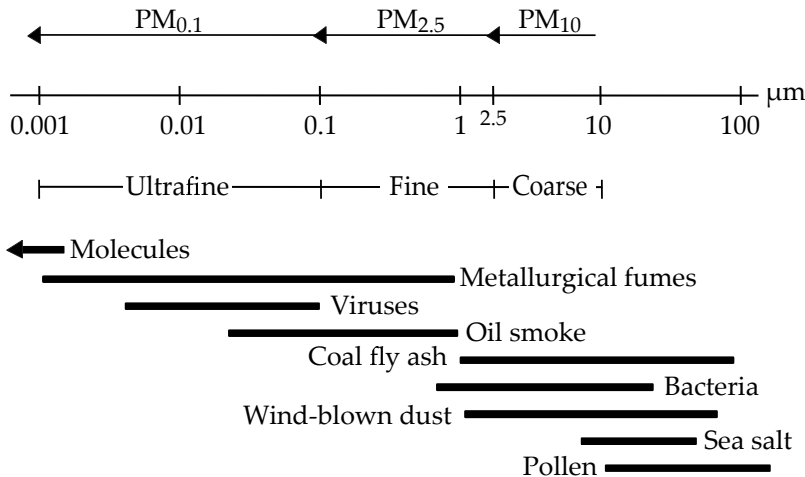


**Fig. 2.1:** Classification of particles based on their aerodynamic diameter from different sources (adapted from [32]).



Ambient particle pollution originates from both anthropogenic and natural sources [36–38]. Natural emission sources of primary and secondary particulates include vegetation, volcanoes, oceans, wildfires and mineral dust from arid and semi-arid regions. Typical anthropogenic activities that are responsible for particle emission include the combustion of fuels from vehicles, industrial processes, agricultural procedures and construction and demolition activities. On a global scale, data shows that airborne particles from natural sources are predominant rather than those of anthropogenic origin (98 wt% versus 2 wt%) [29, 37]. Sea salt and mineral dust are the largest contributors to total mass fluxes. Furthermore,  $\sim 99$  wt% of the particles of natural origin consists of primary particles, whereas secondary aerosol particles are  $\sim 50$  wt% for the anthropogenic flux. On a local scale, the proportions are completely different. In urban environments, anthropogenic particles account for 80% of total airborne particles. Vehicle combustion, biomass burning, anthropogenic nitrate and sulphate are the main contributors to total flux in urban environments [29, 37].

Particles are constituted of different chemical components, which also depend on the particles' origin. The major chemical constituents are sulphate, nitrate, ammonium, organic compounds, inorganic carbonaceous materials (including black carbon and elemental carbon) and metals such as Pb, Zn, Mn and Cr [39–41]. Further details on particle composition and sources grouped by size are presented in Table 2.1.

Ambient particles' distribution as a function of particle size can be based on particle number, surface area or mass. Different particle size ranges contribute differently to the total distribution depending on which distribution type is considered. Ultrafine particles account for the majority of particles by number, but due to their small size, they account for only a few percent of the total mass of airborne particles. Fine particles constitute most of the particle surface area and a considerable part of the particle mass. The coarse particles contribute most of the total particle mass distribution [40, 41].

### 2.1.2 Outdoor gaseous pollutants

Gaseous air pollution is emitted by several natural sources, such as forest fires and volcanoes, and also comes from anthropogenic emissions related to industrial activities [42]. The major outdoor gaseous air pollutants are sulphur dioxide ( $\text{SO}_2$ ), oxides of nitrogen ( $\text{NO}_x = \text{NO} + \text{NO}_2$ ), ozone ( $\text{O}_3$ ), carbon monoxide ( $\text{CO}$ ), carbon dioxide ( $\text{CO}_2$ ) and some organic compounds, like VOCs [32, 43, 44].

The main sources of  $\text{SO}_2$  are primary emissions. Many are anthropogenic, like fossil fuel combustion, thermal power plant emissions, cement factories and industrial

**Table 2.1:** Major chemical components and related sources of airborne particles grouped by size [32, 39–41].

Particle definition	Main components	Main sources
Coarse (PM <sub>10</sub> )	Mineral dust, carbonaceous matter, sodium, chloride, sulphate, nitrate, biogenic aerosol.	Wind erosion, soil resuspension, agricultural and industrial processes, secondary emission due to oxidation of SO <sub>2</sub> and NO <sub>x</sub> , vegetation, volcanic and marine emissions (sea spray).
Fine (PM <sub>2.5</sub> )	Carbonaceous compounds, chloride, sulphate, nitrate, sodium, ammonium, metals, mineral dust.	Automotive, residential and industrial combustion-related process, oxidation of VOCs, sea spray, coagulation of smaller particles.
Ultrafine (PM <sub>0.1</sub> )	Carbonaceous matter, sulphate, elemental carbon, metal oxides.	Fossil fuels, biofuels, and biomass combustion (condensation of hot vapour during combustion processes), some anthropogenic and biogenic noncombustion sources, continental and marine ecosystems, nucleation of atmospheric species.

emissions [32, 43]. SO<sub>2</sub> can also be emitted by natural sources, such as volcanic eruptions and sulphur-containing geothermal sources, including geysers and hot springs [44].

Nitric oxide (NO) is also a primary pollutant. It is formed from the combustion of nitrogen-containing compounds, including fossil fuels (90% of combustion NO<sub>x</sub> production is NO) or by the thermal fixation of atmospheric nitrogen. Nitrogen dioxide (NO<sub>2</sub>) is both a primary and secondary pollutant, as it is both emitted during combustion processes and formed in the atmosphere by chemical reactions [32, 44].

Ozone (O<sub>3</sub>) is a secondary gaseous pollutant and is also defined as a photochemically formed organic oxidant when at ground level [44]. It is a plant-toxic pollutant associated with precursor gases (NO<sub>x</sub> and VOCs) and solar radiation [43]. Nitrogen oxides formed from fossil combustion and emitted to the atmosphere are acted upon by sunlight to yield ozone. O<sub>3</sub> can further react with hydrocarbons and forms compounds like organic acid, epoxy compounds and aldehydes. [44].

CO<sub>2</sub> and CO are two other important outdoor air pollutants that are heavily emitted by the power and industrial sector. The complete combustion of any fuel containing carbon would lead to CO<sub>2</sub>. However, carbon monoxide, which is highly toxic, is always produced as well. CO<sub>2</sub> concentration levels play an important role in the regulation of photosynthesis and, therefore, in plants' carbon and water metabolism [32, 43].

VOCs include hydrocarbons, halocarbons and oxygenates. The major sources of VOCs are manufacturing processes and industrial emissions, solvent use, fuel refining, road transport and emissions from vehicles and the combustion of fossil fuels. Within VOCs,

hydrocarbons have drawn the most attention because of their role in photochemistry [32, 43]. Benzene, formaldehyde and toluene are also VOCs. Benzene is emitted from burning coal and oil and from vehicle exhaust. Formaldehyde's primary source of emission is biomass burning, whereas secondary formaldehyde is produced in the atmosphere via the photochemical oxidation of other VOCs [45].

### 2.1.3 Consequences of outdoor air pollution

#### *Effects on human health*

The general knowledge of the health risks that air pollution poses to humans has advanced in the past years. Several studies have demonstrated the associations between exposure to airborne particles and adverse health effects, including restricted activity or energy level, hospital admission and increased mortality and morbidity [3, 34, 35, 40, 46–48]. Fine and ultrafine particles can penetrate deeper into respiratory systems compared to larger ones. Particles from 1 to 2.5  $\mu\text{m}$  can reach the terminal bronchioles, whereas particles less than 1  $\mu\text{m}$  diameter can reach the alveoli and thus are more likely to cause respiratory health problems, such as cough, asthma, pulmonary inflammation and even increased risk of lung cancer mortality [49]. There is also a strong statistical association between fine particles and cardiovascular disease mortality due to ischaemic heart disease, fatal dysrhythmias, heart failure and cardiac arrest [48]. Long-term exposure to particulate air pollution at concentrations below the European annual mean limit was even associated with natural-cause mortality in Europe [50].

Exposure to gaseous pollutants also contributes heavily to adverse health consequences. Ozone affects lung function and can create inflammatory conditions in the respiratory tract, and it can have a more dramatic effect on asthmatic subjects [51, 52]. Research has provided valuable insights into the relationship between exposure to  $\text{SO}_2$ ,  $\text{NO}_2$  and CO and health effects including respiratory and cardiovascular hospital admission, myocardial infarction and cardiopulmonary mortality [53, 54].

#### *Effects on the environment*

Air pollution is also harmful to the environment and the climate. Even though there are diverse data that show how the climate has always been changing due to natural factors, anthropogenic activities have contributed to changes in the composition of the atmosphere, and research has been working to understand the impact of such changes on the climate [55]. Together with other gas molecules such as methane ( $\text{CH}_4$ ),  $\text{CO}_2$

and ozone are greenhouse gases that influence the global climate [44]. The continuing increasing concentration of these gases in the atmosphere traps radiation (radiant forcing) and therefore prevents energy from escaping to space, which may increase the surface temperature and contribute to global warming [55].

Particle pollution has both a direct and an indirect impact on the environment. Particles cause the direct effect by scattering and absorbing radiation in the atmosphere, increasing the Earth's albedo and cooling the surface [29]. The indirect effect is related to the increased number of cloud condensation nuclei from aerosol particles, which increases clouds' lifetime and Earth's albedo [55]. One effect of  $\text{SO}_2$ , together with  $\text{NO}_2$ , is the increased formation of acid rain [44], which leads to the acidification of water and soil [45]. Furthermore, vegetation is more sensitive to  $\text{SO}_2$  concentrations than animals and humans. Near cities and industrial areas, wild and cultivated plants are harmed by  $\text{SO}_2$  levels, which can reduce the plants' yield [42].

### *Air quality standard*

The World Health Organisation (WHO) has recognised the harmful impact of air pollution on health and the environment and has published air quality guidelines for particles, ozone, nitrogen dioxide, sulphur dioxide and carbon monoxide to offer guidance in reducing the health impacts of air pollution [8].

The European Union has also elaborated its air quality directives (2008/50/EC Directive on Ambient Air Quality for Europe and 2004/107/EC Directive on heavy metals and polycyclic aromatic hydrocarbons in ambient air), which set thresholds for a set of pollutants that should not be exceeded in a specific period [6, 56]. If the limits are exceeded, State Members' authorities are required to develop and implement air quality plans to manage the exceedances.

The WHO guidelines and EU standards are visible in Table 2.2. The assigned periods differ based on the scientific evidence of the health consequences associated over different exposure times for each pollutant. The WHO guidelines based on the protection of health are generally stricter than the EU standards, which were agreed upon politically [56].

## **2.2 Indoor air quality**

Most individuals are aware of the importance of outdoor air quality and the risks that outdoor air pollution can pose for human health and the environment. In contrast, many do not understand the extent to which indoor air pollution can harm them [57].

**Table 2.2:** Current WHO air quality guidelines and EU air quality standards [6, 8].

Pollutant	Averaging period	Legal nature of EU standard*	EU standard concentration	WHO guideline concentration
PM <sub>10</sub>	Annual	Limit value	40 $\mu\text{g m}^{-3}$	15 $\mu\text{g m}^{-3}$
	24-hour	Limit value	50 $\mu\text{g m}^{-3}$	45 $\mu\text{g m}^{-3}$
PM <sub>2.5</sub>	Annual	Limit value	25 $\mu\text{g m}^{-3}$	5 $\mu\text{g m}^{-3}$
	24-hour	-	-	15 $\mu\text{g m}^{-3}$
O <sub>3</sub>	8-hour	Target value	120 $\mu\text{g m}^{-3}$	100 $\mu\text{g m}^{-3}$
NO <sub>2</sub>	Annual	Limit value	40 $\mu\text{g m}^{-3}$	10 $\mu\text{g m}^{-3}$
	Hourly	Limit value	200 $\mu\text{g m}^{-3}$	-
SO <sub>2</sub>	24-hour	-	-	25 $\mu\text{g m}^{-3}$
	24-hour	Limit value	125 $\mu\text{g m}^{-3}$	40 $\mu\text{g m}^{-3}$
CO	Hourly	Limit value	350 $\mu\text{g m}^{-3}$	-
	24-hour	-	-	4 $\mu\text{g m}^{-3}$

\*Under EU law, a limit value is legally binding, while a target value represents an obligation to take necessary measures (without disproportionate costs) to ensure that it is respected; therefore, it is less strict than a limit value [6].

According to the US Environmental Protection Agency, indoor pollutant levels are generally 2–5 times higher than the outdoors, indicating the magnitude of the indoor air problem [58]. Furthermore, most of modern society’s activities are held inside buildings, causing the population to spend most of its time indoors [59]. It is therefore important to understand the factors that affect indoor air pollution, the source of emissions and the consequences of exposure.

The concentration of indoor pollutants may vary due to several factors, such as human activities, outdoor air quality, building and construction materials and equipment and furniture [60, 61]. Indoor pollutants originate from various sources:

- **Cooking:** this activity has been identified in several studies as the main source of indoor pollution [62, 63]. Kong et al. evaluated the particle concentration generated while cooking in the kitchen of a residential home under 12 different ventilation conditions [64]. The study showed that a combination of ventilation devices and natural ventilation is the only effective solution to reduce particle concentration, which otherwise would reach harmful values [64].
- **Tobacco smoke:** cigarette burning is responsible for the release of more than 4,000 chemical compounds that are toxic and carcinogenic [65, 66] and are generated with a high rate of emission [67]. It is one of the largest sources of indoor particles. Second- and thirdhand smoke also represent an issue for indoor air quality and

health [68, 69]. Afshari et al. showed that up to 9% of the ultrafine particles generated by tobacco smoking in an apartment infiltrated the neighbouring flat [68].

- **Heating:** wood-burning stoves and fireplaces have again gained popularity in residential houses in recent years, both because of the warm ambience they create and the lower cost they offer compared to other forms of heating [70]. Salthammer et al. investigated the emissions from seven wood-burning ovens [70]. Ultrafine particles and benzene concentrations increased during operation above average values for non-smoker households, while the effects on CO, CO<sub>2</sub>, NO, NO<sub>2</sub>, TVOCs, formaldehyde and acetaldehyde were small [70]. In modern airtight appliances, the periodic removal of residual ash from the fireplace is responsible for the release of particles that can affect the average concentration during 48-h sampling [71]. In the study of Afshari et al., an electric radiator was investigated and showed a consistent emission of ultrafine particles. However, the radiator is not a primary particle source; the emission is due to the dust deposited on the surface of the heater [67].
- **Cleaning activities:** these activities are responsible for the resuspension and redistribution of deposited particles on indoor surfaces and the generation of gaseous pollutants emitted from various cleaning products. Sweeping and vacuuming affect the resuspension of particles in the coarse fraction. Corsi et al. observed an increase of particles above 10  $\mu\text{m}$  diameter of  $>17 \mu\text{g m}^{-3}$  and a resuspension of particles above 2.5  $\mu\text{m}$  diameter of  $1.1 \mu\text{g m}^{-3}$  during carpet vacuuming in residential apartments [72]. Vicente et al. compared different vacuum cleaner devices and concluded that the bagged vacuum cleaner presents the highest particle emission rate [73]. Emissions from cleaning products (which include terpenes, chlorine and aldehydes that compose the products) can react with ozone and become sources of new VOCs such as formaldehyde and secondary indoor organic aerosol [74, 75], which have an adverse impact on IAQ. In this regard, Stabile et al. have also demonstrated that ozone-initiated reactions can lead to the emission of ultrafine particles [76].
- **Human occupancy:** the human body emits various compounds, even when not performing any specific activity. Human skin surface lipids can react with ozone and increase the indoor concentration of compounds that contain carbonyl, carboxyl or  $\alpha$ -hydroxyl ketone groups [77]. Moreover, particle resuspension is affected by occupants simply walking into and out of a room; this can increase the mass of suspended coarse particles up to 100% [78].

- **Building and furniture materials:** VOCs' indoor concentration is influenced by the materials used for buildings, furniture and other indoor products. Formaldehyde is the most common pollutant released from pressed-wood products used in construction (hardwood, plywood and panelling) [79, 80]. New materials produce higher emissions, which decrease with time; ozone reacts with the material surface layer and, in time, the ozone uptake decreases together with the secondary pollutants' emissions [81].
- **Office equipment:** computers, photocopiers and printers are sources of pollution including particles, VOCs and ozone, which (as already mentioned) can initiate reactions that lead to the formation of secondary pollutants [82]. These devices have the highest impact in offices and schools, where more units are installed. Nevertheless, they can still affect residential building IAQ, as they represent a long-term source of pollution [82].
- **Outdoor air pollution:** the pathways for outdoor air to enter buildings are several and include natural ventilation through windows, the air entering through mechanical ventilation and infiltration through the building envelope. This topic is investigated further in the next section.

Indoor air pollutants can also be re-emitted in the indoor air through the phenomena called the *sink effect*. The sink effect consists of the sorption and desorption of indoor air pollutants, including many VOCs, on the surfaces of furnishing and building materials, including floors and rugs, walls, ceilings and HVAC systems [83]. The consequence of this phenomenon is a higher concentration of VOCs in the indoor air. Such an effect can last for a long period – in some cases, for the building's entire life [83]. Several models have been developed to predict the sink effect and the overall indoor air quality in buildings in relation to this phenomenon [84–87].

### 2.2.1 The relationship between outdoor contaminants and indoor air quality

Understanding the relationship between outdoor and indoor pollutants helps to prevent harmful concentrations indoors. Three mechanisms result in outdoor air entering and affecting the indoor environment: mechanical ventilation, natural ventilation and infiltration. Figure 2.2 schematically represents the pathways of outdoor air inside buildings through these mechanisms. Mechanical ventilation supplies outdoor air, which carries outdoor-originated pollution. While air filters are usually installed in mechanical

ventilation systems, in most cases they cannot clean the air completely from various pollutants, allowing some pollutants to enter indoors. Wind and buoyancy flow are the main drivers that bring outdoor air into buildings through windows and doors, also called natural ventilation. When these types of ventilation are not present, air exchange still occurs through the uncontrolled flow of air through the building envelope due to leaks and cracks, referred to as infiltration [58]. Once outdoor pollution enters the indoor environment, it can be diluted or accumulated depending on the ventilation conditions [88].

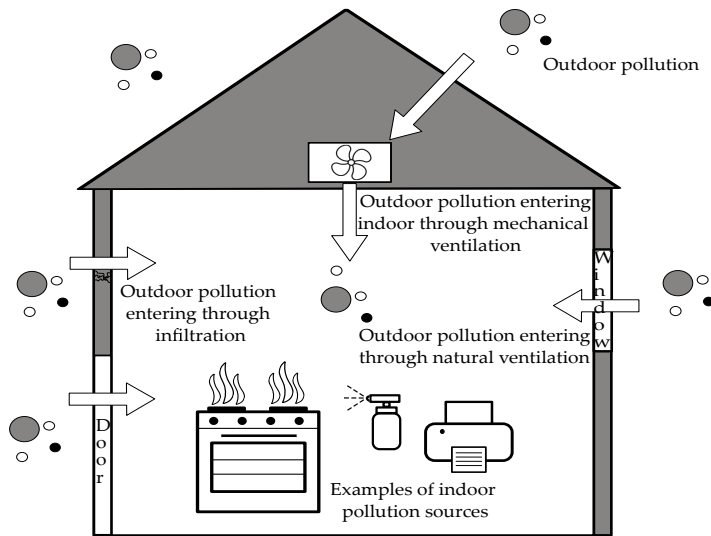


**Fig. 2.2:** Pathways and sources of indoor air pollution.

Several factors affect the relationship between outdoor and indoor pollutants, including the building ventilation rate and airtightness as well as building location, season and weather [89]. Matson detected higher ultrafine particle concentrations both outdoors and indoors in urban areas compared to rural areas [15]. Within a city, the closer a building is located to a busy roadway, the higher the detected indoor particle concentration [90]. Some meteorological parameters influence indoor particle concentration, including wind direction and speed, relative humidity and temperature, which are also season-dependent [91, 92]. Nonetheless, outdoor air pollution is considered the dominant source of indoor particles [17].

The I/O ratio is defined as the ratio between indoor and outdoor pollutants concentrations, which is widely used as it is easily understood [58]. I/O ratio is adopted



to define the I/O relationship of particles [58], but it can be used also to evaluate the relationship between other pollutants' indoor and outdoor concentration, like  $\text{NO}_x$  and  $\text{O}_3$  [93]. Blondeau et al. have found that  $\text{NO}$  and  $\text{NO}_2$  I/O ratios vary from 0.5 to 1 and from 0.88 to 1 respectively, whereas ozone I/O ratio ranged between 0 and 0.45 and showed to be highly dependent on the building air-tightness [93]. In regards to particle pollution, there is a wide range of studies that have investigated the I/O ratio under various measurement conditions and evaluating different particles sizes [15, 94–96]. Chen and Zhao have reviewed the studies on I/O ratio reported in the literature [58]. They found values that ranged between far below 1 to far above 1 and concluded that this parameter is affected by many factors related to indoor particle sources and measurement conditions, which results in a wide range of values without a uniform conclusion. An alternative is to use the infiltration and penetration factors. The first metric is useful for qualifying how many indoor particles come from outdoors, while the second is the most efficient parameter for understanding the penetration mechanisms of particles through building cracks [58].

### 2.2.2 Indoor air pollutants and their impacts

Indoor sources of air pollution emit various air pollutants of different natures. These pollutants include  $\text{NO}_x$ ,  $\text{SO}_2$ ,  $\text{O}_3$ ,  $\text{CO}$ , VOCs, radon and micro-organisms, and they can be categorised as organic, inorganic, biological and radioactive pollutants [88]. Table 2.3 lists the most common indoor air pollutants and their sources, as well as the main impacts they have on human health and the environment.

Indoor pollutants are a topic of increased interest due to their crucial consequences for human health. Many studies are available in the literature that describe the sources, concentrations and consequent health effects of such pollutants [89, 97, 98]. Most indoor pollutants have a direct impact on the respiratory and cardiovascular systems; the severity of this effect varies depending on the duration and intensity of the exposure and on the precedent health condition of the exposed population [88, 99]. Furthermore, developing countries are exposed to higher health risks because they rely on inefficient and highly polluting solid fuels for basic necessities (e.g. the use of open fires for heating and cooking in households) [100]. Besides its health effects, indoor air quality can also affect the productivity of workers in office buildings [101].

Among the pollutants addressed in Table 2.3, ozone plays a special role in indoor chemistry. Indoor reactions involving ozone have been thoroughly investigated in the literature, including gas-phase and surface reactions [102]. Ozone is a strong oxidising

agent that can react with several VOCs that are present indoors and form products that are even more irritating and harmful than their precursors. For example, limonene, a terpene that is a common fragrance component of products such as air fresheners and floor cleaners, reacts with ozone to produce a mixture of products including formaldehydes, sub-micron particles, carbonyls and acids [74, 103].

### 2.2.3 Improving indoor air quality

As the evidence of the critical consequences that a poor IAQ can have on humans and the environment increases, it is important to seek effective solutions to limit emissions and decrease human exposure to the pollutants. There are three applicable methods for improving IAQ: pollution source control, air dilution through ventilation using outdoor air supply and pollutant removal through filtration and air cleaning.

While pollution source control should be the first method to be applied, it is not always practical or possible. Secondly, outdoor air should be supplied in order to dilute and refresh the indoor air. However, when the outdoor air is not clean, this solution exacerbates the issue by worsening the IAQ. Therefore, the third method must be employed. Air filters can be installed as part of the ventilation system or used in the form of a portable air cleaner. When integrated into the HVAC system, the air filter can be used to clean the supplied outdoor air in order to combine the second and third methods. Various air filter technologies are available on the market. Their characteristics, advantages and limitations will be thoroughly addressed in the next chapter.

**Table 2.3:** Sources and impacts of indoor air pollutants [88, 98, 99, 104–106].

Indoor air pollutant	Main sources	Impacts
Particle pollution	Outdoor air, cooking, combustion processes (smoking, fireplaces, candle burning), cleaning activities, product of indoor chemistry (secondary pollutant).	Lung and airway inflammation, causing or aggravating respiratory and cardiovascular diseases (aggravated asthma, decreased lung function, non-fatal heart attack).
O <sub>3</sub>	Outdoor air, air cleaning devices involving high voltage, office equipment.	Triggers allergies and asthma, causes lung damage. Irritation of eyes and nose. Main driver of indoor chemical reactions. Also damages indoor materials.
SO <sub>2</sub>	Outdoor air, cooking stoves, fireplaces.	Irritates eyes, nose, throat and respiratory tract. Increases bronchial reactivity. Asthma and cardiovascular diseases.
NO <sub>2</sub>	Outdoor air, gas-fuelled cooking and heating appliances, fireplaces	Irritates eyes, nose, throat and respiratory tract. Increases susceptibility to infections and bronchial reactivity.
CO	Outdoor air, cooking, combustion processes involving gas appliances, smoking, fireplaces, gasoline powered equipment.	Interferes with transport of oxygen, which causes headache, nausea, dizziness and fatigue, and with high exposure leads to coma and death (700 ppm).
VOCs (including formaldehydes, toluene and turpenes)	Paint, solvents, varnishes, adhesives, waxes, pesticides, air fresheners, incense, building materials and furnishing including plywood and carpets, wood preservatives, printers and photocopiers, perfumes, building occupants and activities	Irritant effects to mucous membranes, fatigue and difficulties in concentrating, carcinogenic. Respiratory irritation. Cause of rhinitis, pruritus, headache, nausea, dizziness, muscular weakness.
Radon	Outdoor air, building materials, soil gas and tap water.	Lung cancer.
Biological pollutants	Pets and humans, house dust, mites, mould, pollen, bacteria, fungus.	Can cause allergic reactions, from rhinitis to asthma. Respiratory infections, digestive problems and chronic respiratory illness.



## Chapter 3

# Air filtration technologies

### 3.1 An introduction to filtration

The general term *filtration* refers to the process of separating one or more phases by using their physical differences, such as particle size or electric charge [107]. This definition covers a wide spectrum of processes involving the separation of completely mixed phases, such as vapourisation and sorption (e.g. distillation, adsorption and diffusion) or distinct phases, such as solids from fluid and liquids from gas (e.g. filtration, sedimentation and electrostatic precipitation) [107].

Filtration involves the passage of a fluid through or across a barrier, called the *filter medium* or *filter*, which is permeable to some components that are suspended or mixed into the fluid [108]. The *filter medium* is the material that enables filtration, while the *filter* includes the device that holds the filter medium. Most filters impose a resistance on the fluid, which passes through them. Fan power is required to overcome the pressure drop caused by the filter, which determines the energy use of operating the filter.

Filtration is achieved by mechanical or physical means. However, some filtration processes involve electrical and mechanical forces, as others include chemical and physical forces [108]. Different mechanisms act on specific contaminants, which may vary in physical nature, size and concentration. Consequently, various treatment methods are used in connection with different filtration or purification technologies to filtrate particles or remove gaseous compounds from a fluid.

Filtration is a widely used process in several commercial, domestic and industrial human activities. Its applications include wastewater treatment plants, mineral processing,

activities involving machinery fluids (e.g. those used in engines and hydraulic systems) and air filtration and purification in ventilation systems for residential and commercial buildings. Filters can be classified based on the filter media, their function, the nature of the filtered fluid or the mechanism of filtration [108]. Table 3.1 describes various filter media in relation to their usual applications.

### 3.1.1 Fundamentals of filtration mechanisms

Although numerous filters exist and they employ diverse mechanisms to hold back the suspended material from the flow, four basic mechanisms can be defined. Figure 3.1 provides a graphic representation of these mechanisms.

- a. Surface straining* (Figure 3.1a) is the mechanism typical of filters that are thin compared to the smallest particle to be removed, so all filtration happens on the surface upstream of the filter medium. It is based completely on the ratio between the particle size and the pore size of the filter. Particles that are larger than the pores of the filter medium will be deposited on the surface, while any particle smaller than the pore diameter will pass through the pore. Some of the larger particles will block some pores until filtration is stopped and the filter is cleaned by brushing or scraping; this occurs when the flow through the filter falls below an acceptable level. This is the main mechanism for screening through perforated plates, plain woven mesh and metal edges and cartridges. It plays a major role in membrane filtration [107, 109].
- b. Depth straining* (Figure 3.1b) applies to most real filter media, which are thicker than their pore diameters. Furthermore, the pore sizes vary along the thickness of the filter. In this case, a particle travels along the pore until it reaches a point where it is stopped because the pore is too small. The pore is then blocked, and the particle is trapped only because of its size. The filter must be replaced or cleaned through reverse flow blowing when it becomes too clogged. This mechanism is typical of felts and non-woven fabrics [107, 109].
- c. Depth filtration* (Figure 3.1c) is a very similar mechanism to depth straining; most of the time they are grouped under the same name of depth filtration. Depth filtration involves several physical mechanisms, such as direct or inertial interception, diffusion and Brownian motion, that allow a particle to be trapped even if it is smaller than the pores at that depth. Particles can also trap one another through Van der Waals or other surface forces, but the pores do not

**Table 3.1:** Various filter media types and their applications [107].

Group	Filter media	Characteristics	Application
Paper and fabrics	Paper media, woven fabric, non-woven fabric, bonded porous media	Based on fibres of various kinds, short or long, spun into a yarn or collected to create random mass.	Broad application, including water and air filtration, food industry, pharmaceutical application, industrial processes.
Sorbent media	Adsorbent media, absorbent media	Adsorbent materials can be added onto a fibre filter or used as a packed bed or columns and act as a mechanical depth filter.	Air and water purification, removal of odours in domestic application or to industrial fume removal, respirators and gas mask.
Woven wires and screens	Woven wires mesh, perforated plate, bar and wires structure	Mostly made of metal. High strength, corrosion and abrasion resistance. Made with apertures of precise sizes.	Separation of solid particles by size, coarse screening of gas and liquid flows of some finer processing stage, sieving and sifting.
Constructed filter cartridges	Edge filters, yarn-wound cartridges	Filter media that, when appropriately assembled in a cartridge, can work as a filter, but they have no filtration capability in themselves. Surface filtration.	Mostly used for clarification: extraction of contamination from a fluid.
Membranes	Different types: porous, non-porous, polymeric or inorganic (ceramics)	Chemically resistant to feed and cleaning fluids, thermally and mechanically stable, high permeability, highly selective, stable in prolonged operations.	Industrial sector: petrochemical, pharmaceutical, chemical, food and beverages process, electronics, biotechnology and water treatment.
Packed beds	Deep-bed media, pre-coat filtration	Unconstrained materials: masses of particulate substances that remove contaminants by depth filtration. Media must be inert, resistant to fracture.	Used in clarification process, especially in water purification.

become absolutely blocked because the fluid can flow between the particles. A fully blocked filter medium must be replaced or cleaned by reverse flow. This mechanism is common for most filter media, in particular in high-efficiency air filters and deep-bed filters [107, 109].

*d. Cake filtration* (Figure 3.1d) defines the mechanism that occurs when a thick layer of particles accumulates on the filter medium and acts as a filter itself, with actual depth filtration within the thickness of the cake and surface straining on its upstream surface. This mechanism occurs at high solid concentrations in the suspension when small particles bridge together across the opening of a pore and form the base of the cake. Cake filtration is employed in some clarification processes [107, 109].

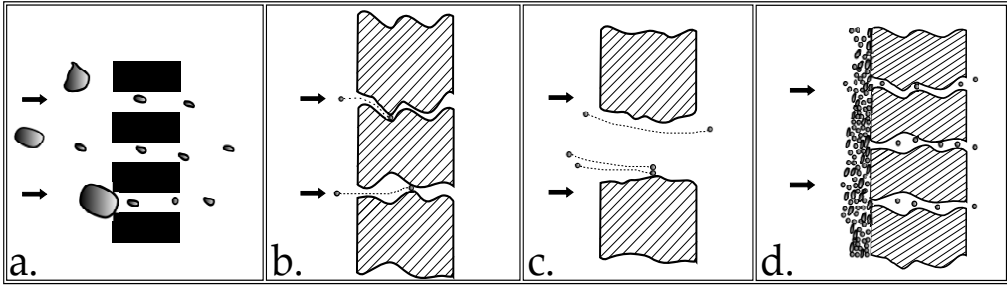


**Fig. 3.1:** Filtration mechanisms: (a.) surface straining, (b.) depth straining, (c.) depth filtration and (d.) cake filtration (adapted from [109]).

In reality, filtration happens mostly as a combination of these mechanisms. These combinations occur depending on the characteristics of the filter medium and the suspension that is being filtered [109].

Another important aspect of the filtration process is the separation between steady stage and non-steady stage [110].

The first stage of the filtration process is called the steady stage because particle efficiency and the pressure drop of the filter do not change over time. The only parameters that influence this part of the process are the intrinsic characteristics of the filter, its geometry and the properties of the air flow and the particles. In air filtration related to buildings, where particle concentration is relatively low, this stage of filtration is important [110]. The surface straining and depth filtration mechanisms are typical of this stage before clogging starts.

The non-steady stage is characterised by a change in particle filtration efficiency and pressure drop over time. During this stage, the filter performance also depends on particle deposition, water vapour, gas erosion, etc. This stage has decisive significance for filters employed in industrial processes [110]. The thickness of the filter varies significantly during the non-steady stage, as the cake filtration mechanism enters into force.



## 3.2 Air filtration in HVAC systems

### 3.2.1 Ventilation strategies

Designing a ventilation system for a specific building is a rather complex process that depends on various building characteristics, including building type and related needs, dimensions, available space and location and climate. Ventilation systems can be divided into three major groups: natural, mechanical and hybrid systems.

#### *Natural ventilation*

Natural ventilation is characterised by air flows through the building that are driven by natural forces such as buoyancy, pressure and the stack effect [111, 112]. In natural ventilation, air moves through ventilation openings such as doors, windows and leakages in the envelope, which makes it the least controllable ventilation type. Ventilation openings can be installed in order to improve control of the ventilation rate [112]. Different natural ventilation strategies are selected based on several factors, such as the ceiling height, the depth of space within ventilation openings, the heat gain and the climate. The most frequently used techniques are single-sided ventilation, cross-ventilation and stack ventilation [111], the basic principles of which are represented in Figure 3.2. The most obvious benefits of naturally ventilated buildings are their lower energy use and environmental impact compared to buildings with mechanical ventilation [113]. Most European residential buildings were ventilated by natural ventilation until recent decades, which means that many existing residential buildings are based on natural ventilation. Implementing mechanical ventilation with heat recovery in new and in energy-retrofitted residential buildings is a requirement in Northern Europe (with few exceptions) [28, 114, 115]. Increasing buildings' airtightness in the attempt to reduce heat loss is one reason for the implementation of mechanical ventilation, as well as the fact that natural ventilation might be unable to provide the required air change rate [111, 116].

#### *Mechanical ventilation*

Mechanical ventilation systems can provide a steady air change rate with a high level of control, which allows them to respond to varying demand based on occupants or pollutant levels [111]. Another benefit of mechanical ventilation is the possibility of integrating heating and cooling, and heat recovery in the air exhaust as a mean of

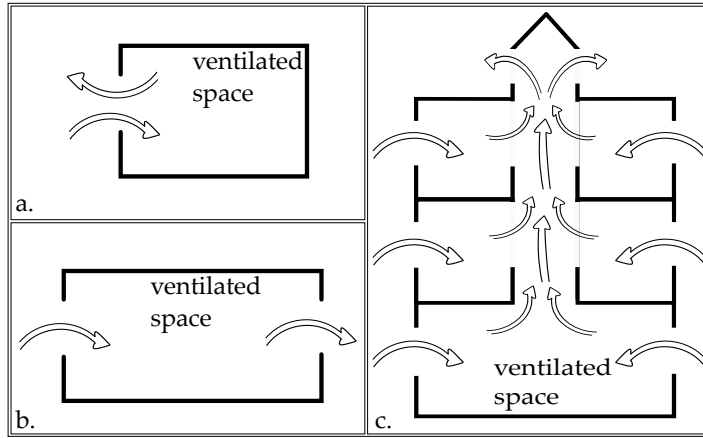


**Fig. 3.2:** Natural ventilation techniques: (a.) single-sided ventilation, (b.) cross-flow ventilation, (c.) stack-ventilation (adapted from [117]).

reducing ventilation energy use. Heat recovery is essential in fully outdoor air supply systems [111]. The main typical mechanical ventilation designs that can be installed in buildings are exhaust mechanical ventilation, supply mechanical ventilation and balanced mechanical ventilation [112] (Figure 3.3).

An exhaust ventilation system uses a fan to remove air from the ventilated space [118]. The optimal operational efficiency of such systems is reached by keeping the internal pressure lower than the external one, so that the air flow is controlled by the mechanical system [116]. In this way, the extracted air is replaced by outdoor air. However, in buildings that are highly airtight or lack sufficient air openings, pressure differences can rise and consequently increase energy use, while the system might not be able to deliver the desired air flow rate [116]. Furthermore, the outdoor air supply cannot be conditioned (and is generally not filtered) before coming indoors.

Supply mechanical ventilation is based on mechanically introducing filtrated and conditioned air into the building. As this system avoids the ingress of infiltrated air, all the supplied air is pre-cleaned and thermally conditioned [116]. It also introduces a slight overpressure, so the indoor air leaves by exfiltration through leakage or installed air outlets [118]. This ventilation type is not recommended in residential buildings, especially in cold climates, as there is a risk of indoor generated moisture penetrating the building material where condensation can occur [116].

Balanced ventilation combines the supply and extract systems in a separated ducted

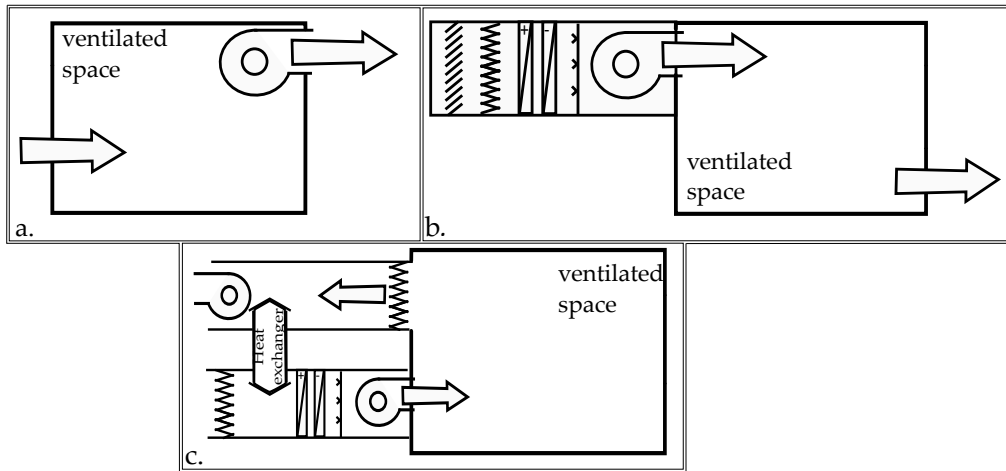


**Fig. 3.3:** Principles of mechanical ventilation systems: (a.) mechanical extract ventilation, (b.) mechanical supply ventilation, (c.) balanced mechanical ventilation (adapted from [112]).

network. These systems usually incorporate heat recovery to pre-heat the incoming air ‘for free’ [116]. For optimal performance, balance systems must be highly airtight. This is because balanced mechanical ventilation systems do not significantly influence the indoor pressure in relation to the outdoors, so infiltration driven by wind or temperature differences can occur [116].

Mechanical ventilation systems use more energy and incur higher costs for maintenance and component replacement compared to naturally ventilated buildings [116]. These aspects must be taken into account when considering mechanical ventilation, especially because the inadequate maintenance of ventilation systems can severely compromise indoor environmental quality.

### *Hybrid ventilation*

Hybrid ventilation systems consist of ventilation processes based on a combination of natural and mechanical driving forces. These systems can be based on two modes that operate separately depending on the season or within individual days [113]. Some hybrid systems are mixed- or single-mode and run using wind and/or thermal stacks with an assisted fan [119]. There are three main hybrid ventilation principles upon which these systems are based: natural and mechanical ventilation, fan-assisted natural ventilation and stack- and wind-assisted mechanical ventilation [117]. The first type is based on an

intelligent control strategy that switches between two autonomous systems based on the task to be performed, mostly related to occupancy levels and seasonality. Fan-assisted natural ventilation relies on an extract or supply (low pressure) fan that runs when demand increases or natural driving forces are weak. The last principle is based on mechanical ventilation that optimally exploits natural driving forces. These systems are usually based on very small pressure losses that can be partly covered by natural driving forces [117]. As for natural ventilation, hybrid systems are well accepted by occupants because they offer a high degree of control of the indoor climate and visible and direct responses to user decisions [113]. Moreover, they fulfil the requirements of indoor environmental performance without compromising on energy savings and sustainable development [117].

#### *Air filters in ventilation systems*

At first, air filters within HVAC systems were intended to protect the ventilation system components; keeping coils, fans and ducts clean would avoid malfunctions and pressure drop increases. However, scientific research has highlighted the impacts of air quality on human health and the environment and raised awareness about the importance of indoor air quality. In this context, the primary purpose of air filters within HVAC systems has been recognised as the reduction of air pollutants in the indoor environment [120]. It is estimated that 50% of outdoor airborne pollutants are carried into buildings, and supplied air pollution is the main factor of exposure to air pollutants and the primary link to health risks [120]. Air filtration can reduce the indoor air pollutant concentration, removing pollutants either with air cleaning devices or by reducing the outdoor-to-indoor transport of pollutants, thus improving the health and productivity of the building occupants [120].

Regardless of the ventilation system adopted in a building, the requirement of a fresh outdoor air supply must be met. One of the main differences between natural and mechanical ventilation systems lies in the use of fans to distribute the air, and consequently in the pressure drop that each system type can handle. Natural ventilation systems are usually not equipped with air filters because, even given properly designed air ventilation openings, conventional air filters may impose a pressure drop that is too high for the air to penetrate the building. This fact has served as the starting point of this research project, which aimed to fabricate a single thin-layer filter that would impose a negligible resistance to air. Such a filter could be employed in low-energy ventilation systems such as in natural ventilation or fan-assisted natural ventilation systems.

### 3.2.2 Air filter performance

The performance of air filters is based on two main characteristics: the filtration efficiency towards air pollutants and the pressure drop. These parameters depend on the filter structure (in the case of fibre filters, the packing density and fibre radius), the characteristics of the filtered pollutant (concentration, solid or gaseous state, particle size or molecule type) and operating conditions, such as temperature and face velocity [121]. Other parameters to consider while evaluating a filter's long-term performance are regeneration capacity and the lifetime of the filter medium.

When evaluating the filter performance, the face velocity at which the investigation is carried out must be addressed. Indeed, there is a direct relationship between face velocity and both pressure drop and filtration efficiency. Furthermore, different ventilation systems are characterised by different ranges of face velocity. In mechanical ventilation, the air velocity in the ducts can reach  $1.5\text{--}2\text{ m s}^{-1}$ , whereas natural ventilation is characterised by face velocities through the ventilation openings starting from  $0.05\text{ m s}^{-1}$  to  $0.5\text{ m s}^{-1}$ . The face velocity ( $\text{m s}^{-1}$ ) is defined as the airflow velocity through the cross-section of the filter:

$$V_f = \frac{Q}{A \cdot 3,600} \quad (3.1)$$

where  $Q$  is the flow rate in  $\text{m}^3\text{ h}^{-1}$  and  $A$  is the cross-sectional area of the air filter in  $\text{m}^2$  [110].

#### *Filtration efficiency*

Filtration efficiency defines the filtration efficiency/removal capacity of the filter media. The term *filtration efficiency* is mostly used in relation to particle filtration, while *removal capacity* is preferred in connection to the removal of gaseous compounds. In experimental studies in which a particle counter or a gas analyser is used to assess the concentration of pollutants before and after the filter, the filtration efficiency or removal capacity  $\eta$  (%) is calculated with the following equation:

$$\eta = \frac{C_{up} - C_{down}}{C_{up}} \cdot 100 \quad (3.2)$$

where  $C_{up}$  and  $C_{down}$  are the concentrations of the pollutant upstream and downstream of the filter, respectively. The concentration can be defined in particle mass in  $\text{mg m}^{-3}$  or particle number, whereas the unit can be either ppb or ppm in the case of a gaseous pollutant. The particle filtration efficiency can be calculated as the overall efficiency or

in relation to specific particle sizes.

The particle filtration efficiency  $\eta$  for fibrous filters is the result of the combination of the filtration mechanisms operating within a filter: interception, inertial impaction, Brownian diffusion and electrostatic effects (Figure 3.4).

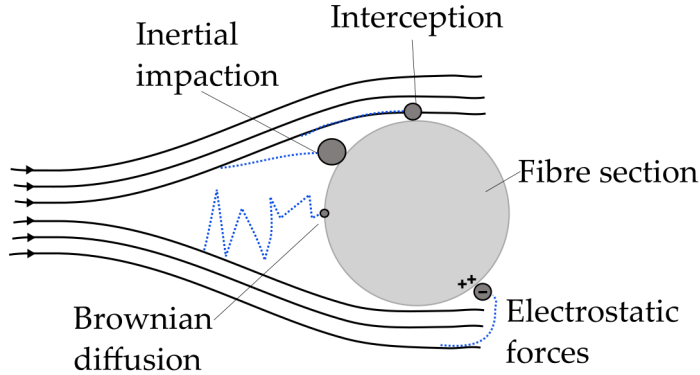


**Fig. 3.4:** Illustration of the different filtration mechanisms involved in mechanical filtration (adapted from [120]).

All four mechanisms are influenced by particle size. Interception occurs when a particle that follows the air stream collides with a fibre of the filter because of its size [122]. Inertial impaction describes a particle that cannot follow the streamline around a fibre. The particle deviates from the air stream due to particle inertia, colliding with the fibre. An increased air velocity and particle size would increase the inertial force [120]. Brownian diffusion influences the movements of particles smaller than  $1\ \mu\text{m}$ . Such particles deviate randomly from the air stream due to the Brownian movement of air molecules and strike the fibres, becoming attached to them [120]. This mechanism is dominant for ultrafine particles ( $<0.1\ \mu\text{m}$ ). In fibrous filters, electrostatic attraction can occur and plays a minor role. Small particles can be retained by the fibre due to weak electrostatic forces present on the fibres [122]. Generally, capture by interception and impaction is dominant for larger particles, while diffusion is dominant for smaller particles.

The particle filtration efficiency of a clean fibrous filter can be assessed also with theoretical modelling of the filter. The overall efficiency of a fibrous filter is related to the penetration  $P$  by the equation  $P = 1 - \eta$  ( $\eta$  is here considered a dimensionless number between 0 and 1).  $P$ , defined as the ratio between the aerosol concentration downstream of the filter to the upstream concentration, can be expressed as follows [123]:

$$P = \exp\left(-\frac{4\eta_f\alpha Z}{\pi(1-\alpha)d_f}\right) \quad (3.3)$$

and consequently,

$$\eta = 1 - \exp\left(-\frac{4\eta_f\alpha Z}{\pi(1-\alpha)d_f}\right) \quad (3.4)$$

where  $\alpha$  is the filter packing density,  $d_f$  is the fibre diameter,  $Z$  is the thickness of the filter and  $\eta_f$  is the particle filtration efficiency of a single fibre [123]. The filter packing density  $\alpha$  is the ratio between the volume of fibres and the total volume of the filter and it is related to the porosity  $\varepsilon$  by  $\alpha = 1 - \varepsilon$  [124, 125]. This correlation assumes that the filter can be approximated by an array of parallel cylinders [126]. The overall filtration efficiency of a fibrous filter medium is therefore determined based on the single-fibre efficiency  $\eta_f$ , which is defined as the sum of the efficiencies of the individual mechanisms just described [123]:

$$\eta_f = \sum_i \eta_{f,i} = \eta_D + \eta_I + \eta_R \quad (3.5)$$

where  $\eta_D$ ,  $\eta_I$  and  $\eta_R$  are the single fibre efficiencies of diffusion, impaction and interception, respectively [123]. In air filtration, equation 3.5 is used assuming that the different mechanisms act independently [123]. Several studies have proposed methods to calculate the single fibre efficiencies of the various mechanisms [126–129]. Lee and Liu have proposed a semi-empirical correlation to calculate  $\eta_D$  and  $\eta_R$  considering the filtration of particles from 0.1 to 0.3  $\mu\text{m}$  (impaction plays a minor role in such conditions) and in a continuous-flow regime characterised by a negligible Knudsen number [128]. The Knudsen number ( $\text{Kn} = 2\lambda/d_f$ ) is negligible when the fibre diameter  $d_f$  is considerably larger than the mean free path of the gas molecules  $\lambda$  ( $\lambda = 65 \text{ nm}$  for air molecules) [130]. When this condition is not met and the diameter of the fibre is of the same magnitude as  $\lambda$ , the slip flow must be considered due to the discontinuity of the fluid around the fibre [129]. Payet et al. have further developed the model from Lee and Liu to include the slip-flow effect in the correlation [129]. The authors reported a high level of agreement between their model and the experimental data collected using particles in the size range

0.08–0.4  $\mu\text{m}$  [129]. This model defines the single fibre efficiencies as follows [129]:

$$\eta_R = 0.6 \left( \frac{1 - \alpha}{Ku} \right) \left( 1 + \frac{Kn}{R} \right) \left( \frac{R^2}{1 + R} \right) \quad (3.6)$$

$$\eta_D = 1.6 \left( \frac{1 - \alpha}{Ku} \right)^{1/3} Pe^{-2/3} C_1 C_2 \quad (3.7)$$

$$C_1 = 1 + 0.388 Kn \left( \frac{(1 - \alpha) Pe}{Ku} \right)^{1/3} \quad (3.8)$$

$$C_2 = \frac{1}{1 + 1.6 \left( \frac{1 - \alpha}{Ku} \right)^{1/3} Pe^{-2/3} C_1} \quad (3.9)$$

$$Ku = -\frac{1}{2} \ln \alpha + \alpha - \frac{1}{4} \alpha^2 - \frac{3}{4} \quad (3.10)$$

$$Pe = \frac{V_f d_f}{D} \quad (3.11)$$

$$R = \frac{D_p}{d_f} \quad (3.12)$$

where  $D_p$  is the particle diameter,  $D$  is the diffusion coefficient,  $R$  is the interception parameter,  $Ku$  is the Kuwabara factor and  $Pe$  is the Peclet number, which represents the effect of Brownian diffusion [129].

The single-fibre efficiency of inertial impaction depends on the Stokes number, which is a dimensionless parameter that describes the behaviour of a particle suspended in a fluid flow [126]. Particles with a high Stokes number will deviate from the streamlines around the fibre due to inertia [121]. If they are captured by the fibre due to such deviation, they are captured because of impaction. One of the empirical correlations reported in the literature defines the single-fibre efficiency of impaction as [126]

$$\eta_I = \frac{St^3}{St^3 + 0.77 St^2 + 0.22} \quad (3.13)$$

$$St = \frac{D_p^2 \rho V_f}{18 \mu_a d_f} \quad (3.14)$$

where  $\rho$  is the particle density and  $\mu$  is the coefficient of viscosity.



### *Pressure drop*

The pressure drop across the filter describes the resistance of the filter to the air flow. The higher the pressure drop, the more fan power is needed for the filter operation within a ventilation system. The optimal filter has a small pressure drop in order to impact the building energy use as little as possible. It is also important to assess the filter pressure drop because ventilation systems will be designed and the fan will be sized depending on the filter pressure drop. An inaccurate assessment of the filter pressure drop could lead to system malfunctions. Another aspect to consider is the change in pressure drop over time due to filter clogging and cake formation during particle filtration. Such phenomena increase the pressure drop, and the filter must be replaced once the pressure drop exceeds a threshold value.

Since the pressure drop across a filter is closely related to the pattern of the flowing air, it can be calculated only when the basic pattern is known. The air flow is affected by four intrinsic properties: inertia, viscosity, elasticity and molecular properties [126]. The velocity of the air and the dimensions of the system determine whether the inertia or viscosity dominates the air flow, which is evaluated by the Reynolds number,  $Re$ :

$$Re = \frac{\rho_a V_f d_f}{\mu_a} \quad (3.15)$$

where  $\rho_a$  is the density of air, approximated to  $1.2 \text{ kg m}^{-3}$  and  $\mu_a$  is the air coefficient of viscosity,  $1.81 \times 10^{-5} \text{ kg (m s)}^{-1}$ . As airflow through a fibrous filter is usually well-approximated by Stokes flow, inertia is completely neglected and  $Re$  is assumed to be zero [126]. In such conditions of stationary flow, the pressure drop across the filter depends on its thickness  $Z$ , the air velocity, the fibre diameter and the coefficient of viscosity, which is the only significant intrinsic parameter [126]. Darcy's law is the most frequently used correlation of filtration theory:

$$\Delta p = \frac{4\mu_a V_f Z}{d_f^2} F(\alpha) \quad (3.16)$$

The fibre-packing density  $\alpha$  is included through a dimensionless function  $F$ , also called the drag force coefficient. Various models in the literature describe such a coefficient [131–133]. The theoretical models of Happel [132] and Kuwabara [131] were not consistent with the experimental data from Davies [133] because they assumed a viscous flow perpendicular to an array of parallel cylinder. In reality, air filters differ from this simplified geometry because they have randomly oriented fibres. The

Davies correlation is the most used because it has been validated with a large body of experimental data. Moreover, it is validated for fibrous filters with  $d_f$  between 1.6 and 80  $\mu\text{m}$  and  $0.006 < \alpha < 0.3$  [133]:

$$F(\alpha) = 16\alpha^{1.5}(1 + 56\alpha^3) \quad (3.17)$$

This correlation is valid when molecular effects in the air flow can be neglected and the air flow can be treated as a continuous fluid. Such conditions stand as long as the  $d_f$  is significantly larger than the mean free path of the air molecules, which is 0.065  $\mu\text{m}$ . When the fibres are in the sub-micrometre size, slip-flow phenomena must be taken into account. In this respect, the Knudsen number (Kn) defines the flow regime that is dominant at specific conditions. There are four flow regime types: continuum flow, slip flow, transition flow and free molecule flow (Figure 3.5). The slip flow should be considered for  $Kn > 0.1$  but it is dominant for  $Kn > 0.25$ , and therefore for fibre diameters below 500 nm [134]. As the aerodynamic slip is significant, the tangential direction of the air velocity at the surface of the fibre is non-zero, and so the drag force on the air decreases significantly [135].

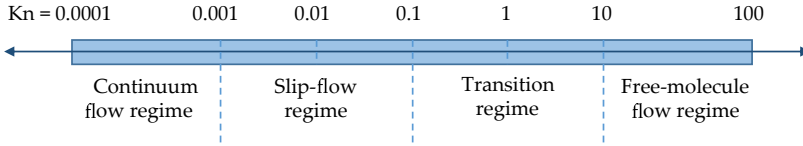


**Fig. 3.5:** Schematic representation of the flow regime in relation to the Knudsen number (adopted from [136]).

The consequence of such phenomena is that the pressure drop through sub-micron fibrous filters is lower than for microfibre filters, and consequently lower than the one calculated from equation 3.16. Kirsch et al. [137, 138] developed a generalised correlation that defines the pressure drop across a nanofibre filter made of cylinder nanofibres with irregular arrangements, in which the drag force coefficient  $F$  is expressed as [139]:

$$\frac{1}{F} = \frac{1}{F_0} + \frac{\tau\phi}{4\pi}(1 - \alpha)Kn \quad (3.18)$$

$$F_0 = \frac{4\pi}{-ln2t + \frac{1}{2} + \frac{t^2}{3}} \quad (3.19)$$

where  $F_0$  is the dimensionless force under hydrodynamic flow conditions ( $Kn = 0$ ),  $\tau$  is a constant coefficient,  $t$  is a dimensionless parameter and  $\phi$  is a function that depends on

the arrangement of the fibres [135, 139]. The theoretical model from Kirsch et al. has been validated recently by Xia et al. [135], who used extensive experimental data from the literature to assess the correlation, demonstrating its validity.

It is important to highlight that all the theories presented depend on parameters that are fixed once the filter is fabricated ( $d_f$ ,  $\alpha$ ,  $Z$ ,  $\phi$ ) except for the face velocity. If the viscosity of air can be considered constant (i.e. if it does not vary significantly with temperature), the pressure drop across the filter is directly proportional to the face velocity of the air flow [135]. This proportion is described by a constant term that has been defined in the literature as the air resistance coefficient,  $\beta$  ( $\text{Pa} \cdot \text{s m}^{-1}$ ) [135]. Therefore, equation 3.16 can be written as

$$\Delta p = \frac{4\mu V_f Z}{d_f^2} F(\alpha) \equiv \beta V_f \quad (3.20)$$

#### *Quality factor*

The quality factor ( $\text{Pa}^{-1}$ ), also known as the figure of merit, is a criterion to evaluate and compare the overall performance of air filters [126]. It is defined as

$$Q_f = \frac{-\ln(1 - \eta)}{\Delta p} \quad (3.21)$$

Therefore, the quality factor represents the ratio between filtration efficiency and pressure drop, which is an indication of a filter's energy expenditure. It is an adequate method to compare the energy efficiency of filter media [121]. As the aim of filter performance is to achieve high filtration efficiency with a low pressure drop, larger values of the quality factor indicate a filter with better quality.

### **3.2.3 Classification of HVAC filters**

Air filters for ventilation purposes are classified according to a European Standard that assesses their technical requirements and specifications. The current standard is ISO 16890, which came into force in mid-2018 and replaced the previous EN 779. The classification method is based on the percentage of dust collected in a filter [140]. The last update classifies the filters on the basis of the particle size classification system recommended by the WHO (in the previous version, the classification was based on filters' filtration efficiency for  $0.4 \mu\text{m}$  particles). ISO 16890 considers the mass concentration of particles with an optical diameter  $>0.3 \mu\text{m}$ , divided in  $\text{PM}_{10}$ ,  $\text{PM}_{2.5}$  and  $\text{PM}_{1.0}$ . The

standard uses the symbol  $ePM_x$  to refer to the filtration efficiency of an air filter for particles with an optical diameter between  $0.3 \mu\text{m}$  and  $x \mu\text{m}$  [140]. In Table 3.2, the minimum initial efficiency values used to classify a filter in one of the four groups and the final maximum pressure drop are reported from ISO 16890. A filter is classified in a given group when the initial efficiency and discharged efficiency are above 50% for the corresponding particle size. When the value drops below the threshold, the filter automatically drops to the inferior group. The efficiencies are reported in steps of 5% [140].

**Table 3.2:** Classification and requirements of air filters (ISO 16890) [140]

Group	$ePM_{1,min}$	$ePM_{2.5,min}$	$ePM_{10}$	Final $\Delta p$
ISO Coarse	-	-	$< 50\%$	200 Pa
ISO $ePM_{10}$	-	-	$\geq 50\%$	300 Pa
ISO $ePM_{2.5}$	-	$\geq 50\%$	-	300 Pa
ISO $ePM_1$	$\geq 50\%$	-	-	300 Pa

### 3.2.4 Air filtration and purification technologies

Today, various air filtration or purification technologies are available. These are based on different mechanisms and therefore can remove different pollutants. The removal of air pollutants with distinct physical states (particles and gaseous pollutants) is usually managed with different technologies because different mechanisms are required to remove such pollutants effectively. The simultaneous removal of such pollutants has usually involved multi-stage or hybrid filtration systems. The main air purification/filtration technologies available are briefly described in the following paragraphs, focusing on the pollutants the technologies can remove and their advantages and limitations.

#### *Mechanical filtration*

Mechanical filtration refers to filters that rely on physical mechanisms to remove suspended particles from the air. Such devices are fibrous filters and are essential components in all air conditioning systems [141]. High-efficiency particulate air (HEPA) filters are a typical example of mechanical filters and can achieve a filtration efficiency of 99.97% of particles above  $0.3 \mu\text{m}$  diameter [142]. Together with HEPA filters, ultra-low penetration air (ULPA) filters are commonly used in cleanrooms, hospitals and laboratories, whereas fine, medium and coarse filters are used mostly in residential and commercial

buildings [143]. While mechanical filters do not retain gaseous compounds, they have removed ozone as reported in a few studies [144, 145].

As described in Chapter 3.2.2, the filtration efficiency of fibrous filters depends on a combination of the mechanisms such as interception, diffusion and impaction. Furthermore, the performance of a mechanical filter changes over time as it gets saturated by particles. The filter can become clogged with a consequent increase of collection efficiency, pressure drop and the required energy use of the fan. When this occurs, the filter must be replaced. Mechanical filters can also become sources of contamination from harmful micro-organisms that can grow on the filter surface [146].

### *Electronic filtration*

There are various types of electronic filters, which are effective in the removal of suspended particles. Electret air filters are polarised fibrous filters made of dielectric materials, which can be produced with different processes such as corona charging, induction charging and triboelectric charging [147]. The quasi-permanent electrical charge on the filter material implies the electrostatic attraction of smaller particles as the dominant filtration mechanism. This means that electret air filters can consist of a lower fibre volume fraction compared to mechanical fibrous filters, achieving less air resistance. However, the electrostatic effect might decrease with operation time, leading to an exponential decrease in filtration efficiency [148].

Electrostatic precipitators (ESPs) are another type of electronic air filtration technology that consists of parallel charged plates. The particles are charged with the opposite polarity of the plates. In the presence of an electric field, the particles are directed and deposited onto the plates once they flow through them [149]. Such filters have a lower overall filtration efficiency compared to HEPA filters or fibre mats [150] but also impose a lower pressure drop [151]. However, ESPs are less effective for sub-micron particles and have been found to generate ozone [152].

Ion generators, or ionisers, remove suspended particles from the air by dispersing charged ions into the air. These ions attach to particles and charge them. Oppositely charged particles can attract each other and form heavier particles, which are easier to deposit. The charged particles may be trapped in the filters or deposit on surfaces such as furniture or walls [141]. Ion generators can generate  $O_3$ , which can react with terpenes and form secondary organic aerosols (SOAs) in the ultrafine range [153].

### Adsorption

The adsorption process is divided into two classes, physical adsorption and chemisorption, depending on the interaction between the adsorbent and the adsorbate. A schematic representation of these two mechanisms is shown in Figure 3.6. Chemisorption indicates a chemical adsorption process driven by a chemical reaction on the surface of the adsorbent [154]; this process is typically non-reversible. Physical adsorption is more significant in the application of separation processes because it involves a low heat of adsorption and the adsorption equilibrium is rapidly established and reversible [155]. In this process, organic molecules are trapped on the surface and in the pores of the adsorbent by the Van der Waals force of attraction [155].

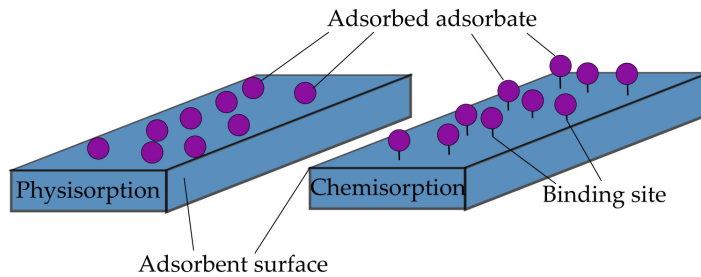


**Fig. 3.6:** Interaction mechanisms between adsorbent and adsorbate during physisorption and chemisorption (adapted from [156]).

Typical adsorbent materials include activated carbon (AC) [157], silica gel, zeolites [158], mineral clay and some polymers [159]. The key for an efficient adsorbent material is a large surface area or a large micropore volume, which is typical of a porous material. AC is one of the most popular adsorbents for VOC removal in indoor air treatment because it has excellent adsorption ability due to its large surface area, cost efficiency and thermo-stability [160].

One drawback of the adsorption technique is related to the influence of relative humidity. Competitive adsorption between water molecules and the target species can occur in humid conditions. As water is rapidly adsorbed within the carbon structure, the volume of porosity that is available for adsorbing the pollutant is reduced [157]. This happens because AC forms hydrogen bonds with water and other polar vapours due to its hydrophilic surfaces, which behave as polar sites [157]. AC is characterised by a vast infrastructure of pores, mostly within the micropore range, which makes it more efficient at lower concentrations and towards VOCs with smaller molecular sizes [146, 160]. The removal of BTEX (benzene, toluene, ethyl benzene and xylenes) at

concentrations between 0.1 and 1 ppm using AC reached 90% efficiency [161]. Activated carbon fibres (ACFs) are a relatively new carbonaceous material that is obtained by the carbonisation and activation of organic fibres at 700–1,000 °C in an atmosphere of carbon dioxide or steam [160]. ACFs have demonstrated a large adsorption capacity towards VOCs [162, 163] and faster adsorption kinetics compared to conventional AC [160]. However, carbonaceous materials cannot adsorb all gaseous compounds because such materials are naturally hydrophobic. Nonpolar and weak molecules like aromatic compounds can be adsorbed on carbonaceous materials, while polar molecules are less likely to be adsorbed [160].

Adsorbent materials saturate over time. Eventually, the adsorbent filter reaches ‘breakthrough’ and the re-emission of pollutants into the air is unavoidable. Some adsorbent materials can be regenerated through the desorption of the pollutants using various methods, such as thermal regeneration, electrothermal heating and vacuum desorption [160]. However, the adsorption capacity is reduced after regeneration [146]. Therefore, these filters must be replaced after a certain period, producing waste that must be properly disposed. Despite the drawbacks of adsorption filters, when compared to other technologies (photocatalytic oxidation, ozonation and cold plasma) for the removal of VOC mixtures, they have been classified as the most effective technology, with removal efficiencies higher than 90% for most pollutants [164]. This guarantees the capture of the most hazardous compounds, such as formaldehyde and acetaldehyde [164].

#### *Photocatalytic oxidation (PCO)*

Photocatalysis is the process that degrades gaseous contaminants in the presence of a catalyst and an irradiation source. The reaction is initiated with the use of a semiconductor material, such as  $\text{TiO}_2$ ,  $\text{ZnO}$ ,  $\text{ZrO}$  or  $\text{SnO}_2$ , which acts as the catalyst of the reaction [165]. Titanium dioxide ( $\text{TiO}_2$ ) activated by UV light has been the most frequently used catalyst [166]. This process converts organic compounds into harmless and odourless products such as water vapour ( $\text{H}_2\text{O}$ ) and carbon dioxide ( $\text{CO}_2$ ). Figure 3.7 illustrates the mechanism of the PCO of VOCs with UV light using  $\text{TiO}_2$  as catalyst. The band-gap energy ( $E_g$ ) is defined as the energy difference between the highest valence band and the lowest conduction band. When the band-gap energy of the catalyst material is lower than the light energy of the excitation source, the photon is adsorbed. This results in the excitation of an electron ( $e_{cb}^-$ ) from the valence band to the conduction band, generating an electron ( $e_{cb}^-$ ) and a hole ( $h^+$ ) [167]. As the electron has a reduction ability and the positive hole has an oxidation ability, they drive the redox process,

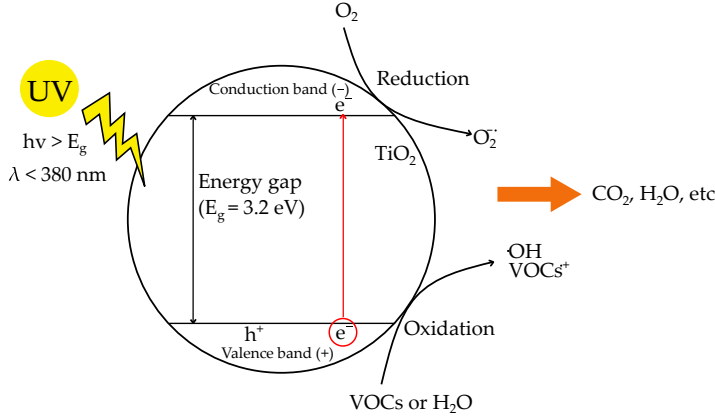
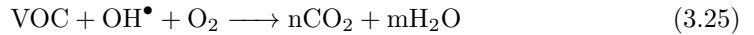
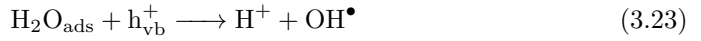


**Fig. 3.7:** Mechanism of the PCO of VOCs with UV light using  $\text{TiO}_2$  as catalyst (adapted from [165]).

reacting with  $\text{O}_2$ , water and the gaseous compounds that are adsorbed on the surface of the photocatalyst [167]. The oxidation reaction of the adsorbed water produces the hydroxyl radical ( $\text{OH}^\bullet$ ), which is the dominant oxidant in the degradation of VOCs. The basic reactions – including activation, oxidation and reduction – of the degradation of VOCs using  $\text{TiO}_2$  as a photocatalyst can be expressed as follows [165, 167]:



PCO has been used for indoor air treatment because it offers several advantages. It is active at room temperature and it degrades a broad spectrum of pollutants due to the oxidant potency of the hydroxyl radical [165]. Most studies are based on experimental investigations in laboratory conditions. In one pilot-scale application, the removal efficiency of a mixture of VOCs at sub-ppm concentrations (0.25–2 ppm) using PCO was investigated [168]. The results showed conversion rates in the 5–60% range, which vary depending on process parameters such as residence time, relative humidity, light source and intensity, VOC type and concentration [168].

Titanium dioxide is a metal oxide that can be found in two crystalline structures, anatase and rutile, with energy bandgaps of 3.23 and 3.02 eV, respectively [166].  $\text{TiO}_2$



Aeroxide P25 (70% anatase and 30% rutile) is the most frequently used photocatalyst for air purification because of its low cost, excellent stability, high availability and performance in degrading several VOCs [169, 170]. Theoretically, a UV light with a wavelength less than 380 nm can initiate photocatalytic oxidation with  $\text{TiO}_2$ . The two UV lights that are used most often are the fluorescent black-light UV lamp (UV-A, 300–400 nm) and the germicidal lamp (UV-C, 254 nm) [169]. The removal efficiency for mixture of VOCs of the two UV lights with the same power output was compared and it was concluded that there was no significant difference between the use of the two light sources [171]. In some studies, an ozone-generating UV light (UV-C/ $\text{O}_3$ , 245 + 185 nm) was employed to increase the removal efficiency of the PCO system, which was then combined with ozonation process [172, 173]. The study suggests that the removal rates are ordered as follows: UV-C/ $\text{O}_3$  > UV-C > UV-A [173].

The most challenging and concerning drawback of PCO is the formation of by-products that can be more harmful than the original pollutants. PCO is a stepwise reaction, and the intermediate steps can generate unwanted products if the conversion is not finalised [174]. The photocatalytic oxidation of toluene generates benzaldehyde, methanol, acetaldehyde and formaldehyde [175]. The generation of by-products is affected by light intensity, residence time, relative humidity and VOC type and concentration [175–177]. Relative humidity in particular has a strong influence on PCO. In the absence of humidity, the photocatalyst is deactivated. However, in high humidity (above 60%), competitive adsorption between water vapour, VOCs and by-products takes place, which reduces the by-products' residence time and leads to their release from the surface [177]. As an example, the removal efficiency of toluene at typical indoor air concentrations (10–500 ppb) varied between 30 to 90% depending on parameters such as relative humidity, residence time and the amount of  $\text{TiO}_2$  [172].

In general, the conversion and efficiency rates of PCO are comparatively low [146]. To enhance PCO's performance and overcome the challenges related to harmful by-products and operation with high relative humidity, PCO has been combined with an adsorbent material as support. In several studies,  $\text{TiO}_2$  has been combined with AC [161, 178–180]. The combination of the two materials has shown improvements to performance in terms of a reduction of by-product release [181], and increased removal efficiency of typical indoor pollutants (from 50 to 89.5% removal efficiency for toluene) [180]. It also mitigates the competition effect between water vapour and pollutants and the inhibition effect of diverse pollutants [181].

### *Non-thermal plasma*

Non-thermal plasma (NTP) is a highly ionised gas commonly used for air purification that consists of electrons, positive ions and neutral particles and is not in thermodynamic equilibrium [141]. In general, there are several ways to produce plasma: direct current, corona discharge with alternate current and dielectric barrier discharge (DBD) [182]. Plasma air cleaners can efficiently remove particles, VOCs and microbes [146, 183, 184]. However, the application of NTP for the treatment of pollutants such as VOCs is mostly limited to the laboratory because it requires a significant investment and adequate technical knowledge [185]. Furthermore, NTPs form harmful by-products during incomplete oxidation, such as CO, O<sub>3</sub>, NO<sub>x</sub> and aerosol particles, which is the main reason for their limited use in indoor air applications [186]. Moreover, NTP has a low energy efficiency, especially for treating low VOCs concentrations [184], and its capacity to remove different pollutants is affected by humidity [187]. NTPs have often been combined with a catalyst in order to increase the overall efficiency of the hybrid system and improve the oxidation efficiency [184].

### *Ozonation*

The use of ozone generators in indoor air cleaning devices peaked in the 1990s. During this period, the technology was marketed for the elimination of odours and microbial agents and the removal of VOCs [188, 189]. Such devices produce O<sub>3</sub> by adding energy to molecules of oxygen (O<sub>2</sub>), temporarily splitting the atoms so they recombine with other oxygen molecules [190]. Corona discharge and UV radiation are the two methods that can be used in this process [190]. Ozone is an oxidising agent that is also known for its harmful effects on human health. Moreover, the reaction with VOCs might not be fast enough to compete with typical ventilation rates when the ozone concentration is below 50 ppb [104]. However, high levels of ozone must be avoided in the presence of animals and people. Furthermore, ozone generators can increase the concentration of fine particles, especially in the presence of terpenes [188]. Ozone generators have been combined with adsorbent materials to increase the overall conversion efficiency of VOCs, thus maintaining a low residual ozone level [191].

## **3.2.5 Combined air filtration systems**

The optimal filter should be able to remove a broad variety of pollutants, solid and gaseous, perform effectively at various temperatures and humidity levels, and involve

little energy use. A universal single filter that can achieve such conditions is difficult to find on the market. However, various filter technologies have been combined to overcome individual mechanisms' drawbacks and improve the overall system performance. Some examples have already been given in the previous section. NTP and catalysts have been combined to avoid or limit by-product formation, while hybrid ozonation systems involve the use of adsorbent materials to decrease the amount of residual ozone in the air. In addition, the synergic use of adsorbent and catalyst materials has been investigated to inhibit the competition effect between water vapour and pollutants, avoid the deactivation of the PCO and increase pollutant conversion rates [141].

However, such combinations do not enhance the capacity of the filters to remove particle and gaseous pollutants simultaneously. Fibrous filters are often combined with AC or other adsorbent filters to simultaneously remove both solid and gaseous compounds [192, 193]. These two filters are usually installed back-to-back in ventilation systems or air-cleaning devices to remove the different pollutants individually [194]. In other cases, activated carbon has also been loaded onto fibrous filters [195]. Both strategies lead to bulky and heavy filtration modules. ACF have also been investigated in the laboratory for the simultaneous removal of particles and gaseous pollutants [194]. However, most studies on ACF are still related to the adsorption of VOCs, and there is not much data available on their performance for particles [160]. Other types of filters have been developed for the removal of both types of pollutants [196–199]. In one study, an electrostatic precipitator was combined with a catalyst material and achieved >99% particle removal in 25 minutes and 80% VOCs degradation in around 45 minutes. The experimental investigation was performed in a test chamber with mixing air [197]. In another study, a metal-organic framework (MOF) was used to coat an electret filter media. The result showed that the coating enabled a toluene removal capacity up to 85%, although the heavy coating led to an increased pressure drop and lower particle holding capacity [196]. A corona reactor reached a particle removal efficiency above 98% and degradation of 80% of formaldehyde [198]. The degradation of formaldehyde was investigated in a 1 m<sup>3</sup> chamber, and it reached an acceptable concentration after around 1 h of treatment; this process was rather slow and produced ozone [198].

Electrospun fibre filters have also been produced and investigated for the simultaneous removal of various pollutants [200, 201]. The advantage of such filters is that their fibres can reach diameters in the nano-dimension range, which leads to a lower pressure drop compared to conventional fibre filters because of the slip-flow effect [136]. Furthermore, electrospinning is a versatile method that makes it possible to functionalise the fibres using additives in order to enhance the removal capacity for gaseous compounds. An

electrospun fibre filter is a thin non-woven mat with a low basis weight. Such a filter can be installed as a single-stage filtration layer even when the available space for the filtration system is limited. The performance of such filters is still part of academic research studies, and they have shown promising results in this field. Therefore, they were chosen as the filter type to be investigated in this Ph.D. project. In the next section, the results from the literature on electrospun fibre filters are presented in detail.

### 3.3 Electrospun fibre filters

Though promising, the application of electrospun fibre mats to air filtration is relatively new. Electrospinning is an electrostatic method used to produce ultrathin fibres (details on the electrospinning process, applications and theory are provided in Chapter 3.4). Electrospun fibre filters have been reported since the 1980s and have since undergone further development. They have become a hot topic in the last 15 years, probably in association with the increasing concern about air pollution [202]. The most advantageous characteristics of such filters are related to their high porosity and specific surface area, low basis weight and uniform fibre size, which are requirements of high-performance filters [203].

The diameter of electrospun fibres can be as small as 40 nm. This peculiarity is rather crucial when it comes to the air resistance of fibrous filters. The general theory of filtration assumes continuous flow around the fibres and a no-slip condition at the fibre surface [126]. However, when the dimension of the fibre is comparable to the movement of the air molecules, the slip-flow model is dominant. In such conditions, the drag force on the fibre surface is smaller than in no-slip flow and, therefore, the pressure drop is lower (the slip-flow phenomenon has been further described in Chapter 3.2.2). Therefore, electrospun fibre filters have the potential to perform better than conventional fibrous filters, as they can achieve high-efficiency filtration with a lower pressure drop and can remove gaseous pollutants once doped with specific additives. In a recent study, Zhao et al. fabricated a PAN-based nanofibre filter with the aim of investigating the slip-flow effect [136]. The authors demonstrated a 40% reduction in the pressure drop (from 15 to 9 Pa) when the fibre diameter dropped from 168 to 71 nm with a face velocity of  $0.053 \text{ m s}^{-1}$ . Wang et al. investigated the quality factor of filters made of a micrometre-fibre substrate and a single nanofibre layer composed of fibres of various sizes [204]. They noticed that higher nanofibre solidity corresponded to a higher pressure drop and higher filtration efficiency. Furthermore, the quality factor of the filter was lower when more of the smallest fibres (20 nm diameter) were present. The quality factor was indeed

improved when there was a higher density of fibres with an average diameter of 780 nm [204]. Moreover, Zhang et al. demonstrated that a filter consisting of multiple thin layers of nanofibres had a higher quality factor compared to a nanofibre mat made of a single layer [205]. Therefore, the number of nanofibres and their fibre diameters must be adjusted to improve the filter performance, in addition to adopting a short-term deposition time [204, 205].

Polymers are the most frequently used materials for the fabrication of electrospun fibres. Researchers have used a broad range of polymers to fabricate electrospun air filters, such as polyacrylonitrile (PAN) [206], polyvinyl alcohol (PVA) [207], polyurethane (PU) [208], polysulfone (PSU) [209] and polyamide (PA) [210]. Such polymers are dissolved in a polymer-solvent solution, which can be employed in an electrospinning setup. The parameters that affect the filtration performance of such filters include the fibre diameter and structure, pore size, specific surface area, basis weight and thickness of the electrospun fibres. These parameters can be controlled to a certain extent with the electrospinning process. Different polymers present different characteristics, which produce different results. Table 3.3 reports the main results of various studies on electrospun fibres applied in air filtration.

PAN nanofibres with an average diameter of 200 nm achieved 95–100% PM<sub>2.5</sub> removal efficiency during a 100-h field test with extreme hazardous air conditions [206]. Electrospinning PA leads to small fibre diameters (90–180 nm) with a large surface area [211]. In one study, Nylon 6,6 electrospun fibres exhibited slightly higher particle filtration efficiency compared to a conventional glass fibre filter but at the expense of three times lower pressure drop [212].

PU is a thermoplastic polymer that exhibits good mechanical properties, and it has been found to be one of the best materials to produce nanofibre mats [213]. It can be dissolved using N,N-dimethylformamide (DMF), a commonly used but toxic organic solvent. PU exhibited adsorption capacity towards VOCs and can also be used in repeated cycles of adsorption and desorption processes under ambient temperatures and pressure, which is an improvement compared to activated carbon [159]. The adsorption capacity of electrospun pristine PU fibres and fly ash/PU fibres were tested using chloroform, benzene, toluene, xylene and styrene. The results showed that PU can sufficiently adsorb the VOCs, though the adsorption capacity increased 2.2–2.8 times when combined with fly ash particles [214].

PVA is a biodegradable and water-soluble polymer and is the largest synthetic resin produced in the world [215]. PVA-based fibres have demonstrated outstanding filtration capacity for particles of various sizes [216, 217], achieving a filtration efficiency (99.95%)

comparable to a HEPA filter but with a higher quality factor [216]. PVA was also electrospun in combination with  $\text{TiO}_2$  to investigate the removal of particles and the degradation of acetone [218]. The results showed a strong relationship between filter performance and retention time when evaluating the removal of both particles and acetone. The filter reached 98% removal efficiency of particles above 200 nm size with a retention time of 2 min. The degradation of acetone was above 99% using a UV-254 nm light, an initial concentration of acetone of 1,500 ppm and a retention time of 10 sec. The removal of acetone decreased to 54% under the same conditions but using a UV-365 nm light [218].

Cellulose acetate (CA) is another polymer that can be used for air filter applications. CA is the most common and most frequently used organic compound, and it is attractive because of its availability and biodegradability [219]. The electrospinning of CA has been investigated and resulted in fibres with good thermal stability, chemical resistance and high porosity [220]. CA nanofibres showed a filtration efficiency of 84–89% for particles in the 0.1–0.3  $\mu\text{m}$  size range with a pressure drop in the range 105–140 Pa at face velocity 0.053  $\text{m s}^{-1}$  [221]. In another study, PAN/CA-based activated carbon nanofibres prepared with electrospinning demonstrated an adsorption capacity for  $\text{SO}_2$  of up to 40  $\text{mg g}^{-1}$  [222]. CA was also combined with  $\text{TiO}_2$  to investigate electrospun fibre filters' capacity to remove both particles and NO with photocatalytic oxidation [223]. The study showed a degradation of NO up to 78.6% using a UVA lamp; the emission peak was 365 nm. Regarding particle filtration, the filters showed an efficiency above 97% for particle sizes between 0.1 to 0.6  $\mu\text{m}$ , reaching a peak of 99.6% for  $\text{PM}_{0.6}$  [223]. The pressure drop was recorded around 30.7 Pa with a face velocity of 0.054  $\text{m s}^{-1}$ .

Xia et al. performed a comprehensive literature review on electrospun nanofibre filters to investigate the relationship between face velocity and pressure drop [135]. The linear relationship between these two parameters had been confirmed (in relation to the theoretical studies from Kirsch et al. [137]), though the study underlined the limitations of current research on electrospun nanofibre filters. These filters have been tested at low face velocities (most are in the range of 0.05–0.1  $\text{m s}^{-1}$ ); this does not correspond to the typical range of face velocities in HVAC systems, which can reach 1–3  $\text{m s}^{-1}$  [135]. The same can be seen by analysing the face velocities presented in Table 3.3. In order to confirm their superior performance in relation to the pressure drop, electrospun fibre filters should be studied at higher air velocity conditions.

To conclude, empirical evidence clearly suggests that electrospun fibre filters can be employed to remove both particles and VOCs. However, most of the research until now has only partially investigated the performance of such filters. Most studies investigated

**Table 3.3:** Air filter performance of electrospun fibre filters.

Materials	Particles ( $\mu\text{m}$ )	Gaseous pollutants	$V_f$ ( $\text{m s}^{-1}$ )	$\eta$	$\Delta p$ (Pa)	Ref.
PU	0.080	-	0.057	99.66%	190	[208]
PVC/PU	0.3–0.5	-	0.053	99.5%	144	[224]
PAN	<2.5	-	0.21	98.11%	206	[206]
PAN/TiO <sub>2</sub>	0.26 <sup>(a)</sup>	Toluene <sup>(b)</sup>	0.053	97% <sup>(a)</sup> , 97.9% <sup>(b)</sup>	145	[225]
PAN/TiO <sub>2</sub>	0.1–1	-	0.80	86–99%	>15,000	[226]
PU/FAPs	-	Chloroform, benzene, toluene, o-xylene, styrene	-	8–45 $\mu\text{g g}^{-1}$ fibre	-	[214]
PU	-	Chloroform, toluene, hexane	-	0.01–0.45 $\mu\text{g g}^{-1}$ fibre	-	[159]
PVA	0.075	-	0.053	99.95%	294–980	[216]
PVA	0.6	-	0.083	~100%	1,530	[217]
PVA	0.3–0.5	-	0.15	91.3%	300	[227]
PVA/TiO <sub>2</sub>	0.1–0.2 <sup>(a)</sup>	Acetone <sup>(b)</sup>	-	60–98% <sup>(a)</sup> , 50–99% <sup>(b)</sup>	-	[218]
PSU/TiO <sub>2</sub>	0.3–0.5	-	0.05	99.997%	45.3	[228]
PSU/PU	0.26	-	0.053	99.93%	255.78	[209]
PLA	0.26	-	0.053	99.999%	93.3	[229]
PAN/silica	0.3–0.5	-	0.14	99.989%	117	[230]
PET/CD	-	Aniline	-	2,600–3,400 ppm	-	[231]
Nylon 6	0.3	-	0.05	99.993%	145	[232]
PVA/PAN	0.3–7	-	0.42	99%	418	[233]
PAN/CA/AC	-	Toluene	0.11	65–72g/ 100g fibre	-	[234]
PVP/TiO <sub>2</sub> ACF	-	SO <sub>2</sub>	-	67.6%	-	[235]
PAN/AC	-	NO	-	>60%	-	[236]
Manganese/ PAN/AC	-	Toluene	0.11	68g/100g fibre	-	[237]
CA/TiO <sub>2</sub>	0.1–0.6 <sup>(a)</sup>	NO <sup>(b)</sup>	0.054	99.5% <sup>(a)</sup> , 78.6% <sup>(b)</sup>	30.7	[223]

the removal of either particles or VOCs, while some have been employed under static conditions and have not evaluated the pressure drop of such filters. Therefore, it is important to investigate such filters further in order to have a clear overview of their overall potential when applied in air filtration.

## 3.4 Electrospinning

Electrospinning nano- and microfibres is a versatile and effective method to produce fibre mats. It was first studied by Formhals in the 1930s [238]. In the 1990s, several research groups showed interest in this technique, triggering more theoretical and experimental studies on electrospinning in the following years [239]. The advantages of this technique include its technical simplicity and easy adaptability. Furthermore, the fibre's diameter and morphology are tuneable by the processing parameters, solution characteristics and environmental conditions [201].

### *Materials and applications*

A wide variety of materials can be spun, including polymers, composites and ceramics [239]. Several bio- and synthetic polymers have been electrospun under various conditions [240]. Polymers can be electrospun alone, as a mixture of polymers or in combination with various additives [241]. Electrospinning is used to produce fibres for various applications, including filtration, protective clothing, reinforcement fibres in composites, biomedical devices, food applications, nanosensors and electrical and optical applications [242, 243]. Table 3.4 provides an overview of commonly electrospun polymers and their applications.

### *Types of electrospinning*

There are two major types of electrospinning: solution electrospinning and melt electrospinning. Solution electrospinning is based on the formation of fibres from a polymer-solvent solution, whereas melt electrospinning involves the use of a polymer melt without any solvent [242]. Solution electrospinning has been widely used, as there is a wide variety of materials (especially polymers) that are soluble in various solvents [281], such as water [282], acetone [252], DMF [283] or mixtures of solvents [159, 224]. Different components can be easily added to the polymer solution, such as nanoparticles or other molecular species, which can add various functionalities to the fibres [239]. Furthermore, solution electrospinning has proven more viable for producing fibres in the nano-range compared to melt electrospinning because of the evaporation of the solvent [242].

In melt electrospinning, a suitable polymeric material is heated above its glass transition point. The plastic melt is transformed into fibres by pulling it in an electrostatic field, as in solution electrospinning. Usually, fibres produced by melt electrospinning have diameters from a few micrometres up to 10 micrometres [281]. The reason for this is that melts usually have higher viscosities and unusual viscoelastic properties



**Table 3.4:** Commonly electrospun polymers and their application.

Polymer	Application	Ref.
Polyurethane (PU)	Filtration, protective clothing, drug delivery systems	[214, 244, 245]
Polyvinyl alcohol (PVA)	Filtration, nanofibre support for enzymes, drug delivery systems	[207, 246, 247]
Polycarbonate (PC)	Filtration, sensors, protective clothing	[244, 248, 249]
Polyamide (PA)	Filtration, protective clothing	[244, 250]
Cellulose acetate (CA)	Filtration, membranes, fabrics, biosensors, drug delivery systems, tissue engineering, nutraceutical delivery, self-cleaning textiles	[251–253]
Polycaprolactone (PCL)	Drug delivery systems, tissue engineering	[254, 255]
Polystyrene (PS)	Catalyst, enzymatic biotransformation, filtration	[256–258]
Polyacrylonitrile (PAN)	Filtration, hydrogen storage, battery electrodes	[259–261]
Polyethylene oxide (PEO)	Filtration, microelectronic wiring	[262, 263]
Poly(lactic acid) (PLA)	Sensors, filtration, drug delivery systems	[264, 265]
Poly(methyl methacrylate) (PMMA)	Enzyme immobilisation	[266]
Poly(vinyl pyrrolidone) (PVP)	Regenerative tissue engineering, drug delivery systems	[247, 267]
Polyvinylchloride (PVC)	Water and air filtration, protective clothing, batteries	[224, 268–270]
Polyethylene terephthalate (PET)	Various biomedical applications, filters	[231, 271]
Polysulfone (PSU)	Filtration	[209, 228]
Polyvinylidene fluoride (PVDF)	Filtration, membrane distillation	[272, 273]
Chitosan	Wound dressing, drug delivery systems, tissue engineering	[255, 274, 275]
Keratin	Tissue engineering, filtration	[276–278]
Collagen	Tissue engineering	[279, 280]

[281]. One advantage of melt electrospinning is that solvents are not needed, which is crucial in areas where solvent accumulation or solvent toxicities are an issue, such as biomedical applications [284]. Another difference with solution electrospinning that can

be advantageous in some applications is that the melt jet is more stable in the flying path towards the collector. Consequently, the fibre deposition is more predictable and less chaotic than in solution electrospinning [285, 286].

#### *Solution electrospinning: Setup and process*

The main components of a solution electrospinning setup include a high voltage power supply, a collector coupled to the ground and a syringe pump, which comprises a needle (connected to the power supply) and connecting tubes, where the polymer solution is carried at a constant and controllable feed rate to reach the tip of the needle (Figure 3.8). During electrospinning, the so-called Taylor cone forms on the tip of the needle when the polymer solution overcomes its surface tension as high voltage is applied. The fluid solution stretches and elongates in the direction of the collector, while the solvent evaporates [287]. In the flying path, the fluid assumes a jet form, which becomes unstable due to bending instability, which is responsible for jet-stretching and looping [287]. In fact, the thread trajectory has a whipping-like geometry that enables the evaporation of the solvent and promotes the elongation of the fibres [288]. Various bending instabilities occur during the jet flight. Every time one bending instability happens, the trajectory of the jet path revolves, increasing the radius around the jet axis until it is fully solidified [289]. Mechanical buckling instability can occur due to compressive forces when the jet lands on the collector [288]. The result of this process is the formation of fibres deposited on the collector with a diameter ranging from 50 nm to 10–15  $\mu\text{m}$  [241]. Additional details about the fibre formation process are discussed in Chapter 3.4.2.

Various spinnerets can be used to prepare fibres, including single needle, multineedle, coaxial needle or needleless spinnerets. The collector can also vary in shape and movement, which makes it possible to collect fibres in different patterns. Figure 3.8 gives a schematic overview of the electrospinning setup and the different equipment possibilities. The various feeding and collecting configurations are further described below.

#### *Feeding configurations*

Fibre formation during electrospinning occurs with the development of the Taylor cone from the solution. This occurs when the solution surface tension is broken by the Coulomb force of the electric field [290]. The curvature on the surface of the solution needed to initiate the process is formed by a droplet located at the tip of the needle or by using a needleless configuration [291].

Simple single-needle electrospinning has been widely investigated [291]. Multi-jet

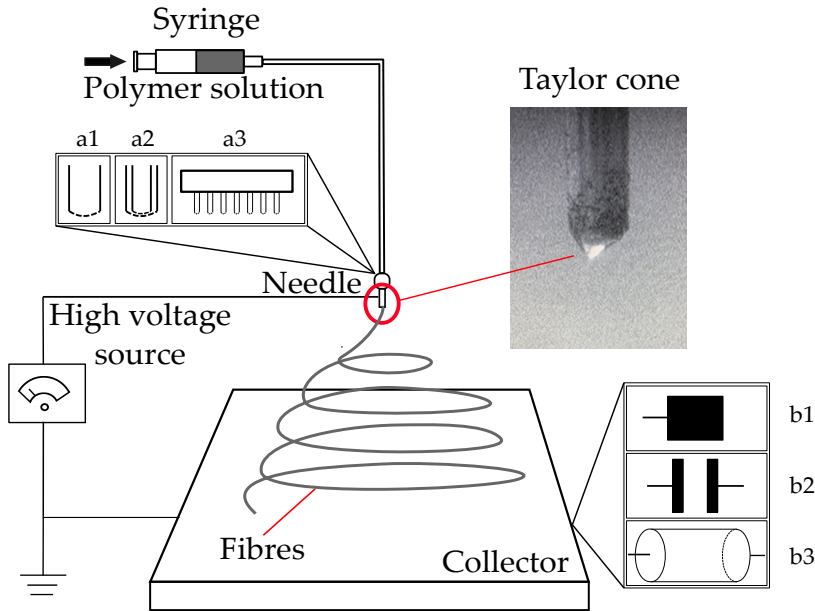


**Fig. 3.8:** Scheme of a basic electrospinning setup. (a) Examples of types of feeding configuration (a1) single needle (a2) coaxial needle (a3) multineedle. (b) Examples of types of collector (b1) flat plate collector (b2) parallel electrodes (b3) rotating drum.

spinnerets have been employed as an alternative up-scaled configuration and have increased fibre productivity [292]. Nevertheless, Yang et al. have demonstrated that multiple nozzles can introduce a strong interference of the electrical field that can prevent the improvement and eventually worsen the fibre production. Jet repulsion was decreased only when the nozzles were kept above a threshold distance, and the electrospinning throughput was similar to the single nozzle configuration [293].

The possibility of forming a droplet without the use of a needle has been investigated through different upwards needleless techniques in which fibres are electrospun directly from an open liquid surface [291]. Compared to the traditional needle electrospinning, those techniques have the potential to achieve higher throughput as they are not depending on the fluidic channel numbers [294]. In fact, needleless electrospinning is used for large scale fibres production [291]. Yarin and Zussman have designed a two-layer-fluid setup which consisted of ferromagnetic suspension which was covered by the polymer solution to be spun. A permanent magnet was placed under the two fluids. Vertical spikes would form on the interlayer interface which during electrospinning become sites

of upwards jetting on the uppermost free surface [295]. Other possibilities include the use of a rotating roller partially immersed into the polymer solution, which slowly rotates, loading the solution onto the roller surface and generating a large amount of jets from the roller surface upwards when applying the high voltage [296]. There are several types of rotating spinnerets that are used in needleless electrospinning, as disk, spiral coil and ball spinneret [291].

Diverse morphologies of electrospun fibres can be achieved using a coaxial needle setup in which a needle is mounted inside an outer needle [297]. This configuration is used to produce fibres using different materials for the outer shell and the inside core, which has been of particular use in biomedical applications (e.g. drug delivery) [298]. The use of a second polymer solution increases the complexity of the process because more parameters affect the electrospinning system, such as the interfacial properties between the two polymeric liquids and shell-to-core feed rate [297]. However, control of these parameters has been achieved, which even allows increasing the number of layers and fabricating triaxial fibres [299].

### *Collector configurations*

There are different ways to collect the electrospun fibres, from a simple plate (stationary collector) to a rotating drum (moving collector), as shown in Figure 3.8. The use of different collectors enables the production of various patterns or fibre alignments. The collector is generally made of a conductive material, such as aluminium foil on a metal plate, that is electrically grounded to ensure a stable potential between the needle and collector [300]. However, it is possible to place other materials on top of the collector to collect fibres in diverse configurations [301].

The 2D flat plate collector is the most widely used to collect randomly oriented fibres, as it is a simple and efficient solution; the resulting mesh is called a non-woven mat [287]. In order to align fibres with a stationary collector, it is possible to use sharp edges such as two parallel plates or wires [302]. This straightforward method can achieve a high degree of orientation [288].

Moving collectors create the possibility of dynamically assembling the electrospun fibres. Such collectors can have the shape of a cylinder [225] or a rotating disk [303]. A rotating drum makes it possible to align fibres along the circumference of the cylinder. However, the use of a rotating collector can lead to fibre breakage if the rotation speed is too high [279]. Rotating drums are also useful in assisting the collection of dry fibres. A solvent with a high boiling point, such as DMF, may result in collected wet fibres, as

the solvent does not fully evaporate. The rotating collector increases the evaporation rate of the solvent and gives more time for the solvent to evaporate, improving the fibres' morphology [300, 304].

Moving collection can also be achieved through the controlled X-Y motion of the collector or spinneret using a pre-programmed track via a computer. Some electrospinning equipment, including the setup used in this project, allows the controlled movement of the arm where the needle is kept. In the case of a flat plate collector, this function allows a more homogeneous distribution of fibres onto the collector surface [305]. It also supports the formation of more complex patterns and precise fibre deposition in so-called direct writing electrospinning and near-field electrospinning [305].

### 3.4.1 Electrospinning governing parameters

The morphology and properties of the electrospun fibres are influenced by several parameters, which can be classified into three groups (Table 3.5): processing, solution and ambient parameters [201, 306].

**Table 3.5:** Electrospinning governing parameters.

<b>Process parameters</b>	Applied voltage
	Feed rate
	Tip-to-collector distance (TCD)
<b>Solution parameters</b>	Polymer concentration
	Viscosity
	Surface tension
	Molecular weight of the polymer
	Solvent boiling point
<b>Ambient parameters</b>	Temperature
	Humidity

#### *Processing parameters*

Processing parameters that affect the electrospun fibre properties include the applied voltage, the feed rate of the polymer solution and the distance between the nozzle and the collector (called the tip-to-collector distance; TCD).

When the electrostatic force overcomes the surface tension of the polymer solution, the Taylor cone forms on the nozzle [201]. An increase in the applied voltage raises the deposition rate by increasing the mass of polymer fed out of the tip of the needle [306]. The applied voltage is strongly related to the presence of bead defects in the fibre morphology. Deitzel et al. experimentally demonstrated that the electrospun fibres present a higher density of beads above a critical voltage value. This is correlated to a steep increase in the spinning current observed when reaching this crucial voltage value, as well as an increase in the instability of the jet at the tip of the needle [307]. A higher presence of beads decreases the fibres' surface area, which has a negative effect on their filtration capacities [306].

Givchi et al. have shown that increasing the tip-to-collector distance decreased the fibre diameter, also resulting in more uniform fibres [308]. The TCD affects the electric field, which decreases exponentially as the TCD increases. However, a longer distance increases the time for the solvent to evaporate and for the jet fluid to stretch, resulting in thinner fibres [308].

Lastly, the polymer solution feed rate has a direct effect on the jet velocity between the needle and the collector. Megelski et al. have noted that an increase in the solution feed rate led to an increase in fibre and pore diameter and to more pronounced beaded morphology [309]. Furthermore, it is necessary to tune the flow rate to its optimal value in order to generate the Taylor cone during the electrospinning process. A higher feed rate can cause a build-up of the solution on the edge of the needle, whereas a lower feed rate can create a vacuum inside the syringe [310].

### *Solution parameters*

The solvent characteristics and the polymer concentration, viscosity and surface tension of the solution are the most relevant solution parameters to the fibres' morphology. The viscosity of the polymer solution is related to the molecular weight of the polymer, which reflects the number of polymer chain entanglements in a solution [311].

The boundary between the electrospray phenomenon and the fibres' formation is defined by the solution concentration, as it determines the solution surface tension and viscosity. When concentration – and viscosity – are very low, surface tension governs the process and prevents the solution from forming fibres, resulting in droplet formation (so-called electrospray) [307]. When fibres are produced from less concentrated solution, they present more beads because they are more difficult to dry before they reach the collector [232]. As the polymer concentration increases, viscosity increases and becomes

dominant over surface tension; the result is less bead formation and more uniform fibres [232]. If the concentration is too high, the cohesive nature of the solution (i.e. its high viscosity) prevents the formation of fibres [307]. Furthermore, increasing the polymer concentration also increases the fibre diameter and may produce more uniform and cylindrical fibres [287].

The solvent solubility, surface tension and boiling point are also essential factors to consider prior to electrospinning because they affect the process [310]. It is also important to consider whether the selected solvent is hazardous [309]. A low boiling point is a beneficial characteristic for a solvent because it promotes the evaporation of the solvent in conventional atmospheric conditions, ensuring the deposition of the fibres in a dry state [242]. However, an excessively low boiling point results in very fast evaporation and clogs the needle tip, while solvents with boiling points that are too high lead to ribbon-shaped fibres because the solvent does not completely evaporate before depositing onto the collector. Therefore, solvent volatility has a direct effect on fibre characteristics such as diameter, shape and porosity [310].

#### *Ambient parameters*

Ambient temperature and humidity also influence the electrospun fibres' morphology. Wang et al. have shown that increased temperature increases the evaporation rate of the solvent; this decreases the time it takes for the jet to solidify and elongate, resulting in thicker fibres [312]. In the same study, nanofibre membranes were electrospun at a high relative humidity (RH) above 75%. Beads-on-a-string fibres were formed at an RH of 75%, as the solvent could not fully evaporate during elongation [312]. Therefore, humidity also affects the fibres' morphology.

### **3.4.2 Fundamentals of the theoretical background and phenomena governing the electrospinning process**

Several theoretical and experimental studies have attempted to understand the electrospinning process [262, 289, 290, 313–320]. In particular, researchers have sought to understand how, during electrospinning, a fluid solution is transformed into solid micro- and nanofibres through a capillary tube that is four to five orders of magnitude larger in diameter than the fibres [305]. Understanding the electrospinning process also leads to better control over the resulting fibre morphology.

According to the literature, fibre formation can be divided into three phases according to various physical phenomena: (1) Taylor cone formation, jet initiation and straight

elongation of the charged jet; (2) the onset of bending instabilities and further elongation; and (3) jet solidification and deposition of the micro- or nanofibres onto the collector. The major principles that are employed in all the analysing works are Newton's law (for an object's force analysis) and the conservation laws (for system analysis) [242].

*Taylor cone, jet initiation and straight elongation*

The formation of a droplet at the tip of the needle or a curved liquid surface is the first step towards fibre initiation. Before electrospinning starts, and therefore in the absence of an electric field, the equilibrium shape of the droplet is governed by gravity and surface-energy distribution [281]. As the electric field is applied, the electric force is the driving force that will initiate the electrospinning process. In the case of needle electrospinning, the droplet of the charged solution reduces its size under the effect of the electric force in order to maintain the force balance [305]. As the applied voltage increases, the fluid droplet assumes a prolate shape in the direction of the electric field. The equilibrium states of the prolate shapes are controlled by the equilibrium between the electric forces and the surface tension. As the electric field increases further and approaches a critical value, the droplet overcomes its surface tension and assumes a cone shape, called a Taylor cone [321]. Under this critical potential difference, the onset of a jet fluid from the droplet is observed. Taylor was the first to describe these phenomena in the 1960s [290, 321] and he defined the critical electric potential  $V_c$  needed for electrospinning as

$$V_c^2 = 4 \frac{H^2}{h^2} \left( \ln \left( \frac{2h}{R} \right) - 1.5 \right) (0.117\pi R\gamma) \quad (3.26)$$

where  $\gamma$  is the solution surface tension,  $H$  is the distance between the needle tip and the collector and  $h$  is the length of the needle with outer radius  $R$  [242]. Taylor considered only inviscid fluids in this calculation [242]. In his experimental work, Taylor predicted that the Taylor cone angle that defines the equilibrium is  $49.3^\circ$  [290]. Later, Yarin et al. demonstrated that the cone assumes a critical shape with a smaller angle of  $33.5^\circ$  [313]. To control the jet profile and the diameter of the fibres, the Taylor cone has to be controlled. This is why a vast amount of work, both theoretical and experimental, has applied Newton's first law to analyse the force balance of the Taylor cone [242].

The electrically charged jet develops on a straight line for a few centimetres as long as no instabilities become dominant [281]. Until this condition is met, the Coulomb forces that act on the charges carried with the leading segment of the jet pull the jet towards



the collector; the jet accelerates while the surface tension and the viscoelastic stresses within the jet play against the stretching [289]. At this stage, the jet accelerates at up to  $600 \text{ m s}^{-2}$ , which is two orders of magnitude higher than gravitational acceleration [281]. Indeed, gravitational force does not play a significant role in electrospinning, which is why bottom-up electrospinning configurations also work [281]. The jet deviates from the straight path only when the total tensile stress within the jet has decayed enough for the instabilities to become dominant. He et al. has proposed the following equation to estimate the critical length  $L$  of the straight jet [322]

$$L = \frac{4kQ^3}{\pi\rho^2I^2}(R_0^{-2} - r_0^{-2}) \quad (3.27)$$

where  $k$  is the dimensionless conductivity,  $Q$  is the flow rate,  $\rho$  is the density of the solution,  $I$  is the current through the jet,  $R_0 = (2\sigma Q/\pi k\rho E)^{1/3}$ ,  $\sigma$  is the surface charge,  $E$  is the applied electric field and  $r_0$  is the initial radius of the jet [322]. This critical length is strongly related to the applied voltage, as confirmed by experimental findings [281].

#### *Electrical bending instabilities and further elongation*

Originally, the electrospinning mechanism was believed to be the result of the splitting of the main jet, as described by Doshi and Reneker [323]. Later, bending instabilities were understood to be the dominating mechanism. The straight jet elongates and its diameter decreases as the distance from the tip increases until it becomes unstable due to the onset of various electrically driven instabilities. It is at this point that it starts to bend and to perform spiralling and looping motions [281, 305]. These instabilities are due to the excess charge that cannot be redistributed along the length of the jet as it elongates, which bend and deform the jet [289]. This bending or whipping instability repeats itself on a smaller scale as the jet diameter decreases, leading to further reduction [281]. The result is a series of progressively smaller coils with increasing radius at each bending turn, as well as the continuous elongation of each segment in response to the Coulomb repulsion of the charge carried with the jet [289]. In this phase, the jet motion towards the counter-electrode is characterised by velocities on the order of metres per second [287].

Reneker, Yarin and their colleagues [313, 314, 324], Hohman et al. [315, 316] and Shin et al. [319, 320] analysed which instabilities exist and when they occur and have formed several mathematical models to describe them and the development of the jet. Their works indicate that there are three main instabilities that can occur; these dominate one another depending on the chosen spinning parameters and the consequent jet radius and

surface charge of the fluid element [319]. The first is the classical Rayleigh instability, which is axisymmetric and dominated by surface tension. It appears in weak electric fields and will be suppressed when the electric field and the surface charge density exceed a threshold [319]. The second axisymmetric instability occurs at stronger electric fields than the first [305]. The third is a non-axisymmetric instability that occurs with the strongest electric field, and it is also called the whipping or bending instability [305]. The last two modes are independent of the surface tension [319]. Fridikh et al. developed a model to describe the charged liquid with bending instability [325].

In addition to the electrical bending instabilities, other instabilities such as branching or the formation of physical beads can occur [289]. A jet-branching effect can occur more frequently for more concentrated and viscous solutions and at electric fields stronger than the minimum threshold for producing one jet [289]. Yarin et al. developed a theoretical model to predict branching instability [326]. The formation of beads along the fibres is the result of another effect called capillary instability [289]. This phenomenon causes a cylindrical jet of liquid to collapse into separated droplets and leads to the formation of beaded fibres [289, 327]. The beads aligned along the fibre can be prevented by varying the spinning parameters [287]. Beads and branches are rarely observed at the same time, as branches occur at high charges per unit area while beads are formed at low charges per unit area [289].

#### *Fibre solidification and deposition*

At the final stage of electrospinning, the fibre approaches the solid state and the jet becomes so thin that the bending instability cannot govern the process. Therefore, as the final step of electrospinning, the solidified nano- or microfibres are deposited on the counter-electrode [281]. The elongation of the fibre along the straight path and the whipping phase is accompanied by the evaporation of the solvent, which plays an important role in the jet-thinning process and in the final fibre diameter deposited onto the collector. As the bending process progresses, evaporation intensifies, increasing the polymer fraction in the jet and leading to solidification [324]. Yarin et al. included solvent evaporation in their mathematical expression of the bending electrospinning process and derived an equation that describes the volume variation and mass change of the jet due to evaporation [324].

During deposition, buckling deformations can occur due to the presence of longitudinal compressive forces on the jet at the impaction on the collector surface [289]. Such forces are independent of the electrical bending instability [328]. Buckling instability results in

the formation of narrowly looped fibres with various pattern structures such as sinuous, recurring curves and figures of eight [328]. If a high solvent concentration or a solvent with a high boiling point is used, soft fibres may be deposited depending on the relative humidity, creating partial coalescence effects [281]. Such effects happen when two soft fibres come into contact or cross each other, yielding distinct adhesion geometries at the junction points. Figure 3.9 shows the result of the electrospinning of a PU in DMF solution during an experiment of this Ph.D. project.

To conclude, fibres with diameters down to a few nanometres can be produced thanks to the above-described instabilities during electrospinning. The fibre formation process is characterised by an overall stretching ratio on the order of  $10^5$  and a stretching rate up to  $10^5 \text{ s}^{-1}$ . These extremely high values are not accessible through other fibre formation methods [287].

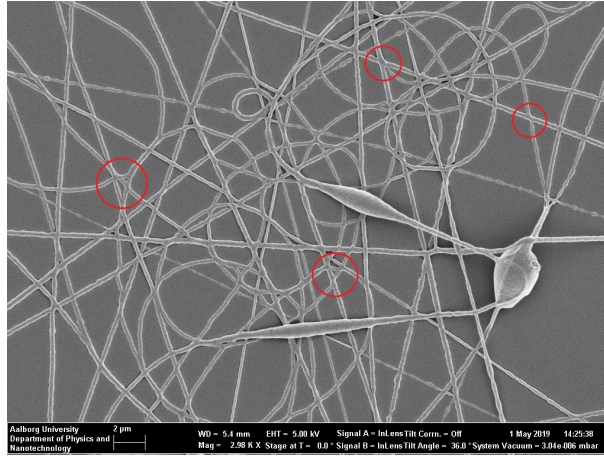


**Fig. 3.9:** Coalescence of PU nanofibres. DMF is the solvent used for dissolving the polymer.



Part II

Research Papers



# Introduction to research papers

In the following chapters, the research papers that were published as part of the Ph.D. project are reprinted. The author of this thesis is the first author of all the papers, and the papers were all written in collaboration with the Ph.D. supervisors, Professor Alireza Afshari and Associate Professor Peter Fojan, as senior authors. The other co-authors present in the papers have been essential parts of the Ph.D. project thanks to the collaborations that have been established during the past three years.

The first paper is the result of a literature study on the performance of air filtration technologies, including pressure drop, removal capacity and the formation of by-products. Several technologies were reviewed in order to investigate their potential related to the simultaneous removal of particles and gaseous pollutants. This paper offers insight into the most common air filters in the market and in scientific research. It is also the first paper that established the collaboration with Professor Jinhan Mo from the Department of Building Science at Tsinghua University, China.

The second and third papers present the results from the so-called ‘first generation of filters’ of this Ph.D. project. These electrospun nanofibre filters were prepared using two different polymers: PU (Paper II) and PVA (Paper III), doped with activated charcoal and titanium dioxide (separately). Paper II reports the preliminary results of the study, describing the electrospinning process and reporting the pressure drop and filtration performance for particles in the range 11.8–478.2 nm, as well as the toluene removal of the PU-based filters, using a face velocity of  $0.053 \text{ m s}^{-1}$ . Paper III covers the same ground for the PVA-based nanofibres with the use of additives, but the investigation is extended to the morphology of the nanofibres, including the fibres’ average diameters and chemical characterisation. The filters were also assessed in terms of specific surface area, pore volume, pore size and basis weight. Partial work reported in these papers was conducted in collaboration with Professor Matthew S. Johnson and his research group from the Department of Chemistry at the University of Copenhagen.

The first generation's strengths and weaknesses pointed the way to the second generation of filters, which was fabricated with the aim of improving and optimising the results of the first study. The last two papers report the data collected while investigating different electrospun CA-based fibre filters. The polymer was selected in order to achieve higher porosity and lower pressure drop compared to the previous generation. Moreover, the doping process was changed to improve the removal capacity for VOCs, while the selected additives remained the same. Paper IV reports the results regarding the fibre morphology, filtration efficiencies towards particles between 0.3 to 10  $\mu\text{m}$  and the pressure drop at face velocities from 0.035 to 1  $\text{m s}^{-1}$ , addressing the effect of the additives on such parameters. This paper also discussed the quality factor ( $Q_f$ ) of the filters and compared it to the  $Q_f$  of other electrospun fibre filters reported in the literature. Some of the results of this paper were achieved in collaboration with Professor Jinhan Mo and his research group at Tsinghua University. The fifth and last paper describes a further investigation of the removal capacity of the CA-based filters for toluene, addressing the adsorption and photocatalytic oxidation of the VOC promoted by the two additives. This paper proposes a final filter type, which explores a third doping method employing a coaxial electrospinning setup.

The common denominator of these papers is that each addresses fabrication and characterisation methods of electrospun fibre filters that aim to remove multiple air pollutant types at the cost of a negligible pressure drop for future use in residential buildings.



## Chapter 4

### Paper I

# Single-Stage Air Filtration of Particles and Gaseous Contaminants in Buildings: A Literature Study

Roberta Orlando, Peter Fojan, Jinhan Mo, Niels C. Bergsøe and Alireza Afshari

The paper has been published in the  
*IOP Conf. Ser.: Earth Environ. Sci.* Vol. 588, 032073, 2020.



# Single-Stage Air Filtration of Particles and Gaseous Contaminants in Buildings: A Literature Study

Roberta Orlando<sup>1</sup> Peter Fojan<sup>2</sup> Jinhan Mo<sup>3</sup> Niels C. Bergsøe<sup>1</sup> and Alireza Afshari<sup>1</sup>

<sup>1</sup>Department of the Built Environment, Aalborg University, DK-2450 Copenhagen, Denmark

<sup>2</sup>Department of Materials and Production, Aalborg University, DK-9220 Aalborg, Denmark

<sup>3</sup>Department of Building Science, Tsinghua University, Beijing 100084, China

Email: roo@sbi.aau.dk

**Abstract.** A variety of air filtration technologies are commercially available for reducing particles and gaseous contaminants that may enter buildings from outside. According to the World Health Organization (WHO), there is an increasing range of adverse health effects linked to air pollution, at even-lower concentration of pollutants. This article presents a short literature overview of air filtration technologies, which focus on assessing their ability in removing both particles and gaseous compounds. The aim is to provide information about current research development of air filtration technologies as well as their advantages, limitations and performance in terms of removal efficiency, pressure drop and formation of by-products. Mechanical filters and electrostatic filters are efficiently used for the removal of particles. Photocatalytic oxidant and adsorbent air filters are commonly used for gas removal. These last two types of filters are not feasible for particles removal. Air filtration using electrospun nanofiber filters have been studied, however, the performance of such filters for the removal of particles and gaseous contaminants at the same time has to be further investigated.

## 1. Introduction

In this study, air pollutants are distinguished by their physical state between particles and gaseous contaminants as Volatile Organic Compounds (VOCs) that may be present in the indoor air in buildings. A large variety of air filtration technologies are commercially available for removing different types of pollutants. Simultaneous removal of particles and VOCs is required in order to improve Indoor Air Quality. The present review focuses partly in investigating the removal efficiency of the available filtration technologies towards particles and VOCs in order to assess whether there is the possibility to use a single-stage filter for removing both pollutant types. The present study also discusses the challenges facing the future air filtration directions and development in achieving sustainable ventilation and acceptable indoor air quality in residential buildings, in accordance with the UN Sustainable Development Goal (UN SDG) “Good Health and Well Being”. A comprehensive literature search through Scopus yielded 1429 relevant hits in the period between 2000 and 2019. Only original papers without conference articles have been considered in the current study, as articles that do not refer to indoor air in buildings have been disregarded. Twenty-three most relevant publications have been selected for this short review.



## 2. Removal efficiency towards particles and gaseous compounds

Seven air filter technologies are investigated and compared in their ability of removing particles and gaseous compounds, as shown in Table 1. Filter technologies are rather selective in terms of which pollutants they can remove. Mechanical and electrostatic air filters are efficient and commercially used in the removal of particles. High Efficiency Particulate Air (HEPA) filters remove up to 99.97% of particles with 0.3  $\mu\text{m}$  diameter or larger [1]. Electrostatic air filters present lower removal efficiencies compared to mechanical filters [2][3]. Ardkapan et al. (2014) showed that the filtration efficiency for an electret filter can vary from 45% to 80% depending on the particle concentration and particle sizes [2]. None of the above mentioned air filters is capable of removing gaseous compounds. Indeed, adsorbent filters are highly efficient on the removal of gaseous pollutants, through materials such as activated carbon or zeolites. Chen et al. (2005) have stated that sorption materials are the most effective technology for the removal of indoor VOCs. Activated carbon cannot remove very volatile gases alone but the removal efficiency can be improved when combined with other sorption media [4]. An alternative to adsorbent materials is degradation of VOCs through photocatalytic oxidation (PCO) [5]. The photocatalytic degradation of VOCs using titanium dioxide  $\text{TiO}_2$  as catalyst has been investigated with initial VOCs concentration close to indoor air conditions (ppbv levels) [5]–[7]. In the study of Vildozo et al. (2011), the removal efficiency of VOCs ranged from 50% at a gas flow's relative humidity of 60%, and 100% removal in dry conditions [6]. Both adsorbent and PCO filters are not effective in removing particles from the air. Another filtration technology presents in the literature is Non-Thermal Plasma (NTP) filters. NTP filters precipitate particles and promote oxidation of VOCs, although it operates unsteadily and with low efficiency [8],[9]. Electrospun nanofiber filters have shown promising results in the simultaneous removal of particles and VOCs [10], [11]. Those filters have demonstrated high particle removal efficiency, comparable to HEPA filters, as well as degradation of VOCs through  $\text{TiO}_2$ . Indeed, the electrospinning technique allows the use of additives as activated carbon or  $\text{TiO}_2$  which enhances the capture selectivity of the nanofibrous filters. Chuang et al. (2014) prepared an electrospun nanofiber filter with a 99% acetone removal efficiency and 90% removal efficiency of particles above 200 nm diameter [11].

## 3. Pressure Drop

The energy consumption of a fan in a ventilation system is affected by the pressure drop applied by the operating air filter. Therefore the pressure drop across the filter needs to be addressed when evaluating different air filter technologies. Mechanical filters are characterized by an increase of pressure drop over time, due to clogging of the filters [12]. A characteristic of HEPA filters is their relative high pressure drop, in the range between 250-500 Pa [13]. Electrostatic air filters present a lower pressure drop compared to mechanical fibrous filters [2]. The air resistance imposed by nanofiber filters is lower compared to conventional mechanical filters made by microfibers, due to a slip flow dominance in the air flow [14]. Wan et al. (2014) demonstrated that the use of additives as  $\text{TiO}_2$  on electrospun nanofiber filters promoted a decrease of pressure drop compared to the pure nanofiber filter [15]. Electrospun nanofiber filters have been investigated mostly at face velocities around 0.05-0.2 m/s in a controlled environment [16]. In the future works, the pressure drop of such filters has to be evaluated under realistic ventilation face velocities in buildings (1-1.5 m/s), in order to assess the filtration performance of nanofiber filters in comparison to conventional microfiber filters. Table 1 summarizes also the pressure drop of the investigated air filtration technologies.

## 4. By-products

The aim of air filters is to improve the indoor air quality. When a filter becomes a source of secondary pollution releasing particles or introducing by-products, the indoor air quality is degraded. Indeed, mechanical filters can be a source of contamination from micro-organism, as electrostatic filters may increase the concentration of ultrafine particles, ozone and formaldehyde [17], [18]. Adsorbent air filters

are not generating by-products but there is a possibility of pollutant reemission when saturation occurs. PCO and NTP filters are both sources of by-products [9], [19]. When partial oxidation occurs during PCO filter operation, its products can be reemitted in the air stream and they can affect people's health to an even greater extent than the oxidation reactants [19]. As summary, Table 1 includes information about filters as source of by-products.

**Table 1.** Summary of air filter technologies' performance

Air filter technology	Particles removal	VOCs removal	Remarks	Ref
Mechanical filters	+	-	99.99% efficient for particle size > 0.3 $\mu\text{m}$ . Economic. In time pressure drop increase, efficiency decrease and release odor. Source of contamination.	[1], [12], [13], [17]
Electrostatic filters	+	-	Lower pressure drop compared to mechanical filter, lower particle removal efficiency. Source of ozone and other compounds. Require high maintenance.	[2], [3], [18], [20]
Adsorbent filter	-	+	Most efficient commercial technology in VOCs removal. Saturation, cause of re-emission. Need regeneration. Humidity and temperature affect the adsorption.	[4], [21]
Photocatalytic oxidant (PCO)	-	+	TiO <sub>2</sub> most investigated photocatalyst. Can degrade a broad range of pollutants. Affected by water vapour and pollutants concentration. Production of harmful by-product.	[5]–[7], [19], [22]
Non-Thermal Plasma (NTP)	+	+	NTP degrades VOC and it removes also particle with low efficiency. Formation of by-products. High energy consumption and low energy efficiency.	[8], [9]
Electrospun nanofiber filters	+	+	High surface-to-volume ratio. Slip flow dominance – lower pressure drop compared to microfiber filter. Versatile. Emerging technology, mostly tested at very low face velocity (0.05-0.20 m/s).	[10], [11], [14]–[16], [23]

## 5. Conclusion

The present review discussed the challenges facing the future air filtration directions and development in achieving sustainable ventilation and acceptable indoor air quality in residential buildings. The results have shown that electrospun nanofiber filters are an emerging technology with promising filtration performance with regards to the simultaneous removal of particle and harmful gases. However, it is necessary to conduct more investigations of such filters in terms of filtration efficiency and pressure drop under realistic ventilation system conditions.

## References

- [1] American Society of Mechanical Engineers 2004 *Addenda to ASME AG-1–2003 Code on Nuclear Air and Gas Treatment*. ASME AG-1a–2004 (ASME).
- [2] Ardkapan S R, Johnson M S, Yazdi S, Afshari A and Bergsøe N C 2014 Filtration efficiency of an electrostatic fibrous filter: Studying filtration dependency on ultrafine particle exposure and composition. *J. Aerosol Sci.* **72** 14–20.
- [3] Lin W, Chang Y, Lien C and Kuo C 2011 Separation Characteristics of Submicron Particles in an Electrostatic Precipitator with Alternating Electric Field Corona Charger. *Aerosol Sci. Technol.* **45** 393–400.
- [4] Chen W, Zhang J S and Zhang Z. 2005 Performance of Air Cleaners for Removing Multiple Volatile Organic Compounds in Indoor Air. *ASHRAE Trans.* **111** 1101–14.

- [5] Debono O, Thevenet F, Gravejat P, Hequet V, Raillard C, Lecoq L and Locoge N 2011 Toluene photocatalytic oxidation at ppbv levels: Kinetic investigation and carbon balance determination. *Appl. Catal. B Environ.* **106** 600–608.
- [6] Vildoza D, Portela R, Ferronato C and Chovelon JM 2011 Photocatalytic oxidation of 2-propanol/toluene binary mixtures at indoor air concentration levels. *Appl. Catal. B Environ.* **107** 347–354.
- [7] Quici N, Vera M, Choi H, Puma G L, Dionysiou D D, Litter M I, Destailats H 2010 Effect of key parameters on the photocatalytic oxidation of toluene at low concentrations in air under 254 + 185 nm UV irradiation. *Appl. Catal. B Environ.* **95** 312–319.
- [8] Yu B F, Hu Z B, Liu M, Yang H L, Kong Q X, and Liu Y H 2009 Review of research on air-conditioning systems and indoor air quality control for human health. *Int. J. Refrig.* **32** 3–20.
- [9] Park J H, Byeon J H, Yoon K Y and Hwang J 2008 Lab-scale test of a ventilation system including a dielectric barrier discharger and UV-photocatalyst filters for simultaneous removal of gaseous and particulate contaminants. *Indoor Air* **18** 44–50.
- [10] Su J, Yang G, Cheng C, Huang C, Xu H and Ke Q 2017 Hierarchically structured TiO<sub>2</sub>/PAN nanofibrous membranes for high-efficiency air filtration and toluene degradation. *J. Colloid Interface Sci.* **507** 386–396.
- [11] Chuang Y H, Hong G B and Chang C T 2014 Study on particulates and volatile organic compounds removal with TiO<sub>2</sub>/nonwoven filter prepared by electrospinning. *J. Air Waste Manag. Assoc.* **64** 738–742.
- [12] Joubert A, Laborde J C, Bouilloux L, Callé-Chazelet S and Thomas D 2010 Influence of humidity on clogging of flat and pleated HEPA filters. *Aerosol Sci. Technol.* **44** 1065–76.
- [13] Chuaybamroong P, Chotigawin R, Supothina S, Sribenjalux P, Larpiattaworn S and Wu C Y 2010 Efficacy of photocatalytic HEPA filter on microorganism removal. *Indoor Air* **20** 246–254.
- [14] Park H and Park Y O 2005 Filtration Properties of Electrospun Ultrafine Fiber Webs. **22** 165–172.
- [15] Wan H, Wang N, Yang J, Si Y, Chen K, Ding B, Sun G, El-Newehy M, Al-Deyab S S and Yu 2014 Hierarchically structured polysulfone/titania fibrous membranes with enhanced air filtration performance. *J. Colloid Interface Sci.* **417** 18–26.
- [16] Xia T, Bian Y, Zhang L and Chen C 2018 Relationship between pressure drop and face velocity for electrospun nanofiber filters. *Energy Build.* **158** 987–999.
- [17] Simmons R B and Crow S A 1995 Fungal colonization of air filters for use in heating, ventilating, and air conditioning (HVAC) systems. *J. Ind. Microbiol.* **14** 41–45.
- [18] Waring M S and Siegel J A 2011 The effect of an ion generator on indoor air quality in a residential room. *Indoor Air* **21** 267–276.
- [19] Mo J, Zhang Y, Xu Q, Lamson J J and Zhao R 2009 Determination and risk assessment of by-products resulting from photocatalytic oxidation of toluene. *Appl. Catal. B Environ.* **89** 570–576.
- [20] Day D B, Xiang J, Mo J, Clyde M A, Weschler C J, Li F, Gong J, Chung M, Zhang Y, Zhang J 2018 Combined use of an electrostatic precipitator and a high-efficiency particulate air filter in building ventilation systems: Effects on cardiorespiratory health indicators in healthy adults. *Indoor Air* **28** 360–372.
- [21] Jo W K and Yang C H 2009 Granular-activated carbon adsorption followed by annular-type photocatalytic system for control of indoor aromatic compounds. *Sep. Purif. Technol.* **66** 438–442.
- [22] Mo J, Zhang Y and Xu Q 2013 Effect of water vapor on the by-products and decomposition rate of ppb-level toluene by photocatalytic oxidation. *Appl. Catal. B Environ.* **132–133** 212–218.
- [23] Sundarrajan S, Tan K L, Lim S H and Ramakrishna S 2014 Electrospun nanofibers for air filtration applications. *Procedia Eng.* **75** 159–163.

## Chapter 5

## Paper II

# Electrospun nanofiber air pollution filters: An experimental study

Roberta Orlando, Peter Fojan, Matthew S. Johnson, Niels C. Bergsøe and  
Alireza Afshari

The paper has been published in the  
*Proceedings of the 16th Conference of the International Society of Indoor Air Quality  
and Climate, Indoor Air 2020.*





## Electrospun nanofiber air pollution filters: An experimental study

Roberta Orlando<sup>1</sup>, Peter Fojan<sup>2</sup>, Matthew S. Johnson<sup>3</sup>, Niels C. Bergsøe<sup>1</sup> and Alireza Afshari<sup>1\*</sup>

<sup>1</sup>Department of the Built Environment, Aalborg University, Copenhagen, Denmark

<sup>2</sup>Department of Materials and Production, Aalborg University, Aalborg, Denmark

<sup>3</sup>Department of Chemistry, University of Copenhagen, Copenhagen, Denmark

*\*Corresponding email: aaf@build.aau.dk*

### SUMMARY

The aim of this study is to develop and assess the performance of electrospun nanofiber air pollution filters for removing particles and gaseous compounds. The performance of the novel filters will be evaluated in terms of electrospinning processes, nanofiber characterization and the filters' pressure drop. Polyurethane (PU) was used to fabricate the nanofibers. The nanofiber surfaces were functionalized using activated carbon (AC) and titanium dioxide TiO<sub>2</sub> to enhance the filters' ability to capture and degrade pollutants. The nanofibers presented different morphologies depending on the presence of the additives. The use of additives decreased the filter pressure drop. Toluene was used to assess the removal of gaseous pollutants from the air stream while ultrafine particles were monitored to quantify particle filtration. The PU filter recorded the highest particle filtration efficiency of 98.1% but it has at the same time a very high pressure drop (3092 Pa), whereas PU/AC achieved a high efficiency of 93.7% with a lower pressure drop of 809 Pa. PU/TiO<sub>2</sub> showed better reactivity towards Toluene while PU/AC has not shown any adsorption probably due to the mixing of AC inside the polymer solution prior to electrospinning.

### KEYWORDS

Electrospinning, nanofibers, air filters, polyurethane, indoor air quality

### 1 INTRODUCTION

Air pollution is a major threat to public health and the environment. Outdoor air pollution entering into buildings contributes to poor indoor air quality, also in combination with indoor sources of pollution (World Health Organization 2006). The removal of air pollutants such as particles and gaseous contaminants is one approach to improving indoor air quality. A large variety of air filtration technologies can be used as part of ventilation systems to reduce the pollutants' concentration in buildings. However, air filtration technologies can be rather selective in which pollutants they remove. In recent years electrospun nanofiber filters have become of increasing interest as their large surface-to-volume ratio promises high removal efficiency for different types of pollutants. The unique opportunities for integrating active catalysts onto the filters' surface inspire interest in electrospun nanofiber filters as a solution that can provide simultaneous filtration of particles and removal of gaseous compounds. Electrospinning is a versatile and effective method to produce nanofiber mats which allows a high variety of materials to be spun, as polymers, polymer composites and ceramics (Li and Xia 2004). Polyurethane (PU) nanofiber filters have been previously fabricated and their filtration performance investigated (Scholten et al. 2011; Wang et al. 2014). The PU nanofibers filters showed toluene sorption capacity comparable to activated carbon (0.32 g toluene/g fiber

for polyurethane compared to 0.35 g toluene/g fiber for activated carbon with a 10% toluene in nitrogen stream) (Scholten et al. 2011). Furthermore, porous nanofibers with TiO<sub>2</sub> showed 99% removal efficiency of acetone with an ultraviolet (UV) light source of 254 nm. The filter also performed well for particulate matter, with a removal efficiency of 90% for particulate sizes over 200 nm (Chuang, Hong, and Chang 2014). Activated carbon can also be incorporated into electrospun nanofiber materials. Activated carbon nanofibers have shown high gas adsorption capacity thanks to their large specific surface area (Lee et al. 2010; Oh et al. 2008). In the current work, polyurethane nanofibers in pure form and with AC and TiO<sub>2</sub> have been prepared using electrospinning. The experimental electrospinning phase and the characterization of the nanofibers are described in this paper. Further, the filtration performance in terms of removal of ultrafine particles and toluene, and the filters' pressure drop have been investigated.

## **2 METHODS**

### **Materials**

In this study the following materials were used: Polyurethane (PU) in a pharmaceutical grade, the organic solvent N,N-dimethylformamide (DMF), Activated Charcoal (AC) in powder form and Aeroxide Titanium Dioxide P25 in a nanopowder form.

### **Preparation of electrospun nanofibers**

Three different solutions were prepared and used in this study. The first solution was a PU solution (9wt%), prepared mixing 9.5 g of PU in 96 g of DMF. The solution was heated to 100-110 °C for 1 hour under vigorous stirring, which was stored for 24 h after cooling. The second solution was prepared mixing 20 ml of PU 9wt% solution with 0.8 g of TiO<sub>2</sub> (tapped density 130 g/L), obtaining a solution of PU 9wt% TiO<sub>2</sub> 3w/v% based on the total solution volume. In the same way, the third solution was prepared with 20 ml of PU 9wt% solution and 0.6 g of Activated Charcoal (density 1.95 g/mL), resulting in a solution of PU 9wt% AC 3w/v%. Nanofiber filters were prepared through downwards vertical electrospinning (Electrospinner 2.2.D-500 – Yflow). The different solutions were loaded in a 10 mL syringe and mounted on the syringe pump inside the electrospinner. The polymer solutions were pumped through a needle of 1.1 mm diameter at a constant rate of 1.3 ml/h and at ambient temperature. The voltage ranged between 12.4 kV to 17.9 kV. The nanofibers were collected on a grounded flat collector wrapped with aluminium foil at a distance of 16.5 cm from the needle.

### **Characterization of nanofibers**

The morphologies and the structures of the nanofibers were investigated using a field emission scanning electron microscope (SEM, Zeiss XB1540) operating at 5 kV. Each sample was coated with a thin layer of gold before scanning.

### **Filtration performance experiment**

The filters' performance was evaluated in terms of pressure drop, VOCs removal and ultrafine particle filtration using the setups presented in Figure 1. Electrospun nanofiber filters with a diameter of 5 cm were placed in the reactor shown in Figure 2, exposing a filtering area of 4 cm diameter. The pressure drop analysis was performed using a Testo 480 differential pressure sensor with resolution of  $\pm 0.1$  Pa and accuracy of  $\pm 0.3$  Pa. The pressure drop was evaluated at different face velocities: 5.3 cm/s, 7.95 cm/s and 10.6 cm/s, to investigate the linear dependency between pressure drop and face velocity defined by Xia et al. 2018. Compressed air was used and the flow divided into wet, dry and polluted streams to reach a face velocity of 5.3 cm/s for

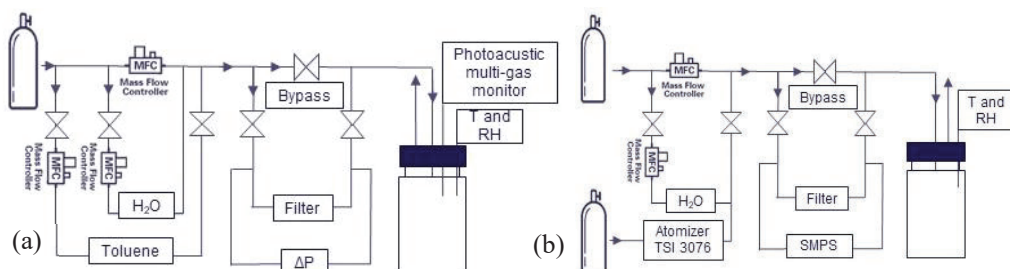


Figure 1. Schematic diagram of the experimental set ups: (a) for VOC removal and pressure drop, (b) for ultrafine particle removal.

both particle and toluene removal experiments. The relative humidity ranged from 47% to 54%. The temperature ranged from 20 to 24 °C. Toluene at 1-1.5 ppm concentration was used to characterise the ability of the AC and TiO<sub>2</sub> doped filters to adsorb and degrade volatile organic compounds (VOC). Toluene was kept in four 1.5 ml GC vials (MACHEREY-NAGEL GmbH & Co. KG) inside a 250 ml gas-washing bottle (Lenz Laborglas GmbH & CO.KG). The concentration of toluene was monitored before and after the filter using the bypass, with a photo-acoustic multi-gas monitor (Model 1302, Bruel&Kjaer) with a filter for TVOC. Water content was also recorded using the same monitor in order to observe the water content variation during the experiments, relevant especially during the photocatalytic oxidation and for cross-compensation purpose. Photocatalytic oxidation was activated using a Xenon lamp through a bandpass filter, with a peak wavelength of 335 nm. NaCl in a Milli-Q water solution at a concentration of 0.00012 g/cm<sup>3</sup> was used as the basis for particle formation from a constant output atomizer (Model 3076, TSI). Total average particle mass density was 91.1 µg/m<sup>3</sup>, monitored using a Scanning Mobility Particle Sizer (SMPS, Model 3080C, TSI) for particle sizes between 11.8 nm and 478.3 nm. Only ultrafine particles were monitored as the typical Most Penetrating Particle Sizes for most filters is in between 0.1 and 0.3 µm (Kadam, Wang, and Padhye 2018). The filtration efficiency  $\eta$  was calculated using the following formula



Figure 2. Filter's reactor

$$\eta = (C_1 - C_2)/C_1 \times 100 \quad (1)$$

where  $C_1$  and  $C_2$  are concentrations of toluene (ppm) or particles (µg/m<sup>3</sup>) before and after the filters, respectively.

### 3 RESULTS AND DISCUSSIONS

#### Characterization of PU nanofibers

SEM images of the pure PU filter and the filters with PU/AC and PU/TiO<sub>2</sub> are shown in Figures 3(a), (b), (c) and (d). The three filters have a non-uniform nanofiber morphology. The SEM images show a tendency for adhesion among adjacent fibers. This phenomenon is attributed to the physical properties of the solvent, DMF, which has a high boiling point (153 °C) resulting in a slow evaporation rate. Therefore, the DMF had not fully evaporated between the tip of the needle and the collector during electrospinning, yielding the structure that can be seen in Figure 3. Adhesion of PU fibers manufactured using DMF has been reported in previous studies (Jeong, Yang, and Youk 2007; Wang et al. 2014). The bead formations visible in Figures 3a and 3b are

related to the non-complete evaporation of DMF during electrospinning. In Figure 3c and 3d TiO<sub>2</sub> is clearly visible in the form of agglomerate of nanoparticles.

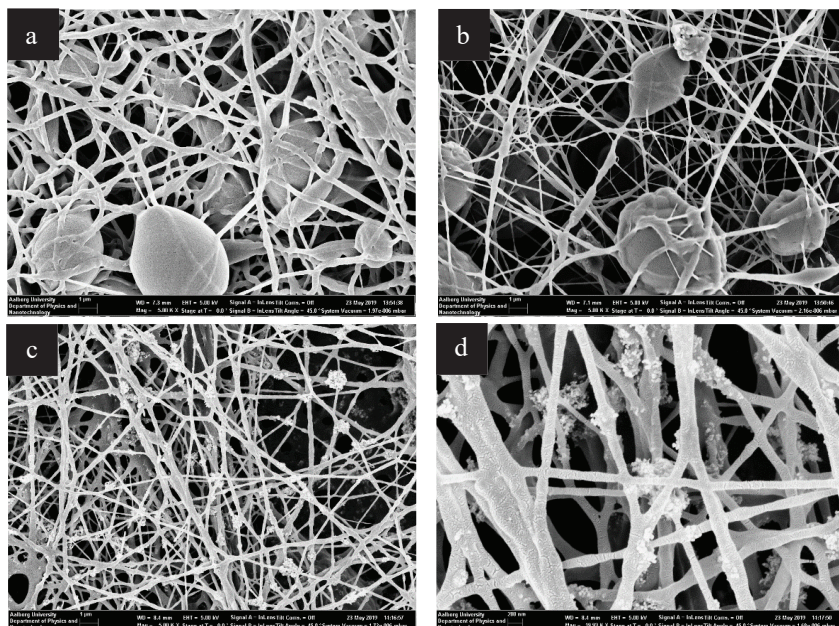


Figure 3. SEM pictures of (a) pure PU, (b) PU/AC and (c) and (d) PU/TiO<sub>2</sub> electrospun nanofibers.

### Pressure drop

The linear regression and its coefficient of determination ( $R^2$ ) was used to investigate the relation between pressure drop and face velocity, as shown in Figure 4. The results confirmed the linear dependency with  $R^2$  above 0.989. The lowest pressure drop was seen for the PU/AC filter, with a pressure drop of 809 Pa at a face velocity of 5.3 cm/s. The use of additives decreases the pressure drop of the filters, with a reduction of 73.8% for PU/AC and 26% for PU/TiO<sub>2</sub> compared to the pure PU nanofiber filter. This phenomenon has also been observed by Wan et al. 2014 for TiO<sub>2</sub> doped polysulfone-based nanofibers.

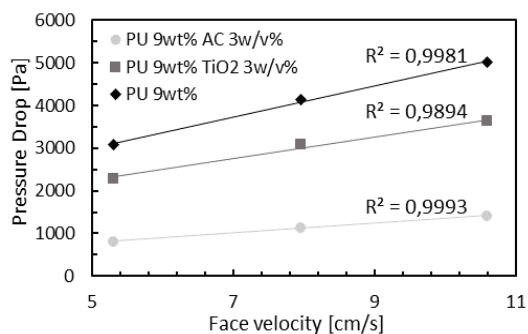


Figure 4. Pressure drop versus face velocity for PU, PU/AC and PU/TiO<sub>2</sub>

### VOC adsorption and degradation

The pure PU and PU/AC filters did not show any toluene removal through adsorption. As Scholten et al. 2011 explained in their study, PU is a polymer with a specific (mass-weighted) adsorbent ability comparable to activated carbon. The question is what surface the samples present to the airstream, which depends on the method of preparation. PU was not synthesized in the same way in this study as in the literature, as it was prepared through a commercial preparation. In previous studies, activated carbon was formed on the nanofiber surface through carbonization, after electrospinning (Lee et al. 2010; Oh et al. 2008). In contrast, in the work



presented here, activated carbon was added into the polymer solution in a powder form prior to electrospinning. In this configuration, the dissolved polymer is likely to wet the surface of the AC, covering it when the solvent evaporates. The performance of the PU/TiO<sub>2</sub> filters are shown in Figure 5a. When the toluene flowed into the filter, no change of concentration was detected by the multi-gas monitor. When the Xenon light was switched on, a steep increase of TVOC was observed until the light has been removed. At the same time, the water content in the air stream also increased. This indicates that the photocatalytic oxidation of toluene is activated, as water and other by-products in the form of VOCs are produced in the photocatalysis of toluene. The multi-gas monitor shows the TVOC concentration and does not distinguish between different product VOCs.

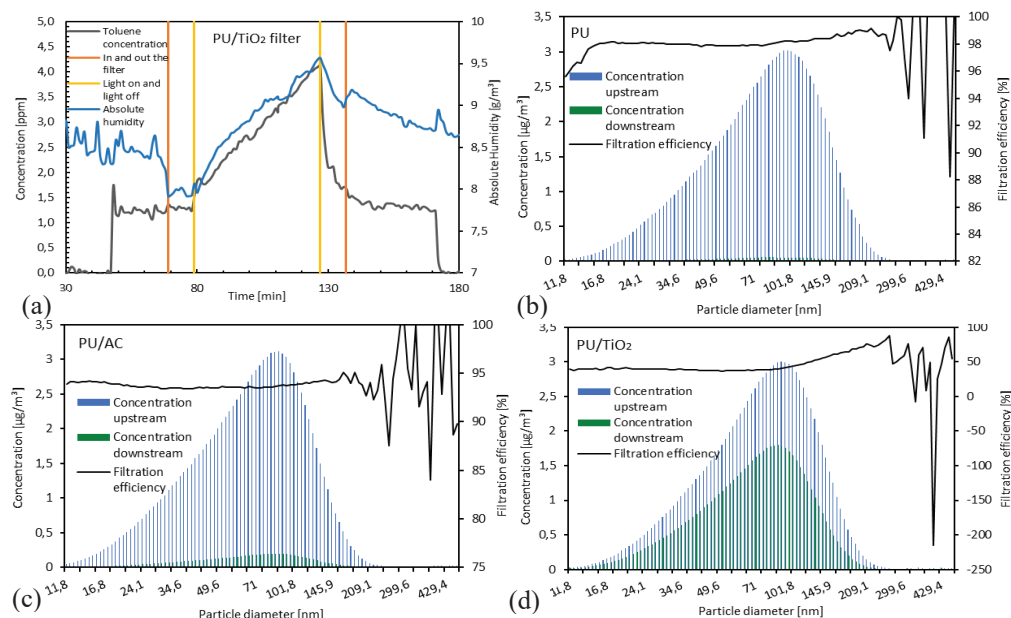


Figure 5. Results from (a) photocatalytic oxidation of toluene with PU/TiO<sub>2</sub> filter and ultrafine particle removal using (b) PU, (c) PU/AC and (d) PU/TiO<sub>2</sub>.

### Ultrafine particle removal efficiency

The filters' removal efficiency as a function of particle size is shown in Figure 5b, 5c and 5d. The PU filter has a total removal efficiency of 98.1%, while PU/AC filter showed an efficiency of 93.7% and PU/TiO<sub>2</sub>, 42.8%. These results have an expanded uncertainty of maximum 5.0% within the confidence interval of 95%. The lower efficiency of the PU/TiO<sub>2</sub> filter could be due to static electrical charging (Ding and Yu 2014). Aerosols in the atmosphere carry small positive or negative static charges. Similarly, particles created by the atomizer have an electric charge, which was not neutralized. Some of the electrons excited in the photocatalyst by light can leave the surface resulting in a net positive surface charge, repulsing the positively charged particles and absorbing neutral and negatively charged ones. The PU filter showed stable efficiency around 98% with particle sizes between 15.1 nm and 98.2 nm. For particle sizes below 15.1 nm, the efficiency is lower with a minimum of 95.6% for particle size 11.8 nm. Above 98.2 nm, the filtration efficiency rose, reaching a peak of 99.2% for particles with size 216.7 nm. Above this size, there were not enough particles to get a statistically meaningful result. A decrease of efficiency for small particles is not observed in PU/AC filter. PU/AC filter achieved a stable efficiency of around 94%. The PU/TiO<sub>2</sub> filtration efficiency varied between 37% and 41% for particle sizes below 94.7 nm. Above this size value, the efficiency showed a steep increase, reaching a maximum at 87.9% removal for size 259.5 nm.

## 5 CONCLUSIONS

The PU, PU/AC and PU/TiO<sub>2</sub> filters showed a pressure drop respectively of 3092 Pa, 809 Pa and 2287 Pa. The PU and PU/AC filters did not adsorb toluene, while photocatalytic oxidation in the PU/TiO<sub>2</sub> filter was successfully activated using a Xenon light. Ultrafine particles were removed with a total removal efficiency of 98.1% for PU, 93.7% for PU/AC and 42.8% for PU/TiO<sub>2</sub> filter. The filters are not suitable for indoor air quality application as part of a ventilation system due to their high pressure drop.

## 6 ACKNOWLEDGEMENT

The author would like to thank the Research Technician Peter Kjær Kristensen from the Department of Materials and Production at Aalborg University for his support. The project is financially supported by Grundejernes Investeringsfond, the Department of the Built Environment and the Department of Materials and Production at Aalborg University.

## 7 REFERENCES

- Chuang, Yi Hsuan, Gui Bing Hong, and Chang Tang Chang. 2014. "Study on Particulates and Volatile Organic Compounds Removal with TiO<sub>2</sub>nonwoven Filter Prepared by Electrospinning." *Journal of the Air and Waste Management Association* 64(6):738–42.
- Ding, Bin and Jianyong Yu. 2014. *Electrospun Nanofibers for Energy and Environmental Applications*. edited by D. J. Lockwood and National Research Council of Canada. Springer.
- Jeong, Eun Hwan, Jie Yang, and Ji Ho Youk. 2007. "Preparation of Polyurethane Cationomer Nanofiber Mats for Use in Antimicrobial Nanofilter Applications." *Materials Letters* 61(18):3991–94.
- Kadam, Vinod V., Lijing Wang, and Rajiv Padhye. 2018. "Electrospun Nanofibre Materials to Filter Air Pollutants – A Review." *Journal of Industrial Textiles* 47(8):2253–80.
- Lee, Kyung Jin, Nanako Shiratori, Gang Ho Lee, Jin Miyawaki, Isao Mochida, Seong Ho Yoon, and Jyongsik Jang. 2010. "Activated Carbon Nanofiber Produced from Electrospun Polyacrylonitrile Nanofiber as a Highly Efficient Formaldehyde Adsorbent." *Carbon* 48(15):4248–55.
- Li, Dan and Younan Xia. 2004. "Electrospinning of Nanofibers: Reinventing the Wheel?" *Advanced Materials* 16(14):1151–70.
- Oh, Gil Young, Young Wan Ju, Hong Ryun Jung, and Wan Jin Lee. 2008. "Preparation of the Novel Manganese-Embedded PAN-Based Activated Carbon Nanofibers by Electrospinning and Their Toluene Adsorption." *Journal of Analytical and Applied Pyrolysis* 81(2):211–17.
- Scholten, Elke, Lev Bromberg, Gregory C. Rutledge, and T. Alan Hatton. 2011. "Electrospun Polyurethane Fibers for Absorption of Volatile Organic Compounds from Air." *ACS Applied Materials and Interfaces* 3(10):3902–9.
- Wan, Huigao, Na Wang, Jianmao Yang, Yinsong Si, Kun Chen, Bin Ding, Gang Sun, Mohamed El-Newehy, Salem S. Al-Deyab, and Jianyong Yu. 2014. "Hierarchically Structured Polysulfone/Titania Fibrous Membranes with Enhanced Air Filtration Performance." *Journal of Colloid and Interface Science* 417:18–26.
- Wang, Na, Zhigao Zhu, Junlu Sheng, Salem S. Al-Deyab, Jianyong Yu, and Bin Ding. 2014. "Superamphiphobic Nanofibrous Membranes for Effective Filtration of Fine Particles." *Journal of Colloid and Interface Science* 428:41–48.
- World Health Organization. 2006. *WHO. Air Quality Guidelines : Global Update 2005. Particulate Matter, Ozone, Nitrogen Dioxide and Sulfur Dioxide*.
- Xia, Tongling, Ye Bian, Li Zhang, and Chun Chen. 2018. "Relationship between Pressure Drop and Face Velocity for Electrospun Nanofiber Filters." *Energy and Buildings* 158:987–99.

## Chapter 6

### Paper III

# Electrospun Nanofibre Air Filters for Particles and Gaseous Pollutants.

Roberta Orlando, Merve Polat, Alireza Afshari, Matthew S. Johnson and  
Peter Fojan

The paper has been published in  
*Sustainability*, Vol. 13(12), 6553, 2021.





## Article

# Electrospun Nanofibre Air Filters for Particles and Gaseous Pollutants

Roberta Orlando <sup>1</sup>, Merve Polat <sup>2</sup>, Alireza Afshari <sup>1,\*</sup>, Matthew S. Johnson <sup>2</sup> and Peter Fojan <sup>3</sup><sup>1</sup> Department of the Built Environment, Aalborg University, DK-2450 Copenhagen, Denmark; ror@build.aau.dk<sup>2</sup> Department of Chemistry, University of Copenhagen, DK-2100 Copenhagen, Denmark; mp@chem.ku.dk (M.P.); msj@chem.ku.dk (M.S.J.)<sup>3</sup> Department of Materials and Production, Aalborg University, DK-9220 Aalborg, Denmark; fp@mp.aau.dk

\* Correspondence: aaf@build.aau.dk

**Abstract:** Nanofibre filters may offer new properties not available in commercial fibre filters. These include a higher surface area and the ability to include novel materials within the fibres. In addition the small size allows potential gains in performance due to the slip-flow phenomenon in which normal gas viscosity does not apply to objects smaller than the mean free path of the gas. We tested the properties of novel electrospun fibre filters generated from polyvinyl alcohol solutions, optionally embedded with nano-grains of photocatalytic TiO<sub>2</sub> and activated charcoal. The tested materials exhibited pressure drops in the range of 195 Pa to 2693 Pa for a face velocity of 5.3 cm/s and a removal efficiency greater than 97% for 12–480 nm particles. Basis weights for the filters ranged from 16.6 to 67.6 g/m<sup>2</sup> and specific surface areas ranged from 1.4 to 17.4 m<sup>2</sup>/g. Reactivity towards volatile organic compounds (VOCs) was achieved by irradiating the photocatalytic filters with ultraviolet light. It is necessary to solve the problems connected to the absorbance of VOCs and further reduce the resistance to airflow in order for these filters to achieve widespread use. The incorporation of reactive air filtration into building ventilation systems will contribute to improved indoor air quality.



**Citation:** Orlando, R.; Polat, M.; Afshari, A.; Johnson, M.S.; Fojan, P. Electrospun Nanofibre Air Filters for Particles and Gaseous Pollutants. *Sustainability* **2021**, *13*, 6553. <https://doi.org/10.3390/su13126553>

Academic Editor: Luca Stabile

Received: 23 March 2021

Accepted: 4 June 2021

Published: 8 June 2021

**Publisher's Note:** MDPI stays neutral with regard to jurisdictional claims in published maps and institutional affiliations.



**Copyright:** © 2021 by the authors. Licensee MDPI, Basel, Switzerland. This article is an open access article distributed under the terms and conditions of the Creative Commons Attribution (CC BY) license (<https://creativecommons.org/licenses/by/4.0/>).

**Keywords:** poly(vinyl alcohol); electrospinning; nanofibres; air filters; titanium dioxide; activated charcoal

## 1. Introduction

Air pollution is responsible for an estimated global mortality rate of 8.8 million/year and an estimated loss of life expectancy of 2.9 years [1]. This is higher than the mortality rate for tobacco smoke (active and passive), estimated at 7.2 million/year by the World Health Organization (WHO) [2]. The loss of life expectancy from air pollution exceeds that of all forms of violence, HIV/AIDS, and smoking [1]. Several studies have reported correlations between outdoor air pollution and cardiovascular and respiratory diseases [3–6].

As people now spend most of their lives indoors, most exposure to air pollution occurs inside buildings. The origin of such indoor air pollutants is either the outdoor air pollution entering buildings or indoor sources, including cooking, cleaning products, office equipment, chemical reactions with indoor materials, and different biological sources, such as pets, people, and mould [7]. Air pollution is based on a mixture of numerous components, including solid substances, such as particles, and gaseous pollutants, such as volatile organic compounds (VOCs), carbon monoxide (CO), sulphur dioxide (SO<sub>2</sub>), ozone, and nitrogen dioxide (NO<sub>2</sub>) [8]. The removal of pollutants through air filters as part of the building ventilation system is a common solution to ensure adequate indoor air quality. In addition filters are used to ensure sufficient supply of clean air from outside the building.

Particles and VOCs can be filtered or removed using different types of filters available on the market. Conventional fibre filters are commonly used in ventilation systems to remove coarse, fine, and even ultrafine particles. Adsorption, condensation, membrane separation, and thermal or catalytic oxidation are some of the methods available for

the removal or destruction of VOCs [9,10]. Commercial fibrous filters usually achieve a high filtration efficiency combined with the requirement of a high pressure drop (typical behaviour for HEPA filters) because of their multilayered structure of relatively thick fibres in the diameter range from a few to tens of micrometres. Every fibre filter resists the flow of air, resulting in a pressure drop. In SI units, the pressure drop is measured using  $\text{Pa} = \text{J m}^{-3}$ . Multiplying the pressure drop by a flow (e.g.,  $\text{m}^3/\text{s}$ ), results in the Watts of power needed to sustain the flow as  $W = \text{J/s}$ . Thus, a large amount of energy is used to filter air. In commercial buildings with an installed rooftop HVAC unit, the fan energy needed to move the air accounts for 7% of the total building energy use [11].

Nanofibre air filters are of increasing interest because of their larger surface-to-volume ratio, lower air resistance, and enhanced filtration performance compared with conventional microfibre filters [12]. According to theoretical models, the use of nanofibres should lead to a smaller pressure drop than for a microfibre filter of the same particle cleaning efficiency by taking advantage of slip flow. Slip flow is a phenomenon in which the friction of a gas passing an object decreases when the object is smaller than the mean free path of the molecules in the gas, which is around 65 nm for air [13]. Recently, a filter was fabricated and tested, and the authors demonstrated this effect for electrospun nanofibres [14].

Electrospinning is a versatile and effective method for producing polymer-based nanofibres. The electrospinning setup consists of the following basic components: a syringe pump, including tubes and a needle where the polymer solution is kept and carried from the syringe cylinder to the tip of the needle; a high-voltage electric source connected to the needle; and a collector connected to the ground. High voltage is applied to the fluid, which overcomes its surface tension and forms a so-called Taylor cone on the needle tip. The fluid elongates in a jet form, and as it moves towards the collector, the solvent evaporates. The result is nanofibre formation with a diameter ranging from about 50 to 500 nm, deposited on the collector [15]. The critical advantage of electrospinning is related to the unique opportunity of integrating active catalysts onto the fibre surface to provide the simultaneous filtration of particles and the removal of gaseous compounds [16].

A wide variety of materials can be spun, such as polymers, composites, and ceramics [17]. Many high-molecular-weight polymers have been electrospun in previous research studies, including polyurethane [18], polyvinylpyrrolidone [19], polysulfone (PSU) [20], polyacrylonitrile (PAN) [14,21], and poly(vinyl alcohol) (PVA) [22–24]. Zhao et al. [14] fabricated PAN-based electrospun nanofibre membranes to investigate the slip flow phenomenon and evaluate the filtration performance. Optimising the fabrication parameters, the authors obtained a low pressure drop of 29.5 Pa under a face velocity of 5.3 cm/s and the filtration of particulate matter with an aerodynamic diameter below 2.5  $\mu\text{m}$  ( $\text{PM}_{2.5}$ ) of 99.09%. Wang et al. [22] demonstrated that PVA nanofibres electrospun on a conventional cotton scaffold can achieve a higher filtration efficiency for particles under 1  $\mu\text{m}$  compared with conventional fibrous filters. Compared with other polymers, such as PAN, which is soluble in N,N-dimethylformamide, a highly toxic organic solvent, PVA is a water-soluble, biodegradable polymer, which makes it a more sustainable choice for fabricating air filters.

Several additives have been investigated in regards to their capacity to enhance the filtration selectivity of electrospun nanofibre filters, including titanium dioxide ( $\text{TiO}_2$ ) and activated charcoal (AC). Polymer-based activated carbon nanofibres have exhibited doubled formaldehyde absorbance capacity compared with conventional activated carbon fibres with a larger fibre diameter [21], a toluene adsorption capacity of above 65 g of toluene/100 g of composite [25,26] and NO removal in the air at room temperature, as stated in [27]. Activated carbon is usually produced on the nanofibre surface through carbonisation after electrospinning [21,25–27]. Wan et al. [20] demonstrated that a PSU/ $\text{TiO}_2$  membrane has an improved filtration efficiency (99.997%) for 300- to 500-nm sodium chloride particles and a pressure drop (43.5 Pa) under an airflow of 30 L/min compared with a pristine PSU nanofibre filter. Titanium dioxide has been widely used as a catalyst to initiate photocatalytic oxidation and degrade VOCs [10,23]. The PVA/ $\text{TiO}_2$  electrospun nanofibre filter exhibited 99% removal efficiency of acetone with an ultraviolet light source at 254 nm

and a retention time of 100 s. The filter also performed well for air particles, with a removal efficiency of 90% for particles over 200 nm [23].

The hypothesis of this study is that composite electrospun nanofibre filters will be better than conventional fibre filters in simultaneously removing particles and gaseous pollutants, with a reduced pressure drop, including in the context of indoor air quality. The objective of the study is to develop a PVA-based electrospun nanofibre filter that is effective for both particle filtration and gaseous contaminant removal. Ideally, the resulting filter will have a pressure drop that has a minimal impact on building energy use when installed in the HVAC system. The assumption is that the electrospun PVA nanofibre filter will remove particles through interception and diffusion. In contrast, additives, such as  $\text{TiO}_2$  or activated carbon, mixed inside the polymer solution prior to electrospinning, chemically activate the filter towards gaseous compounds and promote the degradation or absorbance of gaseous pollutants. The nanofibre dimension promotes slip flow which will ideally allow the filter to function with minimal pressure drop.

The electrospinning process and nanofibre characterisation are presented in this paper. Furthermore, the experimental study results are described and discussed regarding the filtration performance for the degradation of toluene, the removal of 12- to 480-nm diameter particles, and the filter pressure drop.

Ideally, the filter developed here would find use in improving indoor air quality in residential and office buildings. The low pressure drop would ensure that the use of the filter would impact building energy use as little as possible while simultaneously removing particles and gaseous pollutants with a single stage filtration technology.

## 2. Materials and Methods

### 2.1. Materials

Poly(vinyl alcohol) (PVA, MW 89,000–98,000 g/mol, 99+% hydrolysed) and AC (MW 12.01 g/mol) in powder form were purchased from Sigma-Aldrich. Aeroxide  $\text{TiO}_2$  P25 in nanopowder form was a gift from Evonik Industries. Ethanol 96% vol and distilled water were used as received. The materials were used without further purification.

### 2.2. Fabrication of Electrospun Nanofibre Filters

The solutions were prepared by mixing the materials at different ratios. The PVA (10 w/v%) was prepared by adding 5 g of PVA into 50 mL of distilled water at 90–100 °C under vigorous stirring until the polymer was completely dissolved. In addition, 1 g and 2.5 g of AC were dispersed separately in 10 mL of ethanol and then added to the polymer solutions (5 g of PVA dissolved into 40 mL of distilled water) and stirred for 1 h. Two different solutions were prepared by mixing 2.5 g of  $\text{TiO}_2$  into 15 mL of ethanol. One was added to a solution of 5 g of PVA dissolved into 35 mL of distilled water. The second was mixed into 4 g of PVA dissolved in 35 mL of distilled water.

The electrospinning setup consisted of a syringe pump, a high-voltage power supply, a flat plate, and a 1.1 mm inner diameter needle. Electrospinning was performed in an upward vertical configuration. The different solutions were loaded in 10 mL syringes, which were inserted into the electrospinning setup. The electrospinning parameters were considered and tuned during the experiment to reach stability are the tip-to-collector distance (TCD), applied voltage, and the feed rate of the polymer solution. The TCD was set between 16 and 19.5 cm, whereas the applied voltage ranged from 11.1 to 25.7 kV. The feed rate varied between 0.12 and 1 mL/h.

### 2.3. Nanofibre Characterisation

The surface morphology of the filter samples was evaluated using scanning electron microscopy (SEM; Zeiss XB1540), operating at 5 kV. Before scanning, the samples were coated with a thin layer of gold. The average fibre diameter was determined by analysing the SEM pictures using the DiameterJ plugin to the ImageJ software (NIH, USA). Specific surface areas (SSAs) were characterised using the Brunauer–Emmett–Teller (BET) method.

Total pore volume and pore size were estimated using the Barrett–Joyner–Halenda (BJH) method. A BET instrument from the company Quantachrome, the Autosorb 1-MP, was used for this purpose. The samples were degassed at 50 °C. The surface area of the samples was measured by nitrogen adsorption using the BET equation at 77.3 K. The integrity of the materials and the presence of solvent in the filters were investigated using Fourier transform infrared spectroscopy (FTIR; LUMOS, Bruker Corporation, Billerica, MA, USA) on the pure PVA filter in the spectral range between 600 and 4000  $\text{cm}^{-1}$  with a resolution of 2  $\text{cm}^{-1}$ . Furthermore, the Raman spectra of PVA and PVA/TiO<sub>2</sub> filter samples were recorded using a Renishaw InVia spectrometer with 532 nm laser excitation. Thermogravimetric analysis (TGA; Discovery TGA, TA Instruments, New Castle, DE, USA) was performed on the PVA sample from 26 to 60 °C at a heating rate of 5 °C/min in the air.

#### 2.4. Investigation of Filtration Performance

The filtration performance of the PVA-based filter samples was investigated for pressure drop, particle filtration, and VOC removal. The nanofibre materials were cut into 5.1 cm diameter filters and weighed using an electronic balance to measure the filter basis weight. Each filter was placed into a reactor with a 4 cm diameter filtration area. The pressure drop was evaluated at three different face velocities (5.3 cm/s, 7.95 cm/s, 10.6 cm/s) to investigate the correlation between the pressure drop and face velocity [28]. The Testo 480 differential pressure sensor was used, with a resolution of  $\pm 0.1$  Pa and an accuracy of  $\pm 0.3$  Pa. Before starting the pressure measurement, the background pressure drop of the reactor was measured for each face velocity.

The particle filtration and VOC removal investigations were performed at a face velocity of 5.3 cm/s using compressed air divided into wet, dry, and polluted streams. The air temperature was between 20 and 24 °C. The relative humidity ranged between 47 and 54%.

The setup built to evaluate the pressure drop and VOC removal of the electrospun nanofibre filters is presented in Figure 1. Toluene at a concentration between 1 and 1.5 ppm was used as a reference pollutant to evaluate the ability of the PVA/AC and PVA/TiO<sub>2</sub> filters to adsorb and degrade VOCs. The toluene concentration was adjusted by flowing dry and clean air into a 250 mL gas-washing bottle with four 1.5 mL G-vials of toluene inside. A photo-acoustic multigas monitor (Model 1302, Brüel&Kjær, Nærum, Denmark) with a filter for the total VOCs (TVOCs) was employed to track the concentration before and after the filter through a flow splitter, as illustrated in Figure 1. It was also possible to record the water content through the photo-acoustic monitor, which is relevant for cross-compensation purposes and to understand the photocatalytic oxidation reactions. Photocatalytic oxidation was initiated using a high-pressure Xenon lamp (ILC technology R100-IB) through a bandpass filter with a peak wavelength of 335 nm.

For the particle filtration experiments, the setup in Figure 2 was used. A constant output atomiser (Model 3076, TSI, Shoreview, MN, USA) was used for particle formation, employing sodium chloride in a Milli-Q water solution with a concentration of 0.12 mg/cm<sup>3</sup>. A scanning mobility particle sizer (SMPS, Model 3080C, TSI) examined the particle mass density and size distribution between 12 and 480 nm. The most penetrating particle size for air filters was between 0.1 and 0.3  $\mu\text{m}$ ; therefore, the air filters were only investigated against particles of this size range [15]. The total average particle mass density was 110.5  $\mu\text{g}/\text{m}^3$ .

The filtration efficiency  $\eta$  was calculated using the following equation:

$$\eta = (C_1 - C_2) / C_1 \times 100, \quad (1)$$

where  $C_1$  and  $C_2$  are the toluene mole fraction (ppm) and particle mass density ( $\mu\text{g}/\text{m}^3$ ) before and after the filter, respectively.

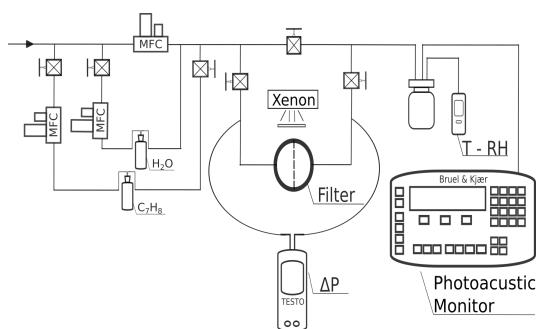


**Figure 1.** Setup used to study the pressure drop and volatile organic compound removal for various filters.

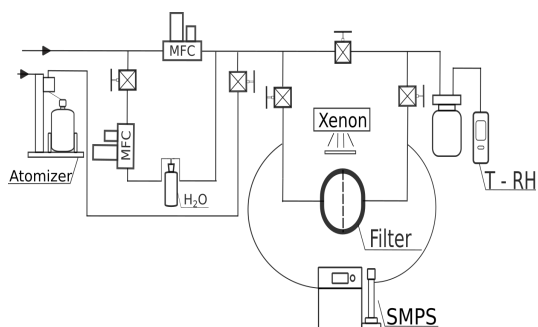


**Figure 2.** Setup used for studying the filtration efficiency of various filters.

### 3. Results and Discussion

#### 3.1. Electrospinning

Polymer solutions were prepared with a PVA concentration from 6  $w/v\%$  to 12  $w/v\%$ , and each was electrospun to assess the electrospinning stability. Once the polymer concentration was selected (10  $w/v\%$ ), the additives were added, and their concentrations were increased until the electrospinning of the polymer/additive solution showed a steady development. The electrospinning results were listed in Table 1, where the polymer/solvent ratio, additive concentration, TCD, applied voltage, and feed rate for each solution are given. Each filter was assigned a tag based on the chemical composition of the electrospun solution to simplify the referencing of the filters. Stable electrospinning depends on the concurrence of factors, such as the polymer concentration and the solvent used, which defined the viscosity and surface tension of the polymer solution and the involved electrospinning parameters (TCD, feed rate, and voltage). The values in Table 1 present stable and constant electrospinning which allowed the formation of the nanofibre filters. The last filter contained a lower polymer concentration than that of the other four samples because the polymer solution viscosity was increased by adding  $\text{TiO}_2$ . Therefore, 8  $w/v\%$  of PVA was sufficient to reach a constant electrospinning condition. Ethanol was used as a solvent with water when the additives were included in the polymer solution. For the AC, ethanol was necessary to decrease the dielectric constant of the solution and avoid the phase separation because AC is very hydrophobic. In addition, ethanol was employed to decrease the surface tension of the polymer solutions and favour the formation of nanofibres.

#### 3.2. Nanofibre Characterisation

##### 3.2.1. Scanning Electron Microscopy, Fibre Diameter and BET Analysis

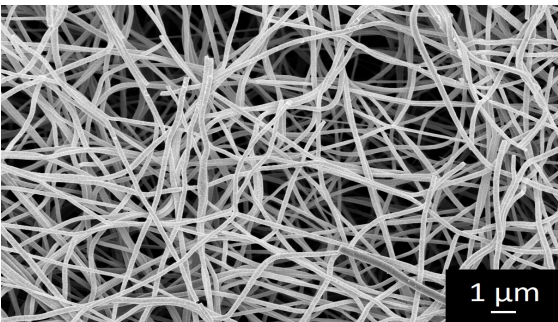
The nanofibre morphologies of the PVA filter and the doped filter with PVA/AC and PVA/ $\text{TiO}_2$  are presented in Figure 3, revealing the randomly oriented structures of the

nanofibres. The pure PVA nanofibres presented a uniform morphology, and although they are rather brittle, as observed by the number of broken fibres in Figure 3a. The use of additives has an important effect on the nanofibre structures. The PVA/AC nanofibres in Figure 3b,c present less uniformity, characterised by the presence of the bead structures. A clear protuberance is visible in Figure 3c, which is formed from an agglomerate of AC nanoparticles. Compared with the smooth pure PVA nanofibres, the PVA/TiO<sub>2</sub> morphology is characterised by a nonuniform and bulky structure, formed by an agglomeration of TiO<sub>2</sub> nanoparticles, as illustrated in Figure 3d,e.

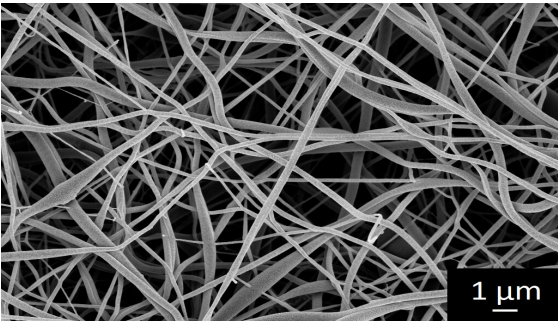
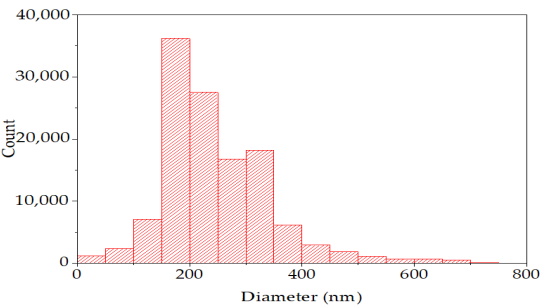
Table 1. Composition of polymer solutions and electrospinning conditions to fabricate filters.

	10PVA	10PVA2AC	10PVA5AC	10PVA5TiO <sub>2</sub>	8PVA5TiO <sub>2</sub>
Solution	PVA 10 w/v%	PVA 10 w/v% AC 2 w/v%	PVA 10 w/v% AC 5 w/v%	PVA 10 w/v% TiO <sub>2</sub> 5 w/v%	PVA 8 w/v% TiO <sub>2</sub> 5 w/v%
PVA (g)	5	5	5	5	4
H <sub>2</sub> O (mL)	50	40	40	35	35
Etanol (mL)	-	10	10	15	15
AC (g)	-	1	2.5	-	-
TiO <sub>2</sub> (g)	-	-	-	2.5	2.5
TCD (cm)	16.5	16	16	19.5	16
Voltage (kV)	20.3–25.7	13.5	13.5	13.5–16.5	11.1
Feed rate (mL/h)	0.23	0.12	0.12	0.12	1

PVA: polyvinyl alcohol; AC: activated charcoal; TCD: tip-to-collector distance.



(a) 10PVA



(b) 10PVA2AC

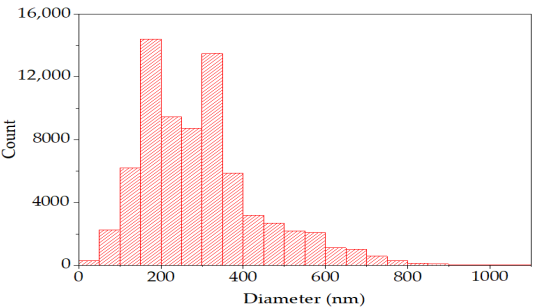
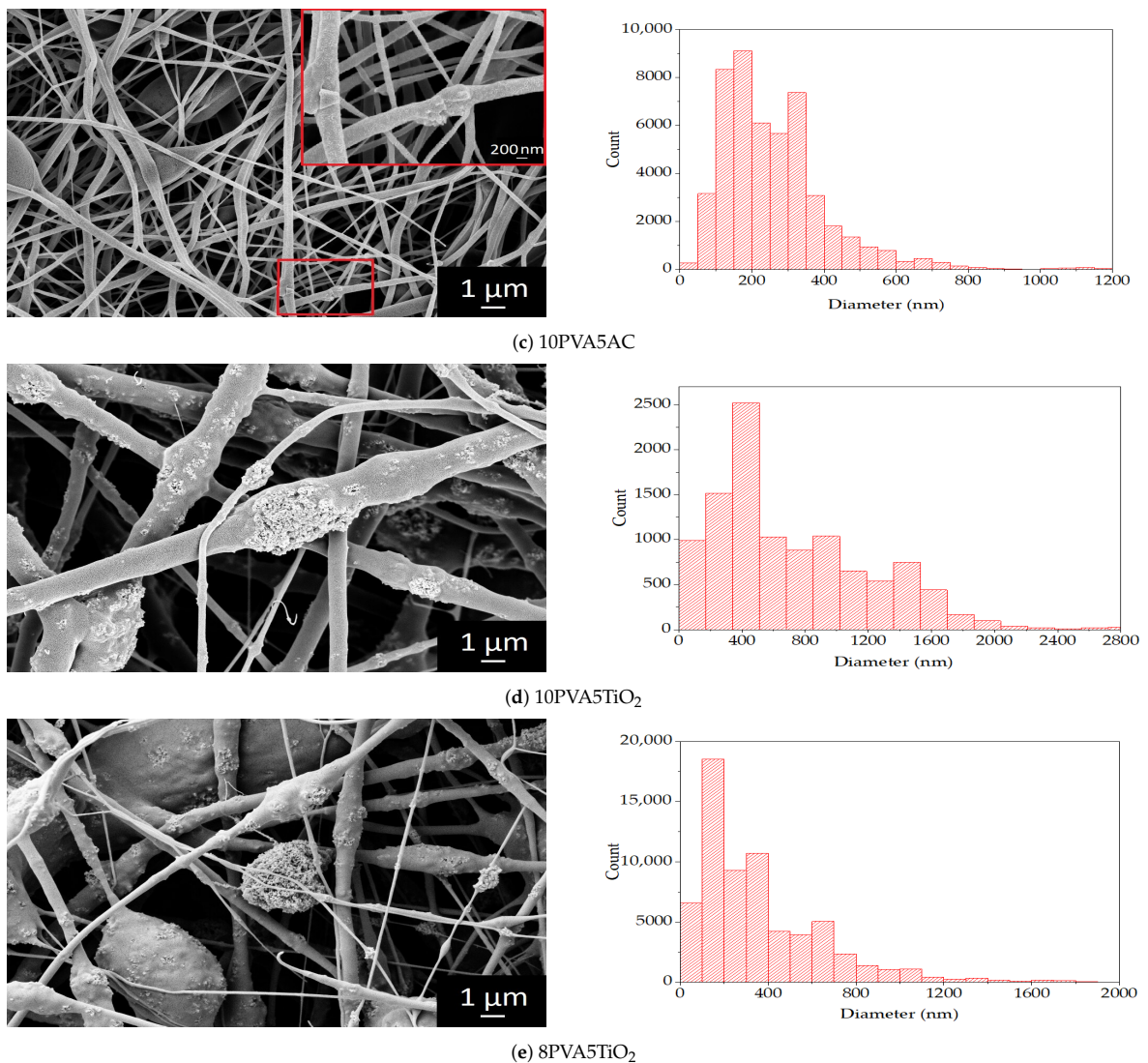


Figure 3. Cont.





**Figure 3.** Scanning electron microscopy images of nanofibre filter samples and the related nanofibre diameter distribution.

The analysis results of the fibre diameters in terms of average size are presented in Table 2, whereas the fibre diameter distribution graphs were displayed in Figure 3. The smallest diameter of the pure PVA nanofibre filter was 213 nm, with a distribution reaching 800 nm. Moreover, the 10PVA5TiO<sub>2</sub> filter has the widest fibres with an average diameter of 430 nm, with fibres that reached 2.8 μm.

The filters present considerably different average diameters due to the different electrospinning conditions employed to fabricate them. The 10PVA filter was electrospun at a voltage higher than 20.3 kV and at a 0.23 mL/h feed rate, compared with 13.5 kV and 0.12 mL/h for the two PVA/AC filters. Decreasing the voltage and feed rate, the 10PVA2AC and 10PVA5AC filters showed an increase in the average diameter of 33% and 24%, respectively. This result indicates that the voltage and feed rate affected the fibre diameter, as mentioned in the literature [29,30]. There is a more significant increase in the diameter

for the two PVA/TiO<sub>2</sub> filters. The average diameter of the fibres in the 10PVA5TiO<sub>2</sub> filter is twice that of the pure PVA nanofibres (430 nm).

**Table 2.** Results of the fibre diameter analysis, basis weight calculation, and BET measurements; specific surface area (SSA), average pore diameter, and total pore volume for pores smaller than 31,917.2 Å.

Filter	Fibre Average Diameter (µm)	STD (µm)	Basis Weight (g/m <sup>2</sup> )	SSA (m <sup>2</sup> /g)	Average Pore Diameter (Å)	Total Pore Volume (cm <sup>3</sup> /g)
10PVA	0.213	0.027	23.5	7.910	30.16	$5.965 \times 10^{-3}$
10PVA2AC	0.283	0.047	16.6	8.519	41.47	$8.889 \times 10^{-3}$ *
10PVA5AC	0.264	0.04	17.6	17.43	31.26	$1.362 \times 10^{-2}$
10PVA5TiO <sub>2</sub>	0.430	0.083	67.6	1.434	32.48	$1.165 \times 10^{-3}$
8PVA5TiO <sub>2</sub>	0.301	0.055	31.8	2.525	40.67	$2.568 \times 10^{-3}$

\* Pores smaller than 31,914.1 Å.

This result is primarily related to using TiO<sub>2</sub> in the PVA solution, contributing to forming large nanoparticle agglomerates and wider fibres. The use of TiO<sub>2</sub> plays an essential role in the average fibre diameter size [20]. When reducing the PVA amount to 8 w/v% (8PVA5TiO<sub>2</sub>), the average fibre diameter was 301 nm. This filter was fabricated using a 1 mL/h feed rate and an applied voltage of 11.1 kV, which are considerably different electrospinning conditions than the other filters, which, combined with a lower polymer concentration, contributed to the formation of thinner nanofibres compared with 10PVA5TiO<sub>2</sub>.

The basis weight of the filters is also reported in Table 2. The 10PVA5TiO<sub>2</sub> filter has the highest basis weight at 67.6 g/m<sup>2</sup>, whereas the 10PVA2AC filter has the lowest at 16.6 g/m<sup>2</sup>. The PVA/TiO<sub>2</sub> filters have the high specific weight due to the use of TiO<sub>2</sub>. In contrast, the higher specific weight of 10PVA compared with the PVA/AC filters indicates a higher number of deposited nanofibres.

The BET results for SSA, pore size, and total pore volume are reported in Table 2. The filters with AC exhibit a higher SSA compared to 10PVA, which is an expected result as AC is a highly adsorbent material with a surface area of 950 to 2000 m<sup>2</sup>/g [31]. As visible in Figure 3, PVA/TiO<sub>2</sub> filters present nonuniform morphology, densely characterized by TiO<sub>2</sub> nanoparticle agglomerates. These bulky structures do not contribute to the SSA, resulting in a lower BET surface area even when compared to 10PVA. A similar result has been reported in [32], where Wang et al. showed that as the TiO<sub>2</sub> ratio and consequent agglomeration increases, the BET surface area of PVA/TiO<sub>2</sub> decreases. Thus, 10PVA presents the smallest average pore diameter. Concomitant with the increased average fibre diameters, the use of additives also contributed to a larger average pore size, as can be seen in Table 2. Moreover, 10PVA5AC and 10PVA5TiO<sub>2</sub> showed a slight increase in average pore size compared to 10PVA2AC and 8PVA5TiO<sub>2</sub>. This result could be related to the nonuniform morphology of the nanofibres.

### 3.2.2. FTIR and Raman Spectroscopy Analysis

The characterisation by the FTIR spectroscopy of the 10PVA filter sample is presented in Figure 4. As mentioned before, the FTIR spectroscopy was performed to investigate the polymer structure. The characteristic bands of PVA are visible in the spectrum. The broad-band marked with the first peak at 3297 cm<sup>-1</sup> is linked to the stretching of the hydroxyl group O–H for intra- and intermolecular hydrogen bonding. The peak at 2919 cm<sup>-1</sup> represents the stretching C–H from the alkyl group. The peak at 1428 cm<sup>-1</sup> refers to the C–H bending vibration of the CH<sub>2</sub> group. The last four peaks, 1328, 1094, 916, and 830 cm<sup>-1</sup> are, respectively, linked to C–H deformation vibrations, C–O stretching of acetyl groups, CH<sub>2</sub> rocking, and the vibration of C–C stretching [33–36]. Peaks between 1750 and 1735 cm<sup>-1</sup> have been reported to be due to the stretching of C=O and C–O from the acetate group.



These peaks are of very low intensity when the polymer presents a very high degree of hydrolysis, indicating that the polymer chain was characterised by only a few acetate groups [34,37]. The PVA used to create the fibres was 99+% hydrolysed; thus, the peak is not visible in the FTIR spectrum of the analysed sample.

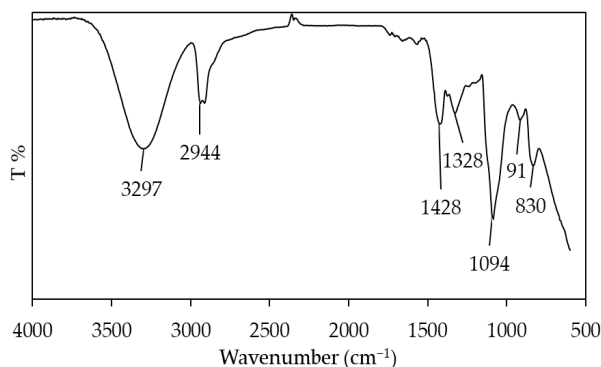


**Figure 4.** FTIR spectra of the 10PVA filter sample.

Raman spectroscopy was performed to investigate the structural characteristics of PVA and the structural changes in the PVA/TiO<sub>2</sub> nanofibres further. Therefore, the Raman spectra of the 10PVA and 10PVA5TiO<sub>2</sub> filters are presented in Figure 5. The two most noticeable peak bands visible on the PVA spectra were at 1430 cm<sup>-1</sup> and 2912 cm<sup>-1</sup>. The first peak is assigned to the stretching vibration of –CH in the PVA molecules, whereas the most intense band at 2912 cm<sup>-1</sup> is attributed to the stretching vibration of –CH<sub>2</sub> [38,39]. In the PVA/TiO<sub>2</sub> spectra, both characteristic peaks were visible but with a lower intensity.

The dominant modes of the PVA/TiO<sub>2</sub> Raman spectra are the six typical Raman active modes of the anatase crystal: 144 (E<sub>g,1</sub>), 197 (E<sub>g,2</sub>), 395 (B<sub>1g,1</sub>), 515 (A<sub>1g</sub>, B<sub>1g,2</sub>), and 639 (E<sub>g,3</sub>) cm<sup>-1</sup> [40,41]. This result is consistent with the crystal characterisation of the aerioxide P25 sample, which predominantly consists of anatase TiO<sub>2</sub>.

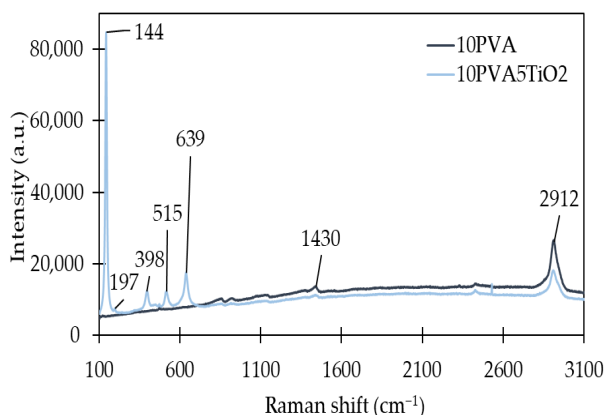


**Figure 5.** Raman spectra of the 10PVA and 10PVA5TiO<sub>2</sub> filter samples.

### 3.2.3. Thermogravimetric Analysis

The TGA curve of the 10PVA nanofibre sample is presented in Figure 6. The TGA reveals that the sample presented three weight-loss phases. At temperatures below 120 °C, a 4% weight loss by mass was detected, which can be ascribed to the weight loss of the adsorbed moisture. The second and most significant stage of weight loss was between

170 °C and 400 °C, where the 60% weight loss was due to the decomposition of the side chain of PVA. A further smaller weight loss of 31.5% was observed in the third stage, between 400 °C and 540 °C, during which the main chain of PVA was decomposed [42,43]. The significant weight loss of 91.5% observed in the range between 170 °C and 540 °C corresponds to the structural decomposition of the PVA. This result suggests that no solvent remains in the fibre.

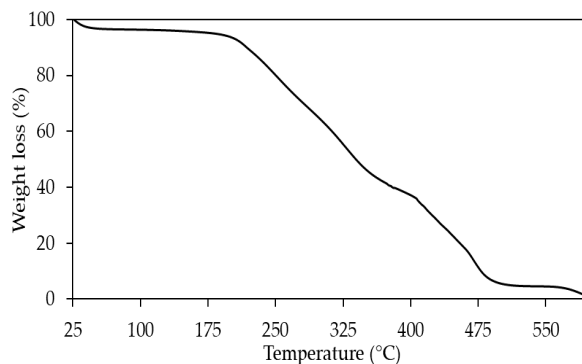


**Figure 6.** Thermogravimetric analysis curve of the 10PVA filter sample.

### 3.3. Filtration Performance

The electrospun nanofibre membranes were cut into filters with 52 mm diameter, as presented in Figure 7, to investigate the filtration performance for the pressure drop, toluene removal, and particle filtration.

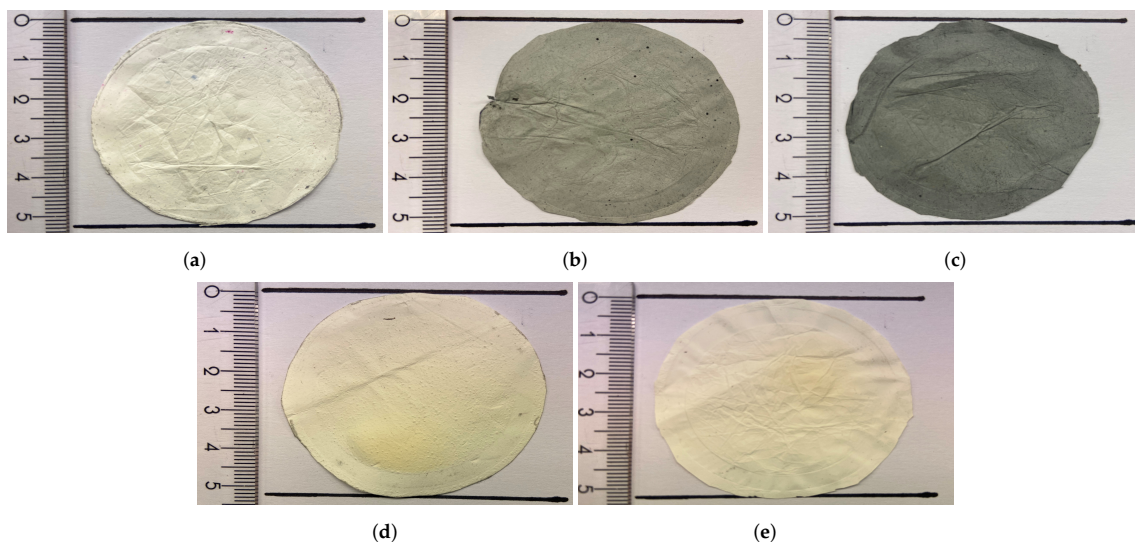


**Figure 7.** Pictures of the electrospun nanofibre filters: (a) 10PVA; (b) 10PVA2AC; (c) 10PVA5AC; (d) 10PVA5TiO<sub>2</sub>; and (e) 8PVA5TiO<sub>2</sub>.

#### 3.3.1. Pressure Drop

The relationship between the face velocity and pressure drop was investigated using linear regression. Figure 8 presents the results for the five filter samples. The linearity of the relationship was confirmed, with  $R^2$  above 0.9992. The highest pressure drop was registered

with the pure PVA filter, reaching 2693 Pa at 5.3 cm/s face velocity. The pressure drop was smaller for PVA/AC filters. The 10PVA2AC filter recorded a pressure drop of 568 Pa, representing a decrease of 78.9% compared with the 10PVA filter. Similarly, the 10PVA5AC filter reached a pressure drop of 336 Pa, 87.5% lower than the pure PVA filter.

The decrease was even more significant for the PVA/TiO<sub>2</sub> filters. The 10PVA5TiO<sub>2</sub> filter had an air resistance that led to a pressure drop of 291 Pa. The best result came from the 8PVA5TiO<sub>2</sub> filter, with a pressure drop of 195 Pa, which decreased 92.8% compared with the pure PVA filter. The use of additives influenced the morphology of the fibres and affected the pressure drop. The beaded morphology of the PVA/TiO<sub>2</sub> filters was responsible for a lower pressure drop, as the beads lead to larger pores, as confirmed by the average pore sizes in Table 2. This result is linked to the fact that the permeability increases with pore diameter, resulting in a decreased pressure drop [44]. This result is interesting in contrast to other studies of polymer-based electrospun nanofibre filters with additives [45,46]. For example, Bortolassi et al. described how a PAN/TiO<sub>2</sub> filter led to a larger pressure drop compared to a pure PAN filter [46]. The explanation is likely due to the role of other parameters like the filter thickness.

The pure PVA filter has the smallest average fibre diameter, corresponding to the highest observed pressure drop. The smallest nanofibres are probably more densely packed, leading to a smaller pore size and higher pressure drop. As mentioned, the slip flow phenomenon was dominant when the diameters of the nanofibres ( $d_f$ ) were comparable to or smaller than the mean free path of the air molecules ( $\lambda$ ), around 65 nm [13]. The transition flow regime is defined when the Knudsen number ( $Kn = 2\lambda/d_f$ ) ranges between 0.1 and 10 [14]. The dimension of the nanofibres of the fabricated filters ranges between 200 and 500 nm, indicating a Knudsen number of between 0.3 and 0.6. The decrease in the fibre diameter increased the pressure drop, although the Knudsen number indicates a transition flow regime, in which the gas slip effect was considered significant.

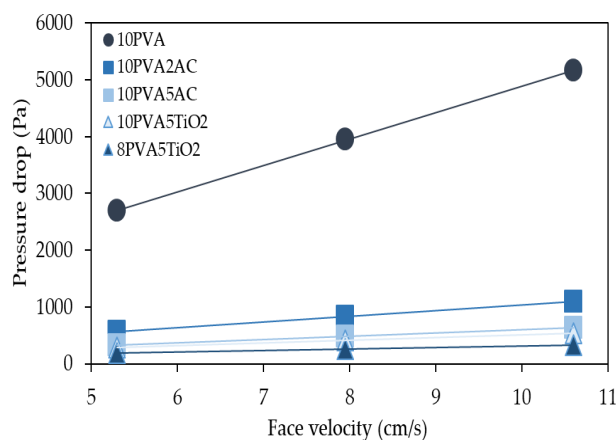


**Figure 8.** Plot of the pressure drop versus the face velocity for each filter. The three measurement points are 5.3, 7.95 and 10.6 cm/s.

Although the PVA/AC filters have a similar morphology to the pure PVA with nanofibre diameters in the same range of 200 to 300 nm, these filters present a significantly lower pressure drop than the 10PVA filter. These results are possibly related to the average pore size and the filter basis weight. Figure 9a presents the pressure drop versus the basis weights of different filters. For the two PVA/AC filters, the lower basis weight compared with 10PVA indicates fewer deposited fibres. Fewer fibres over the same area indicate larger pores in the filter and a lower pressure drop.

A higher basis weight does not correspond to a higher pressure drop for the PVA/TiO<sub>2</sub> compared with the 10PVA filter. Titanium dioxide plays a vital role in terms of the weight

increase in the filter [46]. The pressure drop remained lower than that of the 10PVA filter due to the larger pores and lower fibre density. This conclusion is also supported by the high basis weight of the 10PVA5TiO<sub>2</sub> filter (67.6 g/m<sup>2</sup>) and the relatively small pressure drop change compared to the 8PVA5TiO<sub>2</sub> filter (basis weight 31.8 g/m<sup>2</sup>).

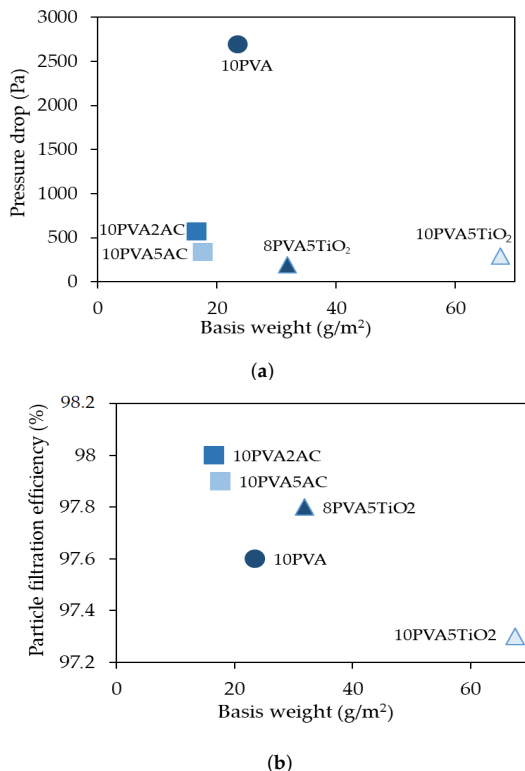


**Figure 9.** Plots of the (a) pressure drop and (b) total particle filtration efficiency versus the basis weight, comparison between filters.

### 3.3.2. Particle Filtration Efficiency

The results of the total filtration efficiency are presented in Table 3. The total filtration efficiency values for the particles are all above 97%. Figure 9b reveals that the filtration efficiency for each filter is presented as a function of the basis weight. The PVA filters with additives follow the same trend: the higher the basis weight, the lower the particle filtration efficiency. This result is in line with the observed pressure drop behaviour of different filters. The basis weight increases due to the extra weight of the additive. The PVA/TiO<sub>2</sub> filters are heavier but characterised by larger pores due to the beaded fibre morphology, resulting in lower particle filtration efficiency. It can be noticed that higher SSA values corresponded to an increase in the total particles' filtration efficiency of the filters, as visible when comparing Tables 2 and 3. However, this increase is not linear. SSA values ranged between 1.4 and 17.4 m<sup>2</sup>/g, while the total filtration efficiencies registered changes all below 1%.

The filtration efficiencies for particles as a function of the particle size for the five different filters are presented in Figure 10. Each of the five filters has lower filtration efficiency values on the smaller particle sizes. The 10PVA filter in Figure 10a exhibited an increasing filtration efficiency for 12 nm diameter particles (95.4%) to 202 nm diameter (99.3%) particles. Similar behaviour for the 10PVA2AC (Figure 10b) and 10PVA5AC (Figure 10c) filters was observed. Respectively, the filters recorded a minimum filtration

efficiency of 96.2% and 94.5% for the smallest particles size (12 nm), reaching a maximum of 99.3% for 209 nm diameter particles and 99% for the 157 nm diameter particles.

The two filters containing  $\text{TiO}_2$  exhibited a slightly different curve regarding their filtration efficiencies as a function of particle size. For 12 nm particles, the filters recorded minimum efficiency values at 95.9% for 10PVA5TiO<sub>2</sub> (Figure 10d) and 95.8% for 8PVA5TiO<sub>2</sub> (Figure 10e). The increasing trend lasted until reaching a particle size of 21 nm for both filters. For the 8PVA5TiO<sub>2</sub> filter, a constant filtration efficiency of 97.7% up to a particle size of 102 nm was observed. Above this threshold, the efficiency constantly increased until the maximum of 98.8% filtration efficiency for the 181 nm particle size. The 10PVA5TiO<sub>2</sub> filter filtration efficiency reached a maximum of 97.5% at a particle size of 26 nm and decreased again to 97% for 85 nm diameter particles, for which the concentration was recorded as one of the highest at around 3  $\mu\text{g}/\text{m}^3$ . Thereafter, the efficiency increased again to reach a maximum of 98.4% at a 181 nm particle size.

For all filters, for particle sizes greater than 217 nm, not enough particles were present to obtain a statistically meaningful result.

**Table 3.** Total particles filtration efficiency for different electrospun nanofibre filters.

	10PVA	10PVA2AC	10PVA5AC	10PVA5TiO <sub>2</sub>	8PVA5TiO <sub>2</sub>
Total filtration efficiency (%)	97.6	98.0	97.9	97.3	97.8

In their recent study, Elkamhawry and Jang characterised a novel hybrid air purification technology with good performance for particulate matter below 10  $\mu\text{m}$  (removal efficiency of 87.3%) in the outdoor environment. There was a trend of decreasing efficiency with decreasing particle size, as below 2.5  $\mu\text{m}$ , the removal efficiency dropped to 73.1% [47]. This study showed that the PVA-based filters investigated are highly efficient at removing particles in the range of the most penetrating particle size between 0.1 and 0.3  $\mu\text{m}$ , and therefore they represent a promising and much needed solution.

### 3.3.3. Toluene Removal

The pure PVA filter did not show any toluene removal, which was an expected result. PVA is a polymer that is not known for its adsorbance. The 10PVA2AC and 10PVA5AC filters have also not presented any toluene adsorption. The preparation method is responsible for the final surface that the samples present to the airstream. In previous experimental studies, activated carbon was formed on the nanofibre surface after electrospinning through carbonisation [21,25]. Activated carbon in powder form was added to the polymer solution prior to electrospinning in the present work. The activated carbon surface is likely wet with the dissolved polymer, which covers the AC surface when the solvent evaporates. This configuration is most probably responsible for the non-adsorption of toluene from the PVA/AC filters.

The performance of the two filters with  $\text{TiO}_2$  is presented in Figure 11, which was investigated using the setup in Figure 1. The graphs show the TVOC concentration in ppm and the absolute humidity in  $\text{g}/\text{m}^3$  that were recorded by the photo-acoustic gas monitor. Toluene was the only VOC added to the technical air to perform the experiment, although photocatalytic oxidation can generate byproducts in the form of VOCs. The orange lines represent when the airstream was first moved from the bypass to the reactor, facing the filter, and then back to the bypass stream. The yellow lines represent when the Xenon light was switched on and off, illuminating the filter surface.

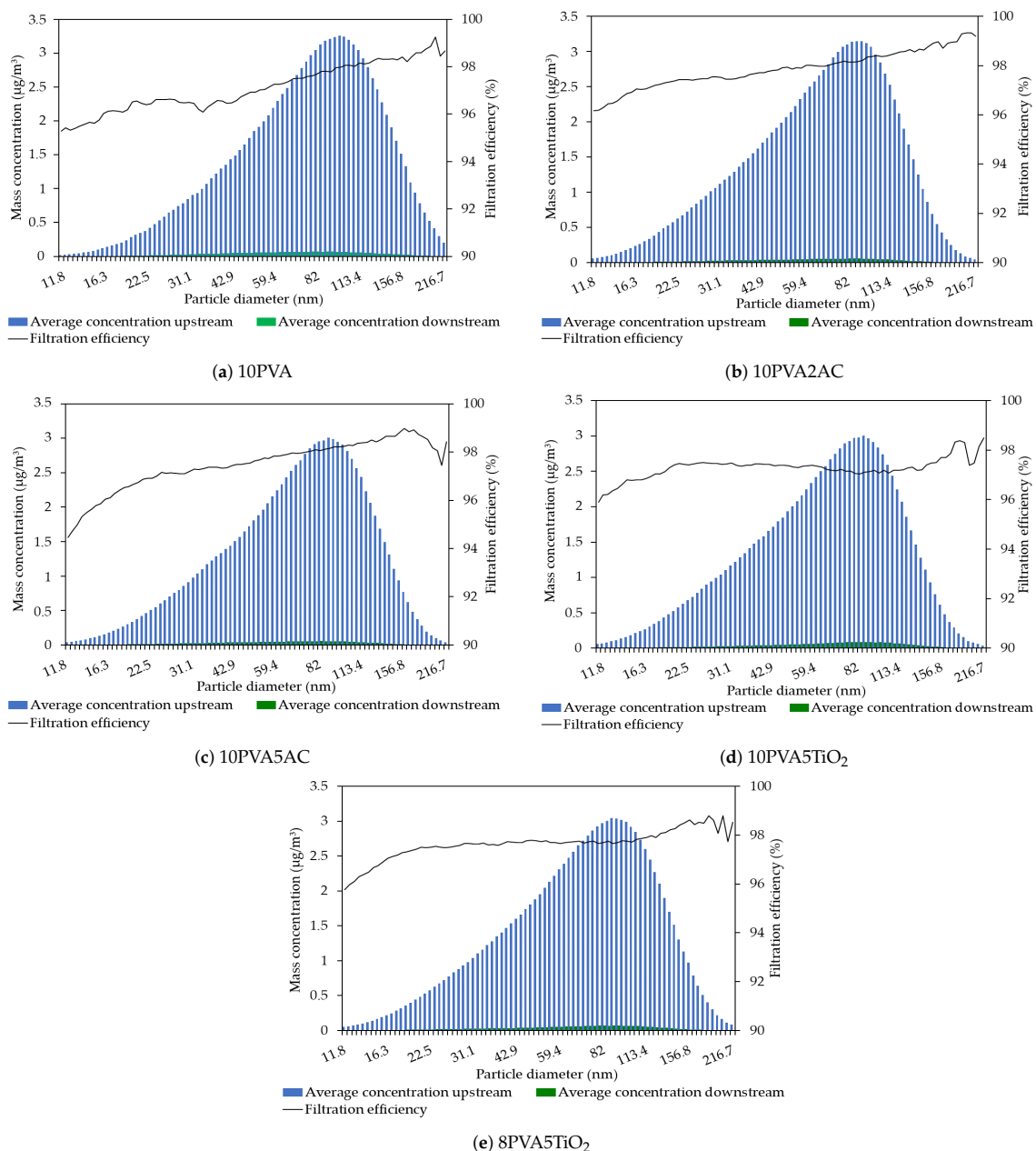


**Figure 10.** Particle size distribution recorded before and after the reactor where the filters were placed and the filtration efficiency was based on particle size.

Figure 11a displays the experiment for the 10PVA5TiO<sub>2</sub> filter. The TVOC concentration was stable at around 1.5 ppm when it entered the reactor. The moment the lamp was switched on, a slight increase in the TVOC concentration was recorded, followed by a consistent drop that stabilised at around 1.1 ppm when the airstream moved to the bypass. The TVOC concentration did not return to the original 1.5 ppm at the end of the experiment, which could lead to the conclusion that the toluene concentration decreased

due to instability in the toluene source. However, the water content in the airstream suggested differently. The graph indicates that the water amount in the airstream increased steeply when the light shined on the filter but then decreased again as soon as the light was switched off and met the initial concentration at the end of the experiment. Water is a product of the photocatalytic oxidation of toluene, presented in the following chemical reaction scheme:

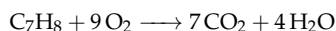
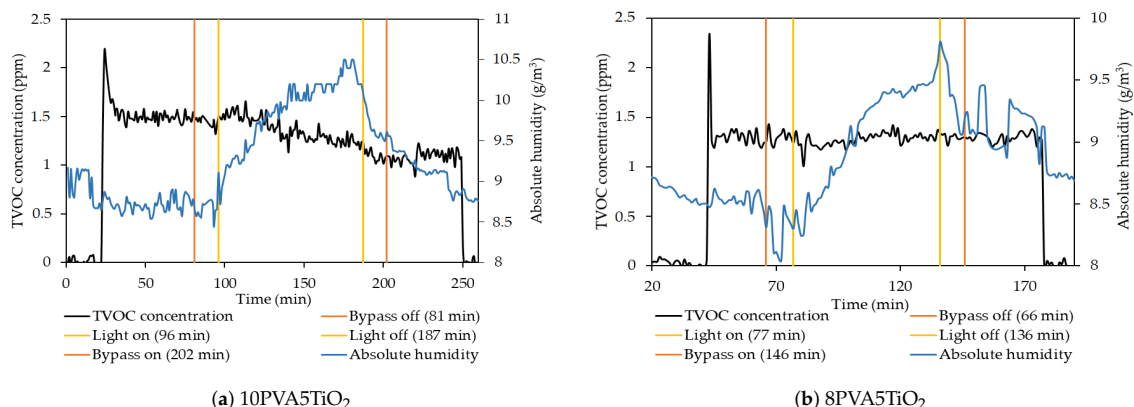


Figure 11b presents the performance of the 8PVA5TiO<sub>2</sub> filter. The situation here is different from the first filter concerning the TVOC concentration, was not been affected throughout the experiment. It stabilised at around 1.3 ppm without consistent changes. However, the water content presented a development similar to the previous filter: it increased steeply when the filter was illuminated, suggesting that the Xenon light initiated oxidation. The two PVA/TiO<sub>2</sub> filters were weighed before and after the experiments to determine whether the increased water content in the airstream could be related to the evaporation of water adsorbed from the filters when the surfaces were exposed to the Xenon light. The 10PVA5TiO<sub>2</sub> filter did not exhibit any weight change, whereas the 8PVA5TiO<sub>2</sub> filter lost 1 mg. The water content increased by 1.3 mg/L of air through the experiment. Such an amount of water content can only be explained by the photocatalytic oxidation of toluene, as it corresponds to the total amount of water produced and is two orders of magnitude higher than the filter weight loss. The resulting water content change indicates that there may also be changes in the relative humidity over time which should be taken into account when evaluating the long-term efficacy of the filter [48].

The results show active photocatalytic oxidation as the water content in the air flow showed a steep increase. The formation of byproducts is very likely the cause of the increased TVOC concentration recorded after the filters. The photocatalytic oxidation of VOCs by TiO<sub>2</sub>-doped filters has been reported in previous studies [23,45], as well as the formation of byproducts as a result of an incomplete reaction [49]. Su et al. have described the photocatalytic activity of their TiO<sub>2</sub>/PAN composite membranes and reported toluene conversion rates from 33.5% to 97.9%, depending on the TiO<sub>2</sub>/PAN mass ratio [45]. The main differences between this study's TiO<sub>2</sub>/PVA filters and the TiO<sub>2</sub>/PAN membranes in [45] are in the doping method and the design of the photocatalytic experiments. In their study, TiO<sub>2</sub> was electrosprayed on the PAN nanofibres, while in this work, TiO<sub>2</sub> nanoparticles were mixed into the PVA solution prior to electrospinning. Electrospraying TiO<sub>2</sub> nanoparticles probably led to a larger TiO<sub>2</sub> surface facing the polluted air and the Xenon light. In addition, Su et al. performed a static experiment, during which toluene was injected into a reactor where TiO<sub>2</sub>/PAN membranes were kept and irradiated using the Xenon light for 2 h. The static experimental design seems to favour good performance by photocatalytic oxidation. This was probably due to the considerably higher retention time used in [45] compared to the photocatalytic experiment designed for the TiO<sub>2</sub>/PVA filters, which were studied under a face velocity of 5.3 cm/s.





**Figure 11.** Development over time of the TVOC concentration and water content during the experiment to evaluate the toluene degradation of PVA/TiO<sub>2</sub> using the Xenon light.

#### 4. Conclusions

In summary, five PVA-based nanofibre filters were fabricated via electrospinning. The use of additives leads to larger fibre diameters and pore size relative to the undoped filter, leading to a lower pressure drop. The investigated filters were still in a transition region between the slip and non-slip flow, as indicated by the Knudsen number. The 8PVA5TiO<sub>2</sub> filter presented the lowest observed pressure drop of 195 Pa, whereas the highest particles filtration efficiency (98%) was recorded for the 10PVA2AC filter. The AC filters did not adsorb any toluene due to the preparation method for the filter. Photocatalytic oxidation was initiated by the Xenon light when investigating the PVA/TiO<sub>2</sub> filter capacity of degrading toluene. This study showed that the efficiency of the filters towards particles and VOCs is promising, but the pressure drop needs further optimization.

**Author Contributions:** Conceptualisation, R.O., A.A., M.S.J. and P.F.; methodology, R.O. and P.F.; validation, R.O.; formal analysis, R.O. and M.P.; investigation, R.O. and M.P.; resources, A.A., M.S.J. and P.F.; project administration, A.A. and P.F.; writing—original draft preparation, R.O.; writing—review and editing, all authors; visualization, R.O.; supervision, A.A., M.S.J. and P.F.; funding acquisition, A.A. and P.F. All authors have read and agreed to the published version of the manuscript.

**Funding:** This research was funded by Grøndejerns Investeringsfond, the Department of the Built Environment, the Department of Chemistry of the University of Copenhagen, and the Department of Materials and Production at Aalborg University.

**Acknowledgments:** The authors thank research technician Peter Kjær Kristensen and laboratory technician Thomas Sørensen Quaade from the Department of Materials and Production at Aalborg University for their support in performing the SEM images and running FTIR and Raman spectroscopy, respectively. We also thank laboratory manager Szymon Kwiatkowski from the Department of Chemistry at the University of Copenhagen for their support.

**Conflicts of Interest:** The authors declare no conflict of interest. The funders had no role in the study design; collection, analyses, or interpretation of data; writing the manuscript, or decision to publish the results.

#### Abbreviations

The following abbreviations are used in this manuscript:

AC	Activated Charcoal
BET	Brunauer–Emmett–Teller method
BJH	Barrett–Joyner–Halenda method
FTIR	Fourier Transform Infrared



HEPA	High Efficiency Particulate Air
HVAC	Heating, Ventilation and Air Conditioning
PVA	Polyvinyl Alcohol
SEM	Scanning Electron Microscopy
SSA	Specific Surface Area
TCD	Tip-to-Collector Distance
TGA	Thermogravimetric Analysis
TVOCs	Total Volatile Organic Compounds
VOCs	Volatile Organic Compounds

## References

1. Lelieveld, J.; Pozzer, A.; Pöschl, U.; Fnais, M.; Haines, A.; Münzel, T. Loss of life expectancy from air pollution compared to other risk factors: A worldwide perspective. *Cardiovasc. Res.* **2020**, *116*, 1910–1917. [CrossRef] [PubMed]
2. World Health Organization. Available online: <https://www.who.int/data/gho> (accessed on 11 January 2021).
3. Mills, N.L.; Donaldson, K.; Hadoke, P.W.; Boon, N.A.; MacNee, W.; Cassee, F.R.; Sandström, T.; Blomberg, A.; Newby, D.E. Adverse cardiovascular effects of air pollution. *Nat. Clin. Pract. Cardiovasc. Med.* **2009**, *6*, 36–44. [CrossRef] [PubMed]
4. Brunekreef, B.; Holgate, S.T. Air pollution and health. *Lancet* **2002**, *360*, 1233–1242. [CrossRef]
5. Katsouyanni, K.; Touloumi, G.; Samoli, E.; Gryparis, A.; Le Tertre, A.; Monopolis, Y.; Rossi, G.; Zmirou, D.; Ballester, F.; Boumghar, A.; et al. Confounding and effect modification in the short-term effects of ambient particles on total mortality: Results from 29 European cities within the APHEA2 project. *Epidemiology* **2001**, *12*, 521–531. [CrossRef]
6. Pope, C.A.; Dockery, D.W. Health effects of fine particulate air pollution: Lines that connect. *J. Air Waste Manag. Assoc.* **2006**, *56*, 709–742. [CrossRef]
7. Fisk, W.J. Health benefits of particle filtration. *Indoor Air* **2013**, *23*, 357–368. [CrossRef]
8. Mannucci, P.M.; Harari, S.; Martinelli, I.; Franchini, M. Effects on health of air pollution: A narrative review. *Intern. Emerg. Med.* **2015**, *10*, 657–662. [CrossRef] [PubMed]
9. Khan, F.I.; Ghoshal, A.K. Removal of Volatic Organic Compounds from polluted air. *J. Loss Prev. Process Ind.* **2000**, *13*, 527–545. [CrossRef]
10. Mamaghani, A.H.; Haghighat, F.; Lee, C.S. Photocatalytic oxidation technology for indoor environment air purification: The state-of-the-art. *Appl. Catal. B Environ.* **2017**, *203*, 247–269. [CrossRef]
11. Zaatari, M.; Novoselac, A.; Siegel, J. The relationship between filter pressure drop, indoor air quality, and energy consumption in rooftop HVAC units. *Build. Environ.* **2014**, *73*, 151–161. [CrossRef]
12. Sundarajan, S.; Tan, K.L.; Lim, S.H.; Ramakrishna, S. Electrospun nanofibers for air filtration applications. *Procedia Eng.* **2014**, *75*, 159–163. [CrossRef]
13. Li, P.; Wang, C.; Zhang, Y.; Wei, F. Air filtration in the free molecular flow regime: A review of high-efficiency particulate air filters based on Carbon Nanotubes. *Small* **2014**, *10*, 4543–4561. [CrossRef] [PubMed]
14. Zhao, X.; Wang, S.; Yin, X.; Yu, J.; Ding, B. Slip-Effect Functional Air Filter for Efficient Purification of PM 2.5. *Sci. Rep.* **2016**, *6*, 1–11. [CrossRef]
15. Kadam, V.V.; Wang, L.; Padhye, R. Electrospun nanofibre materials to filter air pollutants—A review. *J. Ind. Text.* **2018**, *47*, 2253–2280. [CrossRef]
16. Zhu, M.; Han, J.; Wang, F.; Shao, W.; Xiong, R.; Zhang, Q.; Pan, H.; Yang, Y.; Samal, S.K.; Zhang, F.; et al. Electrospun Nanofibers Membranes for Effective Air Filtration. *Macromol. Mater. Eng.* **2017**, *302*. [CrossRef]
17. Li, D.; Xia, Y. Electrospinning of nanofibers: Reinventing the wheel? *Adv. Mater.* **2004**, *16*, 1151–1170. [CrossRef]
18. Scholten, E.; Bromberg, L.; Rutledge, G.C.; Hatton, T.A. Electrospun polyurethane fibers for absorption of volatile organic compounds from air. *ACS Appl. Mater. Interfaces* **2011**, *3*, 3902–3909. [CrossRef]
19. Park, J.Y.; Lee, I.H. Characterization and Morphology of Prepared Titanium Dioxide Nanofibers by Electrospinning. *J. Nanosci. Nanotechnol.* **2010**, *10*, 3402–3405. [CrossRef] [PubMed]
20. Wan, H.; Wang, N.; Yang, J.; Si, Y.; Chen, K.; Ding, B.; Sun, G.; El-Newehy, M.; Al-Deyab, S.S.; Yu, J. Hierarchically structured polysulfone/titania fibrous membranes with enhanced air filtration performance. *J. Colloid Interface Sci.* **2014**, *417*, 18–26. [CrossRef]
21. Lee, K.J.; Shiratori, N.; Lee, G.H.; Miyawaki, J.; Mochida, I.; Yoon, S.H.; Jang, J. Activated carbon nanofiber produced from electrospun polyacrylonitrile nanofiber as a highly efficient formaldehyde adsorbent. *Carbon* **2010**, *48*, 4248–4255. [CrossRef]
22. Wang, H.; Zheng, G.F.; Wang, X.; Sun, D.H. Study on the air filtration performance of nanofibrous membranes compared with conventional fibrous filters. In Proceedings of the 2010 IEEE 5th International Conference on Nano/Micro Engineered and Molecular Systems, NEMS 2010, Xiamen, China, 20–23 January 2010; pp. 387–390. [CrossRef]
23. Chuang, Y.H.; Hong, G.B.; Chang, C.T. Study on particulates and volatile organic compounds removal with TiO<sub>2</sub> nonwoven filter prepared by electrospinning. *J. Air Waste Manag. Assoc.* **2014**, *64*, 738–742. [CrossRef]
24. Givehchi, R.; Li, Q.; Tan, Z. Quality factors of PVA nanofibrous filters for airborne particles in the size range of 10–125 nm. *Fuel* **2016**, *181*, 1273–1280. [CrossRef]

25. Oh, G.Y.; Ju, Y.W.; Jung, H.R.; Lee, W.J. Preparation of the novel manganese-embedded PAN-based activated carbon nanofibers by electrospinning and their toluene adsorption. *J. Anal. Appl. Pyrolysis* **2008**, *81*, 211–217. [\[CrossRef\]](#)
26. Ju, Y.W.; Oh, G.Y. Behavior of toluene adsorption on activated carbon nanofibers prepared by electrospinning of a polyacrylonitrile-cellulose acetate blending solution. *Chem. Eng. J.* **2017**, *34*, 2731–2737. [\[CrossRef\]](#)
27. Wang, M.X.; Huang, Z.H.; Shimohara, T.; Kang, F.; Liang, K. NO removal by electrospun porous carbon nanofibers at room temperature. *Chem. Eng. J.* **2011**, *170*, 505–511. [\[CrossRef\]](#)
28. Xia, T.; Bian, Y.; Zhang, L.; Chen, C. Relationship between pressure drop and face velocity for electrospun nanofiber filters. *Energy Build.* **2018**, *158*, 987–999. [\[CrossRef\]](#)
29. Subbiah, T.; Bhat, G.S.; Tock, R.W.; Parameswaran, S.; Ramkumar, S.S. Electrospinning of nanofibers. *J. Appl. Polym. Sci.* **2005**, *96*, 557–569. [\[CrossRef\]](#)
30. Deitzel, J.M.; Kleinmeyer, J.D.; Harris, D.; Beck Tan, N.C. The effect of processing variables on the morphology of electrospun. *Polymer* **2001**, *42*, 261–272. [\[CrossRef\]](#)
31. Lu, J.D.; Xue, J. Poisoning: Kinetics to Therapeutics. In *Critical Care Nephrology*, 3rd ed.; Elsevier Inc.: Amsterdam, The Netherlands, 2019; pp. 600–629. [\[CrossRef\]](#)
32. Wang, Y.; Zhong, M.; Chen, F.; Yang, J. Visible light photocatalytic activity of TiO<sub>2</sub>/D-PVA for MO degradation. *Appl. Catal. B Environ.* **2009**, *90*, 249–254. [\[CrossRef\]](#)
33. Coates, J. Interpretation of Infrared Spectra, A Practical Approach. In *Encyclopedia of Analytical Chemistry*; Meyers, R.A., Ed.; John Wiley and Sons Ltd.: Hoboken, NJ, USA, 2000.
34. Mansur, H.S.; Sadahira, C.M.; Souza, A.N.; Mansur, A.A. FTIR spectroscopy characterization of poly (vinyl alcohol) hydrogel with different hydrolysis degree and chemically crosslinked with glutaraldehyde. *Mater. Sci. Eng. C* **2008**, *28*, 539–548. [\[CrossRef\]](#)
35. Kharazmi, A.; Faraji, N.; Hussin, R.M.; Saion, E.; Yunus, W.M.M.; Behzad, K. Structural, optical, opto-thermal and thermal properties of ZnS-PVA nanofluids synthesized through a radiolytic approach. *Beilstein J. Nanotechnol.* **2015**, *6*, 529–536. [\[CrossRef\]](#) [\[PubMed\]](#)
36. Bhat, N.V.; Nate, M.M.; Kurup, M.B.; Bambole, V.A.; Sabharwal, S. Effect of  $\gamma$ -radiation on the structure and morphology of polyvinyl alcohol films. *Nucl. Instrum. Methods Phys. Res. Sect. B Beam Interact. Mater. Atoms* **2005**, *237*, 585–592. [\[CrossRef\]](#)
37. Elashmawi, I.S.; Hakeem, N.A.; Selim, M.S. Optimization and spectroscopic studies of CdS/poly(vinyl alcohol) nanocomposites. *Mater. Chem. Phys.* **2009**, *115*, 132–135. [\[CrossRef\]](#)
38. Shi, Y.; Xiong, D.; Li, J.; Wang, K.; Wang, N. In situ repair of graphene defects and enhancement of its reinforcement effect in polyvinyl alcohol hydrogels. *RSC Adv.* **2017**, *7*, 1045–1055. [\[CrossRef\]](#)
39. Ferrari, A.C.; Meyer, J.C.; Scardaci, V.; Casiraghi, C.; Lazzeri, M.; Mauri, F.; Piscanec, S.; Jiang, D.; Novoselov, K.S.; Roth, S.; et al. Raman spectrum of graphene and graphene layers. *Phys. Rev. Lett.* **2006**, *97*, 1–4. [\[CrossRef\]](#)
40. Surmacki, J.; Wroński, P.; Szadkowska-Nicze, M.; Abramczyk, H. Raman spectroscopy of visible-light photocatalyst—Nitrogen-doped titanium dioxide generated by irradiation with electron beam. *Chem. Phys. Lett.* **2013**, *566*, 54–59. [\[CrossRef\]](#)
41. Balachandran, U.; Eror, N.G. Raman spectra of titanium dioxide. *J. Solid State Chem.* **1982**, *42*, 276–282. [\[CrossRef\]](#)
42. Ding, W.; Wei, S.; Zhu, J.; Chen, X.; Rutman, D.; Guo, Z. Manipulated electrospun PVA nanofibers with inexpensive salts. *Macromol. Mater. Eng.* **2010**, *295*, 958–965. [\[CrossRef\]](#)
43. Kim, G.M.; Asran, A.S.; Michler, G.H.; Simon, P.; Kim, J.S. Electrospun PVA/HAP nanocomposite nanofibers: Biomimetics of mineralized hard tissues at a lower level of complexity. *Bioinspir. Biomimetics* **2008**, *3*. [\[CrossRef\]](#)
44. Mancin, S.; Zilio, C.; Cavallini, A.; Rossetto, L. Pressure drop during air flow in aluminum foams. *Int. J. Heat Mass Transf.* **2010**, *53*, 3121–3130. [\[CrossRef\]](#)
45. Su, J.; Yang, G.; Cheng, C.; Huang, C.; Xu, H.; Ke, Q. Hierarchically structured TiO<sub>2</sub>/PAN nanofibrous membranes for high-efficiency air filtration and toluene degradation. *J. Colloid Interface Sci.* **2017**, *507*, 386–396. [\[CrossRef\]](#) [\[PubMed\]](#)
46. Bortolassi, A.C.C.; Guerra, V.G.; Aguiar, M.L.; Soussan, L.; Cornu, D.; Miele, P.; Bechelany, M. Composites based on nanoparticle and pan electrospun nanofiber membranes for air filtration and bacterial removal. *Nanomaterials* **2019**, *9*, 1740. [\[CrossRef\]](#)
47. Elkamhawy, A.; Jang, C.M. Performance evaluation of hybrid air purification system with vegetation soil and electrostatic precipitator filters. *Sustainability* **2020**, *12*, 5428. [\[CrossRef\]](#)
48. Ollier, R.; Pérez, C.; Alvarez, V. Effect of Relative Humidity on the Mechanical Properties of Micro and Nanocomposites of Polyvinyl Alcohol. *Procedia Mater. Sci.* **2012**, *1*, 499–505. [\[CrossRef\]](#)
49. Yu, W.; In 'T Veld, M.; Bossi, R.; Ateia, M.; Tobler, D.; Feilberg, A.; Bovet, N.; Johnson, M.S. Formation of formaldehyde and other byproducts by TiO<sub>2</sub> photocatalyst materials. *Sustainability* **2021**, *13*, 4821. [\[CrossRef\]](#)

## Chapter 7

### Paper IV

# Filtration performance of ultrathin electrospun cellulose acetate filters doped with $\text{TiO}_2$ and activated charcoal

R. Orlando, Y. Gao, P. Fojan, J. Mo and A. Afshari

The paper has been published in  
*Buildings*, Vol. 11(11), 557, 2021.



## Article

# Filtration Performance of Ultrathin Electrospun Cellulose Acetate Filters Doped with TiO<sub>2</sub> and Activated Charcoal

Roberta Orlando <sup>1</sup> , Yilun Gao <sup>2,3</sup> , Peter Fojan <sup>4</sup>, Jinhan Mo <sup>2,3</sup>  and Alireza Afshari <sup>1,\*</sup>

<sup>1</sup> Department of the Built Environment, Aalborg University, DK-2450 Copenhagen, Denmark; ror@build.aau.dk

<sup>2</sup> Department of Building Science, Tsinghua University, Beijing 100084, China;

gyl20@mails.tsinghua.edu.cn (Y.G.); mojinhan@tsinghua.edu.cn (J.M.)

<sup>3</sup> Beijing Key Laboratory of Indoor Air Quality Evaluation and Control, Beijing 100084, China

<sup>4</sup> Department of Materials and Production, Aalborg University, DK-9220 Aalborg, Denmark; fp@mp.aau.dk

\* Correspondence: aaf@build.aau.dk

**Abstract:** Air filters are crucial components of a building ventilation system that contribute to improving indoor air quality, but they are typically associated with relatively high pressure drops. The purpose of the study is to evaluate the effect of additives on ultrathin electrospun filters, the pressure drop, and the particle removal efficiency of uniformly charged particles. The fibres were electrospun under optimised conditions that resulted in a fast-fabricating process due to the properties of the cellulose acetate solution. Different ultrathin electrospun fibre filters based on cellulose acetate (CA) were fabricated: a pure CA electrospun fibre filter, two filters based on CA fibres separately doped with activated charcoal (AC) and titanium dioxide (TiO<sub>2</sub>), respectively, and a composite filter where the two additives, AC and TiO<sub>2</sub>, were embedded between two CA fibres layers. The ultrathin filters exhibited a low pressure drop of between 63.0 and 63.8 Pa at a face velocity of 0.8 m s<sup>−1</sup>. The filtration performance of uniformly charged particles showed a removal efficiency above 70% for particle sizes between 0.3 and 0.5 µm for all filters, rising above 90% for larger particles between 1 and 10 µm, which translates to the average sizes of pollens and other allergenic contaminant particles. Due to the positive impact on the fibre morphology caused by the additives, the composite filter showed the highest filtration performance among the produced filters, reaching 82.3% removal efficiency towards smaller particles and a removal of up to 100% for particle sizes between 5 and 10 µm. Furthermore, cellulose acetate itself is not a source of microparticles and is fully biodegradable compared to other polymers commonly used for filters. These ultrathin electrospun filters are expected to be practical in applications for better building environments.

**Keywords:** cellulose acetate; electrospinning; particle pollution; air filters; titanium dioxide; activated charcoal



**Citation:** Orlando, R.; Gao, Y.; Fojan, P.; Mo, J.; Afshari, A. Filtration Performance of Ultrathin Electrospun Cellulose Acetate Filters Doped with TiO<sub>2</sub> and Activated Charcoal.

*Buildings* **2021**, *11*, 557. <https://doi.org/10.3390/buildings11110557>

Academic Editor: Francesco Nocera

Received: 4 November 2021

Accepted: 17 November 2021

Published: 18 November 2021

**Publisher's Note:** MDPI stays neutral with regard to jurisdictional claims in published maps and institutional affiliations.



**Copyright:** © 2021 by the authors. Licensee MDPI, Basel, Switzerland.

This article is an open access article distributed under the terms and conditions of the Creative Commons Attribution (CC BY) license (<https://creativecommons.org/licenses/by/4.0/>).

## 1. Introduction

Exposure to particle pollution has been linked to negative health effects such as cardiovascular and respiratory disorders and lung cancer, and it can lead to increased mortality [1–4]. Although the World Health Organization (WHO) has defined clear guidelines for annual average outdoor concentration as 5 µg m<sup>−3</sup> for PM<sub>2.5</sub> (particulate matter with an aerodynamic diameter less than 2.5 µm) and 15 µg m<sup>−3</sup> for PM<sub>10</sub> (particulate matter with an aerodynamic diameter less than 10 µm) [5], 91% of the world population lives in areas where these guidelines are not met. Particles originating outdoors can enter residential and non-residential buildings and negatively affect indoor air quality [6,7].

As a significant portion of indoor particles originates outdoors, supply air filters can prevent the outdoor-to-indoor transport of particle pollution and improve indoor air quality. Several air filter technologies can be used to remove particles [8–10]. Commercial fibrous filters, such as HEPA filters, can remove up to 99.97% of particles with diameters larger than 0.3 µm [11] at the expense of a relatively large pressure drop that can negatively

affect the total HVAC energy use [12]. Typically, electrostatic filters achieve lower particle filtration efficiency compared to mechanical filters with the advantage of a much lower air resistance [13]. Most conventional filters require the use of a fan to overcome the pressure drop they impose on the air stream, and therefore, they contribute to an increased energy use from the ventilation system [14]. Air filter contribution can account for between 20 and 50% of the total pressure drop of a ventilation system depending on the loading conditions, filter efficiency, and system configuration [15]. This has a direct impact on the energy use of the ventilation fans, which can account for up to 34% of the total energy use of the HVAC system [14]. The main challenge that air filtration technologies have to overcome today is to optimise the ratio between filtration efficiency and energy use during operation, therefore achieving the highest dust-loading capacity with the lowest air resistance possible. Recent studies have focused on fibre filters produced with electrospinning as a potential solution to overcoming this challenge.

Electrospinning is a versatile and effective method of producing fibres with diameters within the nano- or submicron dimension, which are characterised by various morphologies and properties [16]. When the fibre diameter is reduced to nanoscale, which is comparable to or smaller than the mean free path of air molecules (65 nm), lower air resistance of the filters will occur by introducing a slip effect [17,18]. Thus, electrospun fibre filters aiming at a decreased pressure drop have been fabricated in numerous research studies in recent years [19,20]. A polyacrylonitrile (PAN)-based electrospun nanofibre membrane with a fibre diameter in the range of 50–170 nm was fabricated [17]. The electrospinning process was optimised, and a particle filtration efficiency of 99.09% was obtained, while the pressure drop reached 29 Pa with a face velocity of  $0.053 \text{ m s}^{-1}$  [17]. A silk fibroin/polyvinyl alcohol (SF/PVA) nanofibre air filter was developed aiming at efficient particle capture [21]. The filter reached 99.11% removal efficiency and a pressure drop of 50 Pa at  $0.5 \text{ m s}^{-1}$  air velocity [21]. Moreover, a method to fabricate an electrospun nanofibre filter to minimise the pressure drop when removing particles below  $2.5 \mu\text{m}$  was developed [22]. An optimised approach based on a semi-empirical model was applied on 125 samples, which obtained a decreased pressure drop for 110 cases. The optimal nylon-based filter has achieved 90% filtration efficiency at the cost of 27.18 Pa at a face velocity of  $0.05 \text{ m s}^{-1}$  [22]. Composite electrospun fibre mats have been recently fabricated [23,24]. A polyimide-based electrospun membrane with metal–organic frameworks (MOFs) successfully removed VOCs such as polar formaldehyde (sorption capacity  $124 \text{ mg g}^{-1}$ ) and non-polar toluene ( $142 \text{ mg g}^{-1}$ ), xylene ( $214 \text{ mg g}^{-1}$ ), and mesitylene ( $201 \text{ mg g}^{-1}$ ) from air [23]. A polymeric composite electrospun nanofibre mat was produced to remove air particles and to investigate the antibacterial activity enhanced by the sulfobetaine zwitterionic groups. The materials achieved 99.9% removal of *Klebsiella pneumoniae* and *Staphylococcus aureus* bacteria and exhibited high filtration efficiency ( $>99.9\%$ ) with a pressure drop of 177 Pa at  $5.3 \text{ cm s}^{-1}$  face velocity [24].

The fibre morphology has to be tuned properly in order to achieve an optimal ratio between particle removal and pressure drop. The typical face velocities used in an HVAC system can reach up to  $2 \text{ m s}^{-1}$ , but nanofibre filters are generally tested at much lower face velocities ( $0.05 \text{ m s}^{-1}$ ) [25]. The effect of additives on the morphological filter parameters such as porosity, fibre diameter, and fibre surface roughness has also been a subject of focus [16]. The addition of titanium dioxide was shown to improve the particle filtration efficiency of polymer-based electrospun nanofibre filters [26]. The PSU/TiO<sub>2</sub> membrane has an enhanced filtration efficiency of 99.997% for  $0.3\text{--}0.5 \mu\text{m}$  particles and a pressure drop of 43.5 Pa at a face velocity of  $0.05 \text{ m s}^{-1}$  compared to the pristine PSU filter due to the enhanced porous structure and surface fractal features with irregular rough structures [26]. The combined use of titanium dioxide and activated charcoal when fabricating nanofibres could contribute to the formation of macroporous structures that can decrease the pressure drop [27]. Activated charcoal and titanium dioxide are often used as additives on fibre filters for their properties as an adsorbent and photocatalyst to enhance the removal

capacity of the filters towards gaseous pollutants [28,29], although their influence on particle filtration efficiency has not been widely investigated.

Other researchers have used continuous electrostatic effects on traditional air filters to apply a uniform charge to particles and evaluate the filtration efficiency [30–32]. The particle filtration efficiencies for two commercial HVAC filters have been improved from 5–15% to 40–90% by utilising continuous emission of unipolar ions without affecting the pressure drop [32]. A compact electrostatically assisted air (EAA) filter, which combines corona charging and filter polarising, was developed [33]. The single-pass efficiency for 0.3–0.5  $\mu\text{m}$  charged particles of a polyethylene terephthalate (PET) coarse filter was improved from 0.4% to 99%. The air resistance of the filter led to a pressure drop of 21 Pa at 1.2  $\text{m s}^{-1}$  face velocity [33]. Furthermore, the efficiency for the PET coarse filter could be significantly improved by a thin coating of polydopamine (PDA) via in situ dopamine polymerisation. Using a two-stage EAA filtration device, the PDA@PET filter has a high filtration efficiency of 99.48% for 0.3  $\mu\text{m}$  particles, low air resistance of 9.5 Pa at a filtration velocity of 0.4  $\text{m s}^{-1}$ , and steady performance for up to 30 days [34]. An electrostatically assisted metal foam and PVDF electrospun nanofibres were combined to enhance filtration efficiency by 15% for charged particles with an aerodynamic diameter between 0.3 and 0.5  $\mu\text{m}$  [35]. Moreover, an electrically responsive polyurethane filter with dielectric surface coatings could even achieve 90.50% removal efficiency for ultrafine particles and an ultralow pressure drop at 13.0 Pa at 1  $\text{m s}^{-1}$  face velocity, providing a promising prospect when applied in building ventilation systems [36].

The present study introduces four different ultrathin electrospun fibre filters. These filters exhibit a thickness between 0.1 and 0.2 mm, whereas conventional and commercial filters usually present a thickness ranging from a few to tens of centimetres. The selected polymer was cellulose acetate (CA), which is an abundant and biodegradable organic compound commonly used for application in filters, artificial skin, and protective clothing [37,38]. Employing CA instead of commonly used polymers is beneficial because CA is not a source of microplastic, and it does not increase the plastic load when disposed of, as it is biodegradable. Electrospinning of this polymer has been systematically investigated, reaching fast and stable results [39].

The purpose of this study was to evaluate experimentally the influence of additives such as titanium dioxide and activated charcoal on the filtration performance of uniformly charged particles for CA-based ultrathin electrospun fibre filters. Furthermore, the impact on the performance as measured by filtration efficiency and pressure drop of the different ultrathin filter matrices was also assessed. Compared to the reported electrospun filters in the literature, the novelty of the filters presented here is related to their high porosity and low pressure drop but still maintaining a good filtration efficiency, which is evident from the quality factor. This paper presents the fabrication process via electrospinning of the different fibre filters, which differs in terms of materials and filter configuration. The results from the experimental study of the filtration performance are described and discussed, including the achieved pressure drop and the particle filtration efficiency. The filters were also evaluated and compared in terms of filter quality factors.

## 2. Materials and Methods

### 2.1. Materials

Cellulose acetate (CA, 39.8 wt % acetyl content, MN 30000 GPC) and activated charcoal (AC, MW 12.01  $\text{g mol}^{-1}$ ) in a powder form were purchased from Sigma-Aldrich. Aeroxide TiO<sub>2</sub> P25 in a nanopowder form was a gift from Evonik Industries. Pure acetone, ethanol absolute, and 2-propanol were acquired by Avantor and were used as is. The materials were used without further purification.

## 2.2. Fabrication of Electrospun Fibre Filters

### 2.2.1. Preparation of CA Solution

The polymer solution was prepared by adding 31.25 g of CA to 250 mL of acetone under vigorous stirring for 12 h to obtain a homogeneous solution. The stirring was carried out at room temperature (20 °C).

### 2.2.2. Preparation of TiO<sub>2</sub> and AC Dispersions

First, 1.5 g of TiO<sub>2</sub> was dispersed in a solution of 80 mL 2-propanol and 20 mL ethanol. The mixture was vigorously stirred for an hour, and then, it was ultrasonicated in a bath for 30 min to ensure uniformity. Similarly, 2 g of AC were dispersed in a solution of 80 mL 2-propanol and 20 mL ethanol. The solution was continuously stirred to ensure a homogenous AC distribution.

### 2.2.3. Electrospinning Process

The electrospinning was carried out using an electrospinner from Yflow (2.2.D-500), which is equipped with a flat collector and a remote-controlled arm where the needle is located. A schematic representation of the setup is shown in Figure 1. The electrospinning was performed in a vertical downwards configuration. For the preparation of CA electrospun fibre, the CA solution was loaded in a 20 mL glass syringe (Poulsen & Graf GmbH). The solution was fed at a constant rate of 1 mL min<sup>-1</sup> through a needle with an inner diameter of 1.5 mm. The electrospinning was continuous until 10 mL of the CA solution had been electrospun onto the collector. The voltage applied was 14.8 kV. The tip of the needle was kept at 9 cm distance from the collector. Inside the electrospinner box, the temperature ranged between 19.8 and 20.8 °C, and the relative humidity was kept between 27% and 32%. The needle was remotely controlled at a velocity of 50 mm s<sup>-1</sup> on the collector (20 cm × 20 cm), as shown in Figure 1, to ensure the uniformity of fibre distribution across the filter surface. After electrospinning, the filter was kept in a ventilated oven at 70 °C for 1 h to ensure complete evaporation of the solvent.

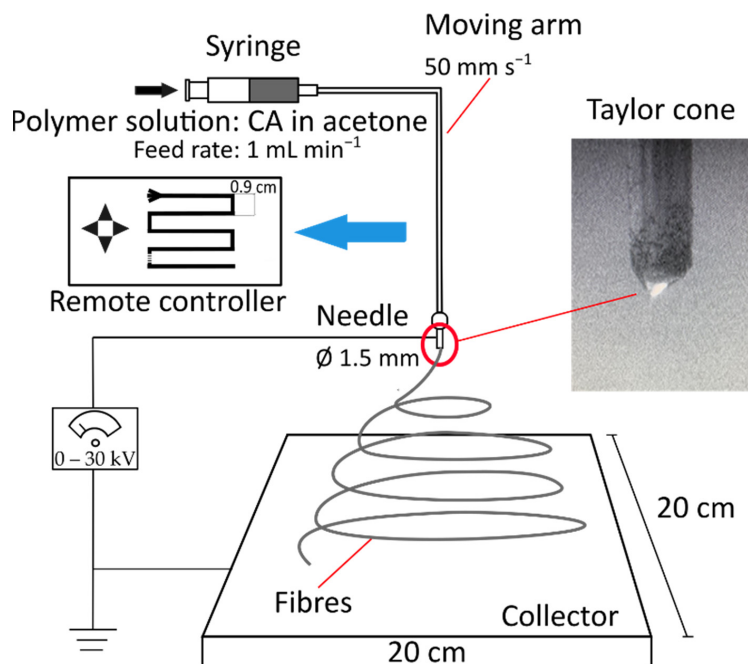


Figure 1. Schematic representation of the electrospinning setup.



#### 2.2.4. Preparation of the Doped Filters

The CA/AC and CA/TiO<sub>2</sub> fibre filters were prepared by spraying the additive dispersion onto the electrospun fibre filter surface using an airbrush. Such a doping method implies that the additives are deposited on the filter, modifying the first layers of the filter surface. The previously electrospun CA membrane was placed in a fume hood onto a metal grid at a distance of 20 cm from the air brush. The filter was sprayed with the respective suspension for 2 min. Then, the filter was dried in the oven at 70 °C for an hour. The airbrush process was repeated twice for each filter.

For the composite filter, the two additive dispersions were separately sprayed between two layers of CA electrospun fibre. The first layer of polymer fibre was made by electrospinning 6 mL of CA solution onto the collector. After drying the membrane for 1 h at 70 °C in the oven, two 2-min rounds of airbrushing of AC dispersion at 10 L min<sup>−1</sup> were applied, which was interspersed with 1 h drying at 70 °C between each application. The third layer of the composite filter consisted of electrospinning 4 mL of CA solution. The fourth and final layer comprised two rounds of airbrushing of the TiO<sub>2</sub> dispersion using the previously described conditions, including 1 h of drying at 70 °C between airbrushing applications.

#### 2.3. Fibre Characterisation

The fibre surface morphology was investigated using scanning electron microscopy (SEM; Zeiss XB1540) operating at 5 kV. The samples were coated with a thin layer of gold before scanning. The average fibre diameter and surface porosity were measured using the DiameterJ plugin for ImageJ (1.51w, NIH, Bethesda, MD, USA) on the SEM images.

The thickness of the filters has been measured with a traditional External Micrometer (Model 965M, Moore & Wright Ltd., Sheffield, UK) with an accuracy of ±0.005 mm. The filters were folded in two and kept between two metal plates during the measurement to avoid compression of the materials.

#### 2.4. Investigation of Filtration Performance

The filtration performance tests were conducted in an acrylic air duct with an inner diameter of 50 mm, as shown in Figure 2. The filtration module is divided into the charging section and collecting section, where the membrane is kept, as shown in Figure 3. The air with ambient airborne particles was driven through the module in the sequence of a diffusion plate, a pin-to-plate charging module for the ionisation of particles, the filter to be tested, and an axial flow fan. The length of the charging pin is 20 mm, and the pin-to-plate distance is 10 mm. The charging pin was connected to an adjustable High-Voltage Direct Current (HVDC) power supply (from 0 to +30 kV, accuracy: 0.1 kV, P30, GENVOLT Co. Ltd., Beijing, China). The back metal ring of the charging module was connected to the ground. The face filtration velocity could be altered by adjusting the frequency of the fan.

The face velocity was measured by a thermo-anemometer (435-1, Testo SE & Co. KGaA, Titisee-Neustadt, Germany) located upstream of the air duct, and it was controlled at 0.8 m s<sup>−1</sup> during the particle removal efficiency test. The number concentration of 0.3–10 µm particles was measured by a particle counter (Aerotrak 9306, TSI Inc., Shoreview, MN, USA) located upstream and downstream of the filters. A sensor (WSZY-1, Tianjian-huayi Tech. Co. Ltd., Beijing, China) was used to monitor the air temperature and relative humidity during testing in the air duct. The pressure drop across the filter was measured using a differential gauge (accuracy: ±1%, DP-CALC 5825, TSI Inc., Shoreview, MN, USA). The pressure drop was measured at several face velocities in the range between 0.035 and 1 m s<sup>−1</sup>.

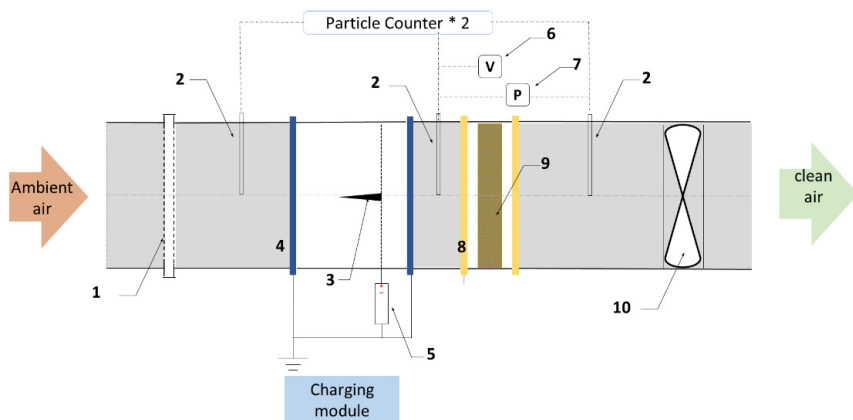


**Figure 2.** Schematic setup representation. 1. Diffusion plate, 2. Sampler, 3. Charging pins, 4. Metal rings, 5. HVDC power, 6. Anemometer, 7. Differential pressure sensor, 8. Metal mesh, 9. Membrane, 10. Fan and frequency converter.

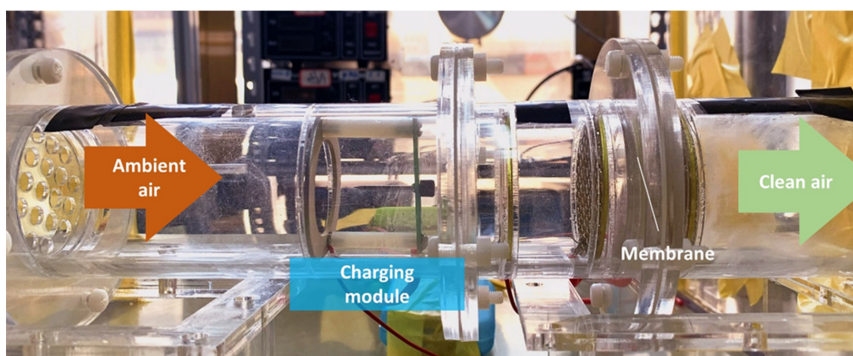


**Figure 3.** Real image of the setup used to investigate the filtration performance of the filter materials.

Each filter was exposed to the polluted air stream for 30 min, and in this period of time, the particle concentration was monitored upstream and downstream the filter. The filtration efficiency  $\eta$  for charged particles based on particle size was calculated using the following equation:

$$\eta(d_p) = \left( \frac{C_{up}(d_p) - C_{down}(d_p)}{C_{up}(d_p)} \right) \times 100 \%, \quad (1)$$

where  $C_{up}$  and  $C_{down}$  are the particles number concentration upstream and downstream the filter respectively, and  $d_p$  is the particle diameter.

The filters were also evaluated in terms of quality factor  $Q_F$  ( $\text{Pa}^{-1}$ ), which was calculated using the equation below.

$$Q_F = \frac{-\ln(1 - \eta_{(0.3-0.5 \mu\text{m})})}{\Delta P}, \quad (2)$$

where  $\eta_{(0.3-0.5 \mu\text{m})}$  represents the single-pass filtration efficiency for particles sized between 0.3 and 0.5  $\mu\text{m}$  at 0.8  $\text{m s}^{-1}$  face velocity, and  $\Delta P$  is the pressure drop at the same face velocity. The quality factor gives a clear understanding of which filter best optimises the ratio between pressure drop and filtration efficiency, and therefore, the ratio between the

energy use related to filter operation and the filter’s contribution to an improved indoor air quality. The quality factor was calculated based on the filtration efficiency of particles with diameters between 0.3 and 0.5  $\mu\text{m}$ , as this is commonly considered the most penetrating particle size.

3. Results and Discussion

3.1. Preparation of Electrospun Fibre Filters

The characteristic parameters that define the electrospinning process of the cellulose acetate solution were adjusted from the optimal conditions mentioned in the study from Christoforou and Doumanidis [39], and these are presented in Table 1. The conditions that stabilised the electrospinning process were based on a high feed rate of 1 mL min<sup>−1</sup>. Compared to other studies, where the feed rates for the polymer solution are in the range of mL h<sup>−1</sup> [40–42], the CA/acetone solution allowed for the fast fabrication of a free-from-beading and uniform fibre filter, owing also to the remotely controlled arm of the electrospinner. The final filter material is visible in Figure 4a. The air spraying of the solutions containing either AC or TiO<sub>2</sub> resulted in the final materials visible in Figure 4b,c, respectively, while the composite material is shown in Figure 4d.

Table 1. Solution, process, and environmental parameters that were used during the electrospinning of CA solution.

Solution Parameters			Process Parameters			Environmental Parameters	
CA Concentration	Solvent	Tip-to-Collector Distance	Voltage	Feed Rate	Needle Inner Ø	Temperature	Relative Humidity
12.5 w/v%	Acetone	9 cm	14.8 kV	1 mL min <sup>−1</sup>	1.5 mm	21 °C ± 0.5 °C	37% ± 3%

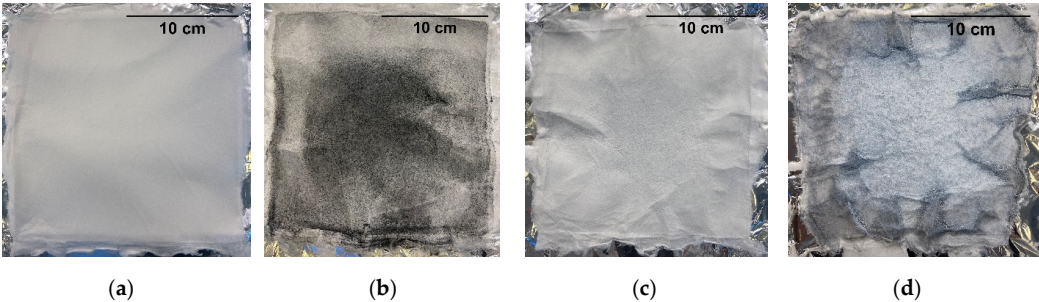
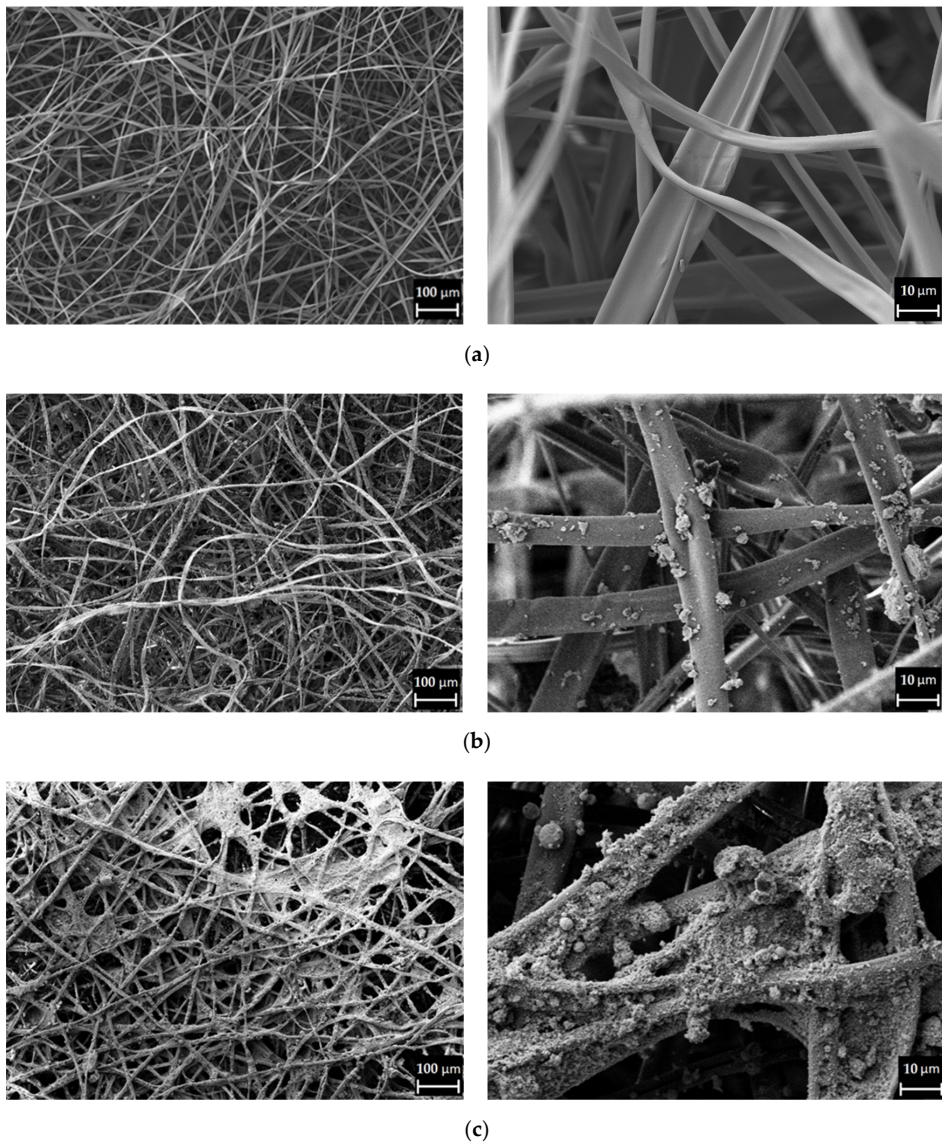


Figure 4. Electrospun filter materials developed in this study: (a) pure CA; (b) CA/AC; (c) CA/TiO<sub>2</sub>; (d) composite.

3.2. Fibre Characterisation

SEM images of different CA fibre filter samples are shown in Figure 5. The pure CA fibre presents a uniform flat-ribbon morphology, which is randomly oriented (Figure 5a). Compared to the smooth fibres of the pure CA membrane, the doped filters show a different fibre surface due to the use of additives. The CA fibre surface is visibly covered by AC (Figure 5b) and TiO<sub>2</sub> (Figure 5c). The dense deposition of TiO<sub>2</sub> highly affects the fibres’ morphology and the pore dimension, as the TiO<sub>2</sub> nanoparticles are forming agglomerates which tend to increase the fibre diameter and clog the pores. The presence of activated charcoal has a milder influence on the fibre morphology. The additive is still clearly visible on the fibre surface, but it does not fully coat it, as does TiO<sub>2</sub>.



**Figure 5.** SEM images of the different electrospun fibre materials: (a) pure CA; (b) CA/AC; (c) CA/TiO<sub>2</sub>.

The composite filter is a combination of the previous two CA/TiO<sub>2</sub> and CA/AC filters. SEM images of the four steps to fabricate each layer of the filters are shown in Figure 6. The presence of additives is clearly visible on the fibre surface on the second and fourth layers in the form of agglomerates.



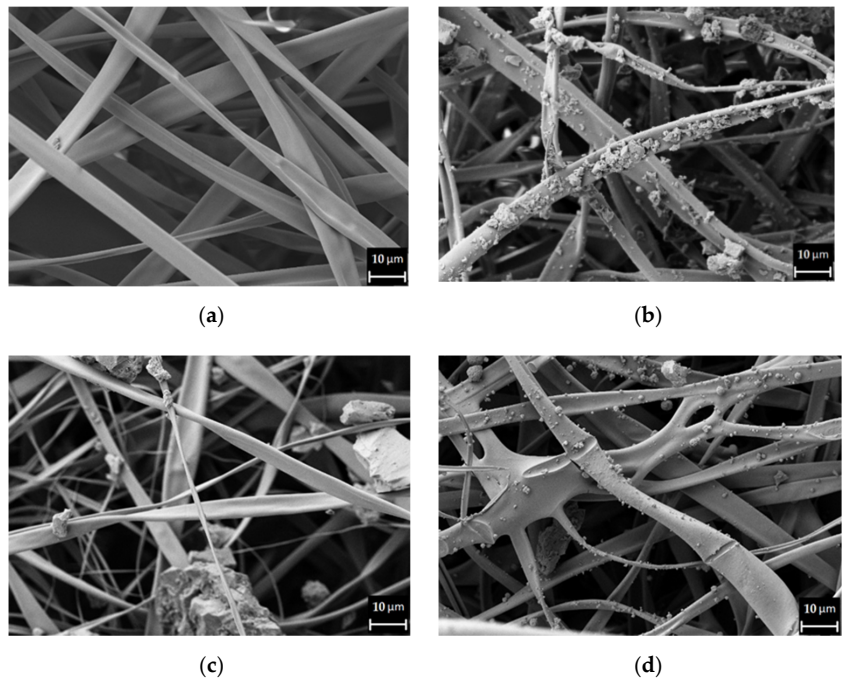


**Figure 6.** SEM images of the composite filter divided into the four layers of fabrication: (a) 1st layer, CA fibres; (b) 2nd layer, AC spray; (c) 3rd layer, CA fibres; (d) 4th layer, TiO<sub>2</sub> spray.

The SEM images of the pure CA fibres have been analysed to investigate the average fibre diameter. The average diameter distribution is presented in Figure 7. The mean fibre diameter is 4.2 µm. The fibres are not falling into the nano-dimension. This is the result of the electrospinning process, which was stable at a rather fast feed rate of 1 mL min<sup>−1</sup> and a short tip to collector distance of 9 cm. The polymer solution jet did not stretch enough to form nanofibres.

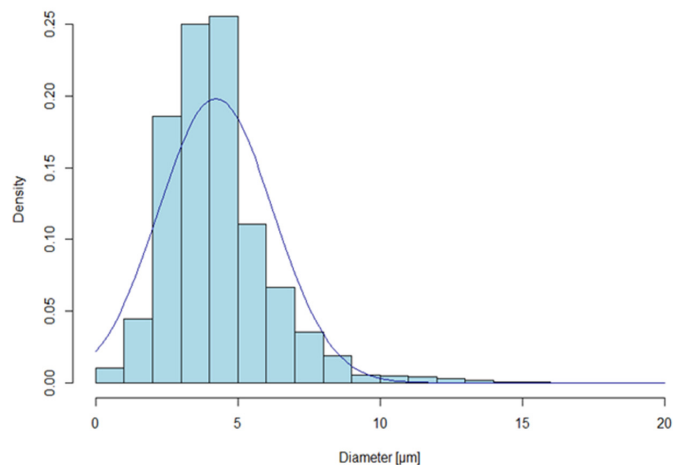


**Figure 7.** Mean fibre diameter distribution.

Furthermore, the surface porosity of the filters has also been determined for each filter material using ImageJ. Such a parameter is used as a comparative term for the use of the additives on the filter surface. The results are shown in Table 2. As previously mentioned, the use of additives reduces the surface porosity of the materials. The pure CA reached the highest surface porosity of 42%, while the surface porosity of CA/TiO<sub>2</sub> dropped to the lowest value of 32.5%.

**Table 2.** Results from the analysis of the filter porosity and thickness.

	CA	CA/AC	CA/TiO <sub>2</sub>	Composite
Surface porosity (%)	42.0 ± 5.4	38.5 ± 2.6	32.5 ± 5.1	34.4 ± 4.5
Thickness (mm)	0.11 ± 0.016	0.14 ± 0.012	0.15 ± 0.005	0.18 ± 0.007

The results of the thickness analysis are also presented in Table 2. The filter thickness ranges between 0.11 and 0.18 mm, and the results are consistent with the use of additives. The pure CA filter is the thinnest filter, whereas the composite filter, which incorporates two layers of additives, is the thickest material among the four samples.

### 3.3. Filtration Performance

The filter materials previously presented were cut into filters to install them into the set up (inner diameter: 50 mm) designed to evaluate the pressure drop and filtration efficiency.

#### 3.3.1. Pressure Drop

The filters' pressure drop was investigated in two different ranges of face velocity. Electrospun fibre filters are mostly tested at face velocity in the range from 10<sup>−2</sup> to 10<sup>−1</sup> m s<sup>−1</sup>; many of those are between 0.2 and 0.053 m s<sup>−1</sup> [25]. The filters developed were also evaluated in the low range of face velocity starting from 0.035 m s<sup>−1</sup> up to 0.087 m s<sup>−1</sup>, which would reproduce the case of a filter installed under natural ventilation conditions. However, such filters could be used in buildings as part of a mechanically ventilated system, where face velocities are as high as 1 m s<sup>−1</sup>. Therefore, the filters were also tested at 0.8 m s<sup>−1</sup> and 1 m s<sup>−1</sup>. The results are shown in Table 3.

**Table 3.** Pressure drop results for the different filters at different face velocities. Filtration efficiency to particle size between 0.3 and 0.5 µm and related quality factor calculated with pressure drop at 0.8 m s<sup>−1</sup> face velocity.

Filter	0.035 m s <sup>−1</sup>	0.053 m s <sup>−1</sup>	0.069 m s <sup>−1</sup>	0.087 m s <sup>−1</sup>	0.8 m s <sup>−1</sup>	1 m s <sup>−1</sup>	$\eta$	Q <sub>F</sub>
CA	3 Pa	3.5 Pa	4.7 Pa	6.6 Pa	63.0 Pa	74.1 Pa	73.3% ± 3.1%	0.020 Pa <sup>−1</sup>
CA/AC	3.2 Pa	3.7 Pa	4.9 Pa	6.8 Pa	63.3 Pa	74.7 Pa	80% ± 3.2%	0.023 Pa <sup>−1</sup>
CA/TiO <sub>2</sub>	3.2 Pa	3.7 Pa	4.9 Pa	7.0 Pa	63.4 Pa	74.8 Pa	76.8% ± 3.1%	0.022 Pa <sup>−1</sup>
Composite	3.3 Pa	3.8 Pa	5.1 Pa	7.0 Pa	63.8 Pa	75.3 Pa	85.3% ± 5.9%	0.027 Pa <sup>−1</sup>

The pure CA fibre filter showed a starting pressure drop of 3.5 Pa at a face velocity of 0.053 m s<sup>−1</sup>. The use of additives increased the pressure drop. The CA/AC and CA/TiO<sub>2</sub> filters show very similar results, with an increase in pressure drop of between 6 and 10% compared to pure CA on the low range of face velocities. When moving towards higher face velocity, the increase is always below 1%. The composite filter produced the highest pressure drop among the fabricated materials. Again, on the low range of face velocity, the impact of the additives seems to be more significant, and the composite filter reached a 10% higher pressure drop than the pure CA membrane. At 1 m s<sup>−1</sup>, the difference between the composite and CA filter pressure drop is around 1.6%.

The difference in pressure drop between filters seems to be strictly connected to the use of additives and their influence on the fibre morphology and filter thickness. The CA fibres were produced using the same electrospinning conditions. Therefore, any morphological change that can affect the filter performance is due to the doping process of the fibre surface. As it was visible from the SEM pictures, the fibre surfaces of the CA/AC and CA/TiO<sub>2</sub>

filters presented rougher characteristics, and the filters presented an increased thickness. Consequently, lower surface porosity was measured for the doped filters compared to pure CA, which resulted in a higher pressure drop. Even though the CA/TiO<sub>2</sub> filter showed lower surface porosity, the composite filter presented a higher pressure drop. The increased thickness from 0.15 to 0.18 mm compared to CA/TiO<sub>2</sub> might be responsible for the higher pressure drop result.

### 3.3.2. Particle Filtration Efficiency

The results of the filtration efficiency of the four different filters are presented in Figure 8. The face velocity was set at 0.8 m s<sup>−1</sup>. The air temperature and relative humidity were measured at 22.4 °C and 36.2%.

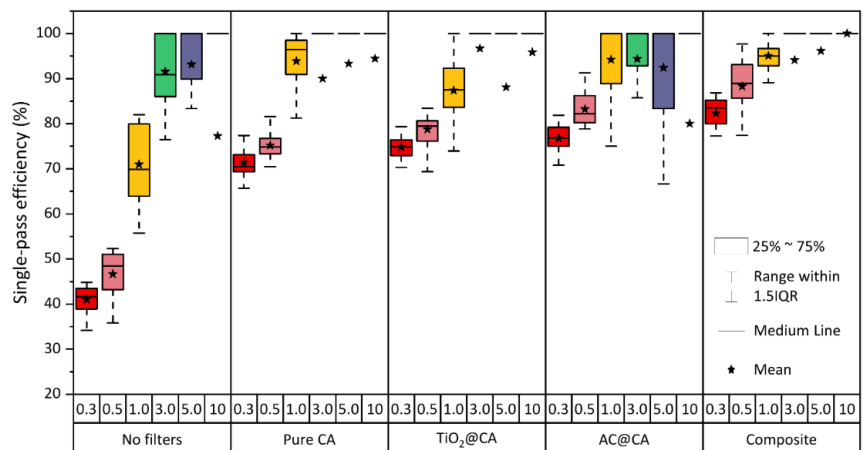


Figure 8. Particle filtration efficiency for the different filters per particle size.

The charging module was investigated in terms of particle removal without the use of any filter. It recorded a peak removal capacity towards 3.0–5.0 μm particle size (above 90%), while smaller particles (0.3–0.5 μm) easily penetrated it, and the removal capacity fell below 47%. Medium-sized particles between 0.5 and 3 μm and large particles between 5 and 10 μm have been removed with an efficiency of 71% and 77.3%, respectively.

The use of the filters had an impact on filtration of all particle sizes, with the most significant improvements registered for the smaller and most harmful particles. As visible from the graph in Figure 8, all ultrathin filters have recorded particle filtration efficiency above 70%. In accordance with the concept of most penetrating particle size (MPPS), the smaller particles penetrate the filters more, resulting in a decreased mean filtration efficiency for 0.3 to 0.5 μm particles compared to larger particle sizes. For particles between 1 and 10 μm diameter, the filters have recorded filtration efficiencies above 90%.

Comparing the performance across the different ultrathin filters, the use of additives affected the filtration capacity. The major and most important impact is again on the filtration of small charged particles between 0.3 and 0.5 μm diameter. The CA/AC and CA/TiO<sub>2</sub> filters recorded an increased filtration efficiency of 9.2% and 4.8 %, respectively, compared to the pure CA filter. The composite filter registered the best performance with an improvement of 16.4%. Moving towards the larger particles, the pure CA filter also performed well in comparison with the CA/AC and CA/TiO<sub>2</sub> filters. The composite filter again achieved the best performance, with 95% removal of particles around 1 μm size and achieving 100% removal of the largest particles between 5 and 10 μm.

Figure 9 shows the relationship between single-pass filtration efficiency for 0.3–0.5 μm particle size, surface porosity, and pressure drop. As supposed, the general tendency demonstrates that the higher the surface porosity, the lower the filtration efficiency and

the pressure drop. The CA/TiO<sub>2</sub> filter does not completely follow the trend because it has shown a lower efficiency compared to CA/AC filter, despite a lower porosity. The difference in the effect seen between AC and TiO<sub>2</sub> surface-modified filters, apart from their differences in surface porosity, is in the inherent nature of the modifying material. AC renders the filter material more hydrophobic, whereas TiO<sub>2</sub> adds negative charges to the filter surface. As it can be seen in Figure 9, the hydrophobic effect surpasses the effect of the negative charge of TiO<sub>2</sub> and thereby renders the CA/AC filter better suited than the CA/TiO<sub>2</sub> filter.

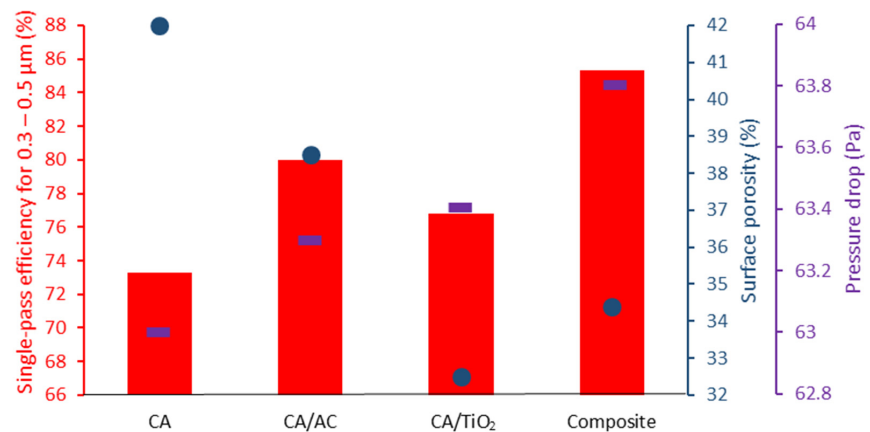


**Figure 9.** Single-pass filtration efficiency for particle size between 0.3 and 0.5  $\mu\text{m}$ , surface porosity, and pressure drop.

Table 3 also shows the calculated quality factor for each of the filters. These parameters give a clear understanding of which filter best optimised the ratio between filtration efficiency and pressure drop. The result revealed that the composite filter best optimises this ratio when comparing it with the other filters developed in this work. The combination of activated charcoal and titanium dioxide in a composite filter reached a considerably higher filtration efficiency at the cost of a slightly increased pressure drop.

Data have been collected from other studies in order to compare the filtration performance of different filters at a face velocity of  $0.8 \text{ m s}^{-1}$ , as reported in Table 4. The filtration efficiency is related to particle sizes between 0.3 and  $0.5 \mu\text{m}$ , and this criterion has been used to select the studies in the literature. In their study, Xia et al. have also highlighted that most of the electrospun fibre filters were evaluated at very low face velocities [25]. In order to compare the studies in the literature with the filter fabricated in this study, pressure drops have been recalculated, assuming a proportional relationship with face velocities [25]. The composite filter developed for this work shows a high-quality factor compared to the others. Only one sample from the study of Zhang et al. has achieved a higher quality factor [43]. The filtration efficiency of the ultrathin composite material is lower compared to the samples from other studies, which instead reached significantly higher pressure drops. The main difference lies in the average fibre diameter of the fabricated composite material and the use of the charging module in order to ensure a uniform charge on the particles. The micro-dimension of the fibres and the use of additives have contributed to forming a surface porosity able to maintain the balance between pressure drop and filtration capacity while using a single ultrathin layer of filter material. The final result is that the composite filter kept a low pressure drop and achieved a relatively high filtration efficiency, optimising the quality factor compared to other electrospun fibre materials.



**Table 4.** Comparison of filtration efficiency for particle size between 0.3 and 0.5  $\mu\text{m}$ , pressure drop and quality factor at  $0.8\text{ m s}^{-1}$  with studies in the literature.

Case	Particle Filtration Efficiency (0.3–0.5 $\mu\text{m}$ ) (%)	Pressure Drop (Pa)	QF ( $\text{Pa}^{-1}$ )	Material	Ref
1	99.98	243	0.0351	Polyimide nanofibres	[43]
2	98	1997	0.0019	Poly(vinyl alcohol)/Poly(acrylic acid) + silica and silver nanoparticles	[44]
3	99.992	1781	0.0053	Polysulfone/Polyacrylonitrile/Polyamide 6	[45]
4	99.997	725	0.0143	Polysulfone/ $\text{TiO}_2$ fibrous membrane	[26]
5	99.99	4315	0.0021	Nylon 6 nanofibre	[46]
6	99.989	659	0.0138	Polyacrylonitrile/silica nanoparticles	[47]
7	82.3	63.8	0.0271	Composite filter CA/AC/CA/ $\text{TiO}_2$	This work

#### 4. Conclusions

In summary, four ultrathin CA-based electrospun fibre filters were fabricated, achieving various configurations with the addition of AC and  $\text{TiO}_2$ , separately and combined. The filters presented an average fibre diameter of  $4.2\text{ }\mu\text{m}$  and a surface porosity between 32.5 and 42%. The use of additives has led to an overall rougher fibre morphology and lower surface porosity compared to the undoped CA filter, reaching an increased particle filtration and a slightly higher pressure drop. The filters presented ultralow pressure drops between 3 and  $3.3\text{ Pa}$  at  $5.3\text{ cm s}^{-1}$  face velocity. The pure CA filter had a thickness of  $0.14\text{ mm}$  and achieved a filtration efficiency of 73.3% for charged particles between 0.3 and  $0.5\text{ }\mu\text{m}$ . The filtration efficiencies improved with the use of the additives. The composite filter, in which both AC and  $\text{TiO}_2$  nanoparticles were embedded, demonstrated a thickness of  $0.18\text{ mm}$  and presented a filtration efficiency of 82% for charged particles sized between 0.3 and  $0.5\text{ }\mu\text{m}$ , reaching 100% removal of  $10\text{ }\mu\text{m}$  particles, at the cost of a pressure drop of  $63.8\text{ Pa}$  at  $0.8\text{ m s}^{-1}$  face velocity. This study showed the positive impact of additives on the particle filtration performance of ultrathin electrospun fibre filters. The ultrathin CA based-composite filter presented filtration performances and quality factors that are significantly improved compared to other electrospun fibre filters found in the literature today.

**Author Contributions:** Conceptualisation, R.O., P.F. and A.A.; methodology, R.O., Y.G., P.F. and J.M.; validation, R.O., Y.G., P.F. and J.M.; formal analysis, R.O. and Y.G.; investigation, R.O. and Y.G.; resources, P.F. and J.M.; writing—original draft preparation, R.O.; writing—review and editing, all authors; visualisation, R.O. and Y.G.; supervision, A.A., P.F., J.M.; project administration, A.A. and P.F.; funding acquisition, A.A. and P.F. All authors have read and agreed to the published version of the manuscript.

**Funding:** This research was funded by Grundejernes Investeringssfond, the Department of the Built Environment, and the Department of Materials and Production at Aalborg University. The research was financially supported by the National Natural Science Foundation of China (No. 52078269).

**Acknowledgments:** The authors thank research technician Peter Kjær Kristensen from the Department of Materials and Production at Aalborg University for his support in performing the SEM images.

**Conflicts of Interest:** The authors declare no conflict of interest. The funders had no role in the design of the study; in the collection, analyses, or interpretation of data; in the writing of the manuscript, or in the decision to publish the results.

#### References

1. Mills, N.L.; Donaldson, K.; Hadoke, P.W.; Boon, N.A.; MacNee, W.; Cassee, F.R.; Sandström, T.; Blomberg, A.; Newby, D.E. Adverse cardiovascular effects of air pollution. *Nat. Clin. Pr. Neurol.* **2008**, *6*, 36–44. [\[CrossRef\]](#)
2. Brunekreef, B.; Holgate, S.T. Air pollution and health. *Lancet* **2002**, *360*, 1233–1242. [\[CrossRef\]](#)
3. Pope, C.A., 3rd; Dockery, D.W. Health Effects of Fine Particulate Air Pollution: Lines that Connect. *J. Air Waste Manag. Assoc.* **2006**, *56*, 709–742. [\[CrossRef\]](#)

4. Katsouyanni, K.; Touloumi, G.; Samoli, E.; Gryparis, A.; Le Tertre, A.; Monopoli, Y.; Rossi, G.; Zmirou, D.; Ballester, F.; Boumghar, A.; et al. Confounding and Effect Modification in the Short-Term Effects of Ambient Particles on Total Mortality: Results from 29 European Cities within the APHEA2 Project. *Epidemiology* **2001**, *12*, 521–531. [\[CrossRef\]](#)
5. World Health Organization. *WHO Global Air Quality Guidelines. Particulate Matter (PM<sub>2.5</sub> and PM<sub>10</sub>), Ozone, Nitrogen Dioxide, Sulfur Dioxide and Carbon Monoxide*; WHO: Geneva, Switzerland, 2021.
6. Xia, T.; Chen, C. Differentiating between indoor exposure to PM<sub>2.5</sub> of indoor and outdoor origin using time-resolved monitoring data. *Build. Environ.* **2019**, *147*, 528–539. [\[CrossRef\]](#)
7. Chen, C.; Zhao, B. Review of relationship between indoor and outdoor particles: I/O ratio, infiltration factor and penetration factor. *Atmos. Environ.* **2011**, *45*, 275–288. [\[CrossRef\]](#)
8. Fazli, T.; Zeng, Y.; Stephens, B. Fine and ultrafine particle removal efficiency of new residential HVAC filters. *Indoor Air* **2019**, *29*, 656–669. [\[CrossRef\]](#)
9. Brincat, J.-P.; Sardella, D.; Muscat, A.; Decelis, S.; Grima, J.; Valdramidis, V.; Gatt, R. A review of the state-of-the-art in air filtration technologies as may be applied to cold storage warehouses. *Trends Food Sci. Technol.* **2016**, *50*, 175–185. [\[CrossRef\]](#)
10. Stephens, B.; Siegel, J.A. Ultrafine particle removal by residential heating, ventilating, and air-conditioning filters. *Indoor Air* **2013**, *23*, 488–497. [\[CrossRef\]](#) [\[PubMed\]](#)
11. ASME. *Addenda to ASME AG-1–2003 Code on Nuclear Air and Gas Treatment*; ASME: New York, NY, USA, 2004.
12. Bourrous, S.; Bouilloux, L.; Ouf, F.-X.; Lemaitre, P.; Nerisson, P.; Thomas, D.; Appert-Collin, J.-C. Measurement and modeling of pressure drop of HEPA filters clogged with ultrafine particles. *Powder Technol.* **2016**, *289*, 109–117. [\[CrossRef\]](#)
13. Ardkapan, S.R.; Johnson, M.S.; Yazdi, S.; Afshari, A.; Bergsøe, N.C. Filtration efficiency of an electrostatic fibrous filter: Studying filtration dependency on ultrafine particle exposure and composition. *J. Aerosol Sci.* **2014**, *72*, 14–20. [\[CrossRef\]](#)
14. COAG. *Guide to Best Practice Maintenance & Operation of HVAC Systems for Energy Efficiency*; COAG: Canberra, ACT, Australia, 2012.
15. Stephens, B.; Siegel, J.A.; Novoselac, A. Energy implications of filtration in residential and light-commercial buildings. *Ashrae Trans.* **2010**, *116*, 346–357.
16. Li, D.; Xia, Y. Electrospinning of Nanofibers: Reinventing the Wheel? *Adv. Mater.* **2004**, *16*, 1151–1170. [\[CrossRef\]](#)
17. Zhao, X.; Wang, S.; Yin, X.; Yu, J.; Ding, B. Slip-Effect Functional Air Filter for Efficient Purification of PM<sub>2.5</sub>. *Sci. Rep.* **2016**, *6*, 35472. [\[CrossRef\]](#) [\[PubMed\]](#)
18. Shou, D.; Ye, L.; Fan, J. Gas transport properties of electrospun polymer nanofibers. *Polymer* **2014**, *55*, 3149–3155. [\[CrossRef\]](#)
19. Li, Y.; Yin, X.; Yu, J.; Ding, B. Electrospun nanofibers for high-performance air filtration. *Compos. Commun.* **2019**, *15*, 6–19. [\[CrossRef\]](#)
20. Zhu, M.; Han, J.; Wang, F.; Shao, W.; Xiong, R.; Zhang, Q.; Pan, H.; Yang, Y.; Samal, S.K.; Zhang, F.; et al. Electrospun Nanofibers Membranes for Effective Air Filtration. *Macromol. Mater. Eng.* **2017**, *302*, 1600353. [\[CrossRef\]](#)
21. Bian, Y.; Wang, R.; Ting, S.H.; Chen, C.; Zhang, L. Electrospun SF/PVA Nanofiber Filters for Highly Efficient PM<sub>2.5</sub> Capture. *IEEE Trans. Nanotechnol.* **2018**, *17*, 934–939. [\[CrossRef\]](#)
22. Niu, Z.; Bian, Y.; Xia, T.; Zhang, L.; Chen, C. An optimization approach for fabricating electrospun nanofiber air filters with minimized pressure drop for indoor PM<sub>2.5</sub> control. *Build. Environ.* **2021**, *188*, 107449. [\[CrossRef\]](#)
23. Topuz, F.; Abdulhamid, M.A.; Hardian, R.; Holtzl, T.; Szekeley, G. Nanofibrous membranes comprising intrinsically microporous polyimides with embedded metal–organic frameworks for capturing volatile organic compounds. *J. Hazard. Mater.* **2021**, *424*, 127347. [\[CrossRef\]](#)
24. Kumar, S.; Jang, J.; Oh, H.; Jung, B.J.; Lee, Y.; Park, H.; Yang, K.H.; Seong, Y.C.; Lee, J.-S. Antibacterial Polymeric Nanofibers from Zwitterionic Terpolymers by Electrospinning for Air Filtration. *ACS Appl. Nano Mater.* **2021**, *4*, 2375–2385. [\[CrossRef\]](#)
25. Xia, T.; Bian, Y.; Zhang, L.; Chen, C. Relationship between pressure drop and face velocity for electrospun nanofiber filters. *Energy Build.* **2018**, *158*, 987–999. [\[CrossRef\]](#)
26. Wan, H.; Wang, N.; Yang, J.; Si, Y.; Chen, K.; Ding, B.; Sun, G.; El-Newehy, M.; Al-Deyab, S.S.; Yu, J. Hierarchically structured polysulfone/titania fibrous membranes with enhanced air filtration performance. *J. Colloid Interface Sci.* **2014**, *417*, 18–26. [\[CrossRef\]](#) [\[PubMed\]](#)
27. Tian, M.-J.; Liao, F.; Ke, Q.-F.; Guo, Y.-P. Synergetic effect of titanium dioxide ultralong nanofibers and activated carbon fibers on adsorption and photodegradation of toluene. *Chem. Eng. J.* **2017**, *328*, 962–976. [\[CrossRef\]](#)
28. Ao, C.; Lee, S.-C. Indoor air purification by photocatalyst TiO<sub>2</sub> immobilized on an activated carbon filter installed in an air cleaner. *Chem. Eng. Sci.* **2005**, *60*, 103–109. [\[CrossRef\]](#)
29. Chuang, Y.-H.; Hong, G.-B.; Chang, C.-T. Study on particulates and volatile organic compounds removal with TiO<sub>2</sub> nonwoven filter prepared by electrospinning. *J. Air Waste Manag. Assoc.* **2014**, *64*, 738–742. [\[CrossRef\]](#)
30. Shi, B.; Ekberg, L. Ionizer Assisted Air Filtration for Collection of Submicron and Ultrafine Particles—Evaluation of Long-Term Performance and Influencing Factors. *Environ. Sci. Technol.* **2015**, *49*, 6891–6898. [\[CrossRef\]](#)
31. Park, J.H.; Yoon, K.Y.; Hwang, J. Removal of submicron particles using a carbon fiber ionizer-assisted medium air filter in a heating, ventilation, and air-conditioning (HVAC) system. *Build. Environ.* **2011**, *46*, 1699–1708. [\[CrossRef\]](#)
32. Agranovski, I.E.; Huang, R.; Pyankov, O.V.; Altman, I.S.; Grinshpun, S.A. Enhancement of the Performance of Low-Efficiency HVAC Filters Due to Continuous Unipolar Ion Emission. *Aerosol Sci. Technol.* **2006**, *40*, 963–968. [\[CrossRef\]](#)
33. Tian, E.; Mo, J. Toward energy saving and high efficiency through an optimized use of a PET coarse filter: The development of a new electrostatically assisted air filter. *Energy Build.* **2019**, *186*, 276–283. [\[CrossRef\]](#)

34. Tian, E.; Yu, Q.; Gao, Y.; Wang, H.; Wang, C.; Zhang, Y.; Li, B.; Zhu, M.; Mo, J.; Xu, G.; et al. Ultralow Resistance Two-Stage Electrostatically Assisted Air Filtration by Polydopamine Coated PET Coarse Filter. *Small* **2021**, *17*, 2102051. [[CrossRef](#)]
35. Xia, F.; Gao, Y.; Tian, E.; Afshari, A.; Mo, J. Fast fabricating cross-linked nanofibers into flameproof metal foam by air-drawn electrospinning for electrostatically assisted particle removal. *Sep. Purif. Technol.* **2021**, *274*, 119076. [[CrossRef](#)]
36. Gao, Y.; Tian, E.; Mo, J. Electrically Responsive Coarse Filters Endowed by High-Dielectric-Constant Surface Coatings toward Efficient Removal of Ultrafine Particles and Ozone. *ACS ES&T Eng.* **2021**, *1*, 1449–1459. [[CrossRef](#)]
37. Entcheva, E.; Bien, H.; Yin, L.; Chung, C.Y.; Farrell, M.; Kostov, Y. Functional cardiac cell constructs on cellulose-based scaffolding. *Biomaterials* **2004**, *25*, 5753–5762. [[CrossRef](#)] [[PubMed](#)]
38. Kwon, M.; Kim, J.; Kim, J. Photocatalytic activity and filtration performance of hybrid TiO<sub>2</sub>-cellulose acetate nanofibers for air filter applications. *Polymers* **2021**, *13*, 1331. [[CrossRef](#)]
39. Christoforou, T.; Doumanidis, C. Biodegradable cellulose acetate nanofiber fabrication via electrospinning. *J. Nanosci. Nanotechnol.* **2010**, *10*, 6226–6233. [[CrossRef](#)] [[PubMed](#)]
40. Su, J.; Yang, G.; Cheng, C.; Huang, C.; Xu, H.; Ke, Q. Hierarchically structured TiO<sub>2</sub>/PAN nanofibrous membranes for high-efficiency air filtration and toluene degradation. *J. Colloid Interface Sci.* **2017**, *507*, 386–396. [[CrossRef](#)]
41. Qin, X.-H.; Wang, S.-Y. Electrospun nanofibers from crosslinked poly(vinyl alcohol) and its filtration efficiency. *J. Appl. Polym. Sci.* **2008**, *109*, 951–956. [[CrossRef](#)]
42. Guibo, Y.; Qing, Z.; Yahong, Z.; Yin, Y.; Yumin, Y. The electrospun polyamide 6 nanofiber membranes used as high efficiency filter materials: Filtration potential, thermal treatment, and their continuous production. *J. Appl. Polym. Sci.* **2013**, *128*, 1061–1069. [[CrossRef](#)]
43. Zhang, R.; Liu, C.; Hsu, P.-C.; Zhang, C.; Liu, N.; Zhang, J.; Lee, H.R.; Lu, Y.; Qiu, Y.; Chu, S.; et al. Nanofiber Air Filters with High-Temperature Stability for Efficient PM<sub>2.5</sub> Removal from the Pollution Sources. *Nano Lett.* **2016**, *16*, 3642–3649. [[CrossRef](#)]
44. Zhu, M.; Hua, D.; Pan, H.; Wang, F.; Manshian, B.; Soenen, S.; Xiong, R.; Huang, C. Green electrospun and crosslinked poly(vinyl alcohol)/poly(acrylic acid) composite membranes for antibacterial effective air filtration. *J. Colloid Interface Sci.* **2018**, *511*, 411–423. [[CrossRef](#)] [[PubMed](#)]
45. Zhang, S.; Tang, N.; Cao, L.; Yin, X.; Yu, J.; Ding, B. Highly Integrated Polysulfone/Polyacrylonitrile/Polyamide-6 Air Filter for Multilevel Physical Sieving Airborne Particles. *ACS Appl. Mater. Interfaces* **2016**, *8*, 29062–29072. [[CrossRef](#)] [[PubMed](#)]
46. Kim, G.T.; Ahn, Y.C.; Lee, J.K. Characteristics of Nylon 6 nanofilter for removing ultra fine particles. *Korean J. Chem. Eng.* **2008**, *25*, 368–372. [[CrossRef](#)]
47. Wang, N.; Si, Y.; Wang, N.; Sun, G.; El-Newehy, M.; Al-Deyab, S.S.; Ding, B. Multilevel structured polyacrylonitrile/silica nanofibrous membranes for high-performance air filtration. *Sep. Purif. Technol.* **2014**, *126*, 44–51. [[CrossRef](#)]



## Chapter 8

### Paper V

# Cellulose Acetate-based composite fibre membranes for toluene removal

R. Orlando, A. Afshari and P. Fojan

The paper has been submitted in the  
*Journal of Industrial Textiles* in November 2021.



# Cellulose Acetate-based composite fibre membranes for toluene removal

Roberta Orlando<sup>a</sup>, Alireza Afshari<sup>a\*</sup> and Peter Fojan<sup>b</sup>

<sup>a</sup>Department of the Built Environment, Aalborg University, DK-2450 Copenhagen, Denmark

<sup>b</sup>Department of Materials and Production, Aalborg University, DK-9220 Aalborg, Denmark

\*Corresponding author e-mail address: aaf@build.aau.dk

## Abstract

Volatile organic compounds (VOCs) are some of the most typical air pollutants emitted from fossil fuel combustion. In indoor environments they originate from cleaning products, cooking and by chemical reactions with building materials. The VOCs removal from polluted air has been achieved using several different methods but primarily through the use of adsorbent materials or through degradation with photocatalytic oxidation. Fibres produced by electrospinning have the possibility to easily incorporate additives into the fibres and onto their surface. This can functionalise them for efficient VOCs removal. Cellulose acetate (CA)-based electrospun fibre membranes have been fabricated and doped with activated charcoal (AC) and titanium dioxide (TiO<sub>2</sub>), either separately or in combination to investigate their toluene removal capacity of the single additive and the synergic effects of adsorption and photocatalytic oxidation. Two different methods of functionalisation of the fibres with AC and TiO<sub>2</sub> have been used. These methods are air spraying and electro-spraying. Several configurations of the final membranes have been investigated. SEM images indicate that the additives have been successfully distributed on the fibre surface and they affect their morphology by increasing the overall roughness and the thickness of the final membranes. Adsorption with activated charcoal achieved 45.5% removal of toluene with a starting concentration of 22.5 ppm. Photocatalytic oxidation was probably initiated using a blacklight blue UV lamp with a peak wavelength of 365 nm as formation of formaldehyde was recorded. The findings suggest that photocatalytic oxidation is affected by the residence time and UV light intensity.

**Keywords:** Cellulose Acetate; Electrospinning; Titanium dioxide; Activated charcoal; Air purification; Volatile organic compounds

## 1. Introduction

In modern society, people spend more than 90% of their daily time in an indoor environment [1] and consequently the indoor air quality (IAQ) has a major impact on people's health, productivity and comfort [2]–[4]. Typical indoor air pollutants are particulates, volatile organic compounds (VOCs), nitrogen oxides ( $\text{NO}_x$ ), carbon oxide (CO) and sulphur dioxide ( $\text{SO}_2$ ). VOCs are a major group of indoor contaminants and the main compounds contain alkenes, alcohol, aromatics and carboxylic acids. Formaldehyde, ethanol and toluene are examples of indoor VOCs [5]. The sources of such pollutants are various and are mostly found inside the building, such as cleaning products, building construction materials and furnishings (plywood products and carpets) as well as office equipment like printers and photocopiers, but also human occupancy and related activities [6]–[9]. Owing to the concerns related to IAQ, several different technologies have been investigated and developed to remove VOCs from indoor air, such as non-thermal plasma [10], adsorption [11], ozonation [12] and photocatalytic oxidation [13].

Plasma based methods are related to the use of a high voltage discharge for the destruction of gaseous pollutants [14]. Non-thermal plasma is associated with the production of unwanted by-products like  $\text{NO}_x$  and ozone, poor energy efficiency and unsteady operation [15], [16]. The use of ozone generators for removal of VOCs was more frequent in the 1990s. Later, it was proven that the efficiency of VOC removal with such technology was rather low [17] and more importantly, ozone has been found to contribute to the formation of harmful secondary organic aerosols [18] and can cause asthma and other health related issues in humans [19]. Adsorption and photocatalytic oxidation have been the two methods that attract most interest in the removal and degradation of VOCs.

Adsorption has proven to successfully retain various contaminants on the surface of the adsorbent materials, like zeolites, some polymers, activated alumina and above all, activated charcoal (AC). Carbon materials have demonstrated to be low-cost, highly efficient and stable in removing VOCs and therefore, despite some disadvantages related to their hygroscopicity, have the most potential as adsorbent materials [20]. Activated carbon fibres have demonstrated better performance in adsorbing VOCs compared to zeolites, silica gel and granular activated carbon when investigated under the same conditions [21]. Activated charcoal adsorption capacity has been investigated for most VOCs including alcohols, aromatic compounds, esters, aldehydes and alkanes and has proven to be effective against a wide range of pollutants [22].

Degradation of VOCs is promoted by photocatalytic oxidation (PCO), which relies on the presence of a semiconductor as a catalyst and an irradiation source that initiates the reaction [15]. The interesting characteristics of PCOs are related to their activity towards various contaminants, formation of benign final products ( $\text{CO}_2$  and  $\text{H}_2\text{O}$ ) and optimal operation at room temperature [23]. Titanium dioxide has been the



most used catalyst for this application because of its promising performance as a photocatalyst under UV light irradiation and chemical stability [24]. The main disadvantage of using PCO is the potential formation of harmful by-products such as aldehydes, ketones or organic acids in cases of an incomplete reaction [25]–[27]. Parameters such as relative humidity, residence time, UV source wavelength, intensity and pollutant concentrations are influencing factors in the reaction process of degrading VOCs [28]–[30]. Toluene conversion efficiency has increased from 30% to 90% when the residence time moved from 120 ms to 1920 ms, indicating the importance of this parameter and highlighting the non-complete conversion in any experimental conditions [29].

In order to enhance the efficiency of PCO, the exposure to light irradiance and to the polluted air should be maximised. This can be achieved with combined use with an adsorbent material as a support. The adsorbent would retain the pollutant from the air close to the photocatalyst and this could mitigate the negative influence of a short residence time. Several studies have investigated the use of AC as a support material for  $\text{TiO}_2$  in removing VOCs from polluted air [31]–[34]. The conversion of toluene using P25  $\text{TiO}_2$  was demonstrated to drop down to about 47% when reducing the residence time from 3.7 to 0.6 min, while the reduction was only about 27% when  $\text{TiO}_2$  was combined with AC [31]. PCO can be used as a regeneration method of AC when located downstream of the adsorbent [34]. Furthermore, the combined use of  $\text{TiO}_2$ /AC has been demonstrated to not only enhance the removal efficiency of the pollutants but also to reduce the amount of intermediate by-products released in the air, as well as delaying the adsorption saturation of AC [33], [35].

In recent years, electrospinning has attracted a large amount of attention, as it is a technique that allows fast and efficient mass production of fibrous materials. Furthermore, the process allows easy functionalisation with a wide variety of materials, such as  $\text{TiO}_2$  and AC, to enhance the removal efficiency of VOCs by the fibres [36]–[39]. Polyvinyl alcohol (PVA)-based fibres doped with  $\text{TiO}_2$  have shown an acetone removal efficiency of 50%, with an initial concentration of 1500 ppm, under a light source of UV-365 nm and a retention time of 10 s [37]. When the retention time was increased from 10 s to 100 s, the removal efficiency of acetone increased to 99% [37]. Polyacrylonitrile (PAN)-based activated carbon electrospun fibres produced by carbonisation and steam activation after electrospinning demonstrated to be an effective adsorbent towards formaldehyde, showing a breakthrough time of 10.5 h at 11 ppm of formaldehyde and in dry conditions [39]. This breakthrough time is remarkably longer compared to conventional activated carbon fibres (FE100), which under the same conditions was 4 h [39].  $\text{TiO}_2$ -AC complex fibres have been prepared by electrospinning and the fibres were investigated for the removal of Prussian blue dyes by solar dye irradiation, reaching a dye removal of 94-99% [40].

The present study introduces five different electrospun fibre membranes made of cellulose acetate and loaded with  $\text{TiO}_2$  and AC either separately or combined to investigate the toluene removal capacity of the single additive and the synergic effect of adsorption and photocatalytic oxidation. The membranes were exposed to toluene, which was chosen because it is a common VOC found in indoor air and used as a standard substance for PCO experiments. Cellulose acetate (CA) was selected because it is a biodegradable organic material, highly available and previously used for protective clothing, artificial skin and air filtration [41]–[43]. The biodegradability of CA is an advantage compared to the typically employed synthetic polymers, as it means CA does not produce microplastic, both while in use and when it is disposed [43].

The electrospun fibres were doped by using air spraying or electrospaying to include, mix and combine the additives in different configurations. The fibre morphology and characteristic and the toluene removal capacity of titanium dioxide and activated charcoal when used as additives on polymer based electrospun fibres was experimentally investigated and compared.

## **2. Experimental**

### **2.1 Materials**

Cellulose Acetate (CA,  $M_N$  30000 GPC, 39.8 wt% acetyl content) was purchased from Sigma-Aldrich, together with powdered-form AC ( $MW$  12.01 g mol<sup>-1</sup>). Nanopowder aerioxide titanium dioxide ( $\text{TiO}_2$  P25) was given by Evonik Industries. Ethanol, acetone, and 2-Propanol were employed as received from Avantor. All materials were used without further purification.

### **2.2 Synthesis of electrospun fibre membranes**

The membranes were prepared using the method described in the previous work [43]. A homogeneous CA-solution was obtained stirring vigorously 31.25 g of cellulose acetate in 250 mL of acetone. The mixing was performed for 12 h at 20°C (room temperature).

Then, three different dispersions were prepared. The first dispersion consisted of 1.5 g of  $\text{TiO}_2$  mixed for 1 h in a 100 mL solution of ethanol and 2-propanol (1:4). To ensure uniformity, the solution was kept 30 min in a ultrasonicated bath. The second dispersion contained 2 g of AC mixed in the same solvent mixture (100 mL ethanol and 2-propanol; 1:4). In this case, to ensure a homogenous dispersion of AC, the solution was kept under continuously stirring before being used [43]. These two dispersions were prepared and used in the air spraying process to dope the electrospun fibre membranes. The third solution was prepared to be used in electrospaying and consisted of 2 g  $\text{TiO}_2$  mixed with 20 mL of acetone.

For the preparation of the CA membranes, electrospinning was performed on a vertical downward configuration with a flat collector, using an electrospinner 2.2.D-500 from Yflow A/S. The electrospinner provides a movable arm that allows for movement of the needle in the X-Y plane via a pre-programmed track. Figure 1a shows a schematic representation of the setup. The prepared polymer solution was transferred to a 20 mL glass syringe (Poulsen & Graf GmbH). The applied voltage was 14.8 kV, the feed rate was kept constant at 1 mL min<sup>-1</sup> through a needle with a 1.5 mm inner diameter, kept at 9 cm from the collector. Continuous electrospinning was performed to use 10 mL of the CA solution for producing a fibre mat [43]. To ensure uniform fibre distribution on the collector surface, the movement of the needle was remotely controlled on a X-Y motion at a constant velocity (50 mm s<sup>-1</sup>) on the 20 cm x 20 cm collector (Figure 1). During electrospinning, the relative humidity was controlled in the range 27-32% and the temperature was registered in the range 19.8-20.8°C inside the electrospinning box. In order to complete evaporate the solvent, the membrane was kept in a ventilated oven at 70°C for 1 h [43].

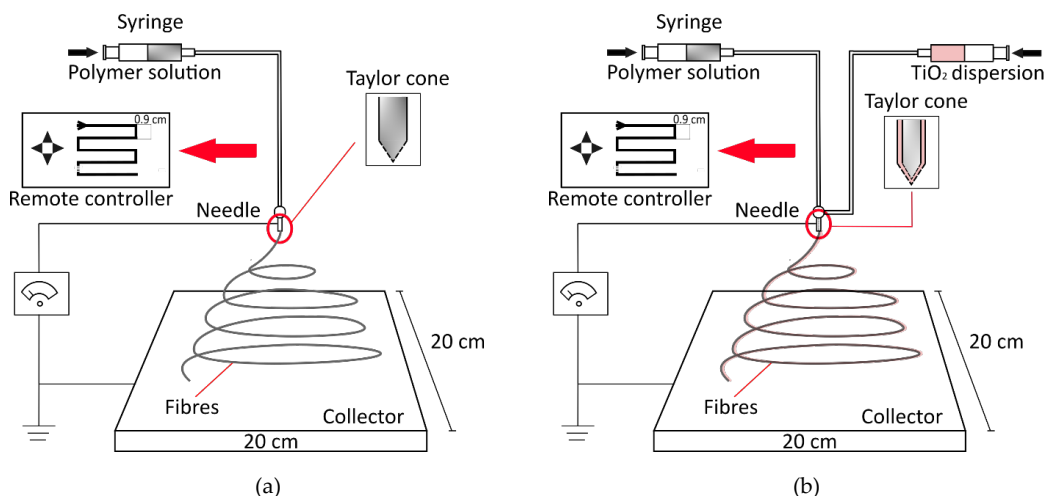


Figure 1. Representation of the two setups used for electrospinning in this research project, (a) single needle, (b) co-axial needle

The pure CA membrane fabricated with electrospinning was the base for three different membrane types: the CA/AC, the CA/TiO<sub>2</sub> and the composite membrane. The first two membranes were made air spraying the respective additive solution with an air brush onto the CA-membrane surface. The spraying process was performed by placing the electrospun CA membrane onto a metal grid in a fume hood. The distance between the grid and the air brush was kept at 20 cm. The process consisted of 2 min spraying at a flow rate of 10 L min<sup>-1</sup> of nitrogen gas. Each membrane was sprayed twice and the process was interspersed with a 1 h drying phase at 70°C [43]. In the composite membrane, two CA electrospun fibre layers were interspersed with spraying of the two additive dispersions containing AC and TiO<sub>2</sub> separately. The four layers of the composite membrane were made up as follows: layer 1, electrospun matrix from 6 mL of CA solution, layer 2, spraying

of AC dispersion, layer 3, electrospun matrix from 4 mL of CA solution and layer 4, spraying of TiO<sub>2</sub> dispersion. Each step was followed by 1 h drying at 70°C. The air spraying process for the two layers of additives was the same adopted for the single-additive membranes [43].

The fifth membrane was produced differently. The CA fibre mat was electrospun with a coaxial needle and the outer needle provided a sheet flow of TiO<sub>2</sub>, leading to a more equal distribution of TiO<sub>2</sub> on the fibre mat. The co-axial setup is presented in Figure 1b. The inner needle contained the polymer solution, while in the outer needle the TiO<sub>2</sub> dispersion flowed. The feed rate of the polymer solution was set at 1.1 mL min<sup>-1</sup> while the dispersion was fed at 0.7 mL min<sup>-1</sup>. The applied voltage was 23 kV and the collector was kept at a distance of 15 cm from the tip of the needle. The temperature and the relative humidity inside the electrospinning box during the experiment were 22.7°C and 60%, respectively.

### 2.3 Fibre Characterisation

Scanning electron microscopy (SEM; Zeiss XB1540) operating at HT of 5 kV was used to investigate the morphology of the fibre surface. Before scanning, a sample of each membrane was coated with a thin layer of gold. DiameterJ plugin for ImageJ (NIH, USA) was employed to assess the average surface porosity of the membranes. A traditional External Micrometer (accuracy  $\pm 0.005$  mm, Model 965M, Moore & Wright Ltd, Sheffield England) was used to measure the thickness of the membranes. To avoid compression of the materials, the membranes were kept between two metal plates during measuring [43].

### 2.4 Toluene removal

Toluene removal capabilities of the fabricated membranes were investigated with the setup, which is schematically presented in Figure 2. Pure nitrogen at 1 bar pressure was used as a carrier gas throughout the experiment. The total flow was controlled at 3.9 L min<sup>-1</sup>. The input gas stream was split into wet and polluted streams. A wet stream was used in order to ensure humidity inside the setup, which is a crucial parameter to ensure adsorption and photocatalytic oxidation of toluene [27], [35]. The wet stream was controlled using

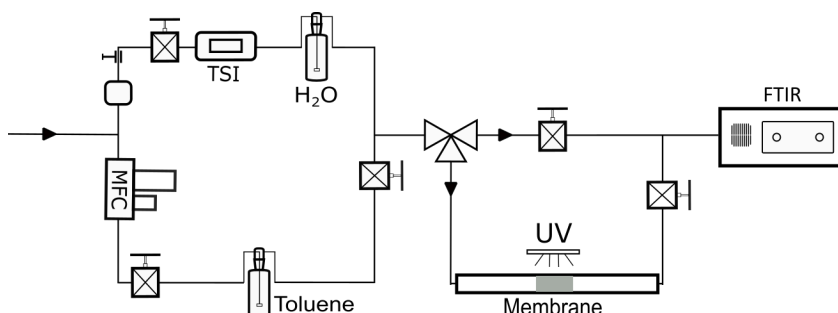


Figure 2. Schematic representation of the setup to assess the capacity of toluene removal of the membranes

a compression valve and measured through a mass flow meter (Model 4043, TSI Incorporated, Shoreview, MN USA), whereas the polluted gas stream was controlled through a mass flow controller (5850TR series, Brooks Instrument B.V., Holland). Milli-Q water and toluene were kept separately in two 250-mL gas-washing bottles, which were immersed in a water bath at 21°C to keep the evaporation rate constant. During the experiment, the membranes were kept in a 1-m fused quartz tube, with an inner diameter of 36 mm. The 20 cm x 20 cm membranes were pleated to fit inside the quartz tube. The tube was kept inside a box with a blacklight blue UV lamp with a peak wavelength of 365 nm, employed to activate TiO<sub>2</sub> present on the fibres and initiate photocatalytic oxidation of toluene. A bypass was built to allow access to the quartz tube while running the experiments and evaluate the toluene concentration before and after passing through the membrane. The flow was directed into a multicomponent FTIR gas analyser (Gasmeter DX4000, Gasmeter Technologies Oy, Vantaa, Finland) to monitor the amount of water vapour and toluene concentration during the different stages of the experiment and therefore assess the effectiveness of the membranes in removing toluene from the air stream.

The toluene removal capacity of each membrane was calculated using the following formula:

$$\eta = \left( \frac{C_{up} - C_{down}}{C_{up}} \right) \times 100 \% \quad (1)$$

where  $C_{up}$  and  $C_{down}$  are average toluene concentration upstream and downstream of the membranes, respectively.

### 3. Results and discussion

#### 3.1 Fabrication of electrospun membranes

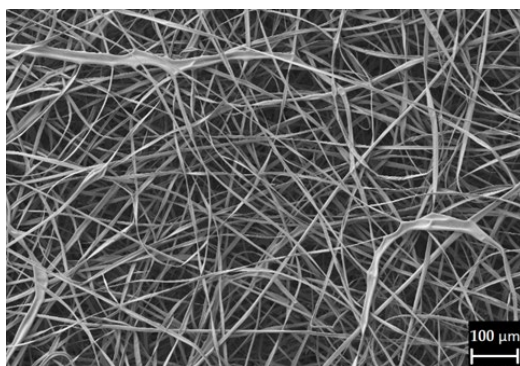
The process parameters used to electrospin the CA fibres were adapted from [44]. The electrospinning of the CA/acetone solutions was kept stable at a feed rate of 1 mL min<sup>-1</sup>, which is a relatively high value compared to most other studies, where electrospinning is conducted at feed rates in the range less than 1 mL h<sup>-1</sup> [45]–[47]. The remotely controlled arm allowed the fabrication of uniformly distributed fibres over the collector surface. The fabrication of the CA/TiO<sub>2</sub> membrane using electrospray involved the use of slightly different characteristic parameters to keep the stability of the process. Table 1 lists the electrospinning and doping conditions that were applied to obtain the various CA-based membranes.

Table 1. Electrospinning and doping conditions used to fabricate the CA-based membranes

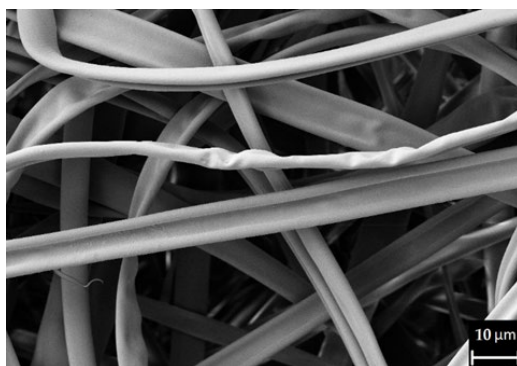
	Electrospinning condition								Doping condition	
	Solution parameters		Process parameters				Ambient parameters		Air spraying	Electrospray
	Polymer	Solvent	TCD	Voltage	Feed rate	Needle inner $\varnothing$	T	RH		
<b>CA</b>	CA 12.5wt%	Acetone	9 cm	14.8 kV	1 mL min <sup>-1</sup>	1.5 mm	21°C $\pm$ 0.5°C	37% $\pm$ 3%	-	-
<b>CA/TiO<sub>2</sub></b>	CA 12.5wt%	Acetone	9 cm	14.8 kV	1 mL min <sup>-1</sup>	1.5 mm	21°C $\pm$ 0.5°C	37% $\pm$ 3%	2x 2 min at 10 L min <sup>-1</sup> of TiO <sub>2</sub> dispersion	-
<b>CA/AC</b>	CA 12.5wt%	Acetone	9 cm	14.8 kV	1 mL min <sup>-1</sup>	1.5 mm	21°C $\pm$ 0.5°C	37% $\pm$ 3%	2x 2 min at 10 L min <sup>-1</sup> of AC dispersion	-
<b>Composite</b>	CA 12.5wt%	Acetone	9 cm	14.8 kV	1 mL min <sup>-1</sup>	1.5 mm	21°C $\pm$ 0.5°C	37% $\pm$ 3%	2x 2 min at 10 L min <sup>-1</sup> of TiO <sub>2</sub> and AC dispersion	-
<b>CA/TiO<sub>2</sub> el.spray</b>	CA 12.5wt%	Acetone	15 cm	23 kV	1.1 mL min <sup>-1</sup>	1.1 mm	22.7°C $\pm$ 0.3°C	60% $\pm$ 1%	-	Feed rate 0.7 mL min <sup>-1</sup> Needle inner $\varnothing$ 1.5 mm

### 3.2 Fibre characterisation

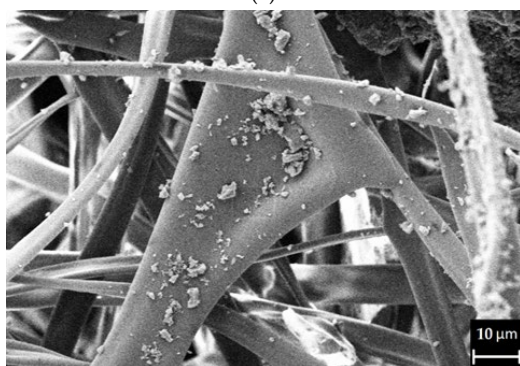
The SEM images of the various membranes are shown in Figure 3 and Figure 4. The pure CA-based electrospun fibres present a flat ribbon shape, as visible in Figure 3a and Figure 3b. Furthermore, they exhibit a uniform morphology and a randomly oriented distribution over the surface of the membrane. The doped fibres with either AC or TiO<sub>2</sub> are visible in Figure 3c and Figure 3d respectively. The images show that the additives have been successfully incorporated onto the surface of the membranes. In contrast with the smooth and uniform pure CA fibres, the additives cover the fibre surface of the doped membranes, affecting their smoothness. In Figure 3d, it is evident how the deposition of TiO<sub>2</sub> in form of agglomerates has densely coated the surface of the CA-based fibres, whereas the AC particles are highly dispersed on the fibre surface of the CA/AC sample (Figure 3c). The additives affect the morphology of the fibres, their surface, and the dimension of the pores. The result is a rougher surface and smaller pores, especially for the CA/TiO<sub>2</sub> membrane (Figure 3d) compared to pure CA (Figure 3a,b) and the AC-doped fibres (Figure 3c).



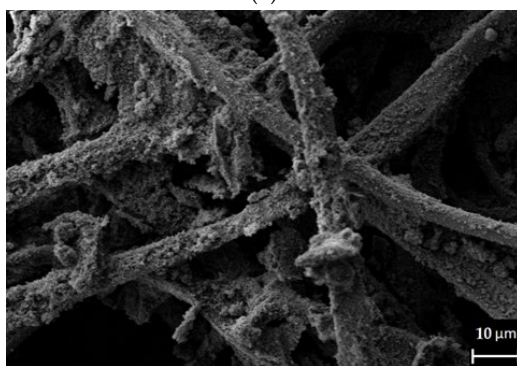
(a)



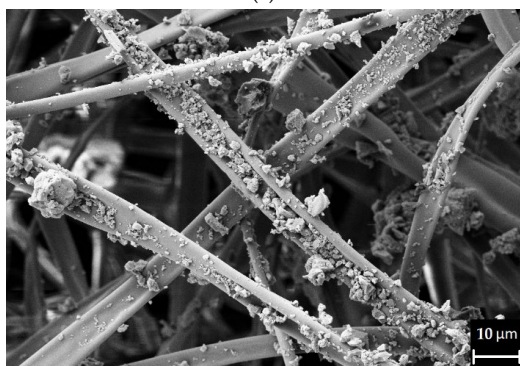
(b)



(c)



(d)



(e)



(f)

*Figure 3: SEM images of (a) and (b) pure CA fibres, (c) AC doped fibres, (d)  $\text{TiO}_2$  doped fibres, (e) composite membranes, second layer, AC doped fibres and (f) composite membranes, fourth layer,  $\text{TiO}_2$  doped fibres.*

The SEM images of the composite membrane are shown in Figure 3e and Figure 3f, where the second and the fourth layer of the membrane are displayed respectively, in order to show the additives on the fibres surface. In this case, the  $\text{TiO}_2$  seems to be less heavily deposited on the fibres (Figure 3f) and morphology is

affected in a milder form compared to the CA/TiO<sub>2</sub> membrane. However, AC is densely present in forms of agglomerates on the second layer of the membrane (Figure 3e).

The fibres from the SEM images of the last membrane, fabricated using electrospraying of TiO<sub>2</sub> as part of the electrospinning process, are presented in Figure 4. The flat ribbon shape has remained unchanged compared to the previously described membranes. Again, TiO<sub>2</sub> has been successfully integrated onto the fibres surface as visible in Figure 4b. Figure 4a revealed the presence of agglomerates of TiO<sub>2</sub> nanoparticles distributed within the fibres and on the membrane surface. These agglomerates could be the result of non-complete evaporation of the solvent during electrospinning and they partly cover the fibres, affecting the surface morphology of the membrane.

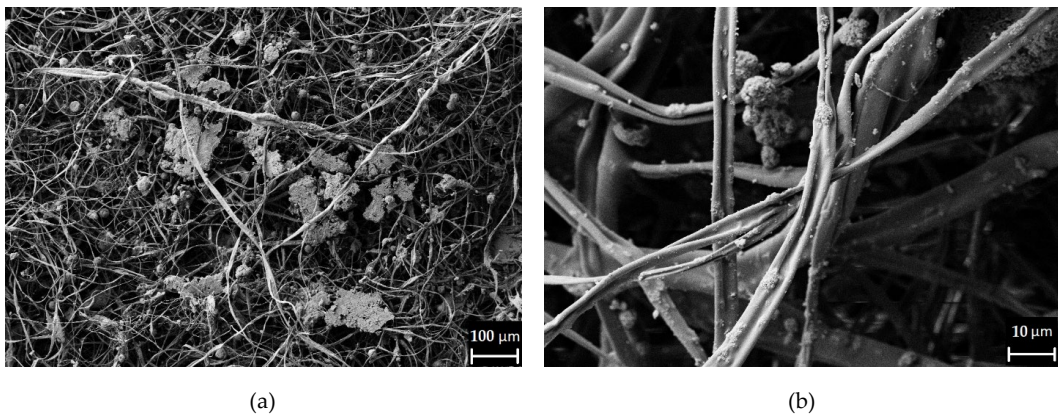


Figure 4. SEM images of electrospun CA fibres with TiO<sub>2</sub> electrospayed using a co-axial setup.

In Table 2 the surface porosity of each membranes is reported. As the main doping method affected the first layers of the membrane, the surface porosity was analysed and used as term of comparison between the different methods. Compared to the pure CA, the membranes where additives have been added after electrospinning recorded a decrease in surface porosity. The surface porosity of the pure CA membrane was 42%, whereas it dropped to 32.5% for CA/TiO<sub>2</sub> [43]. When titanium dioxide was electrospayed during the electrospinning of the polymer solution, the effect on the surface porosity of the membrane was milder and the surface porosity decreased by less than 1% compared to the pure CA. This result reflects the different influence that electrospraying of an additive implicates on the fibre mat, meaning that the additive was distributed among the entire membrane volume. On the contrary, spraying of additives concentrates them only on the membrane surface, resulting in a more significant influence on the surface porosity.

The thickness analysis led to the results presented in Table 2. The use of the additives had a significant influence on these results [43]. The pure CA membrane is 0.11 mm thin, followed by the three single-additive



membranes with a thickness of 0.14 and 0.15 mm. The composite membrane showed an increase in thickness of 82% compared to the pure CA membrane, due to the use of a layered configuration of fibres and additives.

*Table 2: Thickness and surface porosity of the electrospun membranes*

	CA	CA/AC	CA/TiO <sub>2</sub>	Composite	CA/TiO <sub>2</sub> el.spray
Thickness (mm)	0.11 ± 0.016	0.14 ± 0.012	0.15 ± 0.005	0.18 ± 0.007	0.14 ± 0.024
Surface porosity (%)	42.0 ± 5.4	38.5 ± 2.6	32.5 ± 5.1	34.4 ± 4.5	40.9 ± 5.5

### 3.3 Toluene removal

The removal capacity of gaseous compounds was investigated by assessing the degradation through photocatalytic oxidation and adsorption of toluene from the different membranes. The experimental study was done on each sample and one more investigation was performed combining one CA/AC sample with a CA/TiO<sub>2</sub> electrosprayed membrane.

The concentration of toluene inside the setup was stabilised at 22.5 ppm, while the relative humidity was kept at 33% ± 5%. The investigation was run for 40 min on each sample, of which 30 min the UV light was turned on to initiate the photocatalytic oxidation of toluene. Figure 5 shows the results of the experiments displaying the changes of the normalised toluene concentration in time for each tested sample, while the initial removal efficiencies and the residence time are presented in Table 3. The pure CA membrane did not adsorb any toluene, as expected. CA has no adsorption capacity and is used as a negative reference sample. The toluene concentration through the pure CA membrane remained very stable throughout the experiment, with an average deviation from the mean value of 0.15 ppm. The concentration of toluene significantly decreased in a very short time in each sample containing AC, revealing their adsorption capacity. The composite membrane showed an initial removal capacity of 33.1%, while the CA/AC alone and combined with CA/TiO<sub>2</sub> electrospray showed an initial removal capacity of 39.6% and 45.5%, respectively. The registered removal is due to the adsorbance capacity of AC. As can be seen in Figure 5, the concentration of toluene started to increase again with a similar development for each of the three samples containing AC. After 40 min of exposure to the pollutant, the removal efficiencies of the membranes have stabilised around 20%. Therefore, they haven't reached the breakthrough after 40 min of exposure. The enhanced

performance of the combined CA/AC and CA/TiO<sub>2</sub> electro spray might be due to the increased residence time for the reaction that allowed a higher amount of toluene being adsorbed from the activated charcoal.

The two membranes that contained TiO<sub>2</sub> did not show a clear reduction of toluene concentration. It is noticeable that the concentration of toluene did not present the same stability around the average value as it was before placing the membrane in the setup (the average deviation from the mean value was 0.17 ppm) or while testing the pure CA membrane. The CA/TiO<sub>2</sub> and CA/TiO<sub>2</sub> electro spray showed an average deviation from the mean value of 0.34 ppm and 0.56 ppm, respectively. Furthermore, while the two membranes were

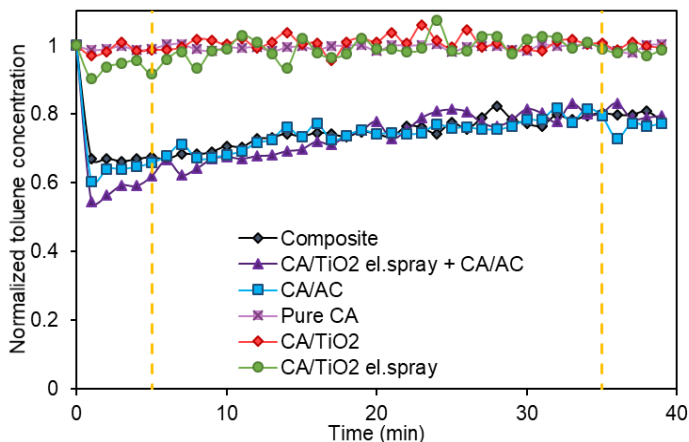


Figure 5: Changes of normalised toluene concentration throughout the experimental study (the yellow dotted lines show the point when the UV light is turned on and off).

irradiated with the UV light, formaldehyde was detected in the air flow, with peaks of 260 and 360 ppb for CA/TiO<sub>2</sub> and CA/TiO<sub>2</sub> electro spray, respectively (Figure 6a and Figure 6b). Formaldehyde is recognised to be one typical by-product of photocatalytic oxidation of toluene [24], [48]. Therefore, it can be concluded that the photocatalytic reaction has been initiated in the set up.

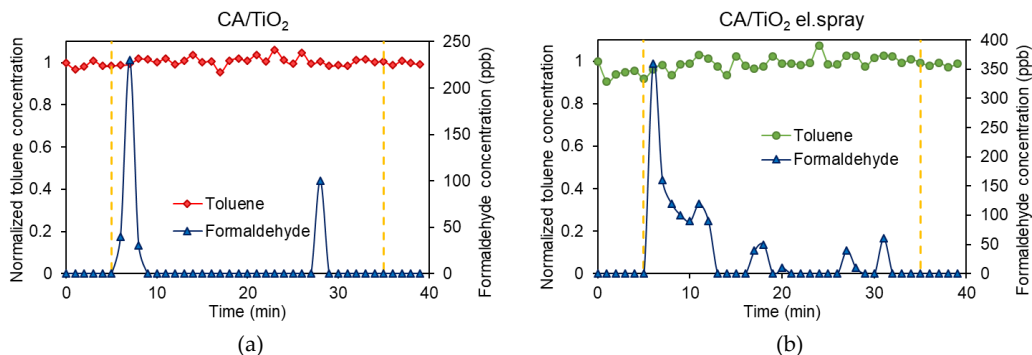


Figure 6. Details on the experimental study of the CA/TiO<sub>2</sub> (a) and CA/TiO<sub>2</sub> (b) el.spray membrane. The development in time of the normalised concentration of toluene and the concentration of formaldehyde in ppm is shown. The yellow dotted lines represent the point in time when the UV lamp was switched on and off.

The reasons behind the inefficient toluene conversion from the  $\text{TiO}_2$  might be related to different factors. First, the UV lamp shines a rather diffusive and low-intensity light rather than directional and intense. This means that the light was placed along the quartz tube where the membranes were kept and the intensity reaching the  $\text{TiO}_2$  might have not been enough to degrade the toluene inside the reactor [30], [33]. The second reason might be related to the contact time, or residence time, which is the time that the gas molecules spend in contact or near the photocatalyst. The residence time involved in this experimental study ranges between 0.067 and 0.172 s, as shown in Table 3. Compared to others, the residence time is kept in the range of seconds to minutes. In a typical air purification system, the residence time ranges from tens to hundreds of milliseconds [49]. This is one main reason behind the difference of performance of photocatalysts, which exhibit acceptable removal efficiencies in the laboratory and demonstrate worse performance under real conditions [49]. Furthermore, the removal of BTEX through photocatalytic oxidation with  $\text{TiO}_2$  has been reported to decrease quickly as the residence time decreases from 3.7 and 0.6 min [32]. Therefore, as the residence time in this experiment was in the range of hundreds of milliseconds, the photocatalytic oxidation might not have been initiated efficiently enough. Lastly, when the additives were combined onto the surface of the membranes, it seems that the activated charcoal prevents the degradation of toluene from the catalyst. No formaldehyde production was recorded, therefore the  $\text{TiO}_2$  might have been deactivated from AC, or the formaldehyde had been retained in the charcoal and could not be observed during the experiment.

Typical indoor gaseous air pollutants are found in ranges of concentrations at the ppb and sub-ppb level [50]–[53]. As already mentioned, the concentration of toluene in the setup was around 22.5 ppm, which represents a relative high concentration compared to the typical indoor and outdoor levels of gaseous compounds. Therefore, the amount of AC deposited on the membrane surface might maintain a higher removal efficiency for a longer period of time when exposed to real conditions.

Table 3: Initial removal efficiencies and residence time for the different fabricated membranes.

Membrane	Pure CA	CA/ $\text{TiO}_2$	CA/AC	Composite	CA/ $\text{TiO}_2$ el.spray	CA/ $\text{TiO}_2$ el.spray + CA/AC
Initial removal efficiency (%)	-	-	39.6%	33.1%	-	45.5%
Residence time (s)	0.067	0.092	0.086	0.111	0.086	0.172

#### 4. Conclusion

In summary, five CA based electrospun fibre membranes doped with AC and  $\text{TiO}_2$  were fabricated to investigate the adsorption and degradation capacity and the possible synergistic effect of these two additives

when combined. A rougher fibre morphology was concluded to be a direct consequence of the use of TiO<sub>2</sub> and activated charcoal and the membranes doped with the additives had an increased thickness compared to the pure CA membrane. The activated charcoal membranes have shown removal efficiencies for toluene up to 45.5% with a residence time of 0.172 s and a toluene concentration of 22.5 ppm. The photocatalytic oxidation was initiated as formaldehyde was detected in the N<sub>2</sub> stream, although the conversion rate of toluene was not large enough to be detected. When the two additives were combined to investigate the synergistic effect on the removal of toluene, activated charcoal adsorbed the pollutant preventing the initiation of photocatalytic oxidation or it has also re-adsorbed the degradation products.

### **Acknowledgments**

For his assistance in performing the SEM images, the authors acknowledge Peter Kjær Kristensen, research technician at the Department of Materials and Production at Aalborg University.

### **Funding**

The funding of this research was provided by Grundejernes Investeringssfond, the Department of the Built Environment, and the Department of Materials and Production at Aalborg University.

### **Declaration of competing interest**

The Author(s) declare(s) that there is no conflict of interest.

### **References**

- [1] N. E. Klepeis *et al.*, "The National Human Activity Pattern Survey (NHAPS): A resource for assessing exposure to environmental pollutants," *J. Expo. Anal. Environ. Epidemiol.*, vol. 11, no. 3, pp. 231–252, 2001, doi: 10.1038/sj.jea.7500165.
- [2] D. P. Wyon, "The effects of indoor air quality on performance, behaviour and productivity," *Pollut. Atmos.*, vol. 14, no. SPECIAL ISSUE, pp. 35–41, 2005.
- [3] J. A. Hoskins, "Health effect due to indoor air pollution," in *Survival and Sustainability*, 2011, pp. 665–676.
- [4] P. Wargocki, L. Lagercrantz, T. Witterseh, J. Sundell, D. P. Wyon, and P. O. Fanger, "Subjective perceptions, symptom intensity and performance: A comparison of two independent studies, both changing similarly the pollution load in an office," *Indoor Air*, vol. 12, no. 2, pp. 74–80, 2002, doi: 10.1034/j.1600-0668.2002.01101.x.

- [5] E. Gallego, X. Roca, J. F. Perales, and X. Guardino, "Determining indoor air quality and identifying the origin of odour episodes in indoor environments," *J. Environ. Sci.*, vol. 21, no. 3, pp. 333–339, 2009, doi: 10.1016/S1001-0742(08)62273-1.
- [6] H. Destailats, R. L. Maddalena, B. C. Singer, A. T. Hodgson, and T. E. McKone, "Indoor pollutants emitted by office equipment: A review of reported data and information needs," *Atmos. Environ.*, vol. 42, no. 7, pp. 1371–1388, 2008, doi: 10.1016/j.atmosenv.2007.10.080.
- [7] S. Kim, J. A. Kim, H. J. Kim, and S. Do Kim, "Determination of formaldehyde and TVOC emission factor from wood-based composites by small chamber method," *Polym. Test.*, vol. 25, no. 5, pp. 605–614, 2006, doi: 10.1016/j.polymertesting.2006.04.008.
- [8] M. S. Waring and J. A. Siegel, "Indoor Secondary Organic Aerosol Formation Initiated from Reactions between Ozone and Surface-Sorbed D-Limonene," *Environ. Sci. Technol.*, vol. 47, no. 12, pp. 6341–6348, 2013, doi: dx.doi.org/10.1021/es400846d.
- [9] C. J. Weschler, "Roles of the human occupant in indoor chemistry," *Indoor Air*, vol. 26, no. 1, pp. 6–24, 2016, doi: 10.1111/ina.12185.
- [10] M. Bahri and F. Haghighat, "Plasma-Based Indoor Air Cleaning Technologies: The State of the Art-Review," *CLEAN-SOIL AIR WATER*, vol. 42, no. 12, pp. 1667–1680, Dec. 2014, doi: 10.1002/clen.201300296.
- [11] A. K. Ghoshal and S. D. Manjare, "Selection of appropriate adsorption technique for recovery of VOCs: An analysis," *J. Loss Prev. Process Ind.*, vol. 15, no. 6, pp. 413–421, 2002, doi: 10.1016/S0950-4230(02)00042-6.
- [12] L. Zhong and F. Haghighat, "Ozonation Air Purification Technology in HVAC Applications," *ASHRAE Trans.*, vol. 120, no. 1, pp. 1–8, 2014.
- [13] J. Mo, Y. Zhang, Q. Xu, J. J. Lamson, and R. Zhao, "Photocatalytic purification of volatic organic compounds in indoor air: a literature review," *Atmos. Environ.*, vol. 43, no. 14, pp. 2229–2246, 2009, doi: 10.1016/j.atmosenv.2009.01.034.
- [14] A. M. Vandenbroucke, R. Morent, N. De Geyter, and C. Leys, "Non-thermal plasmas for non-catalytic and catalytic VOC abatement," *J. Hazard. Mater.*, vol. 195, pp. 30–54, 2011, doi: 10.1016/j.jhazmat.2011.08.060.
- [15] A. Luengas, A. Barona, C. Hort, G. Gallastegui, V. Platel, and A. Elias, "A review of indoor air

treatment technologies," *Rev. Environ. Sci. Biotechnol.*, vol. 14, no. 3, pp. 499–522, 2015, doi: 10.1007/s11157-015-9363-9.

- [16] B. F. Yu, Z. B. Hu, M. Liu, H. L. Yang, Q. X. Kong, and Y. H. Liu, "Review of research on air-conditioning systems and indoor air quality control for human health," *Int. J. Refrig.*, vol. 32, no. 1, pp. 3–20, 2009, doi: 10.1016/j.ijrefrig.2008.05.004.
- [17] C. J. Weschler, "Ozone in indoor environments: Concentration and chemistry," *Indoor Air*, vol. 10, no. 4, pp. 269–288, 2000, doi: 10.1034/j.1600-0668.2000.010004269.x.
- [18] H. F. Hubbard, B. K. Coleman, G. Sarwar, and R. L. Corsi, "Effects of an ozone-generating air purifier on indoor secondary particles in three residential dwellings," *Indoor Air*, vol. 15, no. 6, pp. 432–444, 2005, doi: 10.1111/j.1600-0668.2005.00388.x.
- [19] WHO, "Air Quality Guidelines : Global Update 2005. Particulate Matter, Ozone, Nitrogen Dioxide and Sulfur Dioxide," 2006.
- [20] R. Bradley, "Recent developments in the physical adsorption of toxic organic vapours by activated carbons," *Adsorpt. Sci. Technol.*, vol. 29, no. 1, pp. 1–28, 2011, doi: 10.1260/0263-6174.29.1.1.
- [21] D. Das, V. Gaur, and N. Verma, "Removal of volatile organic compound by activated carbon fiber," *Carbon N. Y.*, vol. 42, no. 14, pp. 2949–2962, 2004, doi: 10.1016/j.carbon.2004.07.008.
- [22] X. Zhang, B. Gao, A. E. Creamer, C. Cao, and Y. Li, "Adsorption of VOCs onto engineered carbon materials: A review," *Journal of Hazardous Materials*. 2017, doi: 10.1016/j.jhazmat.2017.05.013.
- [23] A. H. Mamaghani, F. Haghighat, and C.-S. C. S. C.-S. Lee, "Photocatalytic oxidation technology for indoor environment air purification: The state-of-the-art," *Appl. Catal. B Environ.*, vol. 203, pp. 247–269, 2017, doi: 10.1016/j.apcatb.2016.10.037.
- [24] J. Mo, Y. Zhang, Q. Xu, Y. Zhu, J. J. Lamson, and R. Zhao, "Determination and risk assessment of by-products resulting from photocatalytic oxidation of toluene," *Appl. Catal. B Environ.*, vol. 89, no. 3–4, pp. 570–576, 2009, doi: 10.1016/j.apcatb.2009.01.015.
- [25] Y. Sun, L. Fang, D. P. Wyon, A. Wisthaler, L. Lagercrantz, and P. Strøm-Tejsten, "Experimental research on photocatalytic oxidation air purification technology applied to aircraft cabins," *Build. Environ.*, vol. 43, no. 3, pp. 258–268, 2008, doi: 10.1016/j.buildenv.2006.06.036.
- [26] M. Sleiman, P. Conchon, C. Ferronato, and J.-M. Chovelon, "Photocatalytic oxidation of toluene at indoor air levels (ppbv): Towards a better assessment of conversion, reaction intermediates and

mineralization," *Appl. Catal. B Environ.*, vol. 86, no. 3–4, pp. 159–165, 2009, doi: 10.1016/j.apcatb.2008.08.003.

- [27] J. Mo, Y. Zhang, and Q. Xu, "Effect of water vapor on the by-products and decomposition rate of ppb-level toluene by photocatalytic oxidation," *Appl. Catal. B Environ.*, vol. 132–133, pp. 212–218, 2013, doi: 10.1016/j.apcatb.2012.12.001.
- [28] S. Wang, H. M. Ang, and M. O. Tade, "Volatile organic compounds in indoor environment and photocatalytic oxidation: State of the art," *Environ. Int.*, vol. 33, no. 5, pp. 694–705, 2007, doi: 10.1016/j.envint.2007.02.011.
- [29] N. Quici *et al.*, "Effect of key parameters on the photocatalytic oxidation of toluene at low concentrations in air under 254 + 185 nm UV irradiation," *Appl. Catal. B Environ.*, vol. 95, no. 3–4, pp. 312–319, 2010, doi: 10.1016/j.apcatb.2010.01.009.
- [30] J. Jeong, K. Sekiguchi, and K. Sakamoto, "Photochemical and photocatalytic degradation of gaseous toluene using short-wavelength UV irradiation with TiO<sub>2</sub> catalyst: Comparison of three UV sources," *Chemosphere*, vol. 57, no. 7, pp. 663–671, 2004, doi: 10.1016/j.chemosphere.2004.05.037.
- [31] C. H. Ao and S. C. Lee, "Combination effect of activated carbon with TiO<sub>2</sub> for the photodegradation of binary pollutants at typical indoor air level," *J. Photochem. Photobiol. A Chem.*, vol. 161, no. 2–3, pp. 131–140, 2004, doi: 10.1016/S1010-6030(03)00276-4.
- [32] C. H. Ao and S. C. Lee, "Enhancement effect of TiO<sub>2</sub> immobilized on activated carbon filter for the photodegradation of pollutants at typical indoor air level," *Appl. Catal. B Environ.*, vol. 44, no. 3, pp. 191–205, 2003, doi: 10.1016/S0926-3373(03)00054-7.
- [33] Y. Lu, D. Wang, C. Ma, and H. Yang, "The effect of activated carbon adsorption on the photocatalytic removal of formaldehyde," *Build. Environ.*, vol. 45, no. 3, pp. 615–621, 2010, doi: 10.1016/j.buildenv.2009.07.019.
- [34] W. K. Jo and C. H. Yang, "Granular-activated carbon adsorption followed by annular-type photocatalytic system for control of indoor aromatic compounds," *Sep. Purif. Technol.*, vol. 66, no. 3, pp. 438–442, 2009, doi: 10.1016/j.seppur.2009.02.014.
- [35] C. H. Ao and S. C. Lee, "Indoor air purification by photocatalyst TiO<sub>2</sub> immobilized on an activated carbon filter installed in an air cleaner," *Chem. Eng. Sci.*, vol. 60, no. 1, pp. 103–109, 2005, doi: 10.1016/j.ces.2004.01.073.

- [36] B. Ding, C. K. Kim, H. Y. Kim, M. K. Seo, and S. J. Park, "Titanium dioxide nanofibers prepared by using electrospinning method," *Fibers Polym.*, vol. 5, no. 2, pp. 105–109, 2004, doi: 10.1007/BF02902922.
- [37] Y. H. Chuang, G. B. Hong, and C. T. Chang, "Study on particulates and volatile organic compounds removal with TiO<sub>2</sub> nonwoven filter prepared by electrospinning," *J. Air Waste Manag. Assoc.*, vol. 64, no. 6, pp. 738–742, 2014, doi: 10.1080/10962247.2014.889614.
- [38] P. Sullivan, J. Moate, B. Stone, J. D. Atkinson, Z. Hashisho, and M. J. Rood, "Physical and chemical properties of PAN-derived electrospun activated carbon nanofibers and their potential for use as an adsorbent for toxic industrial chemicals," *Adsorption*, vol. 18, pp. 265–274, 2012.
- [39] K. J. Lee *et al.*, "Activated carbon nanofiber produced from electrospun polyacrylonitrile nanofiber as a highly efficient formaldehyde adsorbent," *Carbon N. Y.*, vol. 48, no. 15, pp. 4248–4255, 2010, doi: 10.1016/j.carbon.2010.07.034.
- [40] M.-J. Jung, E.-G. Jeong, J.-S. Jang, and Y.-S. Lee, "Preparation and Characterization of Electrospun TiO<sub>2</sub>-Activated Carbon Complex Fiber as Photocatalyst," *Carbon Lett.*, vol. 11, no. 1, pp. 28–33, 2010, doi: 10.5714/cl.2010.11.1.028.
- [41] E. Entcheva, H. Bien, L. Yin, C. Y. Chung, M. Farrell, and Y. Kostov, "Functional cardiac cell constructs on cellulose-based scaffolding," *Biomaterials*, vol. 25, no. 26, pp. 5753–5762, 2004, doi: 10.1016/j.biomaterials.2004.01.024.
- [42] M. Kwon, J. Kim, and J. Kim, "Photocatalytic activity and filtration performance of hybrid tio<sub>2</sub>-cellulose acetate nanofibers for air filter applications," *Polymers (Basel)*, vol. 13, no. 8, pp. 1–11, 2021, doi: 10.3390/polym13081331.
- [43] R. Orlando, Y. Gao, P. Fojan, and J. Mo, "Filtration Performance of Ultrathin Electrospun Cellulose Acetate Filters Doped with TiO<sub>2</sub> and Activated Charcoal," *Buildings*, vol. 11, no. 11, 557, 2021.
- [44] T. Christoforou and C. Doumanidis, "Biodegradable cellulose acetate nanofiber fabrication via electrospinning," *J. Nanosci. Nanotechnol.*, vol. 10, no. 9, pp. 6226–6233, 2010, doi: 10.1166/jnn.2010.2577.
- [45] E. Scholten, L. Bromberg, G. C. Rutledge, and T. A. Hatton, "Electrospun polyurethane fibers for absorption of volatile organic compounds from air," *ACS Appl. Mater. Interfaces*, vol. 3, no. 10, pp. 3902–3909, 2011, doi: 10.1021/am200748y.
- [46] N. Wang, A. Raza, Y. Si, J. Yu, G. Sun, and B. Ding, "Tortuously structured polyvinyl



chloride/polyurethane fibrous membranes for high-efficiency fine particulate filtration," *J. Colloid Interface Sci.*, vol. 398, pp. 240–246, 2013, doi: 10.1016/j.jcis.2013.02.019.

- [47] M. Liang *et al.*, "Honeycomb-like polysulphone/polyurethane nanofiber filter for the removal of organic/inorganic species from air streams," *J. Hazard. Mater.*, vol. 347, no. January, pp. 325–333, 2018, doi: 10.1016/j.jhazmat.2018.01.012.
- [48] W. Zhao *et al.*, "Photocatalytic oxidation of indoor toluene: Process risk analysis and influence of relative humidity, photocatalysts, and VUV irradiation," *Sci. Total Environ.*, vol. 438, pp. 201–209, 2012, doi: 10.1016/j.scitotenv.2012.08.081.
- [49] J. Lyu, L. Zhu, and C. Burda, "Considerations to improve adsorption and photocatalysis of low concentration air pollutants on TiO<sub>2</sub>," *Catal. Today*, vol. 225, pp. 24–33, 2014, doi: 10.1016/j.cattod.2013.10.089.
- [50] D. A. Sarigiannis, S. P. Karakitsios, A. Gotti, I. L. Liakos, and A. Katsoyiannis, "Exposure to major volatile organic compounds and carbonyls in European indoor environments and associated health risk," *Environ. Int.*, vol. 37, no. 4, pp. 743–765, 2011, doi: 10.1016/j.envint.2011.01.005.
- [51] S. Harrad *et al.*, "Indoor contamination with hexabromocyclododecanes, polybrominated diphenyl ethers, and perfluoroalkyl compounds: An important exposure pathway for people?," *Environ. Sci. Technol.*, vol. 44, no. 9, pp. 3221–3231, 2010, doi: 10.1021/es903476t.
- [52] R. Golden, "Identifying an indoor air exposure limit for formaldehyde considering both irritation and cancer hazards," *Crit. Rev. Toxicol.*, vol. 41, no. 8, pp. 672–721, 2011, doi: 10.3109/10408444.2011.573467.
- [53] P. Wolkoff, C. K. Wilkins, P. A. Clausen, and G. D. Nielsen, "Organic compounds in office environments - Sensory irritation, odor, measurements and the role of reactive chemistry," *Indoor Air*, vol. 16, no. 1, pp. 7–19, 2006, doi: 10.1111/j.1600-0668.2005.00393.x.



## Part III

# Discussion and Conclusions



## Chapter 9

# Discussion

### 9.1 Air filter performance

The main difference between the two generations of filters is related to the size range of the average fibre diameter. The first generation of filters (Papers II and III) is part of the so-called *electrospun nanofibre filters* with average diameters between 200 and 430 nm, and most of the fibre diameters were below 1  $\mu\text{m}$ . The second production cannot be defined as nanofibre filters, as the average diameter of the CA fibres reported in Papers IV and V was around 4.2  $\mu\text{m}$  with fibre diameters reaching 10  $\mu\text{m}$  and above. The average fibre diameter of the various filters was affected by the electrospinning process, in accordance with the electrospinning review in Chapter 3.4.1. Apart from the different solution parameters – the filters were produced using different polymer/solution matrices – the adopted process parameters like feed rate and tip-to-collector distance were significantly different. The PU fibres (Paper II) and PVA fibres (Paper III) were electrospun at feed rates in the range 0.1–1.3  $\text{ml h}^{-1}$  and the TCD ranged between 16 and 19.5 cm. In contrast, the CA fibres (Papers IV and V) were electrospun at 1  $\text{ml min}^{-1}$ , and the TCD was kept at 9 cm. A shorter TCD decreased the time for the polymer solution jet to stretch [308] and, together with the use of a higher feed rate, increased the average fibre diameter and pore diameter in the CA-fibre filters [309]. Indeed, as reviewed in Chapter 3.4.2, jet-stretching and jet-elongation are the phenomena that define the final fibre morphology and diameter. The flat-ribbon shape of the CA fibre is also a result of an electrospinning process during which jet-stretching and solvent evaporation had limited time to perform [310]. A qualitative analysis of the PU and

PVA filters confirmed a lower porosity compared to the CA filters, which also led to pressure drops with values up to 3,000 Pa at  $0.053 \text{ m s}^{-1}$ . Moreover, CA fibre filters showed improved quality factors, which could be a benefit of the short electrospinning time, in accordance with [205].

Several studies have reported or mentioned the effect of the slip-flow phenomenon, which is dominant when fibres are in the nano-range, and its advantages when it comes to pressure drop [134, 136, 208]. Electrospun nanofibres have been produced with the aim of exploiting the slip effect. Usually, the focus of these studies would be on the fibre diameter, so that it would be comparable to the mean free path of air molecules and the air flow pattern would be within the transitional flow regime (Chapter 3.2.2 and Figure 3.5), thus achieving lower pressure drops compared to conventional microfibre filters. However, comparing the two generations of filters, parameters like porosity and filter packing density have shown significant impacts on the filter air resistance. This is consistent with the models presented in Chapter 3.2.2, which show how the drag coefficient is directly dependent on  $\alpha$ . Even though the filters of the first generation had smaller fibres and were thinner, the resulting pressure drops were two to three orders of magnitude larger than the second generation. Therefore, an adequate porosity and filter packing density are the primary requirements to achieve a negligible pressure drop. The presence of nanofibres should be considered to a limited extent [204].

Furthermore, electrospun fibres have usually been tested at very low face velocities ( $0.05$  to  $0.1 \text{ m s}^{-1}$ ; see Table 3.3 in Chapter 3.3), such that a direct comparison with the performance of conventional filters is not feasible. Indeed, the typical range of face velocities adopted in ventilation systems is generally in the range of  $1\text{--}3 \text{ m s}^{-1}$  [135]. In the case of the nanofibre filters from Papers II and III, a wide range of face velocities could not be reached because the imposed pressure drop would be outside the detection limit of the measuring apparatus available. In contrast, in the study presented in Paper IV, the CA filters' pressure drop could be assessed also at face velocities of  $0.8\text{--}1 \text{ m s}^{-1}$  (see Table 3 in Paper IV).

The pressure drop measurements for the two generations of filters demonstrate that the second generation of filters, which displays a very low pressure drop, represents the most remarkable result accomplished throughout the research work. The pressure drops at face velocities of  $0.053 \text{ m s}^{-1}$  are used to allow comparisons with filters between the two productions and with other results reported in the literature. Figure 9.1 shows the pressure drop recorded for the fabricated filters. A pressure drop between  $3.5\text{--}3.8 \text{ Pa}$  is a result that is not commonly achieved in other studies with electrospun fibre filters (see Table 3.3 for reference). It is interesting to note the different influences the additives

have had on the filters between the two generations. The additives had a positive impact on the pressure drop when they were introduced within the polymer solution prior to electrospinning (PU filters, Paper II and PVA filter, Paper III). The pressure drop of the doped filters decreased significantly compared to the pure polymer fibre filters (Figure 9.1). In contrast, when the additives were sprayed after electrospinning, they slightly increased the pressure drop (Paper IV). The reason for this is related to the distribution of the additives on the filter surface. Air spraying the additives affected only the fibre morphology of the first layers of fibres, decreasing the surface porosity of the doped filter (Table 2 in Paper IV). Conversely, electrospinning the additives in solution modified the morphology of the full volume of fibres, which showed a rougher surface, smaller diameters and, consequently, larger average pore size compared to the corresponding pure polymer filter (Table 2 in Paper III).

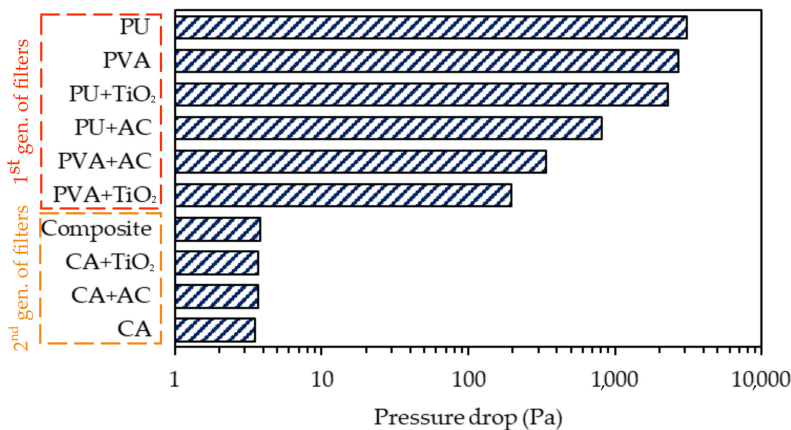


**Fig. 9.1:** Pressure drop of the fabricated filters recorded at a face velocity of  $0.053 \text{ m s}^{-1}$ .

The particle filtration efficiency of the two generations of filters could be compared to a certain extent. Generally, comparing filters is complicated because their performance might have been investigated under different conditions. In the studies reported in Papers II, III and IV, the filters were investigated for the removal of different particle sizes. Even though the filtration efficiency of the first generation of filters was assessed for particles with diameters from 12 nm to 480 nm, there were not enough particles above 200 nm to obtain statistically meaningful results. Therefore, the results are limited to the range 12–200 nm (Paper II and III). The filtration efficiency of the second generation of

filters was studied instead for particle sizes between 0.3 and 10  $\mu\text{m}$  (Paper IV). Therefore, the comparison between the two generations is feasible for particles of 0.3  $\mu\text{m}$  diameter. However, since the first generation of filters had such high filtration efficiencies (most filters were above 94%, while the PU/TiO<sub>2</sub> filter was 88%) for particles below 0.2  $\mu\text{m}$ , which are the most difficult to trap, it can be assumed that the filtration efficiency would not decrease for larger particles (up to 10  $\mu\text{m}$ ). The overall assessment is that the first generation of filters undoubtedly performed better than the second in terms of filtration efficiency for the smallest particles. The larger fibre diameters and higher porosity of the CA filters led to higher small-particle penetration. Indeed, CA filters reached 71–84% removal of 0.3  $\mu\text{m}$  particles, with the doped filters showing improved results compared to the pure CA-fibre filter (Figure 8, Paper IV). The filtration efficiency of the CA filters generally increased for particles between 1 to 10  $\mu\text{m}$ , exceeding 90% for pure and doped filters.

Again, the additives played relevant but different roles in the filtration efficiency results of the different filters. In the case of the PU filters reported in Paper II, the use of additives decreased efficiency (98.1% for the pure PU filter, 93.7% for PU/AC and 42.8% for PU/TiO<sub>2</sub>). Most probably, the additives led to rougher fibre surfaces and therefore larger pore sizes, confirmed by the significant decrease in pressure drop (Figure 4, Paper II). Moreover, in the case of PU/TiO<sub>2</sub>, the severe decrease in filtration efficiency might be related to static electrical charging [215]. The use of additives had a milder effect on the overall particle filtration efficiency of the PVA filters, which reached values between 97 and 98% (Table 3, Paper III). However, an interesting result is related to the different pressure drops imposed from filters with similar filtration efficiencies (Figure 8, Paper III). The PVA pure filter showed a pressure drop of 2,700 Pa at 0.053 m s<sup>-1</sup>, while PVA/TiO<sub>2</sub> showed 195 Pa; these filters had particle filtration efficiencies of 97.6% and 97.8%, respectively. Therefore, the morphology of the fibres characterised by rougher surfaces enhanced the particle filtration even for filters with larger pore sizes (Table 2, Paper III).

Furthermore, the additives significantly increased the filtration efficiency of the CA-based filters. Spraying AC and TiO<sub>2</sub> on the electrospun fibres resulted in an overall improvement of the particle filtration efficiency of all particle sizes (Figure 8, Paper IV). The most remarkable improvement is related to the small particles (0.3–0.5  $\mu\text{m}$ ), which increased from 73% for the pure CA filter to 84% for the composite filter, in which both AC and TiO<sub>2</sub> were embedded in two separate layers (Table 3, Paper IV). This result is explained by the decrease in surface porosity imposed on the outer fibre layers by the presence of the additives and the increase in fibre surface roughness. In conclusion,



the use of additives not only enhances the removal capacity of the filters for gaseous compounds but also has a significant impact on particle filtration efficiency.

Nevertheless, the quality factor is the most appropriate parameter to compare the performance of the filters in terms of the ratio between particle filtration and pressure drop and to assess the overall impact of the additives on the filter performance. The quality factors ( $Q_f$ ) were re-calculated for all the produced filters and are presented in Table 9.1 to allow for a comparative discussion between the different polymer-based filters. To do so, the  $Q_f$  were calculated using performance assessed under comparable conditions. The filtration efficiencies at a face velocity of  $0.053 \text{ m s}^{-1}$  were used to calculate the  $Q_f$  of the first generation of filters. The filtration efficiencies for the second generation were recorded at  $0.8 \text{ m s}^{-1}$ , which might underestimate their quality factors. The particle sizes considered for the filtration efficiencies are around  $0.2\text{--}0.25 \text{ }\mu\text{m}$  for the first generation of filters and  $0.3 \text{ }\mu\text{m}$  for the second generation. Regardless of the different impacts that the additives showed on particle filtration and pressure drops as described above, the quality factors generally increased for the doped filters compared to their respective pure polymer filters. The only exception is related to the PU/TiO<sub>2</sub> filter, in which the decrease of filtration efficiency was larger than the decrease in pressure drop, resulting in a lower quality factor than for the pure PU filter. Nevertheless, the results confirm the higher quality of the second generation of filters based on CA, which achieved values up to two orders of magnitude higher than the first generation. Moreover, the composite filter achieved a significantly higher improvement of the quality factor ( $0.49 \text{ Pa}^{-1}$ ). To the best of the author's knowledge,  $Q_f$  as high as those of the CA filters are rarely reported in other studies involving electrospun fibre filters investigated under comparable conditions.

**Table 9.1:** Quality factors of the produced filters.

<b>1<sup>st</sup> generation</b>				<b>2<sup>nd</sup> generation</b>	
Filter	$Q_f \text{ (Pa}^{-1}\text{)}$	Filter	$Q_f \text{ (Pa}^{-1}\text{)}$	Filter	$Q_f \text{ (Pa}^{-1}\text{)}$
PU	0.0016	PVA	0.0014	CA	0.3567
PU/AC	0.0035	PVA/AC	0.0116	CA/AC	0.3949
PU/TiO <sub>2</sub>	0.0009	PVA/TiO <sub>2</sub>	0.0196	CA/TiO <sub>2</sub>	0.3725
				Composite	0.4872

Regarding the VOC removal capacity of the filters, the CA-based filters employing activated charcoal removed 45.5% of toluene from the polluted air stream even at high

toluene concentrations (22.5 ppm, Paper V), whereas the AC-doped filters from the first generation did not adsorb any toluene when exposed to low concentrations (1–1.5 ppm, Papers II and III). Two factors could explain this difference. As mentioned earlier, the doping method involved spraying the additive on the fibre surface to ensure that the additive surface would be in direct contact with the polluted air stream. In contrast, when the additives have been mixed in the polymer solution, their surface might have been wet by the polymer, preventing adsorption. Secondly, the improved performance could be related to the longer residence time when assessing the performance of the second generation of filters. The face velocities used in the two experimental studies are comparable ( $0.053 \text{ m s}^{-1}$  in Paper II and III and  $0.064 \text{ m s}^{-1}$  in Paper V). However, the CA-based filters were pleated inside the setup. Therefore, the filter surface area and volume are increased, resulting in a higher residence time throughout the investigation compared to the experimental studies with the PU and PVA filters.

The use of  $\text{TiO}_2$  to initiate the photocatalytic oxidation of toluene achieved similar results when investigating the two generation of filters. The use of FTIR to investigate the CA-based filters allowed a quantitative analysis of by-product formation from the oxidation of toluene, and formaldehyde was detected. In the first investigation, the formation of by-products could only be hypothesised since they could not be directly detected. In the literature, successful photocatalytic oxidation has involved residence times in the range of tens of seconds to minutes [181, 218]. By comparison, the residence time of Paper V was in the range of milliseconds. Furthermore, a xenon light was used in the first study (Paper II and III), which has a considerably higher intensity than the UV lamp employed in the second (Paper V). Higher light intensity leads to a higher conversion rate of VOCs when involving photocatalytic oxidation [169]. The intensity of the lamp used in the second study (Paper V) may have been too low to show a significant toluene conversion.

The combined use of the two additives has shown a positive effect with regards to the particle filtration for the composite filter. In previous studies, such additive combinations improved the overall performance of a filter [179, 180]. Once there is significant oxidation of the pollutant, the combined use of AC would be beneficial; AC could either adsorb potential by-products formed by incomplete VOC oxidation or immobilise the pollutant on the filter surface and thereby increase the residence time, allowing oxidation to occur [179, 181].

## 9.2 Overall discussion

The electrospinning process significantly influenced the fibre morphology and diameter, which then influenced filter parameters such as porosity and fibre density. The use of additives affected the fibre surface and the porosity of the filter, which affected air filter performance and filter quality factors. The presented studies provide evidence that final porosity and filter packing density significantly influenced air filter performance, in accordance with theory (Chapter 3.2.2). The fibre diameter range especially influenced the filtration efficiency for small particles ( $<0.3 \mu\text{m}$ ). Nevertheless, nanofibre filters imposed a pressure drop from 195 to 3,092 Pa, while the CA microfibre filters showed a pressure drop between 3 to 4 Pa at  $0.053 \text{ m s}^{-1}$ . Therefore, the CA-based filter achieved a quality factor of  $0.487 \text{ Pa}^{-1}$ . To further improve the filter's quality factor, the nanofibres could be restricted to a few layers to avoid an excessive increase in the pressure drop of the filter and to improve the removal of particles below  $0.5 \mu\text{m}$  size [204, 205].

In fact, the novelty of the CA filters is related to the described performance. Typically, the electrospun fibre filters reported by other groups are thin. However, to achieve a remarkable particle filtration efficiency, the filters must be very dense and are thus always associated with a rather significant pressure drop. The novelty of the filters reported in this thesis lies in the fact that the fabricated ultrathin fibre filters had minor pressure drops (3–4 Pa) and adequate particle filtration efficiencies (above 78%), rendering them suitable for natural ventilation systems. The quality factor confirmed the improved quality of the filters, as such values are rarely reported in the literature for similar filters. Furthermore, the reported CA filters presented a more sustainable alternative to the synthetic polymers commonly used (Tables 3.3 and 3.4, Chapter 3); biodegradable polymers based on renewable materials – which do not contribute to microplastic formation during use and upon disposal – could be used instead.

The doping methods had a significant influence on the final performance of the filters (Papers II, III and IV). Depending on the method used, the presence of the additives increased (spraying after electrospinning – Paper IV, Table 3) or decreased (mixing prior to electrospinning – Paper II, Figure 4 and Paper III, Figure 8) the filters' pressure drop. Overall, the use of additives had a positive influence on the particle filtration efficiency among the different generations (Papers II, III and IV), but especially when spraying the additives after electrospinning. In this technique, the doped filters presented a significantly improved filtration efficiency compared to the pure fibre filters (Paper IV, Table 3 and Figures 8 and 9).

Based on the results on gaseous removal capacity, the doping method based on

additive-in-solution is not preferable because it requires the continuous adjustment of the electrospinning process. Moreover, as shown in Papers II and III, the additive surface might be wet with the polymer, which could prevent reaction with the VOCs. Electro- and air-spraying are favoured methods to functionalise the fibres because the additives are deposited on the fibre surface (Paper V). Indeed, the CA/AC fibre filter doped with air spraying achieved 45.5% VOC removal (Paper V), whereas the PVA/AC and PU/AC filters, in which the catalyst was mixed in the polymer solution prior to electrospinning, showed no significant adsorption of gaseous pollutants (Papers II and Paper III). The reason for the PU/AC and PVA/AC results could be that AC was embedded in the polymer and saturated by the hydrophobic solvent needed to dissolve the polymer.

The use of  $\text{TiO}_2$  as a photocatalyst for treating polluted air has been shown to produce by-products such as formaldehyde (Paper V). The conversion of VOCs was not sufficient to see a notable reduction of toluene concentration, but the formation of by-products confirmed that photocatalytic oxidation was initiated. The reason for this result is related to the residence time and the UV light intensity in the study conditions. A potential solution to this issue might be to increase the UV light intensity on the filter surface to achieve complete VOC oxidation while also increasing the layers of the photocatalytic filter, thus lengthening the residence time and improving the VOC degradation rate.

The CA-based filters have great potential for use in naturally ventilated buildings. Traditionally, such buildings are not designed for the installation of supply air filtration (see Chapter 3.2.1), allowing outdoor pollutants to increase indoor pollution levels. Indeed, as reported previously, the dominant source of indoor particles is outdoor air [17]. As presented in Table 2.3 (Chapter 2), the negative impacts of pollutants such as particles and VOCs on human health are critical. Furthermore, as mentioned in Part I, existing natural ventilation systems might only be able to handle very low pressure drops because either there is no mechanical fan or a single fan is present to assist extraction. Existing buildings with such ventilation designs might have ventilation openings on the facade that offer limited space for modifications or the installation of spacious air filtration devices. The ultrathin electrospun filters reported in Papers IV and V could be installed in such conditions, undoubtedly improving the indoor air quality compared to the existing conditions without affecting the energy use of the building.

# Chapter 10

## Conclusions

### 10.1 Conclusion

Electrospun fibre filters represent a potential alternative to commonly used filters for improving the indoor air quality of residential buildings while causing a negligible increase in building energy use.

The use of electrospinning to fabricate a thin non-woven fibre material makes it possible to tune the porosity during fibre formation. It is possible to produce filters with diverse characteristics and configurations, from multi-layers to sandwich filters, and to embed additives within fibre layers. Indeed, electrospun fibres can be functionalised with active chemistry, and various types of catalysts can be used to dope the filters either before, during or after the electrospinning process. The flexibility of the achievable results makes electrospinning a versatile and reasonably fast method to produce materials for various filtration purposes.

The novelty of the studied filters is related to their polymer matrix, which is based on cellulose acetate, a biodegradable and sustainable material. Compared to common filters made from synthetic polymers based on mineral oil, cellulose acetate is a biopolymer. Therefore, it does not pose any risk of either releasing micro-plastics in the air or increasing the plastic load upon filter disposal.

The use of additives has been shown to improve the air filters' performance. The particle filtration efficiencies of the doped filters increased compared to undoped filters. Mixing the additive in the polymer solution prior to electrospinning led to a decreased pressure drop compared to the pure fibre filter, while doping after electrospinning resulted

in a slight increase in the observed pressure drop. Nevertheless, the doped filters showed higher quality factors than pure polymer filters.

The filters have been demonstrated to remove various air pollutants. Particles in the range from 0.3 to 10  $\mu\text{m}$  were removed with average filtration efficiencies of 78% (0.3–0.5  $\mu\text{m}$ ), 93% (1–3  $\mu\text{m}$ ) and 90% (>5  $\mu\text{m}$ ), including variously charged particles. The same filters have shown an obtainable VOC removal of 45.5%. These performances were achieved at the cost of a pressure drop between 3 to 4 Pa at a 0.053  $\text{m s}^{-1}$  face velocity. The results represent remarkable achievements that have not been reported elsewhere as of today. Indeed, ‘highly efficient’ electrospun filters usually display pressure drops one or two orders of magnitude higher than the presented ones. Therefore, the cellulose acetate-based filters have successfully optimised the ratio between filtration efficiency and pressure drop, obtaining improved quality factors compared to similar filters previously reported in the literature.

## 10.2 Future research

The fabricated filters were tested in a controlled environment in the laboratory. Additional research should investigate the filters’ long-term performance, estimate their lifetime under real conditions in a building and evaluate whether it is possible to regenerate the filter materials. The incorporation of flame retardant additives and their effect on overall filter performance should also be studied.

The possibility of negative synergistic effects among particles and VOCs should be studied to assess the overall performance of the filters.

Finally, for a deeper understanding of the inner workings of this kind of filter, a multi-scale and multi-parameter physics model should be developed.

# Bibliography

- [1] D. A. Glencross, T. R. Ho, N. Camiña, C. M. Hawrylowicz, and P. E. Pfeffer, “Air pollution and its effects on the immune system,” *Free Radical Biology and Medicine*, vol. 151, no. October 2019, pp. 56–68, 2020.
- [2] N. L. Mills, K. Donaldson, P. W. Hadoke, N. A. Boon, W. MacNee, F. R. Cassee, T. Sandström, A. Blomberg, and D. E. Newby, “Adverse cardiovascular effects of air pollution,” *Nature Clinical Practice Cardiovascular Medicine*, vol. 6, no. 1, pp. 36–44, 2009.
- [3] C. A. Pope and D. W. Dockery, “Health effects of fine particulate air pollution: Lines that connect,” *Journal of the Air and Waste Management Association*, vol. 56, no. 6, pp. 709–742, 2006.
- [4] I. Manisalidis, E. Stavropoulou, A. Stavropoulos, and E. Bezirtzoglou, “Environmental and Health Impacts of Air Pollution: A Review,” *Frontiers in Public Health*, vol. 8, no. February, pp. 1–13, 2020.
- [5] C. A. Pope III, R. T. Burnett, M. J. Thun, E. E. Calle, D. Krewski, and G. D. Thurston, “Lung Cancer, Cardiopulmonary Mortality, and Long-term Exposure to Fine Particulate Air Pollution,” *The Journal of the American Medical Association*, vol. 287, no. 9, pp. 1132–1141, 2002.
- [6] European Commission, “Air quality standards.” [Online]. Available: <https://ec.europa.eu/environment/air/quality/standards.htm>

- [7] Ministry of Environment of Denmark, “Air pollution monitoring programme.” [Online]. Available: <https://eng.mst.dk/air-noise-waste/air/air-pollution-monitoring-programme/>
- [8] World Health Organization, “WHO Global Air Quality Guidelines. Particulate matter (PM<sub>2.5</sub> and PM<sub>10</sub>), ozone, nitrogen dioxide, sulfur dioxide and carbon monoxide.” World Health Organization, Geneva, Tech. Rep., 2021.
- [9] WHO, “Guidelines for indoor air quality. Selected pollutants,” World Health Organization, Tech. Rep., 2010.
- [10] World Health Organization, “Air Pollution.” [Online]. Available: <https://www.who.int/health-topics/air-pollution>
- [11] J. Lelieveld, A. Pozzer, U. Pöschl, M. Fnais, A. Haines, and T. Münzel, “Loss of life expectancy from air pollution compared to other risk factors: A worldwide perspective,” *Cardiovascular Research*, vol. 116, no. 11, pp. 1910–1917, 2020.
- [12] P. Wolkoff, “Indoor air pollutants in office environments: Assessment of comfort, health, and performance,” *International Journal of Hygiene and Environmental Health*, vol. 216, no. 4, pp. 371–394, 2013.
- [13] J. Schwartz, D. Slater, T. V. Larson, W. E. Pierson, and J. Q. Koenig, “Particulate Air Pollution and Hospital Emergency Room Visits for Asthma in Seattle,” *American Review of Respiratory Disease*, vol. 147, no. 4, pp. 826–831, 1993.
- [14] D. P. Wyon, “The effects of indoor air quality on performance, behaviour and productivity,” *Pollution Atmospherique*, vol. 14, no. SPECIAL ISSUE, pp. 35–41, 2005.
- [15] U. Matson, “Indoor and outdoor concentrations of ultrafine particles in some Scandinavian rural and urban areas,” *Science of the Total Environment*, vol. 343, no. 1-3, pp. 169–176, 2005.
- [16] W. J. Fisk, “Health benefits of particle filtration,” *Indoor Air*, vol. 23, no. 5, pp. 357–368, 2013.
- [17] W. J. Riley, T. E. McKone, A. C. Lai, and W. W. Nazaroff, “Indoor particulate matter of outdoor origin: Importance of size-dependent removal mechanisms,” *Environmental Science and Technology*, vol. 36, no. 2, pp. 200–207, 2002.



- [18] IEA, “The Critical Role of Buildings,” 2019. [Online]. Available: <https://www.iea.org/reports/the-critical-role-of-buildings>
- [19] CORDIS EU Research results, “EnE-HVAC - Energy Efficient Heat Exchangers for HVAC Applications.” [Online]. Available: <https://cordis.europa.eu/project/id/314648>
- [20] REHVA, “REHVA Covid19 HVAC Guidance,” Federation of European Heating, Ventilation and Air Conditioning Associations, Tech. Rep., 2020.
- [21] ASHRAE, “Guidance for Re-Opening Buildings,” 2020. [Online]. Available: <https://www.ashrae.org/filelibrary/technicalresources/covid-19/guidance-for-re-opening-buildings.pdf>
- [22] IEA, “Energy Efficiency 2020,” 2020. [Online]. Available: <https://www.iea.org/reports/energy-efficiency-2020/buildings>
- [23] COAG, “Guide to Best Practice Maintenance & Operation of HVAC Systems for Energy Efficiency,” Council of Australian Governments, National Strategy on Energy Efficiency, Tech. Rep. January, 2012.
- [24] B. Stephens, J. A. Siegel, and A. Novoselac, “Energy implications of filtration in residential and light-commercial buildings,” *ASHRAE Transactions*, vol. 116 PART 1, no. January 2010, pp. 346–357, 2010.
- [25] European Commission, “Energy Efficiency Directive.” [Online]. Available: [https://ec.europa.eu/energy/topics/energy-efficiency/targets-directive-and-rules/energy-efficiency-directive\\_en](https://ec.europa.eu/energy/topics/energy-efficiency/targets-directive-and-rules/energy-efficiency-directive_en)
- [26] —, “Report from the Commission to the European Parliament and the council,” 2020.
- [27] The European Parliament and the Council of the European Union, “Energy Performance of Buildings Directive (EPBD) 2010/31/EU,” 2010.
- [28] Ministry of Transport Building and Housing, “Executive order on building regulations 2018 (BR18),” 2018.
- [29] R. Gieré and X. Querol, “Solid particulate matter in the atmosphere,” *Elements*, vol. 6, no. 4, pp. 215–222, 2010.

- [30] J. A. Bernstein, N. Alexis, C. Barnes, I. L. Bernstein, J. A. Bernstein, A. Nel, D. Peden, D. Diaz-Sanchez, S. M. Tarlo, and P. B. Williams, "Health effects of air pollution," *Journal of Allergy and Clinical Immunology*, vol. 114, no. 5, pp. 1116–1123, 2004.
- [31] G. McGranahan and F. Murray, *Air pollution and health in rapidly developing countries*. Earthscan Publication Ltd, 2003.
- [32] J. Colls, *Air pollution*, 2nd ed. Spon Press, 2002.
- [33] W. Hinds, *Aerosol Technology: Properties, Behavior, and Measurement of Airborne Particles.*, 2nd ed., ser. A Wiley-Interscience publication., W. C. Hinds, Ed. John Wiley & Sons, 1999.
- [34] N. Englert, "Fine particles and human health - A review of epidemiological studies," *Toxicology Letters*, vol. 149, no. 1-3, pp. 235–242, 2004.
- [35] J. Schwartz, D. W. Dockery, and L. M. Neas, "Is Daily Mortality Associated Specifically with Fine Particles?" *Journal of the Air and Waste Management Association*, vol. 46, no. 10, pp. 927–939, 1996.
- [36] N. Liora, A. Poupkou, T. M. Giannaros, K. E. Kakosimos, O. Stein, and D. Melas, "Impacts of natural emission sources on particle pollution levels in Europe," *Atmospheric Environment*, vol. 137, pp. 171–185, 2016.
- [37] M. Viana, J. Pey, X. Querol, A. Alastuey, F. de Leeuw, and A. Lükewille, "Natural sources of atmospheric aerosols influencing air quality across Europe," *Science of the Total Environment*, vol. 472, pp. 825–833, 2014.
- [38] U. Im, A. Poupkou, S. Incecik, K. Markakis, T. Kindap, A. Unal, D. Melas, O. Yenigun, S. Topcu, M. T. Odman, M. Tayanc, and M. Guler, "The impact of anthropogenic and biogenic emissions on surface ozone concentrations in Istanbul," *Science of the Total Environment*, vol. 409, no. 7, pp. 1255–1265, 2011.
- [39] K. Adams, D. S. Greenbaum, R. Shaikh, A. M. van Erp, and A. G. Russell, "Particulate matter components, sources, and health: Systematic approaches to testing effects," *Journal of the Air and Waste Management Association*, vol. 65, no. 5, pp. 544–558, 2015.
- [40] M. R. Heal, P. Kumar, and R. M. Harrison, "Particles, air quality, policy and health," *Chemical Society Reviews*, vol. 41, no. 19, pp. 6606–6630, 2012.

- [41] J. H. Seinfeld and S. N. Pandis, *Atmospheric Chemistry and Physics: From Air Pollution to Climate Change*, 3rd ed. John Wiley & Sons, Inc., 2016.
- [42] B. Freedman, "Gaseous Air pollution," in *Environmental Science: A Canadian Perspective*, 1998, p. 857.
- [43] P. Agarwal, M. Sarkar, B. Chakraborty, and T. Banerjee, "Phytoremediation of Air Pollutants: Prospects and Challenges," in *Phytomanagement of Polluted Sites: Market Opportunities in Sustainable Phytoremediation*. Elsevier, 12 2018, pp. 221–241.
- [44] J. J. Peirce, R. F. Weiner, and P. A. Vesilind, "Air Pollution," in *Environmental Pollution and Control*. Butterworth-Heinemann, 1998.
- [45] S. Kwiatkowski, M. Polat, W. Yu, and M. S. Johnson, "Industrial Emissions Control Technologies: Introduction," in *Encyclopedia of Sustainability Science and Technology*, R. A. Meyers, Ed. Springer, New York, NY, 2019, pp. 1–35.
- [46] H. R. Anderson, S. A. Bremner, R. W. Atkinson, R. M. Harrison, and S. Walters, "Particulate matter and daily mortality and hospital admissions in the west midlands conurbation of the United Kingdom: Associations with fine and coarse particles, black smoke and sulphate," *Occupational and Environmental Medicine*, vol. 58, no. 8, pp. 504–510, 2001.
- [47] T. M. de Kok, H. A. Driece, J. G. Hogervorst, and J. J. Briedé, "Toxicological assessment of ambient and traffic-related particulate matter: A review of recent studies," *Mutation Research - Reviews in Mutation Research*, vol. 613, no. 2-3, pp. 103–122, 2006.
- [48] C. A. Pope, R. T. Burnett, G. D. Thurston, M. J. Thun, E. E. Calle, D. Krewski, and J. J. Godleski, "Cardiovascular Mortality and Long-Term Exposure to Particulate Air Pollution: Epidemiological Evidence of General Pathophysiological Pathways of Disease," *Circulation*, vol. 109, no. 1, pp. 71–77, 2004.
- [49] D. E. Schraufnagel, "The health effects of ultrafine particles," *Experimental and Molecular Medicine*, vol. 52, no. 3, pp. 311–317, 2020.
- [50] R. Beelen, O. Raaschou-Nielsen, M. Stafoggia, Z. J. Andersen, G. Weinmayr, B. Hoffmann, K. Wolf, E. Samoli, P. Fischer, M. Nieuwenhuijsen, P. Vineis, W. W. Xun, K. Katsouyanni, K. Dimakopoulou, A. Oudin, B. Forsberg, L. Modig,

- A. S. Havulinna, T. Lanki, A. Turunen, B. Oftedal, W. Nystad, P. Nafstad, U. De Faire, N. L. Pedersen, C. G. Östenson, L. Fratiglioni, J. Penell, M. Korek, G. Pershagen, K. T. Eriksen, K. Overvad, T. Ellermann, M. Eeftens, P. H. Peeters, K. Meliefste, M. Wang, B. Bueno-De-Mesquita, D. Sugiri, U. Krämer, J. Heinrich, K. De Hoogh, T. Key, A. Peters, R. Hampel, H. Concin, G. Nagel, A. Ineichen, E. Schaffner, N. Probst-Hensch, N. Künzli, C. Schindler, T. Schikowski, M. Adam, H. Phuleria, A. Vilier, F. Clavel-Chapelon, C. Declercq, S. Grioni, V. Krogh, M. Y. Tsai, F. Ricceri, C. Sacerdote, C. Galassi, E. Migliore, A. Ranzi, G. Cesaroni, C. Badaloni, F. Forastiere, I. Tamayo, P. Amiano, M. Dorronsoro, M. Katsoulis, A. Trichopoulou, B. Brunekreef, and G. Hoek, “Effects of long-term exposure to air pollution on natural-cause mortality: An analysis of 22 European cohorts within the multicentre ESCAPE project,” *The Lancet*, vol. 383, no. 9919, pp. 785–795, 2014.
- [51] M. Longphre, L. Y. Zhang, J. R. Harkema, and S. R. Kleeberger, “Ozone-induced pulmonary inflammation and epithelial proliferation are partially mediated by PAF,” *Journal of Applied Physiology*, vol. 86, no. 1, pp. 341–349, 1999.
- [52] B. Vagaggini, M. Taccola, S. Cianchetti, S. Carnevali, M. L. Bartoli, E. Bacci, F. L. Dente, A. D. Franco, D. Giannini, and P. L. Paggiaro, “Ozone exposure increases eosinophilic airway response induced by previous allergen challenge,” *American Journal of Respiratory and Critical Care Medicine*, vol. 166, no. 8, pp. 1073–1077, 2002.
- [53] S. M. Tarlo, I. Broder, P. Corey, M. Chan-Yeung, A. Ferguson, A. Becker, C. Rogers, M. Okada, and J. Manfreda, “The role of symptomatic colds in asthma exacerbations: Influence of outdoor allergens and air pollutants,” *Journal of Allergy and Clinical Immunology*, vol. 108, no. 1, pp. 52–58, 2001.
- [54] P. J. Koken, W. T. Piver, F. Ye, A. Elixhauser, L. M. Olsen, and C. J. Portier, “Temperature, air pollution, and hospitalization for cardiovascular diseases among elderly people in Denver,” *Environmental Health Perspectives*, vol. 111, no. 10, pp. 1312–1317, 2003.
- [55] S. E. Harnung and M. S. Johnson, *Chemistry and the environment*. Cambridge University Press, 2012.

- [56] European Environment Agency, “Air quality standards,” 2020. [Online]. Available: <https://www.eea.europa.eu/themes/air/air-quality-concentrations/air-quality-standards>
- [57] J. M. Seguel, R. Merrill, D. Seguel, and A. C. Campagna, “Indoor Air Quality,” *American Journal of Lifestyle Medicine*, vol. 11, no. 4, pp. 284–295, 2017.
- [58] C. Chen and B. Zhao, “Review of relationship between indoor and outdoor particles: I/O ratio, infiltration factor and penetration factor,” *Atmospheric Environment*, vol. 45, no. 2, pp. 275–288, 2011.
- [59] J. Sundell, “On the history of indoor air quality and health,” *Indoor Air, Supplement*, vol. 14, no. SUPPL. 7, pp. 51–58, 2004.
- [60] Z. Peng, W. Deng, and R. Tenorio, “Investigation of indoor air quality and the identification of influential factors at primary schools in the north of China,” *Sustainability (Switzerland)*, vol. 9, no. 7, 2017.
- [61] M. Marc, M. Smielowska, J. Namiesnik, and B. Zabiegala, “Indoor air quality of everyday use spaces dedicated to specific purposes—a review,” *Environmental Science and Pollution Research*, vol. 25, pp. 2065–2082, 2018.
- [62] E. Abt, H. H. Suh, G. Allen, P. Koutrakis, and P. Koutrakis2, “Characterization of indoor particle sources: A study conducted in the metropolitan Boston area,” *Environmental Health Perspectives*, vol. 108, no. 1, pp. 35–44, 2000.
- [63] C. He, L. Morawska, J. Hitchins, and D. Gilbert, “Contribution from indoor sources to particle number and mass concentrations in residential houses,” *Atmospheric Environment*, vol. 38, no. 21, pp. 3405–3415, 2004.
- [64] H. K. Kong, D. K. Yoon, H. W. Lee, and C. M. Lee, “Evaluation of particulate matter concentrations according to cooking activity in a residential environment,” *Environmental Science and Pollution Research*, vol. 28, no. 2, pp. 2443–2456, 2021.
- [65] National Research Council, *Risk Assessment in the Federal Government: Managing the Process*. Washington, DC: The National Academies Press, 1983.
- [66] N. E. Klepeis, W. R. Ott, and J. L. Repace, “The effect of cigar smoking on indoor levels of carbon monoxide and particles,” *Journal of Exposure Analysis and Environmental Epidemiology*, vol. 9, no. 6, pp. 622–635, 1999.

- [67] A. Afshari, U. Matson, and L. E. Ekberg, "Characterization of indoor sources of fine and ultrafine particles: A study conducted in a full-scale chamber," *Indoor Air*, vol. 15, no. 2, pp. 141–150, 2005.
- [68] A. Afshari, B. Shi, N. C. Bergsøe, L. A. Ekberg, and T. Larsson, "Quantification of ultrafine particles from second-hand tobacco smoke," *Proceedings of Clima 2010: 10th REHVA World Congress 'Sustainable Energy use in Buildings'*, p. 9, 2010.
- [69] J. P. Winickoff, J. Friebely, S. E. tanski, C. Sherrod, G. E. matt, M. F. Hovell, and R. C. McMillen, "Beliefs about the health effects of "thirdhand" smoke and home smoking bans," *Pediatrics*, vol. 123, no. 1, 2009.
- [70] T. Salthammer, T. Schripp, S. Wientzek, and M. Wensing, "Impact of operating wood-burning fireplace ovens on indoor air quality," *Chemosphere*, vol. 103, pp. 205–211, 2014.
- [71] D. Frasca, M. Marcoccia, L. Tofful, G. Simonetti, C. Perrino, and S. Canepari, "Influence of advanced wood-fired appliances for residential heating on indoor air quality," *Chemosphere*, vol. 211, pp. 62–71, 2018.
- [72] R. L. Corsi, J. A. Siegel, and C. Chiang, "Particle resuspension during the use of vacuum cleaners on residential carpet," pp. 232–238, 2008.
- [73] E. D. Vicente, A. M. Vicente, M. Evtugina, A. I. Calvo, F. Oduber, C. Blanco Alegre, A. Castro, R. Fraile, T. Nunes, F. Lucarelli, G. Calzolari, S. Nava, and C. A. Alves, "Impact of vacuum cleaning on indoor air quality," *Building and Environment*, vol. 180, no. May, 2020.
- [74] A. W. Nørgaard, V. Kofoed-Sørensen, C. Mandin, G. Ventura, R. Mabilia, E. Perreca, A. Cattaneo, A. Spinazzè, V. G. Mihucz, T. Szigeti, Y. De Kluizenaar, H. J. Cornelissen, M. Trantallidi, P. Carrer, I. Sakellaris, J. Bartzis, and P. Wolkoff, "Ozone-initiated terpene reaction products in five European offices: Replacement of a floor cleaning agent," *Environmental Science and Technology*, vol. 48, no. 22, pp. 13 331–13 339, 2014.
- [75] M. S. Waring and J. A. Siegel, "Indoor Secondary Organic Aerosol Formation Initiated from Reactions between Ozone and Surface-Sorbed D-Limonene," *Environmental Science and Technology*, vol. 47, no. 12, pp. 6341–6348, 2013.

- [76] L. Stabile, G. De Luca, A. Pacitto, L. Morawska, P. Avino, and G. Buonanno, "Ultrafine particle emission from floor cleaning products," *Indoor Air*, vol. 31, no. 1, pp. 63–73, 2021.
- [77] C. J. Weschler, "Roles of the human occupant in indoor chemistry," *Indoor Air*, vol. 26, no. 1, pp. 6–24, 2016.
- [78] T. L. Thatcher and D. W. Layton, "Deposition, resuspension, and penetration of particles within a residence," *Atmospheric Environment*, vol. 29, no. 13, pp. 1487–1497, 1995.
- [79] T. J. Kelly, D. L. Smith, and J. Satola, "Emission rates of formaldehyde from materials and consumer products found in California homes," *Environmental Science and Technology*, vol. 33, no. 1, pp. 81–88, 1999.
- [80] S. Kim, J. A. Kim, H. J. Kim, and S. Do Kim, "Determination of formaldehyde and TVOC emission factor from wood-based composites by small chamber method," *Polymer Testing*, vol. 25, no. 5, pp. 605–614, 2006.
- [81] G. C. Morrison and W. W. Nazaroff, "The rate of ozone uptake on carpet: Mathematical modeling," *Atmospheric Environment*, vol. 36, no. 11, pp. 1749–1756, 2002.
- [82] H. Destailats, R. L. Maddalena, B. C. Singer, A. T. Hodgson, and T. E. McKone, "Indoor pollutants emitted by office equipment: A review of reported data and information needs," *Atmospheric Environment*, vol. 42, no. 7, pp. 1371–1388, 2008.
- [83] Y. An, J. S. Zhang, and C. Y. Shaw, "Sink Effect Study for Common Building Materials," National Research Council Canada, Tech. Rep. June, 1997.
- [84] B. A. Tichenor, Z. Guo, J. E. Dunn, L. E. Sparks, and M. A. Mason, "The Interaction of Vapour Phase Organic Compounds with Indoor Sinks," *Indoor Air*, vol. 1, no. 1, pp. 23–35, 1991.
- [85] D. Zhao, J. C. Little, and S. S. Cox, "Characterizing Polyurethane Foam as a Sink for or Source of Volatile Organic Compounds in Indoor Air," *Journal of Environmental Engineering*, vol. 130, no. 9, pp. 983–989, 2004.
- [86] M. Kraenzmer, "Modeling and continuous monitoring of indoor air pollutants for identification of sources and sinks," *Environment International*, vol. 25, no. 5, pp. 541–551, 1999.

- [87] C. S. Lee, F. Haghighat, and W. S. Ghaly, "A study on VOC source and sink behavior in porous building materials - Analytical model development and assessment," *Indoor Air*, vol. 15, no. 3, pp. 183–196, 2005.
- [88] D. Y. Leung, "Outdoor-indoor air pollution in urban environment: Challenges and opportunity," 2015.
- [89] J. A. Hoskins, "Health effect due to indoor air pollution," in *Survival and Sustainability*, 2011, pp. 665–676.
- [90] Z. Tong, Y. Chen, A. Malkawi, G. Adamkiewicz, and J. D. Spengler, "Quantifying the impact of traffic-related air pollution on the indoor air quality of a naturally ventilated building," *Environment International*, vol. 89-90, pp. 138–146, 2016.
- [91] L. Zhao, C. Chen, P. Wang, Z. Chen, S. Cao, Q. Wang, G. Xie, Y. Wan, Y. Wang, and B. Lu, "Influence of atmospheric fine particulate matter (PM<sub>2.5</sub>) pollution on indoor environment during winter in Beijing," *Building and Environment*, vol. 87, pp. 283–291, 2015.
- [92] T. Schneider, K. Alstrup Jensen, P. A. Clausen, A. Afshari, L. Gunnarsen, P. Wåhlin, M. Glasius, F. Palmgren, O. J. Nielsen, and C. L. Fogh, "Prediction of indoor concentration of 0.5-4  $\mu\text{m}$  particles of outdoor origin in an uninhabited apartment," pp. 6349–6359, 2004.
- [93] P. Blondeau, V. Iordache, O. Poupard, D. Genin, and F. Allard, "Relationship between outdoor and indoor air quality in eight French schools," *Indoor Air*, vol. 15, no. 1, pp. 2–12, 2005.
- [94] S. E. Chatoutsidou, J. Ondráček, O. Tesar, K. Tørseth, V. Ždímal, M. Lazaridis, J. Ondr, O. Tesar, K. Tørseth, V. Zdímal, and M. Lazaridis, "Indoor/outdoor particulate matter number and mass concentration in modern offices," pp. 462–474, 2015.
- [95] N. Tippayawong, P. Khuntong, C. Nitatwichit, Y. Khunatorn, and C. Tantakitti, "Indoor/outdoor relationships of size-resolved particle concentrations in naturally ventilated school environments," *Building and Environment*, vol. 44, no. 1, pp. 188–197, 2009.
- [96] I. Colbeck, Z. A. Nasir, and Z. Ali, "Characteristics of indoor/outdoor particulate pollution in urban and rural residential environment of Pakistan," *Indoor Air*, vol. 20, no. 1, pp. 40–51, 2010.



- [97] J. A. Bernstein, N. Alexis, H. Bacchus, I. L. Bernstein, P. Fritz, E. Horner, N. Li, S. Mason, A. Nel, J. Oullette, K. Reijula, T. Reponen, J. Seltzer, A. Smith, and S. M. Tarlo, "The health effects of nonindustrial indoor air pollution," *Journal of Allergy and Clinical Immunology*, vol. 121, no. 3, pp. 585–591, 2008.
- [98] V. Van Tran, D. Park, and Y. C. Lee, "Indoor air pollution, related human diseases, and recent trends in the control and improvement of indoor air quality," *International Journal of Environmental Research and Public Health*, vol. 17, no. 8, 2020.
- [99] R. Perez-Padilla, A. Schilman, and H. Riojas-Rodriguez, "Respiratory health effects of indoor air pollution," *International Journal of Tuberculosis and Lung Disease*, vol. 14, no. 9, pp. 1079–1086, 2010.
- [100] N. Bruce, E. Rehfuess, S. Mehta, G. Hutton, K. Smith, and S. Asia, "Indoor Air Pollution," in *Disease control priorities in developing countries*, 2002, p. 24.
- [101] P. Wargocki, L. Lagercrantz, T. Witterseh, J. Sundell, D. P. Wyon, and P. O. Fanger, "Subjective perceptions, symptom intensity and performance: A comparison of two independent studies, both changing similarly the pollution load in an office," *Indoor Air*, vol. 12, no. 2, pp. 74–80, 2002.
- [102] C. J. Weschler, "Chemistry in indoor environments: 20years of research," *Indoor Air*, vol. 21, no. 3, pp. 205–218, 2011.
- [103] C. J. Weschler and H. C. Shields, "Indoor ozone/terpene reactions as a source of indoor particles," *Atmospheric Environment*, vol. 33, no. 15, pp. 2301–2312, 1999.
- [104] C. J. Weschler, "Ozone in indoor environments: Concentration and chemistry," *Indoor Air*, vol. 10, no. 4, pp. 269–288, 2000.
- [105] J. Zhang and K. R. Smith, "Indoor air pollution: A global health concern," *British Medical Bulletin*, vol. 68, pp. 209–225, 2003.
- [106] R. C. Bruno, "Sources of indoor radon in houses: A review," *Journal of the Air Pollution Control Association*, vol. 33, no. 2, pp. 105–109, 1983.
- [107] K. Sutherland, *Filters and Filtration Handbook*. Butterworth-Heinemann, 2008.
- [108] —, *A-Z of Filtration and Related Separations*. Elsevier Advanced Technology, 2005.

- [109] D. B. Purchas and K. Sutherland, *Handbook of filter media*. Elsevier Advanced Technology, 2002.
- [110] Z. Xu and B. Zhou, *Fundamentals of air cleaning technology and its application in cleanrooms*. Springer, 2014.
- [111] H. Awbi, *Ventilation of Buildings*. Spon Press, 2004.
- [112] H. B. Awbi, *Ventilation Systems - Design and performance*. Taylor & Francis, 2008.
- [113] P. Heiselberg, “Characteristics of natural and hybrid ventilation systems,” in *Ventilation Systems: Design and Performance*, H. Awbi, Ed., 2008.
- [114] The Swedish National Board of Housing Building and Planning, “Boverket’s mandatory provisions and general recommendations, BBR, BFS 2011:6 with amendments up to BFS 2018:4,” 2018.
- [115] The Ministry of the Environment, “National building Code of Finland. Decree of the Ministry of the Environment and the Energy Performance of New Buildings.” 2018.
- [116] Liddament M., “A guide to energy efficient ventilation,” *Phys. Rev. B*, vol. 51, no. 24, p. 274, 1996.
- [117] P. Heiselberg, “Principles of hybrid ventilation,” *IEA Annex 35: Hybrid ventilation in new and retrofitted office buildings*, vol. 803, pp. 795–803, 2002.
- [118] C.-A. Roulet, “Characteristics of mechanical ventilation systems,” in *Ventilation Systems: Design and Performance*, H. B. Awbi, Ed. Taylor and Francis Ltd., 2008.
- [119] S. Terkildsen, “Development of mechanical ventilation system with low energy consumption for renovation of buildings,” Ph.D. dissertation, Technical University of Denmark, 2013.
- [120] J. Gustavsson, A. Ginestet, P. Tronville, and M. Hyttinen, *Air Filtration in HVAC System. REHVA Guidebook*. REHVA, 2010.
- [121] J. Montgomery, “Air filtration: predicting and improving indoor air quality and energy performance,” Ph.D. dissertation, The University of British Columbia, 2015.

- [122] Department of Health and Human Services, "Guidance for Filtration and Air-Cleaning Systems to Protect Building Environment from Airborne Chemical, Biological, or radiological Attacks," National Institute for Occupational Safety and Health, Tech. Rep., 2003.
- [123] P. Contal, J. Vendel, D. Leclerc, V. Renaudin, P. Penicot, and D. Thomas, "Modelling pressure drop in hepa filters during dynamic filtration," *Journal of Aerosol Science*, vol. 30, no. 2, pp. 235–246, 1999.
- [124] D. Thomas, P. Penicot, P. Contal, D. Leclerc, and J. Vendel, "Clogging of fibrous filters by solid aerosol particles Experimental and modelling study," *Chemical Engineering Science*, vol. 56, no. 11, pp. 3549–3561, 2001.
- [125] A. Podgórski, A. Bałazy, and L. Gradoń, "Application of nanofibers to improve the filtration efficiency of the most penetrating aerosol particles in fibrous filters," *Chemical Engineering Science*, vol. 61, no. 20, pp. 6804–6815, 2006.
- [126] R. C. Brown, *Air filtration - an integrated approach to the theory and the application of fibrous filter*. Pergamon Press, 1993.
- [127] C. Y. Chen, "Filtration of aerosols by fibrous media," *Chemical Reviews*, vol. 55, no. 3, pp. 595–623, 1955.
- [128] K. W. Lee and B. Y. Liu, "Theoretical study of aerosol filtration by fibrous filters," *Aerosol Science and Technology*, vol. 1, no. 2, pp. 147–161, 1982.
- [129] S. Payet, D. Boulaud, G. Madelaine, and A. Renoux, "Penetration and pressure drop of a HEPA filter during loading with submicron liquid particles," *Journal of Aerosol Science*, vol. 23, no. 7, pp. 723–735, 1992.
- [130] I. Colbeck and M. Lazaridis, *Aerosol Science. Technology and Applications*. John Wiley and Sons Ltd, 2014.
- [131] S. Kuwabara, "The forces experienced by randomly distributed parallel circular cylinders," *Journal of the physical society of Japan*, vol. 14, no. 4, pp. 527–532, 1959.
- [132] J. Happel, "Viscous flow relative to arrays of cylinders," *AIChE Journal*, vol. 5, no. 2, pp. 174–177, 1959.
- [133] C. N. Davies, "The Separation of Airborne Dust and Particles," pp. 185–213, 1953.

- [134] R. S. Barhate and S. Ramakrishna, “Nanofibrous filtering media : Filtration problems and solutions from tiny materials,” *Journal of Membrane Science*, vol. 296, pp. 1–8, 2007.
- [135] T. Xia, Y. Bian, L. Zhang, and C. Chen, “Relationship between pressure drop and face velocity for electrospun nanofiber filters,” *Energy and Buildings*, vol. 158, pp. 987–999, 2018.
- [136] X. Zhao, S. Wang, X. Yin, J. Yu, and B. Ding, “Slip-Effect Functional Air Filter for Efficient Purification of PM 2.5,” *Scientific reports*, vol. 6, 2016.
- [137] A. A. Kirsch, I. B. Stechkina, and N. A. Fuchs, “Effect of gas slip on the pressure drop in fibrous filters,” *Aerosol Science*, vol. 4, pp. 287–293, 1973.
- [138] —, “Gas flow in aerosol filters made of polydisperse ultrafine fibres,” *Journal of Aerosol Science*, vol. 5, no. 1, pp. 39–45, 1974.
- [139] A. A. Kirsch, I. Stechkina, and N. A. Fuchs, “Effect of Gas Slip on the Pressure Drop in a System of Parallel Cylinders at Small Reynolds Numbers,” *Journal of Colloid and Interface Science*, vol. 37, no. 2, pp. 458–461, 1971.
- [140] ISO 16890, “Air filters for general ventilation,” 2016.
- [141] A. Luengas, A. Barona, C. Hort, G. Gallastegui, V. Platel, and A. Elias, “A review of indoor air treatment technologies,” *Reviews in Environmental Science and Biotechnology*, vol. 14, no. 3, pp. 499–522, 2015.
- [142] ASME, “Addenda to ASME AG-1–2003 Code on Nuclear Air and Gas Treatment,” American Society of Mechanical Engineers, Tech. Rep., 2004.
- [143] A. Afshari and O. Seppänen, “Effect of Portable Air Cleaners on Indoor Air Quality: Particle Removal from Indoor Air,” *REHVA Journal*, pp. 29–38, 2021.
- [144] G. Bekö, O. Halás, G. Clausen, and C. J. Weschler, “Initial studies of oxidation processes on filter surfaces and their impact on perceived air quality,” *Indoor Air*, vol. 16, no. 1, pp. 56–64, 2006.
- [145] P. Zhao, J. A. Siegel, and R. L. Corsi, “Ozone removal by HVAC filters,” *Atmospheric Environment*, vol. 41, no. 15, pp. 3151–3160, 2007.

- [146] B. F. Yu, Z. B. Hu, M. Liu, H. L. Yang, Q. X. Kong, and Y. H. Liu, "Review of research on air-conditioning systems and indoor air quality control for human health," *International Journal of Refrigeration*, vol. 32, no. 1, pp. 3–20, 2009.
- [147] R. Thakur, D. Das, and A. Das, "Electret air filters," *Separation and Purification Reviews*, vol. 42, no. 2, pp. 87–129, 2013.
- [148] R. C. Brown, D. Wake, R. Gray, D. B. Blackford, and G. J. Bostock, "Effect of industrial aerosols on the performance of electrically charged filter material," *Annals of Occupational Hygiene*, vol. 32, no. 3, pp. 271–294, 1988.
- [149] A. Afshari, L. Ekberg, L. Forejt, J. Mo, S. Rahimi, J. Siegel, W. Chen, P. Wargocki, S. Zurami, and J. Zhang, "Electrostatic precipitators as an indoor air cleaner—a literature review," *Sustainability (Switzerland)*, vol. 12, no. 21, pp. 1–20, 2020.
- [150] J.-P. Brincat, D. Sardella, A. Muscat, S. Decelis, J. N. Grima, V. Valdramidisb, and R. Gatt, "A review of the state-of-the-art in air filtration technologies as may be applied to cold storage warehouses," *Trends in Food Science and Technology*, vol. 50, pp. 175–185, 4 2016.
- [151] E. M. Kettleson, J. M. Schriewer, R. M. L. Buller, and P. Biswas, "Soft-X-ray-enhanced electrostatic precipitation for protection against inhalable allergens, ultrafine particles, and microbial infections," *Applied and Environmental Microbiology*, vol. 79, no. 4, pp. 1333–1341, 2013.
- [152] S. H. Huang and C. C. Chen, "Filtration characteristics of a miniature electrostatic precipitator," *Aerosol Science and Technology*, vol. 35, no. 4, pp. 792–804, 2001.
- [153] M. S. Waring, J. A. Siegel, and R. L. Corsi, "Ultrafine particle removal and generation by portable air cleaners," *Atmospheric Environment*, vol. 42, no. 20, pp. 5003–5014, 2008.
- [154] J. Pei and J. S. Zhang, "Critical review of catalytic oxidization and chemisorption methods for indoor formaldehyde removal," *HVAC and R Research*, vol. 17, no. 4, pp. 476–503, 2011.
- [155] F. I. Khan and A. K. Ghoshal, "Removal of Volatic Organic Compounds from polluted air," *Journal of Loss Prevention in the process industries*, vol. 13, pp. 527–545, 2000.

- [156] K. K. Kennedy, K. J. Maseka, and M. Mbulo, "Selected Adsorbents for Removal of Contaminants from Wastewater: Towards Engineering Clay Minerals," *Open Journal of Applied Sciences*, vol. 8, no. 8, pp. 355–369, 2018.
- [157] R. Bradley, "Recent developments in the physical adsorption of toxic organic vapours by activated carbons," *Adsorption Science and Technology*, vol. 29, no. 1, pp. 1–28, 2011.
- [158] K. J. Kim and H. G. Ahn, "The effect of pore structure of zeolite on the adsorption of VOCs and their desorption properties by microwave heating," *Microporous and Mesoporous Materials*, vol. 152, pp. 78–83, 2012.
- [159] E. Scholten, L. Bromberg, G. C. Rutledge, and T. A. Hatton, "Electrospun polyurethane fibers for absorption of volatile organic compounds from air," *ACS Applied Materials and Interfaces*, vol. 3, no. 10, pp. 3902–3909, 2011.
- [160] X. Zhang, B. Gao, A. E. Creamer, C. Cao, and Y. Li, "Adsorption of VOCs onto engineered carbon materials: A review," 2017.
- [161] W. K. Jo and C. H. Yang, "Granular-activated carbon adsorption followed by annular-type photocatalytic system for control of indoor aromatic compounds," *Separation and Purification Technology*, vol. 66, no. 3, pp. 438–442, 2009.
- [162] D. Das, V. Gaur, and N. Verma, "Removal of volatile organic compound by activated carbon fiber," *Carbon*, vol. 42, no. 14, pp. 2949–2962, 2004.
- [163] K. J. Lee, N. Shiratori, G. H. Lee, J. Miyawaki, I. Mochida, S. H. Yoon, and J. Jang, "Activated carbon nanofiber produced from electrospun polyacrylonitrile nanofiber as a highly efficient formaldehyde adsorbent," *Carbon*, vol. 48, no. 15, pp. 4248–4255, 2010.
- [164] W. Chen, J. S. Zhang, and Z. Zhang, "Performance of Air Cleaners for Removing Multiple Volatile Organic Compounds in Indoor Air," *ASHRAE Transactions*, vol. 111, no. 1, pp. 1101–1114, 2005.
- [165] J. Mo, Y. Zhang, Q. Xu, J. J. Lamson, and R. Zhao, "Photocatalytic purification of volatic organic compounds in indoor air: a literature review," *Atmospheric Environment*, vol. 43, no. 14, pp. 2229–2246, 2009.
- [166] A. Fujishima, X. Zhang, and D. A. Tryk, "TiO<sub>2</sub> photocatalysis and related surface phenomena," *Surface Science Reports*, vol. 63, no. 12, pp. 515–582, 2008.

- [167] W. Yu, "Analysis of photocatalysis for control of indoor air pollution," Ph.D. dissertation, University of Copenhagen, 2021.
- [168] L. Zhong, F. Haghighat, C. S. C.-S. Lee, and N. Lakdawala, "Performance of ultra-violet photocatalytic oxidation for indoor air applications: Systematic experimental evaluation," *Journal of Hazardous Materials*, vol. 261, pp. 130–138, 2013.
- [169] A. H. Mamaghani, F. Haghighat, and C.-S. C. S. C.-S. Lee, "Photocatalytic oxidation technology for indoor environment air purification: The state-of-the-art," *Applied Catalysis B: Environmental*, vol. 203, pp. 247–269, 2017.
- [170] S. Wang, H. M. Ang, and M. O. Tade, "Volatile organic compounds in indoor environment and photocatalytic oxidation: State of the art," *Environment International*, vol. 33, no. 5, pp. 694–705, 2007.
- [171] R. M. Alberici and W. F. Jardim, "Photocatalytic destruction of VOCS in the gas-phase using titanium dioxide," *Applied Catalysis B: Environmental*, vol. 14, no. 1-2, pp. 55–68, 1997.
- [172] N. Quici, M. L. Vera, H. Choi, G. L. Puma, D. D. Dionysiou, M. I. Litter, and H. Destaillats, "Effect of key parameters on the photocatalytic oxidation of toluene at low concentrations in air under 254 + 185 nm UV irradiation," *Applied Catalysis B: Environmental*, vol. 95, no. 3-4, pp. 312–319, 2010.
- [173] J. Jeong, K. Sekiguchi, and K. Sakamoto, "Photochemical and photocatalytic degradation of gaseous toluene using short-wavelength UV irradiation with TiO<sub>2</sub> catalyst: Comparison of three UV sources," *Chemosphere*, vol. 57, no. 7, pp. 663–671, 2004.
- [174] L. Zhong and F. Haghighat, "Photocatalytic air cleaners and materials technologies - Abilities and limitations," *Building and Environment*, vol. 91, pp. 191–203, 2015.
- [175] J. Mo, Y. Zhang, Q. Xu, Y. Zhu, J. J. Lamson, and R. Zhao, "Determination and risk assessment of by-products resulting from photocatalytic oxidation of toluene," *Applied Catalysis B: Environmental*, vol. 89, no. 3-4, pp. 570–576, 2009.
- [176] J. Jeong, K. Sekiguchi, W. Lee, and K. Sakamoto, "Photodegradation of gaseous volatile organic compounds (VOCs) using TiO<sub>2</sub> photoirradiated by an ozone-producing UV lamp: decomposition characteristics, identification of by-products and water-soluble organic intermediates," *Journal of Photochemistry and Photobiology A: Chemistry*, vol. 169, no. 3, pp. 279–287, 2005.

- [177] J. Mo, Y. Zhang, and Q. Xu, "Effect of water vapor on the by-products and decomposition rate of ppb-level toluene by photocatalytic oxidation," *Applied Catalysis B: Environmental*, vol. 132-133, pp. 212–218, 2013.
- [178] Y. Lu, D. Wang, C. Ma, and H. Yang, "The effect of activated carbon adsorption on the photocatalytic removal of formaldehyde," *Building and Environment*, vol. 45, no. 3, pp. 615–621, 2010.
- [179] C. H. Ao and S. C. Lee, "Enhancement effect of TiO<sub>2</sub> immobilized on activated carbon filter for the photodegradation of pollutants at typical indoor air level," *Applied Catalysis B: Environmental*, vol. 44, no. 3, pp. 191–205, 2003.
- [180] —, "Indoor air purification by photocatalyst TiO<sub>2</sub> immobilized on an activated carbon filter installed in an air cleaner," *Chemical Engineering Science*, vol. 60, no. 1, pp. 103–109, 2005.
- [181] —, "Combination effect of activated carbon with TiO<sub>2</sub> for the photodegradation of binary pollutants at typical indoor air level," *Journal of Photochemistry and Photobiology A: Chemistry*, vol. 161, no. 2-3, pp. 131–140, 2004.
- [182] Y. Zhang, J. Mo, Y. Li, J. Sundell, P. Wargocki, J. Zhang, J. C. Little, R. Corsi, Q. Deng, M. H. K. Leung, L. Fang, W. Chen, J. Li, and Y. Sun, "Can commonly-used fan-driven air cleaning technologies improve indoor air quality? A literature review," *Atmospheric Environment*, vol. 45, no. 26, pp. 4329–4343, 2011.
- [183] M. Babaie, P. Davari, P. Talebizadeh, Z. Ristovski, H. Rahimzadeh, and R. J. Brown, "Study of particulate matter removal mechanism by using non-thermal plasma technology," *ICESP 2013 : XIII International Conference on Electrostatic Precipitation*, no. September, 2013.
- [184] A. M. Vandenbroucke, R. Morent, N. De Geyter, and C. Leys, "Non-thermal plasmas for non-catalytic and catalytic VOC abatement," *Journal of Hazardous Materials*, vol. 195, pp. 30–54, 2011.
- [185] M. Schiavon, V. Torretta, A. Casazza, and M. Ragazzi, "Non-thermal Plasma as an Innovative Option for the Abatement of Volatile Organic Compounds: a Review," *Water, Air, and Soil Pollution*, vol. 228, no. 10, 2017.
- [186] M. Bahri and F. Haghighat, "Plasma-Based Indoor Air Cleaning Technologies: The State of the Art-Review," *CLEAN-SOIL AIR WATER*, vol. 42, no. 12, pp. 1667–1680, 12 2014.



- [187] Z. Bo, J. H. Yan, X. D. Li, Y. Chi, K. F. Cen, and B. G. Chéron, “Effects of oxygen and water vapor on volatile organic compounds decomposition using gliding arc gas discharge,” *Plasma Chemistry and Plasma Processing*, vol. 27, no. 5, pp. 546–558, 2007.
- [188] H. F. Hubbard, B. K. Coleman, G. Sarwar, and R. L. Corsi, “Effects of an ozone-generating air purifier on indoor secondary particles in three residential dwellings,” *Indoor Air*, vol. 15, no. 6, pp. 432–444, 2005.
- [189] M. F. Boeniger, “Use of ozone generating devices to improve indoor air quality,” *American Industrial Hygiene Association Journal*, vol. 56, no. 6, pp. 590–598, 1995.
- [190] A. Afshari, O. Seppänen, B. W. Olesen, and J. Mo, “Effect of Portable Gas-Phase Air Cleaner on Indoor Air Quality,” *REHVA Journal*, no. 2, pp. 28–35, 2021.
- [191] C. W. Kwong, C. Y. H. Chao, K. S. Hui, and M. P. Wan, “Removal of VOCs from indoor environment by ozonation over different porous materials,” *Atmospheric Environment*, vol. 42, no. 10, pp. 2300–2311, 2008.
- [192] G. Bekö, G. Clausen, and C. J. Weschler, “Sensory pollution from bag filters, carbon filters and combinations,” *Indoor Air*, vol. 18, no. 1, pp. 27–36, 2008.
- [193] A. Ginestet, D. Pugnet, A. Tissot, and M. Henninot, “On-Site Particle and Gas Filtration Efficiencies of Air Handling Unit Filters in Industrial and Non Industrial Building,” *International Journal of Ventilation*, vol. 12, no. 2, pp. 151–158, 2013.
- [194] S. Yang, Z. Zhu, F. Wei, and X. Yang, “Carbon nanotubes / activated carbon fiber based air filter media for simultaneous removal of particulate matter and ozone,” *Building and Environment*, vol. 125, pp. 60–66, 2017.
- [195] I. E. Agranovski, S. Moustafa, and R. D. Braddock, “Performance of activated carbon loaded fibrous filters on simultaneous removal of particulate and gaseous pollutants,” *Environmental Technology*, vol. 26, no. 7, pp. 757–766, 2005.
- [196] Y. Zhang, X. He, Z. Zhu, W. N. Wang, and S. C. Chen, “Simultaneous removal of VOCs and PM<sub>2.5</sub> by metal-organic framework coated electret filter media,” *Journal of Membrane Science*, vol. 618, no. July 2020, p. 118629, 2021.
- [197] Y. Zeng, R. Xie, J. Cao, Z. Chen, Q. Fan, B. Liu, X. Lian, and H. Huang, “Simultaneous removal of multiple indoor-air pollutants using a combined process

- of electrostatic precipitation and catalytic decomposition,” *Chemical Engineering Journal*, vol. 388, no. 132, p. 124219, 2020.
- [198] K. Shimizu, Y. Kurokawa, and M. Blajan, “Basic Study of Indoor Air Quality Improvement by Atmospheric Plasma,” *IEEE Transactions on Industry Applications*, vol. 52, no. 2, pp. 1823–1830, 2016.
  - [199] J. H. Park, J. H. Byeon, K. Y. Yoon, and J. Hwang, “Lab-scale test of a ventilation system including a dielectric barrier discharger and UV-photocatalyst filters for simultaneous removal of gaseous and particulate contaminants,” *Indoor Air*, vol. 18, no. 1, pp. 44–50, 2008.
  - [200] S. Sundarrajan, K. L. Tan, S. H. Lim, and S. Ramakrishna, “Electrospun nanofibers for air filtration applications,” *Procedia Engineering*, vol. 75, pp. 159–163, 2014.
  - [201] M. Zhu, J. Han, F. Wang, W. Shao, R. Xiong, Q. Zhang, H. Pan, Y. Yang, S. K. Samal, F. Zhang, and C. Huang, “Electrospun Nanofibers Membranes for Effective Air Filtration,” *Macromolecular Materials and Engineering*, vol. 302, no. 1, 2017.
  - [202] V. Thavasi, G. Singh, and S. Ramakrishna, “Electrospun nanofibers in energy and environmental applications,” *Energy and Environmental Science*, vol. 1, no. 2, pp. 205–221, 2008.
  - [203] A. K. Selvam and G. Nallathambi, “Polyacrylonitrile/silver nanoparticle electrospun nanocomposite matrix for bacterial filtration,” *Fibers and Polymers*, vol. 16, no. 6, pp. 1327–1335, 2015.
  - [204] J. Wang, S. C. Kim, and D. Y. Pui, “Investigation of the figure of merit for filters with a single nanofiber layer on a substrate,” pp. 323–334, 2008.
  - [205] Q. Zhang, J. Welch, H. Park, C. Y. Wu, W. Sigmund, and J. C. M. Marijnissen, “Improvement in nanofiber filtration by multiple thin layers of nanofiber mats,” pp. 230–236, 2010.
  - [206] C. Liu, P.-c. Hsu, H.-w. Lee, M. Ye, G. Zheng, N. Liu, W. Li, and Y. Cui, “Transparent air filter for high efficiency PM2.5 capture,” *Nature Communications*, vol. 6, pp. 1–9, 2015.
  - [207] Y. Bian, R. Wang, S. H. Ting, C. Chen, and L. Zhang, “Electrospun SF/PVA nanofiber filters for highly efficient PM2.5 capture,” *IEEE transactions on nanotechnology*, vol. 17, no. 5, pp. 934–939, 2018.

- [208] W. Sambaer, M. Zatloukal, and D. Kimmer, "3D air filtration modeling for nanofiber based filters in the ultrafine particle size range," *Chemical Engineering Science*, vol. 82, pp. 299–311, 2012.
- [209] M. Liang, Y. Xu, X. Jin, C. Huang, H. Xu, X. Chen, Q. Ke, and Y. Fang, "Honeycomb-like polysulphone/polyurethane nanofiber filter for the removal of organic/inorganic species from air streams," *Journal of Hazardous Materials*, vol. 347, no. January, pp. 325–333, 2018.
- [210] S. Yan, Y. Yu, R. Ma, and J. Fang, "The formation of ultrafine polyamide 6 nanofiber membranes with needleless electrospinning for air filtration," *Polymers for Advanced Technologies*, vol. 30, no. 7, pp. 1635–1643, 2019.
- [211] P. Heikkilä, A. Taipale, M. Lehtimäki, and A. Harlin, "Electrospinning of Polyamides With Different Chain Compositions for Filtration Application," *Polymer Engineering and Science*, vol. 48, pp. 1168–1176, 2008.
- [212] H.-S. Park and Y. O. Park, "Filtration Properties of Electrospun Ultrafine Fiber Webs," *Korean Journal of Chemical Engineering*, vol. 22, no. 1, pp. 165–172, 2005.
- [213] E. H. Jeong, J. Yang, and J. H. Youk, "Preparation of polyurethane cationomer nanofiber mats for use in antimicrobial nanofilter applications," *Materials Letters*, vol. 61, no. 18, pp. 3991–3994, 2007.
- [214] H. J. Kim, H. R. Pant, N. J. Choi, and C. S. Kim, "Composite electrospun fly ash/polyurethane fibers for absorption of volatile organic compounds from air," *Chemical engineering journal*, vol. 230, pp. 244–250, 2013.
- [215] B. Ding and J. Yu, *Electrospun nanofibers for energy and environmental applications*, D. J. Lockwood and National Research Council of Canada, Eds. Springer, 2014.
- [216] J. Li, F. Gao, L. Q. Liu, and Z. Zhang, "Needleless electro-spun nanofibers used for filtration of small particles," *Express Polymer Letters*, vol. 7, no. 8, pp. 683–689, 2013.
- [217] X. H. Qin and S. Y. Wang, "Filtration properties of electrospinning nanofibers," *Journal of Applied Polymer Science*, vol. 102, no. 2, pp. 1285–1290, 2006.
- [218] Y. H. Chuang, G. B. Hong, and C. T. Chang, "Study on particulates and volatile organic compounds removal with TiO<sub>2</sub>nonwoven filter prepared by electrospinning,"

- Journal of the Air and Waste Management Association*, vol. 64, no. 6, pp. 738–742, 2014.
- [219] T. Christoforou and C. Doumanidis, “Biodegradable cellulose acetate nanofiber fabrication via electrospinning,” *Journal of Nanoscience and Nanotechnology*, vol. 10, no. 9, pp. 6226–6233, 2010.
- [220] Y. E. Greish, M. A. Meetani, E. A. Al Matroushi, and B. A. Shamsi, “Effects of thermal and chemical treatments on the structural stability of cellulose acetate nanofibers,” *Carbohydrate Polymers*, vol. 82, no. 3, pp. 569–577, 2010.
- [221] J. Matulevicius, L. Kliucininkas, T. Prasauskas, D. Buivydiene, and D. Martuzevicius, “The comparative study of aerosol filtration by electrospun polyamide, polyvinyl acetate, polyacrylonitrile and cellulose acetate nanofiber media,” *Journal of Aerosol Science*, vol. 92, pp. 27–37, 2016.
- [222] Y.-B. Wu, J. Bi, T. Lou, T.-B. Song, and H.-Q. Yu, “Preparation of a novel PAN/cellulose acetate-Ag based activated carbon nanofiber and its adsorption performance for low-concentration SO<sub>2</sub>,” *International Journal of Minerals, Metallurgy and Materials*, vol. 22, no. 4, pp. 437–445, 2015.
- [223] M. Kwon, J. Kim, and J. Kim, “Photocatalytic activity and filtration performance of hybrid tio<sub>2</sub>-cellulose acetate nanofibers for air filter applications,” *Polymers*, vol. 13, no. 8, pp. 1–11, 2021.
- [224] N. Wang, A. Raza, Y. Si, J. Yu, G. Sun, and B. Ding, “Tortuously structured polyvinyl chloride/polyurethane fibrous membranes for high-efficiency fine particulate filtration,” *Journal of Colloid and Interface Science*, vol. 398, pp. 240–246, 2013.
- [225] J. Su, G. Yang, C. Cheng, C. Huang, H. Xu, and Q. Ke, “Hierarchically structured TiO<sub>2</sub>/PAN nanofibrous membranes for high-efficiency air filtration and toluene degradation,” *Journal of Colloid and Interface Science*, vol. 507, pp. 386–396, 2017.
- [226] D. Cho, A. Naydich, M. W. Frey, and Y. L. Joo, “Further improvement of air filtration efficiency of cellulose filters coated with nanofibers via inclusion of electrostatically active nanoparticles,” *Polymer*, vol. 54, no. 9, pp. 2364–2372, 2013.

- [227] H. Wang, G. F. Zheng, X. Wang, and D. H. Sun, "Study on the air filtration performance of nanofibrous membranes compared with conventional fibrous filters," *2010 IEEE 5th International Conference on Nano/Micro Engineered and Molecular Systems, NEMS 2010*, pp. 387–390, 2010.
- [228] H. Wan, N. Wang, J. Yang, Y. Si, K. Chen, B. Ding, G. Sun, M. El-Newehy, S. S. Al-Deyab, and J. Yu, "Hierarchically structured polysulfone/titania fibrous membranes with enhanced air filtration performance," *Journal of Colloid and Interface Science*, vol. 417, pp. 18–26, 2014.
- [229] Z. Wang and Z. Pan, "Preparation of hierarchical structured nano-sized/porous poly(lactic acid) composite fibrous membranes for air filtration," *Applied Surface Science*, vol. 356, pp. 1168–1179, 2015.
- [230] N. Wang, Y. Si, N. Wang, G. Sun, M. El-Newehy, S. S. Al-Deyab, and B. Ding, "Multilevel structured polyacrylonitrile/silica nanofibrous membranes for high-performance air filtration," *Separation and Purification Technology*, vol. 126, pp. 44–51, 2014.
- [231] F. Kayaci and T. Uyar, "Electrospun Polyester/Cyclodextrin Nanofibers for Entrapment of Volatile Organic Compounds," *Polymer Engineering and Science*, vol. 54, no. 12, pp. 2970–2978, 2014.
- [232] Y. C. Ahn, S. K. Park, G. T. Kim, Y. J. Hwang, C. G. Lee, H. S. Shin, and J. K. Lee, "Development of high efficiency nanofilters made of nanofibers," *Current Applied Physics*, vol. 6, no. 6 SPEC. ISS., pp. 1030–1035, 2006.
- [233] Z. Cheng, Y. Zhang, Z. Han, L. Cui, L. Kang, and F. Zhang, "A novel preparation of anti-layered poly(vinylalcohol)-polyacrylonitrile (PVA/PAN) membrane for air filtration by electrospinning," *RSC Advances*, vol. 6, no. 88, pp. 85 545–85 550, 2016.
- [234] Y.-W. Ju and G.-Y. Oh, "Behavior of toluene adsorption on activated carbon nanofibers prepared by electrospinning of a polyacrylonitrile-cellulose acetate blending solution," *Chemical engineering journal*, vol. 34, pp. 2731–2737, 2017.
- [235] T. B. Song, Y. B. Wu, P. Sun, and J. Bi, "Preparation of TiO<sub>2</sub>-ACF by electrospinning and its adsorption performance for low concentration SO<sub>2</sub>," *Advanced Materials Research*, vol. 852, pp. 51–55, 2014.

- [236] M. X. Wang, Z. H. Huang, T. Shimohara, F. Kang, and K. Liang, "NO removal by electrospun porous carbon nanofibers at room temperature," *Chemical Engineering Journal*, vol. 170, no. 2-3, pp. 505–511, 2011.
- [237] G. Y. Oh, Y. W. Ju, H. R. Jung, and W. J. Lee, "Preparation of the novel manganese-embedded PAN-based activated carbon nanofibers by electrospinning and their toluene adsorption," *Journal of Analytical and Applied Pyrolysis*, vol. 81, no. 2, pp. 211–217, 2008.
- [238] A. Formhals, "Process and apparatus for preparing artificial threads," pp. 1–4, 1934.
- [239] D. Li and Y. Xia, "Electrospinning of nanofibers: Reinventing the wheel?" *Advanced Materials*, vol. 16, no. 14, pp. 1151–1170, 2004.
- [240] Z. M. Huang, Y. Z. Zhang, M. Kotaki, and S. Ramakrishna, "A review on polymer nanofibers by electrospinning and their applications in nanocomposites," *Composites Science and Technology*, vol. 63, no. 15, pp. 2223–2253, 2003.
- [241] V. V. Kadam, L. Wang, and R. Padhye, "Electrospun nanofibre materials to filter air pollutants – A review," *Journal of Industrial Textiles*, vol. 47, no. 8, pp. 2253–2280, 2018.
- [242] F. K. Ko and Y. Wan, *Introduction to Nanofiber Materials*. Cambridge University Press, 2014.
- [243] L. T. Lim, A. C. Mendes, and I. S. Chronakis, "Electrospinning and electrospraying technologies for food applications," *Advances in Food and Nutrition Research*, vol. 88, pp. 167–234, 1 2019.
- [244] H. Schreuder-Gibson, P. Gibson, K. Senecal, M. Sennett, J. Walker, W. Yeomans, D. Ziegler, and P. P. Tsai, "Protective textile materials based on electrospun nanofibers," *Journal of Advanced Materials*, vol. 34, no. 3, pp. 44–55, 2002.
- [245] G. Verreck, I. Chun, J. Rosenblatt, J. Peeters, A. Van Dijck, J. Mensch, M. Noppe, and M. E. Brewster, "Incorporation of drugs in an amorphous state into electrospun nanofibers composed of a water-insoluble, nonbiodegradable polymer," *Journal of Controlled Release*, vol. 92, no. 3, pp. 349–360, 2003.

- [246] J. Xie and Y.-L. Hsieh, "Ultra-high surface fibrous membranes from electrospinning of natural proteins: casein and lipase enzyme," *Journal of Materials Science*, vol. 38, pp. 2125–2133, 2003.
- [247] S. Thakkar, N. More, D. Sharma, G. Kapusetti, K. Kalia, and M. Misra, "Fast dissolving electrospun polymeric films of anti-diabetic drug repaglinide: formulation and evaluation," *Drug Development and Industrial Pharmacy*, vol. 45, no. 12, pp. 1921–1930, 2019.
- [248] S. J. Kim, Y. S. Nam, D. M. Rhee, H. S. Park, and W. H. Park, "Preparation and characterization of antimicrobial polycarbonate nanofibrous membrane," *European Polymer Journal*, vol. 43, no. 8, pp. 3146–3152, 2007.
- [249] P. Kunzo, P. Lobotka, V. Smatko, and I. Vavra, "Polyaniline-functionalized polycarbonate filter as a flow-through gas sensor," *2013 Transducers and Eurosensors XXVII: The 17th International Conference on Solid-State Sensors, Actuators and Microsystems, TRANSDUCERS and EUROSENSORS 2013*, no. June, pp. 270–273, 2013.
- [250] Y. Guibo, Z. Qing, Z. Tahong, Y. Yin, and Y. Yumin, "The electrospun polyamide 6 nanofiber membranes used as high efficiency filter materials: Filtration potential, thermal treatment, and their continuous production," *Journal of Applied Polymer Science*, vol. 128, no. 2, pp. 1061–1069, 2013.
- [251] S. Anitha, B. Brabu, D. John Thiruvadigal, C. Gopalakrishnan, and T. S. Natarajan, "Optical, bactericidal and water repellent properties of electrospun nano-composite membranes of cellulose acetate and ZnO," *Carbohydrate Polymers*, vol. 97, no. 2, pp. 856–863, 2013.
- [252] H. Liu and Y. L. Hsieh, "Ultrafine fibrous cellulose membranes from electrospinning of cellulose acetate," *Journal of Polymer Science, Part B: Polymer Physics*, vol. 40, no. 18, pp. 2119–2129, 2002.
- [253] R. Konwarh, N. Karak, and M. Misra, "Electrospun cellulose acetate nanofibers: The present status and gamut of biotechnological applications," *Biotechnology Advances*, vol. 31, no. 4, pp. 421–437, 2013.
- [254] E. R. Kenawy, F. I. Abdel-Hay, M. H. El-Newehy, and G. E. Wnek, "Processing of polymer nanofibers through electrospinning as drug delivery systems," *Materials Chemistry and Physics*, vol. 113, no. 1, pp. 296–302, 2009.

- [255] S. V. G. Nista, J. Bettini, and L. H. I. Mei, "Coaxial nanofibers of chitosan-alginate-PEO polycomplex obtained by electrospinning," *Carbohydrate Polymers*, vol. 127, pp. 222–228, 2015.
- [256] H. Jia, G. Zhu, B. Vugrinovich, W. Kataphinan, D. H. Reneker, and P. Wang, "Enzyme-carrying polymeric nanofibers prepared via electrospinning for use as unique biocatalysts," *Biotechnology Progress*, vol. 18, no. 5, pp. 1027–1032, 2002.
- [257] J. Wu, X. Lu, F. Shan, J. Guan, and Q. Lu, "Polydiacetylene-embedded supramolecular electrospun fibres for a colourimetric sensor of organic amine vapour," *RSC Advances*, vol. 3, no. 45, pp. 22 841–22 844, 2013.
- [258] T. Uyar, R. Havelund, Y. Nur, J. Hacaloglu, F. Besenbacher, and P. Kingshott, "Molecular filters based on cyclodextrin functionalized electrospun fibers," *Journal of Membrane Science*, vol. 332, no. 1-2, pp. 129–137, 2009.
- [259] L. Zhang, A. Aboagye, A. Kelkar, C. Lai, and H. Fong, "A review: Carbon nanofibers from electrospun polyacrylonitrile and their applications," *Journal of Materials Science*, vol. 49, no. 2, pp. 463–480, 2014.
- [260] P. Carol, P. Ramakrishnan, B. John, and G. Cheruvally, "Preparation and characterization of electrospun poly(acrylonitrile) fibrous membrane based gel polymer electrolytes for lithium-ion batteries," *Journal of Power Sources*, vol. 196, no. 23, pp. 10 156–10 162, 2011.
- [261] P. Sullivan, J. Moate, B. Stone, J. D. Atkinson, Z. Hashisho, and M. Rood, "Physical and chemical properties of PAN-derived electrospun activated carbon nanofibers and their potential for use as an adsorbent for toxic industrial chemicals," *Adsorption*, vol. 18, pp. 265–274, 2012.
- [262] A. Theron, E. Zussman, and A. L. Yarin, "Electrostatic field-assisted alignment of electrospun nanofibres," *Nanotechnology*, vol. 12, no. 3, pp. 384–390, 2001.
- [263] P. P. Tsai, H. Schreuder-Gibson, and P. Gibson, "Different electrostatic methods for making electret filters," *Journal of Electrostatics*, vol. 54, no. 3-4, pp. 333–341, 2002.
- [264] M. Bognitzki, W. Czado, T. Frese, A. Shaper, M. Hellwig, M. Steinhart, A. Greiner, and J. H. Wendorff, "Nanostructured fibers via electrospinning," *Advanced Materials*, vol. 13, no. 1, pp. 70–72, 2001.



- [265] E. R. Kenawy, G. L. Bowlin, K. Mansfield, J. Layman, D. G. Simpson, E. H. Sanders, and G. E. Wnek, "Release of tetracycline hydrochloride from electrospun poly(ethylene-co-vinylacetate), poly(lactic acid), and a blend," *Journal of Controlled Release*, vol. 81, no. 1-2, pp. 57-64, 2002.
- [266] J. P. Chen, K. H. Ho, Y. P. Chiang, and K. W. Wu, "Fabrication of electrospun poly(methyl methacrylate) nanofibrous membranes by statistical approach for application in enzyme immobilization," *Journal of Membrane Science*, vol. 340, no. 1-2, pp. 9-15, 2009.
- [267] J. I. Lim, H. Im, and W. K. Lee, "Fabrication of porous chitosan-polyvinyl pyrrolidone scaffolds from a quaternary system via phase separation," *Journal of Biomaterials Science, Polymer Edition*, vol. 26, no. 1, pp. 32-41, 2015.
- [268] S. Sundarrajan and S. Ramakrishna, "Fabrication of nanocomposite membranes from nanofibers and nanoparticles for protection against chemical warfare stimulants," *Journal of Materials Science*, vol. 42, no. 20, pp. 8400-8407, 2007.
- [269] C. V. Reddy, Q. Y. Zhu, L. Q. Mai, and W. Chen, "Electrochemical studies on PVC/PVdF blend-based polymer electrolytes," *Journal of Solid State Electrochemistry*, vol. 11, no. 4, pp. 543-548, 2007.
- [270] R. Asmatulu, H. Muppalla, Z. Veisi, W. S. Khan, A. Asaduzzaman, and N. Nuraje, "Study of hydrophilic electrospun nanofiber membranes for filtration of micro and nanosize suspended particles," *Membranes*, vol. 3, no. 4, pp. 375-388, 2013.
- [271] S. Jafari, S. S. Hosseini Salekdeh, A. Solouk, and M. Yousefzadeh, "Electrospun polyethylene terephthalate (PET) nanofibrous conduit for biomedical application," *Polymers for Advanced Technologies*, vol. 31, no. 2, pp. 284-296, 2020.
- [272] R. Gopal, S. Kaur, Z. Ma, C. Chan, S. Ramakrishna, and T. Matsuura, "Electrospun nanofibrous filtration membrane," *Journal of Membrane Science*, vol. 281, no. 1-2, pp. 581-586, 2006.
- [273] Y. Liao, R. Wang, M. Tian, C. Qiu, and A. G. Fane, "Fabrication of polyvinylidene fluoride (PVDF) nanofiber membranes by electro-spinning for direct contact membrane distillation," *Journal of Membrane Science*, vol. 425-426, pp. 30-39, 2013.

- [274] H. Chen, J. Huang, J. Yu, S. Liu, and P. Gu, “Electrospun chitosan-graft-poly (ε-caprolactone)/poly (ε-caprolactone) cationic nanofibrous mats as potential scaffolds for skin tissue engineering,” *International Journal of Biological Macromolecules*, vol. 48, no. 1, pp. 13–19, 2011.
- [275] Y. Zhang, X. Huang, B. Duan, L. Wu, S. Li, and X. Yuan, “Preparation of electrospun chitosan/poly(vinyl alcohol) membranes,” *Colloid and Polymer Science*, vol. 285, no. 8, pp. 855–863, 2007.
- [276] A. Figoli, C. Ursino, D. O. Sanchez Ramirez, R. A. Carletto, C. Tonetti, A. Varesano, M. P. De Santo, A. Cassano, and C. Vineis, “Fabrication of electrospun keratin nanofiber membranes for air and water treatment,” *Polymer Engineering and Science*, vol. 59, no. 7, pp. 1472–1478, 2019.
- [277] I. Oh, S. Lanceros-Mendez, G. Maria Fortunato, D. F. Ros, F. Da Ros, S. Bisconti, A. De Acutis, F. Biagini, A. Lapomarda, C. Magliaro, C. De Maria, F. Montemurro, D. Bizzotto, P. Braghetta, and G. Vozzi, “Electrospun Structures Made of a Hydrolyzed Keratin-Based Biomaterial for Development of in vitro Tissue Models,” *Front. Bioeng. Biotechnol.*, vol. 7, p. 174, 2019.
- [278] A. Aluigi, C. Vineis, C. Tonin, C. Tonetti, A. Varesano, and G. Mazzuchetti, “Wool keratin-based nanofibres for active filtration of air and water,” *Journal of Biobased Materials and Bioenergy*, vol. 3, no. 3, pp. 311–319, 2009.
- [279] J. A. Matthews, G. E. Wnek, D. G. Simpson, and G. L. Bowlin, “Electrospinning of collagen nanofibers,” *Biomacromolecules*, vol. 3, no. 2, pp. 232–238, 2002.
- [280] J. X. Law, L. L. Liau, A. Saim, Y. Yang, and R. Idrus, “Electrospun Collagen Nanofibers and Their Applications in Skin Tissue Engineering,” *Tissue Engineering and Regenerative Medicine*, vol. 14, 2017.
- [281] J. H. Wendorff, S. Agarwal, and A. Greiner, *Electrospinning. Materials, Processing and Applications*. Wiley-VCH Verlag, 2012.
- [282] B. Ding, H. Y. Kim, S. C. Lee, C. L. Shao, D. R. Lee, S. J. Park, G. B. Kwag, and K. J. Choi, “Preparation and characterization of a nanoscale poly(vinyl alcohol) fiber aggregate produced by an electrospinning method,” *Journal of Polymer Science, Part B: Polymer Physics*, vol. 40, no. 13, pp. 1261–1268, 2002.

- [283] P. O. Rujitanaroj, N. Pimpha, and P. Supaphol, "Preparation, characterization, and antibacterial properties of electrospun polyacrylonitrile fibrous membranes containing silver nanoparticles," *Journal of Applied Polymer Science*, vol. 116, no. 4, pp. 1967–1976, 2010.
- [284] P. D. Dalton, K. Klinkhammer, J. Salber, D. Klee, and M. Möller, "Direct in vitro electrospinning with polymer melts," *Biomacromolecules*, vol. 7, no. 3, pp. 686–690, 2006.
- [285] T. D. Brown, P. D. Dalton, and D. W. Hutmacher, "Melt electrospinning today: An opportune time for an emerging polymer process," *Progress in Polymer Science*, vol. 56, pp. 116–166, 2016.
- [286] D. W. Hutmacher and P. D. Dalton, "Melt electrospinning," *Chemistry - An Asian Journal*, vol. 6, no. 1, pp. 44–56, 2011.
- [287] A. Greiner and J. H. Wendorff, "Electrospinning: A fascinating method for the preparation of Ultrathin fibers," *Angewandte Chemie*, pp. 5670–5703, 2007.
- [288] P. E. Silva, F. Vistulo De Abreu, and M. H. Godinho, "Shaping helical electrospun filaments: A review," *Soft Matter*, vol. 13, no. 38, pp. 6678–6688, 2017.
- [289] D. H. Reneker and A. L. Yarin, "Electrospinning jets and polymer nanofibers," *Polymer*, vol. 49, no. 10, pp. 2387–2425, 2008.
- [290] G. Taylor and P. R. S. L. A, "Electrically driven jets," *Proceedings of the Royal Society of London. A. Mathematical and Physical Sciences*, vol. 313, no. 1515, pp. 453–475, 1969.
- [291] H. Niu and T. Lin, "Fiber generators in needleless electrospinning," *Journal of Nanomaterials*, vol. 2012, 2012.
- [292] A. Varesano, R. A. Carletto, and G. Mazzuchetti, "Experimental investigations on the multi-jet electrospinning process," *Journal of Materials Processing Technology*, vol. 209, no. 11, pp. 5178–5185, 2009.
- [293] E. Yang, J. Shi, and Y. Xue, "Influence of electric field interference on double nozzles electrospinning," *Journal of Applied Polymer Science*, vol. 116, no. 6, pp. 3688–3692, 2010.

- [294] H. Niu, X. Wang, and T. Li, "Needleless Electrospinning: Developments and Performances," *Nanofibers - Production, Properties and Functional Applications*, 2011.
- [295] A. L. Yarin and E. Zussman, "Upward needleless electrospinning of multiple nanofibers," *Polymer*, vol. 45, no. 9, pp. 2977–2980, 2004.
- [296] O. Jirsak, F. Sanetrik, D. Likas, V. Kotek, L. Martinova, and J. Chaloupek, "A method of nanofibers production from a polymer solution using electrostatic spinning and a device for carrying out the method." 2005.
- [297] J. Yoon, H. S. Yang, B. S. Lee, and W. R. Yu, "Recent Progress in Coaxial Electrospinning: New Parameters, Various Structures, and Wide Applications," *Advanced Materials*, vol. 30, no. 42, pp. 1–23, 2018.
- [298] T. T. T. Nguyen, C. Ghosh, S. G. Hwang, N. Chanunpanich, and J. S. Park, "Porous core/sheath composite nanofibers fabricated by coaxial electrospinning as a potential mat for drug release system," *International Journal of Pharmaceutics*, vol. 439, no. 1-2, pp. 296–306, 2012.
- [299] Z. Shami, N. Sharifi-Sanjani, S. Khoei, and R. Faridi-Majidi, "Triple Axial Coelectrospun Multifunctional Double-Shell TiO<sub>2</sub>@ZnO Carbon Hollow Nanofibrous Mat Transformed to C-Attached TiO<sub>2</sub> Brush-Like Nanotube Arrays: An Mo<sup>6+</sup> Adsorbent Nonwoven Mat," *Industrial and Engineering Chemistry Research*, vol. 53, no. 39, pp. 14963–14973, 2014.
- [300] S. Ramakrishna, K. Fujihara, W.-E. Teo, T.-c. Lim, and Z. Ma, *An introduction to electrospinning and nanofibers*. World Scientific Publishing Company, 2005.
- [301] J. Xu, C. Liu, P. C. P.-C. Hsu, K. Liu, R. Zhang, Y. Liu, and Y. Cui, "Roll-to-Roll Transfer of Electrospun Nanofiber Film for High-Efficiency Transparent Air Filter," *Nano Letters*, vol. 16, no. 2, pp. 1270–1275, 2016.
- [302] D. Li, Y. Wang, and Y. Xia, "Electrospinning of polymeric and ceramic nanofibers as uniaxially aligned arrays," *Nano Letters*, vol. 3, no. 8, pp. 1167–1171, 2003.
- [303] R. Inai, M. Kotaki, and S. Ramakrishna, "Structure and properties of electrospun PLLA single nanofibres," *Nanotechnology*, vol. 16, no. 2, pp. 208–213, 2005.

- [304] L. Wannatong, A. Sirivat, and P. Supaphol, "Effects of solvents on electrospun polymeric fibers: Preliminary study on polystyrene," *Polymer International*, vol. 53, no. 11, pp. 1851–1859, 2004.
- [305] B. Sun, Y. Z. Long, H. D. Zhang, M. M. Li, J. L. Duvail, X. Y. Jiang, and H. L. Yin, "Advances in three-dimensional nanofibrous macrostructures via electrospinning," *Progress in Polymer Science*, vol. 39, no. 5, pp. 862–890, 2014.
- [306] T. Subbiah, G. S. Bhat, R. W. Tock, S. Parameswaran, and S. S. Ramkumar, "Electrospinning of nanofibers," *Journal of Applied Polymer Science*, vol. 96, no. 2, pp. 557–569, 2005.
- [307] J. M. Deitzel, J. D. Kleinmeyer, D. Harris, and N. C. Beck Tan, "The effect of processing variables on the morphology of electrospun," *Polymer*, vol. 42, pp. 261–272, 2001.
- [308] R. Givehchi, Q. Li, and Z. Tan, "Quality factors of PVA nanofibrous filters for airborne particles in the size range of 10–125 nm," *Fuel*, vol. 181, pp. 1273–1280, 2016.
- [309] S. Megelski, J. S. Stephens, D. Bruce Chase, and J. F. Rabolt, "Micro- and nanostructured surface morphology on electrospun polymer fibers," *Macromolecules*, vol. 35, no. 22, pp. 8456–8466, 2002.
- [310] R. K. Mishra, P. Mishra, K. Verma, A. Mondal, R. G. Chaudhary, M. M. Abolhasani, and S. Loganathan, "Electrospinning production of nanofibrous membranes," *Environmental Chemistry Letters*, vol. 17, no. 2, pp. 767–800, 2018.
- [311] M. Mohammadian and A. K. Haghi, "Systematic parameter study for nano-fiber fabrication via electrospinning process," *Bulgarian Chemical Communications*, vol. 46, no. 3, pp. 545–555, 2014.
- [312] N. Wang, X. Wang, B. Ding, J. Yu, and G. Sun, "Tunable fabrication of three-dimensional polyamide-66 nano-fiber/nets for high efficiency fine particulate filtration," *Journal of Materials Chemistry*, vol. 22, no. 4, pp. 1445–1452, 2012.
- [313] A. L. Yarin, S. Koombhongse, and D. H. Reneker, "Taylor cone and jetting from liquid droplets in electrospinning of nanofibers," *Journal of Applied Physics*, vol. 90, no. 9, pp. 4836–4846, 2001.

- [314] D. H. Reneker, A. L. Yarin, H. Fong, and S. Koombhongse, "Bending instability of electrically charged liquid jets of polymer solutions in electrospinning," *Journal of Applied Physics*, vol. 87, no. 9 I, pp. 4531–4547, 2000.
- [315] M. M. Hohman, M. Shin, G. Rutledge, and M. P. Brenner, "Electrospinning and electrically forced jets. II. Applications," *Physics of Fluids*, vol. 13, no. 8, pp. 2221–2236, 2001.
- [316] —, "Electrospinning and electrically forced jets. I. Stability theory," *Physics of Fluids*, vol. 13, no. 8, pp. 2201–2220, 2001.
- [317] W. Zuo, M. Zhu, W. Yang, H. Yu, Y. Chen, and Y. Zhang, "Experimental study on relationship between jet instability and formation of beaded fibers during electrospinning," *Polymer Engineering and Science*, vol. 45, no. 5, pp. 704–709, 2005.
- [318] D. H. Reneker, A. L. Yarin, E. Zussman, and H. Xu, "Electrospinning of Nanofibers from Polymer Solutions and Melts," *Advances in Applied Mechanics*, vol. 41, 2007.
- [319] Y. M. Shin, M. M. Hohman, M. P. Brenner, and G. C. Rutledge, "Electrospinning: A whipping fluid jet generates submicron polymer fibers," *Applied Physics Letters*, vol. 78, no. 8, pp. 1149–1151, 2001.
- [320] —, "Experimental characterization of electrospinning: The electrically forced jet and instabilities," *Polymer*, vol. 42, no. 25, pp. 09 955–09 967, 2001.
- [321] G. Taylor, "Disintegration of water drops in an electric field," *Proceeding of the Royal Society London Series Mathematical, Physical and Engineering Science*, 1964.
- [322] J. H. He, Y. Wu, and W. W. Zuo, "Critical length of straight jet in electrospinning," *Polymer*, vol. 46, no. 26, pp. 12 637–12 640, 2005.
- [323] J. Doshi and D. H. Reneker, "Electrospinning process and applications of electrospun fibers," *Journal of Electrostatics*, vol. 35, no. 2, pp. 151–160, 1995.
- [324] A. L. Yarin, S. Koombhongse, and D. H. Reneker, "Bending instability in electrospinning of nanofibers," *Journal of Applied Physics*, vol. 89, no. 5, pp. 3018–3026, 2001.

- [325] S. V. Fridrikh, J. H. Yu, M. P. Brenner, and G. C. Rutledge, “Controlling the Fiber Diameter during Electrospinning,” *Physical Review Letters*, vol. 90, no. 14, p. 4, 2003.
- [326] A. L. Yarin, W. Kataphinan, and D. H. Reneker, “Branching in electrospinning of nanofibers,” *Journal of Applied Physics*, vol. 98, no. 6, 2005.
- [327] H. Fong, I. Chun, and D. H. Reneker, “Beaded nanofibers formed during electrospinning,” *Polymer*, vol. 40, no. 16, pp. 4585–4592, 1999.
- [328] T. Han, D. H. Reneker, and A. L. Yarin, “Buckling of jets in electrospinning,” *Polymer*, vol. 48, no. 20, pp. 6064–6076, 2007.

ISSN (online): 2446-1636  
ISBN (online): 978-87-7573-967-7

AALBORG UNIVERSITY PRESS